Impact of Static Sea Surface Topography Variations on Ocean Surface Waves

Yik Keung YING

Technische Universiteit Delft

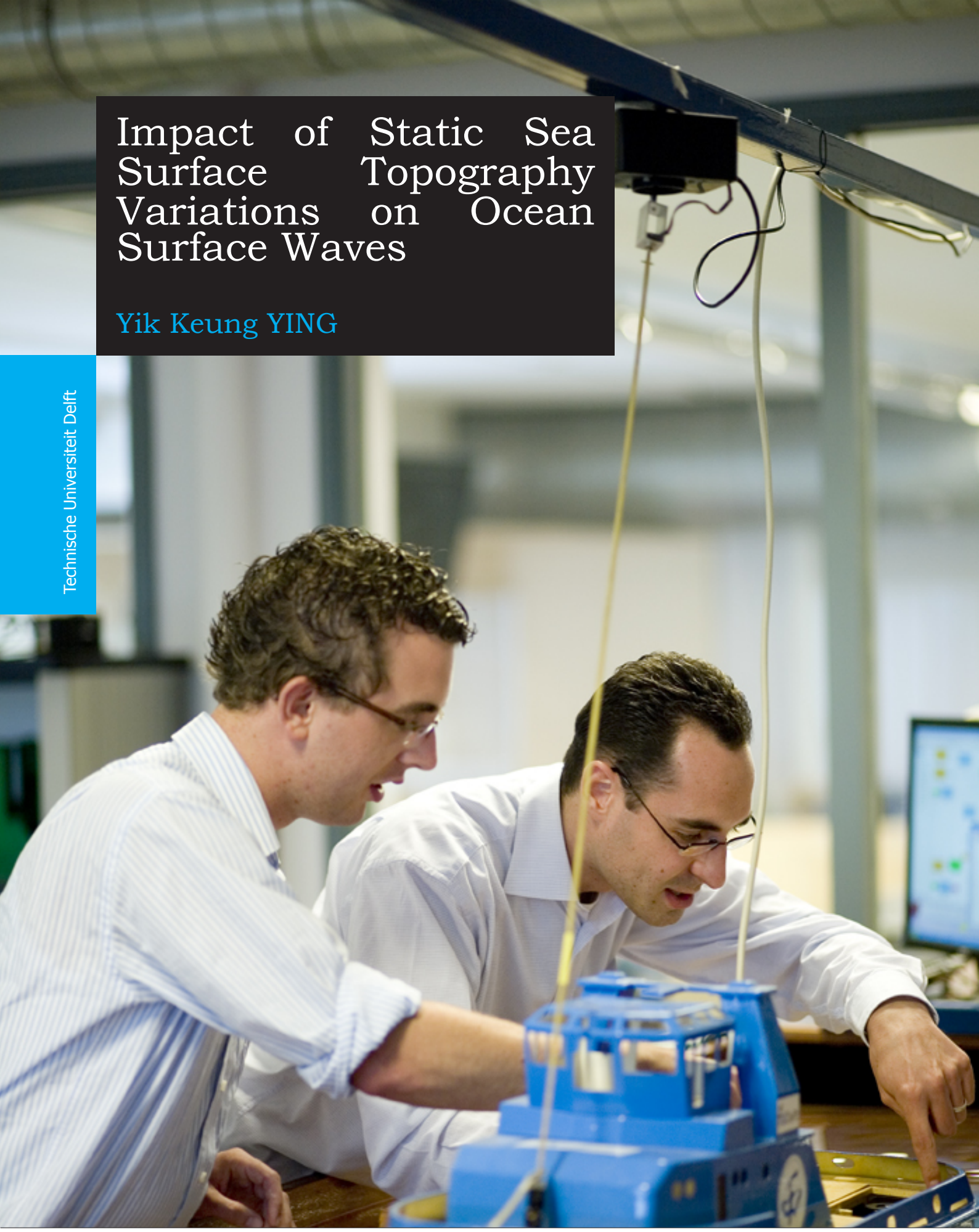

TU Delft Delft University of Technology

Challenge the future

Impact of Static Sea Surface Topography Variations on Ocean Surface Waves

by

Yik Keung YING

in partial fulfillment of the requirements for the degree of

Master of Science
in Applied Mathematics

at the Delft University of Technology,
to be defended publicly on Tuesday August 1, 2016 at 1:00 PM.

Supervisor:	Prof. dr. ir. C. Vuik, Prof. dr. ir. L. R. Maas	
Thesis committee:	Prof. dr. ir. C. Vuik,	TU Delft
	Dr. ir. W. T. van Horssen,	TU Delft
	Prof. dr. ir. L. R. Maas,	Koninklijk Nederlands Instituut voor Onderzoek der Zee

This thesis is confidential and cannot be made public until August 30, 2016.

An electronic version of this thesis is available at http://repository.tudelft.nl/.

TU Delft Delft University of Technology

Preface

I would like to express my gratitude towards everyone I met over the past two years in Europe. Without any of you my life would not have been so joyful and fulfilling.

In particular, I would like to thank Dr. Vadym Aizinger from FAU and Dr. Vera Fofonova from AWI for bringing me to the icy Lena delta. I hope sooner or later I can involve in the discussion between you two in Russian language.

I would also like to thank Prof Kees Vuik and Prof Leo Maas for their patience and advice towards my ill-organised idea and erroneous writing. I don't speak much Dutch but I absolutely love the dutch people and the dutch ways of working things out.

Special thanks also goes to the European Commission and the COSSE Consortium for providing many opportunities and financing my studies. Without the kind support I don't think I have a chance to leave my home country and explore Europe.

Danke schoen. Dankje wel.

Yik Keung YING
Delft, August 2016

Contents

1

Introduction

The shape of the Earth has long been one of the biggest and most frequently-asked questions of humanity. While ancient Chinese believed the Earth is a square plane covered by a hemisphere sky, the ancient Egyptians had long spotted the Earth is curved and even gave an estimate to the curvature and size of the Earth. Yet it was not until Ferdinand Magellan succeeded the circumnavigation in year 1521 that human-beings first confirmed experimentally that the Earth is a closed sphere. Yet it is not really a sphere - the remote sensing techniques developed alongside with the space technology in the last century revealed that the Earth's shape is a 'spheroid', meaning 'almost sphere', whose surface is indeed much rougher than anyone expected.

The shape of the Earth, modernly described by the so-called mean-sea level, is indeed a time-independent equipotential of the conservative gravitational field, governed by the Poisson equation. With an uneven distribution of mass both on the surface and in the interior of the Earth, the resulting gravity field is also spatially non-uniform.

Although small in magnitude, the spatial variation of gravitational attraction does lead to observable 'topography' on the ocean, namely, the hypothetically motionless sea-surface does not lie on a perfect sphere but a rough-surfaced spheroid. Consequently, the gravity vector, which is defined to be the gradient vector of the equipotential lines, does not always point in the same direction. The magnitude of the gravity at the mean-sea level is also not uniform at all.

The causes and empirical determination of the mean-sea level have been addressed by geophysicists. In this project, however, it is the consequence of the non-uniform gravity that concerns us. In particular, the surface waves in fluid in a spatially varying gravity field is the topic of this thesis.

In the classical treatment of surface waves, the gravity field is assumed to be uni-directionally constant everywhere. The gravity together with the fluid pressure constitute the restoring mechanisms of oscillations on the fluid surface, thus creating the surface gravity waves.

In this project, the assumption of uniform gravity, used in most, if not all, of the analytical and numerical studies of surface waves, will be relaxed. Focus is especially put on conservative gravitational force fields, due to their relevance to the actual gravity field on Earth. In Chapter 2 basic terminologies and notations will be introduced. The research topic starts with the shallow water waves in Chapter 3, in which the standard shallow water model will be adapted to cater for the non-uniformity in the gravity field. The adapted shallow water model and the linearised shallow water waves will be derived in this Chapter.

In Chapter 4, the adapted one-dimensional shallow water waves are analysed. Analytic solutions to the adapted shallow water wave equations are derived, and validated by numerical simulations with the aid of the open-source numerical solver CLAWPACK. Two features of surface waves in the one-dimension studies are reviewed, namely the wave amplitudes and wavenumber.

Chapter 5 continues the discussion of the adapted shallow water model in the two-dimensional space. While limited analytic studies are presented, the two-dimensional equations are solved numerically by CLAWPACK based on both hypothetical and physical scenarios. In addition to the wave amplitudes and wavenumbers, the refraction and scattering of waves by the spatially-varying gravity field is focused also in the two-dimensional studies.

A twist is found in Chapter 6. In this chapter the shallowness assumption is relaxed and Airy's linear wave theory, which is a fundamental and widely-applied theory to study surface gravity waves, is generalised for spatially-varying conservative gravity fields. The generalisation is, however, limited to only the two-dimensional space, and thus one-dimensional waves. The surface waves in the full three-dimensional remains an unresolved problem left for further research. Despite this, it is demonstrated that the one-dimensional waves turns out to be consistent with the adapted shallow water waves, discussed in Chapter 3 and 4.

The summary and conclusions are given in Chapter 7. Several unanswered questions in this thesis are also outlined for future research.

2

Basis Terminology

2.1. Governing Equations

2.1.1. Equations of Motion in a Non-rotating Coordinate System

The governing equations for fluid are given by the continuum equations of motions.

Denote

$$\frac{D}{dt} \equiv \frac{\partial}{\partial t} + \mathbf{u} \cdot \nabla \tag{2.1}$$

to be the total derivative following individual fluid elements.

Denote $\mathbf{x}$ to be the position vector, $\rho = \rho(\mathbf{x}, t)$ to be the density of fluid and $\mathbf{u} = \frac{dx}{dt}(\mathbf{x}, t)$ is the velocity field. The continuity equation is given by:

$$\frac{D\rho}{dt} + \rho \nabla \cdot \mathbf{u} = 0 \tag{2.2}$$

In this thesis the fluid is taken to be *incompressible*, so that the continuity equation reads:

$$\nabla \cdot \mathbf{u} = 0 \tag{2.3}$$

Denote $p = p(\mathbf{x}, t)$ to be the pressure field, $\Phi = \Phi(\mathbf{x}, t)$ is the potential for conservative force fields and $\mathbf{F} = \mathbf{F}(\mathbf{x}, \mathbf{u}, t)$ is the non-conservative forces. The momentum equation is given by:

$$\rho \frac{D\mathbf{u}}{dt} = -\nabla p - \rho \nabla \Phi + \mathbf{F} \tag{2.4}$$

2.1.2. Equations of Motion in a Rotating Coordinate System

Consider a reference frame which is rotating at uniform angular speed □ relative to the inertial frame. The continuity equation remains invariant in both rotating and non-rotating coordinate system. The momentum equation, however, is transformed into the following form:

$$\rho \left[\frac{D\mathbf{u}}{dt} + 2\square \times \mathbf{u} \right] = -\nabla p - \rho \nabla (\Phi + \Phi_c) + \mathbf{F} \tag{2.5}$$

where Φ_c is the conservative centrifugal potential associated to the centrifugal force due to the rotation of reference frame.

2.2. Transformation of Coordinates

2.2.1. Notations

The Cartesian coordinates (x, y, z) are commonly used to study geophysical fluid dynamics when the scale of motion is not too large in the sense that the length scale of motion L is much less than the radius of Earth $R_E \approx 6400$km.

For specific problems, it may happen that the use of an transformed coordinate system can simplify the analysis. In the following text, a specific transformation on the vertical coordinates z will be performed. A general description is given below.

Suppose r is a general vertical coordinate which is monotonic with z. Transformation from (x, y, z, t) to (x, y, r, t) requires a transformation function $T(x, y, z, t)$, which maps $(x, y, z, t) \in \mathcal{R}^4$ into $(x, y, r, t) \in \mathcal{R}^4$.

$$(x, y, r, t) = T(x, y, z, t), \tag{2.6}$$

Since the coordinates x, y and remains invariant in the transformation given by T, r can also be seen as a scalar function that maps (x, y, z, t) to a scalar, which is given by

$$r = r(x, y, z, t) \tag{2.7}$$

If r is monotonic, there exist an inverse $\tilde{z}$ to r, which maps (x, y, r, t) back to a scalar, which is given by

$$\tilde{z} = \tilde{z}(x, y, r, t) \tag{2.8}$$

The equation (2.8) can be interpreted as 'reading' the vertical position in the physical coordinate using data from the transformed coordinates (x, y, r, t).

2.2.2. Transformation of scalar fields

Any scalar field $F = F(x, y, z, t)$ can then be rewritten in the new coordinates $F = F(x, y, z(x, y, r, t), t) = \tilde{F}(x, y, r, t)$. Applying the chain rule yields

$$\left.\frac{\partial \tilde{F}}{\partial x}\right|_r = \left.\frac{\partial F}{\partial x}\right|_z + \left.\frac{\partial F}{\partial z}\frac{\partial \tilde{z}}{\partial x}\right|_r \tag{2.9a}$$

$$\left.\frac{\partial \tilde{F}}{\partial y}\right|_r = \left.\frac{\partial F}{\partial y}\right|_z + \left.\frac{\partial F}{\partial z}\frac{\partial \tilde{z}}{\partial y}\right|_r \tag{2.9b}$$

$$\left.\frac{\partial \tilde{F}}{\partial t}\right|_r = \left.\frac{\partial F}{\partial t}\right|_z + \left.\frac{\partial F}{\partial z}\frac{\partial \tilde{z}}{\partial t}\right|_r \tag{2.9c}$$

where the vertical bar refers to partial differentiation maintaining the suffix constant.

Meanwhile along the transformed 'vertical' coordinates, the 'vertical' gradient of the scalar field $\tilde{F}$ is given by

$$\frac{\partial \tilde{F}}{\partial r} = \frac{\partial F}{\partial z}\frac{\partial \tilde{z}}{\partial r} \tag{2.10}$$

Denote $\hat{e_1}, \hat{e_2}$ and $\hat{e_3}$ to be the unit vector in the Cartesian coordinates. the horizontal gradient ∇_h and $\tilde{\nabla}_h$ is given by

$$\nabla_h F = \left.\frac{\partial F}{\partial x}\right|_z \hat{e_1} + \left.\frac{\partial F}{\partial y}\right|_z \hat{e_2} \tag{2.11}$$

$$\tilde{\nabla}_h \tilde{F} = \left.\frac{\partial \tilde{F}}{\partial x}\right|_r \hat{e_1} + \left.\frac{\partial \tilde{F}}{\partial y}\right|_r \hat{e_2}. \tag{2.12}$$

Hence, based on the chain rules (2.9) and equation (2.10), the full gradient operator in the basis of Cartesian unit vector with respect to (x, y, r, t) can be obtained:

$$\nabla F = \nabla_h F + \frac{\partial F}{\partial z}\hat{e_3} \tag{2.13}$$

$$= \left[\tilde{\nabla}_h \tilde{F} - \frac{\partial \tilde{F}}{\partial r}\frac{\partial r}{\partial z}\tilde{\nabla}_h(\tilde{z})\right] + \frac{\partial \tilde{F}}{\partial r}\frac{\partial r}{\partial z}\hat{e_3} \tag{2.14}$$

Note that the reciprocal rule for partial derivatives $\frac{\partial r}{\partial z} = 1/\frac{\partial \tilde{z}}{\partial r}$ has been used to obtain the full gradient operator. The reciprocal rule is valid as long as both $\frac{\partial r}{\partial z}$ and $\frac{\partial \tilde{z}}{\partial r}$ does not vanish.

To summarise this section, the relation between $\nabla_h F$ and $\tilde{\nabla}_h \tilde{F}$ highlighted:

$$\nabla_h F = \tilde{\nabla}_h \tilde{F} - \frac{\partial \tilde{F}}{\partial r}\frac{\partial r}{\partial z}\tilde{\nabla}_h(\tilde{z}), \tag{2.15}$$

which will play crucial roles in the following sections when equations are transformed.

REMARK 1: In the following text, if a variable, a scalar function, or a vector function is marked with a tilde, it implicitly means that the transformed coordinates (x, y, r, t) is used to express it.

REMARK 2: All equations and their derivations in this chapter can be found in the lecture note by Adcroft. Hence the detailed derivation of some equations will be omitted in this text. Interested readers may refer to Adcroft et al.(2015).

2.2.3. Transformation of vector fields

Similarly for any vector field $\mathbf{F}(x, y, z, t) = F_1(x, y, z, t)\hat{e_1} + F_2(x, y, z, t)\hat{e_2} + F_3(x, y, z, t)\hat{e_3}$ in Cartesian coordinates, define the horizontal vector $\mathbf{F}_h = F_1\hat{e_1} + F_2\hat{e_2}$ and horizontal divergence $\nabla_h \cdot$ and $\tilde{\nabla}_h \cdot$

$$\nabla_h \cdot \mathbf{F}_h = \left.\frac{\partial F_1}{\partial x}\right|_z + \left.\frac{\partial F_2}{\partial y}\right|_z \tag{2.16}$$

$$\tilde{\nabla}_h \cdot \tilde{\mathbf{F}}_h = \left.\frac{\partial \tilde{F}_1}{\partial x}\right|_r + \left.\frac{\partial \tilde{F}_2}{\partial y}\right|_r \tag{2.17}$$

Again based on the chain rules (2.9) and equation (2.10) for each component of the vector field $\mathbf{F}$, it then follows the full divergence is given by

$$\nabla \cdot \mathbf{F} = \nabla_h \cdot \mathbf{F}_h + \frac{\partial F_3}{\partial z} \tag{2.18}$$

$$= \left[\tilde{\nabla}_h \cdot \tilde{\mathbf{F}}_h - \frac{\partial \tilde{\mathbf{F}}_h}{\partial r}\frac{\partial r}{\partial z} \cdot \tilde{\nabla}_h(\tilde{z})\right] + \frac{\partial \tilde{F}_3}{\partial r}\frac{\partial r}{\partial z} \tag{2.19}$$

The relation between $\nabla_h \cdot \mathbf{V}_h$ and $\tilde{\nabla}_h \cdot \tilde{\mathbf{V}}_h$ is also highlighted:

$$\nabla_h \cdot \mathbf{V}_h = \tilde{\nabla}_h \cdot \tilde{\mathbf{V}}_h - \frac{\partial \tilde{\mathbf{V}}_h}{\partial r}\frac{\partial r}{\partial z} \cdot \tilde{\nabla}_h(\tilde{z}), \tag{2.20}$$

which will also play significant role in the next section when the equations are transformed.

2.2.4. Transformation of equations

In the new coordinate system (x, y, r, t), the vertical velocity $\dot{r} = \frac{dr}{dt}$ and its relation with the vertical velocity $w = \frac{dz}{dt}$ in the physical coordinates has to be handled with care.

The relation between $\dot{r}$ and w

Consider the total derivative of coordinate function $r = r(x, y, z, t)$,

$$\frac{dr}{dt} = \frac{\partial r}{\partial t} + \frac{\partial r}{\partial x}\frac{dx}{dt} + \frac{\partial r}{\partial y}\frac{dy}{dt} + \frac{\partial r}{\partial z}\frac{dz}{dt} \tag{2.21}$$

Note that $u = \frac{dx}{dt}$, $v = \frac{dy}{dt}$ and $w = \frac{dz}{dt}$ are respectively the velocities in x, y and z directions. Hence a handy expression for $\dot{r} = \frac{dr}{dt}$ with respect to the physical coordinates (x, y, z, t) is obtained

$$\dot{r} = \frac{\partial r}{\partial t} + \mathbf{u}_h \cdot \nabla_h(r) + w\frac{\partial r}{\partial z} \tag{2.22}$$

On the other hand, consider the vertical position $\tilde{z}$ in the physical frame of reference as a function of the transformed coordinates $\tilde{z} = \tilde{z}(x, y, r, t)$ via equation (2.8). The total derivative of $\tilde{z}$, which is the vertical velocity $\tilde{w} = \frac{d\tilde{z}}{dt}$, is hence given by

$$\tilde{w} = \left.\frac{\partial \tilde{z}}{\partial t}\right|_r + \tilde{\mathbf{u}}_h \cdot \tilde{\nabla}_h(\tilde{z}) + \dot{r}\frac{\partial \tilde{z}}{\partial r}, \tag{2.23}$$

which relates the vertical velocity $\tilde{w}$ from the viewpoint of the transformed coordinates.

Total Derivative in the Transformed Coordinates

The total derivative of a scalar field $\tilde{F} = \tilde{F}(x, y, r, t)$ is given by:

$$\frac{D\tilde{F}}{dt} = \frac{\partial \tilde{F}}{\partial t}\bigg|_r + \tilde{\mathbf{u}}_h \cdot \tilde{\nabla}_h(\tilde{F}) + \dot{r}\frac{\partial \tilde{F}}{\partial r}. \tag{2.24}$$

An important application to the equation (2.24) is to compute the quantity $\frac{\partial \tilde{w}}{\partial r}$. Consider the scalar field for the vertical velocity $\tilde{w} = \tilde{w}(x, y, r, t)$ with respect to the transformed coordinates (x, y, r, t). The partial derivative $\frac{\partial \tilde{w}}{\partial r}$ can be shown to be:

$$\frac{\partial \tilde{w}}{\partial r} = \frac{\partial}{\partial r}\left(\frac{\partial \tilde{z}}{\partial t}\bigg|_r + \tilde{\mathbf{u}}_h \cdot \tilde{\nabla}_h(\tilde{z}) + \dot{r}\frac{\partial \tilde{z}}{\partial r}\right) \tag{2.25}$$

$$= \frac{D}{dt}\left(\frac{\partial \tilde{z}}{\partial r}\right) + \frac{\partial \tilde{\mathbf{u}}_h}{\partial r} \cdot \tilde{\nabla}_h(\tilde{z}) + \frac{\partial \dot{r}}{\partial r}\frac{\partial \tilde{z}}{\partial r} \tag{2.26}$$

Based on the expression for $\frac{\partial \tilde{w}}{\partial r}$, after some algebraic manipulations, the divergence of velocity field $\mathbf{u}$ in the transformed coordinates (x, y, r, t) can be concisely given by:

$$\nabla \cdot \mathbf{u} = \tilde{\nabla}_h \cdot \tilde{\mathbf{u}}_h + \frac{\partial \dot{r}}{\partial r} + \frac{D}{dt}\left[\ln(\frac{\partial \tilde{z}}{\partial r})\right] \tag{2.27}$$

The detailed derivation to equation (2.27) is given below. Readers who are not interested may skip to the next section. Recall that the divergence operator for a velocity field is given by equation (2.19). Take the vector field $\mathbf{F}$ to be the velocity field $\mathbf{u} = u\hat{e_1} + v\hat{e_2} + w\hat{e_3}$ in equation (2.19):

$$\nabla \cdot \mathbf{u} = \left[\tilde{\nabla}_h \cdot \tilde{\mathbf{u}}_h - \frac{\partial \tilde{\mathbf{u}}_h}{\partial r}\frac{\partial r}{\partial z} \cdot \tilde{\nabla}_h(\tilde{z})\right] + \frac{\partial \tilde{w}}{\partial r}\frac{\partial r}{\partial z}$$

Consider the quantity $\frac{\partial \tilde{w}}{\partial r}\frac{\partial r}{\partial z}$, replacing the expression of $\frac{\partial \tilde{w}}{\partial r}$ using equation (2.26) gives

$$\frac{\partial \tilde{w}}{\partial r}\frac{\partial r}{\partial z} = \left[\frac{D}{dt}\left(\frac{\partial \tilde{z}}{\partial r}\right) + \frac{\partial \tilde{\mathbf{u}}_h}{\partial r} \cdot \tilde{\nabla}_h(\tilde{z}) + \frac{\partial \dot{r}}{\partial r}\frac{\partial \tilde{z}}{\partial r}\right]\frac{\partial r}{\partial z}$$

Note that by the reciprocal rule, $\frac{\partial \tilde{z}}{\partial r}\frac{\partial r}{\partial z} = 1$. Hence the quantity $\frac{\partial \tilde{w}}{\partial r}\frac{\partial r}{\partial z}$ is simply given by

$$\frac{\partial \tilde{w}}{\partial r}\frac{\partial r}{\partial z} = \frac{\partial \dot{r}}{\partial r} + \frac{\left[\frac{D}{dt}\left(\frac{\partial \tilde{z}}{\partial r}\right)\right]}{\frac{\partial \tilde{z}}{\partial r}} + \frac{\partial \tilde{\mathbf{u}}_h}{\partial r}\frac{\partial r}{\partial z} \cdot \tilde{\nabla}_h(\tilde{z})$$

$$= \frac{\partial \dot{r}}{\partial r} + \frac{D}{dt}\left[\ln\left(\frac{\partial \tilde{z}}{\partial r}\right)\right] + \frac{\partial \tilde{\mathbf{u}}_h}{\partial r}\frac{\partial r}{\partial z} \cdot \tilde{\nabla}_h(\tilde{z})$$

Therefore, the term $\frac{\partial \tilde{\mathbf{u}}_h}{\partial r}\frac{\partial r}{\partial z} \cdot \tilde{\nabla}_h(\tilde{z})$ in the divergence of velocity $\nabla \cdot \mathbf{u}$ cancels out. Hence the divergence of velocity in the transformed coordinates (x, y, r, t) is simply given by

$$\nabla \cdot \mathbf{u} = \tilde{\nabla}_h \cdot \tilde{\mathbf{u}}_h + \frac{\partial \dot{r}}{\partial r} + \frac{D}{dt}\left[\ln\left(\frac{\partial \tilde{z}}{\partial r}\right)\right],$$

which completes the proof.

Continuity Equation

It follows that the continuity equation in (x, y, r, t) coordinates becomes:

$$\frac{D\tilde{\rho}}{dt} + \tilde{\rho}\left[\tilde{\nabla}_h \cdot \tilde{\mathbf{u}}_h + \frac{\partial \dot{r}}{\partial r} + \frac{D}{dt}\left(\ln(\frac{\partial \tilde{z}}{\partial r})\right)\right] = 0 \tag{2.28}$$

Momentum Equation

The transformation of momentum equation, is unfortunately more complicated. Here the transformed momentum equation in a rotating coordinate frame will be derived. First consider the horizontal components of the momentum equations:

$$\rho[\frac{D\mathbf{u}_h}{dt} + \left(2\Omega \times \mathbf{u}\right)_h] = -\nabla_h p - \rho\nabla_h(\Phi + \Phi_c) + \mathbf{F}_h \tag{2.29}$$

The equation (2.15) suggests that in the transformed coordinates (x, y, r, t):

$$\nabla_h p = \tilde{\nabla}_h \tilde{p} - \frac{\partial \tilde{p}}{\partial r}\frac{\partial r}{\partial z}\tilde{\nabla}_h(\tilde{z}), \tag{2.30}$$

whereas equation (2.20) suggests that, by defining the sum of potential Φ_s by $\Phi_s = \Phi + \Phi_c$

$$\nabla_h \Phi_s = \tilde{\nabla}_h \tilde{\Phi}_s - \frac{\partial \tilde{\Phi}_s}{\partial r}\frac{\partial r}{\partial z}\tilde{\nabla}_h(\tilde{z}) \tag{2.31}$$

Hence the horizontal components of the momentum equation is obtained:

$$\tilde{\rho}\left[\frac{D\tilde{\mathbf{u}}_h}{dt} + \left(2\tilde{\Omega} \times \tilde{\mathbf{u}}\right)_h\right] = -\tilde{\nabla}_h \tilde{p} - \tilde{\rho}\tilde{\nabla}_h \tilde{\Phi}_s + \tilde{\mathbf{F}}_h + \left[\frac{\partial \tilde{p}}{\partial r} + \tilde{\rho}\frac{\partial(\tilde{\Phi}_s)}{\partial r}\right]\frac{\partial r}{\partial z}\tilde{\nabla}_h(\tilde{z}) \tag{2.32}$$

The derivation of the vertical momentum equation containing $\frac{d^2 r}{dt^2}$ is cumbersome. In the shallow water approximation of the fluid, the vertical momentum equation is not needed. Hence the exact form of vertical momentum equation will not be presented here.

3

Adapted Shallow Water Model

In this chapter, the adapted model will be presented. A adapted wave equation for ocean surface wave defined on geopotential height will be presented. The inertial frame without non-conservative force will be investigated first.

3.1. Basic Definitions

Define Mean-Sea Level Set Msl: It contains a the points (x, y, z) such that

$$\Phi(x, y, z) = \Phi_0 \tag{3.1}$$

where Φ_0 is an empirically found value. In other words, $Msl = \{(x, y, z) : \Phi(x, y, z) = \Phi_0\}$. Given (x, y), there is unique $z_0 = z_0(x, y)$ such that (x, y, z_0) belongs to Msl. The work done required to transport a unit mass from any point to MSl to any arbitrary point (x, y, z) is known as the potential difference between (x, y, z) and MSl, and is given by:

$$\Psi(x, y, z) = -\int_{(\bar{x},\bar{y},\bar{z})}^{(x,y,z)} -\nabla\Phi \cdot d\vec{l} \tag{3.2}$$

where $(\bar{x}, \bar{y}, \bar{z})$ is any point on Msl. Since Φ is a conservative field, the above integral is path independent. Hence an equivalent definition can be given by:

$$\Psi(x, y, z) = \int_{z_0(x,y)}^{z} \frac{\partial\Phi}{\partial\check{z}}(x, y, \check{z})d\check{z} \tag{3.3}$$

which takes a straightly vertical path integral, or,

$$\Psi(x, y, z) = \Phi(x, y, z) - \Phi_0 \tag{3.4}$$

which is essentially the potential difference.

Define the Geopotential height Z as following:

$$Z = Z(x, y, z) = \frac{\Psi(x, y, z)}{g_0} \tag{3.5}$$

where g_0 is a constant reference gravity. Note that Ψ takes into account only the geopotential induced by masses which are time-independent. The geopotential induced by ocean water is neglected. Z has the same physical dimension with physical height z. Given any (x, y), the mapping from Z to z is monotonic and one-to-one.

The geopotential height Z will serve as the variable r in the chapter 2.2 to transform the equations.

3.2. Properties of the Geopotential Height

In this section, several properties of the Geopotential Height transformation will be discussed.

3.2.1. Vertical Gradient of the Geopotential Height

A very nice property of the Geopotential Height Z comes from the fact that

$$\tilde{\Phi} = g_0 Z + \Phi_0, \tag{3.6}$$

by considering equations (3.4) and (3.5). A tilde is added to to Φ because the geopotential Φ is now read in the transformed coordinates (x, y, Z, t). Hence a very handy vertical gradient is given by:

$$\frac{\partial \tilde{\Phi}}{\partial Z} = g_0 \tag{3.7}$$

which is the reference gravity independent of any spatial or temporal coordinates.

3.2.2. Z-transformation

Assume that the gravity $\vec{g}$ is *weakly non-uniform*: $\vec{g}$ consists of a uniform component $-g_0\hat{e_3}$ and a perturbing non-linear conservative component $\vec{g'}(x, y, z) = -\nabla\Phi'(x, y, z)$, such that $\|\vec{g'}\| \ll g_0$. that is:

$$\vec{g}(x, y, z) = -g_0\hat{e_3} + \vec{g'}(x, y, z) \tag{3.8}$$

It follows that, fixing (x, y), the potential difference Ψ between the point (x, y, z) and the mean sea level is given by

$$\begin{aligned}\Psi(x, y, z) &= -\int_{z_0(x,y)}^{z} [-g_0 + \vec{g'}(x, y, z)]ds \\ &= g_0(z - z_0) + \int_{z_0(x,y)}^{z} \nabla\Phi'(x, y, s)ds\end{aligned}$$

$$\Psi(x, y, z) = g_0(z - z_0(x, y)) + [\Phi'(x, y, z) - \Phi'(x, y, z_0(x, y))] \tag{3.9}$$

where $z = z_0(x, y)$ is the mean sea level at horizontal location (x, y). The term $\Phi'(x, y, z)$ can be interpreted as the disturbing geopotential Φ' due to local topographical features.

It follows that the geopotential height Z becomes:

$$\begin{aligned}Z &= \frac{\Psi}{g_0} \\ &= z + \frac{\Phi'(x, y, z)}{g_0} - \left(z_0(x, y) + \frac{\Phi'(x, y, z_0)}{g_0}\right)\end{aligned}$$

Denote $Z_0(x, y) = z_0(x, y) + \frac{\Phi'(x,y,z_0)}{g_0}$, which is independent of z, the transformation from (x, y, z) to (x, y, Z) can be given by

$$Z = z + \frac{\Phi'(x, y, z)}{g_0} - Z_0(x, y) \tag{3.10}$$

Equation (3.10) will be called as Z**-transformation** in the remaining text.

Now the partial derivative of Z with respect to z (keeping x, y constant) is considered, note that $Z_0(x, y)$ is independent of z. Denote $\frac{\partial\Phi'}{\partial z}$ by g'_z.

$$\begin{aligned}\frac{\partial Z}{\partial z} &= 1 + \frac{1}{g_0}\frac{\partial\Phi'}{\partial z} \\ &= 1 + \frac{g'_z}{g_0}\end{aligned}$$

The partial derivative of Z with respect to z

$$\frac{\partial Z}{\partial z} = 1 + \frac{g'_z}{g_0} \tag{3.11}$$

will be the most crucial ingredient in the later derivation of equations and analysis. It is noted that, since $Z = Z(x, y, z)$ is a smooth function, when $\frac{\partial Z}{\partial z} \neq 0$, the reciprocal rule of partial derivative gives,

$$\frac{\partial \tilde{z}}{\partial Z} = \frac{1}{\frac{\partial Z}{\partial z}} = \frac{1}{1 + \frac{g'_z}{g_0}} \tag{3.12}$$

is also valid. The criterion for which $\frac{\partial Z}{\partial z} \neq 0$ will be discussed in the next section.

ATTENTION: Instead of defining $g'_z = -\frac{\partial \Phi'}{\partial z}$, which is the typical way to define force from for conservative potential, here the definition is given by $-g'_z = -\frac{\partial \Phi'}{\partial z}$. The motivation here is that by defining g'_z in this way, the effective gravity $\vec{g}$ in z direction is given by $-(g_0 + g'_z)$, so that when g'_z is positive, the magnitude of gravity in z-direction is $g_0 + g'_z > g_0$.

3.2.3. Inverse Z-transformation

In this section, further analytic properties of the Z-transformation will be examined. In particular, the existence of the inverse transformation will be discussed.

Recall that the Z-transformation is given by equation (3.10)

$$Z = z + \frac{\Phi'(x, y, z)}{g_0} - Z_0(x, y)$$

It is a natural question to ask if the inverse transformation exists. Consider the complete coordinate transformation problem $(x, y, z) \to (x_1, x_2, x_3)$:

$$\begin{aligned} x_1 &= x \\ x_2 &= y \\ x_3 &= Z(x, y, z) \end{aligned}$$

Note that $Z = Z(x, y, z)$ is considered as a coordinate function $Z : \mathcal{R}^3 \to \mathcal{R}$ here. Consider the vector function $\vec{F} : \mathcal{R}^6 \to \mathcal{R}^3$

$$\vec{F}(x_1, x_2, x_3; x, y, z) = \begin{pmatrix} x_1 - x \\ x_2 - y \\ x_3 - Z(x, y, z) \end{pmatrix} \tag{3.13}$$

The coordinate transformation is equivalent to looking for solution of $\vec{F} = \vec{0}$.

The Jacobian matrix of $\vec{F}$ denoted as $J(\vec{F})$ is thus given by

$$J(\vec{F})(x_1, x_2, x_3; x, y, z) = \begin{pmatrix} 1 & 0 & 0 & -1 & 0 & 0 \\ 0 & 1 & 0 & 0 & -1 & 0 \\ 0 & 0 & 1 & -\frac{\partial Z}{\partial x} & -\frac{\partial Z}{\partial y} & -\frac{\partial Z}{\partial z} \end{pmatrix}$$

According to the implicit function theorem, the inverse function $z = Z^{-1}(x_1, x_2, x_3)$ uniquely exists if the columns corresponding to the partial derivatives with respect to the original coordinates (in this case (x, y, z), which corresponds to the last three columns) form an invertible matrix $\bar{J}$, that is

$$\bar{J} = J(\vec{F})(x, y, z) = \begin{pmatrix} -1 & 0 & 0 \\ 0 & -1 & 0 \\ -\frac{\partial Z}{\partial x} & -\frac{\partial Z}{\partial y} & -\frac{\partial Z}{\partial z} \end{pmatrix}$$

is invertible. Hence it suffices to consider the determinant of $\bar{J}$, which is $\det \bar{J} \neq 0$. Note that $\det \bar{J} = -\frac{\partial Z}{\partial z}$, and from equation (3.11), $\frac{\partial Z}{\partial z} = 1 + \frac{g'_z}{g_0}$, hence $\det \bar{J} \neq 0$ implies

$$1 + \frac{g'_z}{g_0} \neq 0 \iff g'_z \neq -g_0 \tag{3.14}$$

In other words, in the physical sense this condition (3.14) suggests that when the excess gravity g'_z does not cancel out the background uniform gravity g_0, the inverse coordinate transformation $\tilde{z} = Z^-1$ which maps from (x, y, Z) to physical coordinates (x, y, z) is well-defined.

In practice, for weakly non-uniform gravitational field such that $\|g_z'\| \ll g_0$, the condition (3.14) is always satisfied. Thus the inverse transformation $\tilde{z} = \tilde{z}(x, y, Z)$ is practically always well-defined. This is also the condition where the reciprocal rule $\frac{\partial Z}{\partial z} = \frac{1}{\frac{\partial \tilde{z}}{\partial Z}}$ holds, and justifies the validity of (3.12) discussed in the previous section.

3.3. Definition of Water Depth

3.3.1. Classical Water Depth

Suppose at time t, with respect to the physical coordinates (x, y, z), the surface elevation $S(x, y, t)$ of the fluid is described by the level set $z = S(x, y, t)$. Meanwhile the bottom boundary $S_B(x, y)$ of the fluid, which is time-independent, is described by the level set $z = S_B$.

The water depth $D(x, y, t)$ at location (x, y) at time t is given by the difference between the surface elevation S and bottom elevation S_B, that is,

$$D(x, y, t) = S(x, y, t) - S_B(x, y) \tag{3.15}$$

It is natural to give an analogous definition to water depth in the transformed Z-coordinates, which will be discussed in the next section.

3.3.2. Adapted Water Depth

Recall the coordinate transformation (3.10):

$$Z = z + \frac{\Phi'(x, y, z)}{g_0} - Z_0(x, y)$$

Suppose the surface elevation $\tilde{S}$ in the transformed coordinates is given by the level set $Z = \tilde{S}(x, y, t)$. $\tilde{S}$ can thus be computed by putting $z = S$ into the transformation formula:

$$\tilde{S}(x, y, t) = S(x, y, t) + \frac{\Phi'(x, y, S(x, y, t))}{g_0} - Z_0(x, y) \tag{3.16}$$

Similarly the bottom boundary $z = S_B$ can be mapped into $Z = \tilde{S}_B$, which is given by

$$\tilde{S}_B(x, y) = +\frac{\Phi'(x, y, S_B(x, y))}{g_0} - Z_0(x, y) \tag{3.17}$$

Define the water depth $\tilde{D}(x, y, t)$ in Z-coordinates by the difference between $\tilde{S}$ and $\tilde{S}_B$:

$$\tilde{D}(x, y, t) = \tilde{S}(x, y, t) - \tilde{S}_B(x, y) \tag{3.18}$$

Using the equations (3.16) and (3.17), and defining $\Delta\Phi'(x, y, t) = \Phi'(x, y, S) - \Phi'(x, y, S_B)$, the relation between D and $\tilde{D}$ becomes clear:

$$\tilde{D}(x, y, t) = D(x, y, t) + \frac{1}{g_0}\Delta\Phi'(x, y, t). \tag{3.19}$$

Note that $\Delta\Phi'(x, y, t)$ physically refers to the potential difference between the surface elevation and the bottom boundary solely due to the non-uniform component of the gravity.

3.3.3. A First-order Approximation to the Adapted Water Depth

In this section a first-order approximation to equation (3.19) will be obtained. The result of this section will be applied in later sections when the adapted shallow water model is derived.

Recall that the definition of $\Delta\Phi'(x, y, t)$ is given by:

$$\Delta\Phi'(x, y, t) = \Phi'(x, y, S) - \Phi'(x, y, S_B)$$

Performing Taylor-series expansion of $\Phi'(x, y, S)$ around the mean-sea level (x, y, z_0) gives

$$\Phi'(x, y, S) = \Phi'(x, y, z_0) + \left[\frac{\partial \Phi'}{\partial z}\right]_{@z_0(x,y)} (S - z_0) + h.o.t.$$

where the subscript $@z_0(x,y)$ refers to the evaluation of quantities in the square bracket $[\,*\,]$ at the mean-sea level $(x,y,z_0(x,y))$, and $h.o.t.$ refers to the higher-order terms in the Taylor-series expansion.

Similarly, the Taylor-expansion of $\Phi'(x,y,S_B)$ can be performed around $(x,y,z_0(x,y))$ also, a similar expression can be obtained

$$\Phi'(x,y,S_B) = \Phi'(x,y,z_0) + \left[\frac{\partial \Phi'}{\partial z}\right]_{@z_0(x,y)} (S_B - z_0) + h.o.t.$$

For a given certain (x,y) at certain time t, $\Delta\Phi'(x,y,t)$ can thus be approximated by

$$\begin{aligned}\Delta\Phi'(x,y,t) &= \left[\frac{\partial \Phi'}{\partial z}\right]_{@z_0(x,y)} (S - S_B) + h.o.t. \\ &= \left[g'_z\right]_{@z_0(x,y)} D + h.o.t.\end{aligned}$$

Note that the Taylor-expansion could have been performed at any vertical coordinate z within or in the neighbourhood of the interval of $[S_B, S]$ to yield an analogous result. The mean-sea level $z = z_0(x,y)$ is chosen because empirical measurement data of g'_z is usually available at this level.

If the higher-order terms are so small such that they can be neglected, then the relation between D and $\tilde{D}$ given by equation (3.19) can be simplified into

$$\begin{aligned}\tilde{D}(x,y,t) &\approx D(x,y,t) + \frac{\left[g'_z\right]_{@z_0(x,y)}}{g_0} D(x,y,t) \\ &\approx D(x,y,t)\left[\left(1 + \frac{g'_z}{g_0}\right)\right]_{@z_0(x,y)}\end{aligned}$$

Note that according to equation (3.11), $1 + \frac{g'_z}{g_0} = \frac{\partial Z}{\partial z}$, hence

$$\tilde{D}(x,y,t) \approx D(x,y,t)\left[\frac{\partial Z}{\partial z}\right]_{@z_0(x,y)}, \tag{3.20}$$

which is a handy expression for analysis in later sections.

3.4. Transformation of equations

In the remaining part of this chapter, the horizontal gradient ∇_h and $\tilde{\nabla}_h$ are understood to be $\hat{e_1}\frac{\partial}{\partial x}\big|_z + \hat{e_2}\frac{\partial}{\partial y}\big|_z$ and $\hat{e_1}\frac{\partial}{\partial x}\big|_Z + \hat{e_2}\frac{\partial}{\partial y}\big|_Z$ respectively.

To transform the equations from (x,y,z,t) to (x,y,Z,t), take $r = Z$ in equation (2.28) and equation (2.32).

Adapted Continuity Equation:

$$\frac{D\tilde{\rho}}{dt} + \tilde{\rho}\left[\tilde{\nabla}_h \cdot \tilde{\mathbf{u}}_h + \frac{\partial \dot{Z}}{\partial Z} + \frac{D}{dt}\left(\ln\left(\frac{\partial \tilde{z}}{\partial Z}\right)\right)\right] = 0 \tag{3.21}$$

Adapted Horizontal Momentum Equation:

$$\tilde{\rho}\left[\frac{D\tilde{\mathbf{u}}_h}{dt}\right] = -\tilde{\nabla}_h\tilde{p} - \tilde{\rho}\tilde{\nabla}_h\tilde{\Phi} + \left(\frac{\partial \tilde{p}}{\partial Z} + \tilde{\rho}\frac{\partial \tilde{\Phi}}{\partial Z}\right)\frac{\partial Z}{\partial z}\tilde{\nabla}_h(\tilde{z}) \tag{3.22}$$

These equations are not easy to deal with. Hence it is necessary to further simplify them before analytically studying the properties of their solutions, which will be presented in 3.5.

Another highlight is the extra terms $\frac{D}{dt}\left(\ln(\frac{\partial \tilde{z}}{\partial Z})\right)$ in the continuity equation (3.21) and $\left(\frac{\partial \tilde{p}}{\partial Z} + \tilde{\rho}\frac{\partial \tilde{\Phi}}{\partial Z}\right)\frac{\partial Z}{\partial z}\tilde{\nabla}_h(\tilde{z})$ in the momentum equation (3.22), in contrast to the standard continuity and momentum equation in the standard Cartesian coordinates. The properties of these two extra terms will be discussed in the two sections 3.6 and 3.7.

3.5. Additional simplifications

3.5.1. Incompressiblity

Density of water on the ocean surface does change due to temperature and salinity variation. However to simplify the analysis, such density variations are omitted. In other words, it is assumed that $\tilde{\rho}(x,y,Z) = \rho_0$, where ρ_0 is a constant. In the later text, the subscript in ρ_0 will be skipped so that $\tilde{\rho}(x,y,Z) = \rho$.

It follows that the continuity equation (3.21) becomes:

$$\tilde{\nabla}_h \cdot \tilde{\mathbf{u}}_h + \frac{\partial \dot{Z}}{\partial Z} + \frac{D}{dt}\left(\ln\left(\frac{\partial \tilde{z}}{\partial Z}\right)\right) = 0 \tag{3.23}$$

3.5.2. Horizontal Gradient of Geopotential

In the (horizontal) momentum equations (3.22) the horizontal gradient of geopotential with respect to Z, i.e. $\tilde{\nabla}_h\tilde{\Phi}$ is involved. However, recalling that $Z = \frac{\Phi-\Phi_0}{g_0}$, it is noticed that keeping Z constant is equivalent to keeping Φ constant. Hence the horizontal gradient of geopotential $\tilde{\nabla}_h\tilde{\Phi}$ simply vanishes.

$$\tilde{\nabla}_h\tilde{\Phi} = \left.\frac{\partial\tilde{\Phi}}{\partial x}\right|_Z \hat{e_1} + \left.\frac{\partial\tilde{\Phi}}{\partial y}\right|_Z \hat{e_2} = \vec{0} \tag{3.24}$$

Hence under the Z-transformation, the momentum equation (3.22) becomes

$$\rho\left[\frac{D\tilde{\mathbf{u}}_h}{dt}\right] = -\tilde{\nabla}_h\tilde{p} + \left(\frac{\partial\tilde{p}}{\partial Z} + \rho\frac{\partial\tilde{\Phi}}{\partial Z}\right)\frac{\partial Z}{\partial z}\tilde{\nabla}_h(\tilde{z}) \tag{3.25}$$

Note that the density ρ is assumed to be a constant followed by the discussion of section 3.5.1 and there is no difference between the density ρ in the physical coordinates (x,y,z,t) and transformed coordinates (x,y,Z,t).

3.5.3. Hydrostatic approximation

Hydrostatic Balance

For large scale oceanic flows, the horizontal length scale, denoted as L_h, is usually much greater than the vertical length scale which is denoted by L_v. The *shallowness* of an oceanic flow is known as the small aspect ratio:

$$\delta = \frac{L_v}{L_h} \ll 1 \tag{3.26}$$

In section 2.8 of Pedlosky 1979, it is justified that for a *shallow* flow with $\delta \ll 1$, the vertical pressure gradient $\frac{\partial p}{\partial z}$ can be approximated by the gradient of gravitational force $\rho\frac{\partial\Phi}{\partial z}$. An analogous result will be derived.

Consider the hydrostatic pressure $p_s = p_s(x,y,z(x,y,Z),t) = \tilde{p}_s(x,y,Z,t)$. The pressure gradient in hydrostatic condition is obtained by setting velocity $\vec{u} = \vec{0}$ in the momentum equation. Hence the full momentum equation equation(2.4) becomes:

$$\nabla p_s = -\rho\nabla\Phi$$

Since it is assumed that the density ρ is constant everywhere, ρ can be included in the gradient operator. Hence it follows that:

$$\nabla p_s = -\nabla(\rho\Phi) \tag{3.27}$$

$$\Rightarrow p_s = -\rho\Phi + p_0 \tag{3.28}$$

where the reference pressure p_0 is an arbitrary constant. Note that the same argument can be applied in the transformed coordinates (x,y,Z,t) and gives:

$$\tilde{p}_s = -\rho\tilde{\Phi} + \tilde{p}_0, \tag{3.29}$$

where $\tilde{p}_0$ is also an arbitrary constant.

Consider the gradient operator ∇ in Cartesian coordinate, along the z-direction, it is noted that:

$$\frac{\partial p_s}{\partial z} = -\rho \frac{\partial \Phi}{\partial z} \tag{3.30}$$

Multiplying both sides with $\frac{\partial \tilde{z}}{\partial Z}$ leads to:

$$\frac{\partial p_s}{\partial z}\frac{\partial \tilde{z}}{\partial Z} = -\rho \frac{\partial \Phi}{\partial z}\frac{\partial \tilde{z}}{\partial Z} \tag{3.31}$$

By the chain rule, the equalities

$$\frac{\partial \tilde{p}_s}{\partial Z} = \frac{\partial p_s}{\partial z}\frac{\partial \tilde{z}}{\partial Z} \tag{3.32}$$

$$\frac{\partial \tilde{\Phi}}{\partial Z} = \frac{\partial \Phi}{\partial z}\frac{\partial \tilde{z}}{\partial Z} \tag{3.33}$$

are justified. Thus the analogy of the hydrostatic pressure gradient in coordinates (x, y, Z, t) is established:

$$\frac{\partial \tilde{p}_s}{\partial Z} = -\rho \frac{\partial \tilde{\Phi}}{\partial Z} = -\rho g_0 \tag{3.34}$$

The last equality follows from equation (3.6)). It is worthwhile to point out that, unlike the classical case with uniformly downwards gravity $\vec{g} = -g_0 \hat{e_3}$, $\frac{\partial \tilde{p}_s}{\partial x}\big|_z \neq 0$ and $\frac{\partial \tilde{p}_s}{\partial y}\big|_z \neq 0$. It is $\frac{\partial \tilde{p}_s}{\partial x}\big|_Z$ and $\frac{\partial \tilde{p}_s}{\partial y}\big|_Z$ that are equal to zero. The proof for $\frac{\partial p_s}{\partial x}\big|_Z = 0$ is shown:

$$\begin{aligned}
\left.\frac{\partial \tilde{p}_s}{\partial x}\right|_Z &= \left.\frac{\partial(-\rho\tilde{\Phi} + \tilde{p}_0)}{\partial x}\right|_Z \text{ (c.f. equation (3.29))} \\
&= -\rho \left.\frac{\partial(g_0 Z + \Phi_0)}{\partial x}\right|_Z + \left.\frac{\partial p_0}{\partial x}\right|_Z \text{ (c.f. equation (3.6))} \\
&= -\rho g_0 \left.\frac{\partial Z}{\partial x}\right|_Z - \rho \left.\frac{\partial \Phi_0}{\partial x}\right|_Z + \left.\frac{\partial p_0}{\partial x}\right|_Z
\end{aligned}$$

Recall that both the reference pressure p_0 and the reference geopotential Φ_0 are constants that are independent of any coordinates. The partial derivative $\frac{\partial Z}{\partial x}\big|_Z$ vanishes because Z is kept invariant. Hence, every term on the right-hand side vanishes and yields:

$$\left.\frac{\partial \tilde{p}_s}{\partial x}\right|_Z = 0$$

The proof for $\frac{\partial \tilde{p}_s}{\partial y}\big|_Z = 0$ can be obtained in a similar fashion. Therefore, the horizontal gradient of hydrostatic pressure $\tilde{p}_s$ becomes:

$$\tilde{\nabla}_h \tilde{p}_s = \vec{0} \tag{3.35}$$

Hydrostatic Approximation

Assume that the pressure $\tilde{p} = \tilde{p}(x, y, Z, t)$ can be decomposed into a hydrostatic part $\tilde{p}_s$ and dynamic part $\tilde{p}_d$, so that

$$\tilde{p}(x, y, Z, t) = \tilde{p}_s(x, y, Z) + \tilde{p}_d(x, y, Z, t) \tag{3.36}$$

The validity of this assumption need to be justified. In particular, an argument which suggests that the order of magnitude of dynamic pressure $\tilde{p}_d$ is much less than that of hydrostatic pressure $\tilde{p}_s$ should be provided. This will be done through the scale analysis discussed in section 3.9.

The vertical gradient of the hydrostatic pressure $\tilde{p}_s$ can be determined by equation (3.28), which suggests

$$\frac{\partial \tilde{p}_s}{\partial Z} = -\rho \frac{\partial \tilde{\Phi}}{\partial Z}$$

so that the vertical gradient of the total pressure $\tilde{p}$ can be expressed by

$$\frac{\partial \tilde{p}}{\partial Z} = \frac{\partial \tilde{p}_s}{\partial Z} + \frac{\partial \tilde{p}_d}{\partial Z} = -\rho \frac{\partial \tilde{\Phi}}{\partial Z} + \frac{\partial \tilde{p}_d}{\partial Z} \tag{3.37}$$

The scale analysis in section 3.9 suggests that the term $\frac{\partial \tilde{p}_d}{\partial Z}\frac{\partial Z}{\partial z}$ is of order of magnitude $\mathcal{O}(\delta \cdot \rho \frac{D\tilde{\mathbf{u}}_h}{dt})$. Therefore, multiplying all quantities in equation (3.37) with $\frac{\partial Z}{\partial z}$ gives

$$\begin{aligned}\frac{\partial \tilde{p}}{\partial Z}\frac{\partial Z}{\partial z} &= -\rho \frac{\partial \tilde{\Phi}}{\partial Z}\frac{\partial Z}{\partial z} + \frac{\partial \tilde{p}_d}{\partial Z}\frac{\partial Z}{\partial z} \\ &= -\rho \frac{\partial \tilde{\Phi}}{\partial Z}\frac{\partial Z}{\partial z} + \mathcal{O}(\delta \cdot \rho \frac{D\tilde{\mathbf{u}}_h}{dt})\end{aligned}$$

In the shallow water where $\delta \ll 1$, the $\mathcal{O}(\delta \cdot \rho \frac{D\tilde{\mathbf{u}}_h}{dt})$ term is typically much smaller than other terms in the above equation. Hence the term $\mathcal{O}(\delta \cdot \rho \frac{D\tilde{\mathbf{u}}_h}{dt})$ is neglected and give rises to the *hydrostatic approximation* in the transformed vertical coordinate Z:

$$\frac{\partial \tilde{p}}{\partial Z}\frac{\partial Z}{\partial z} \approx -\rho \frac{\partial \tilde{\Phi}}{\partial Z}\frac{\partial Z}{\partial z} \tag{3.38}$$

or equivalently, dividing both sides with $\frac{\partial Z}{\partial z}$

$$\frac{\partial \tilde{p}}{\partial Z} \approx -\rho \frac{\partial \tilde{\Phi}}{\partial Z} \tag{3.39}$$

3.6. The Adapted Continuity Equation

3.6.1. An Exact Adapted Continuity Equation

In this section the adapted continuity equation (3.21) will be examined and simplified under the setting of Z-transformation, where the gravity field is weakly non-uniform.

In the incompressible continuity equation (3.23):

$$\tilde{\nabla}_h \cdot \tilde{\mathbf{u}}_h + \frac{\partial \dot{Z}}{\partial Z} + \frac{D}{dt}\left(\ln\left(\frac{\partial \tilde{z}}{\partial Z}\right)\right) = 0,$$

where the last term can be simplified due to the fact that it is time-independent. The material derivative $\frac{D}{dt}$ therefore yields:

$$\begin{aligned}\frac{D}{dt}\left(\ln\left(\frac{\partial \tilde{z}}{\partial Z}\right)\right) &= \left(\tilde{u}\frac{\partial}{\partial x}\bigg|_Z + \tilde{v}\frac{\partial}{\partial y}\bigg|_Z + \dot{Z}\frac{\partial}{\partial Z}\right)\left(\ln\left(\frac{\partial \tilde{z}}{\partial Z}\right)\right) \\ &= \left(\tilde{\mathbf{u}}_h \cdot \tilde{\nabla}_h + \dot{Z}\frac{\partial}{\partial Z}\right)\left[\ln\left(\frac{\partial \tilde{z}}{\partial Z}\right)\right] \\ &= \frac{1}{\frac{\partial \tilde{z}}{\partial Z}}\left(\tilde{\mathbf{u}}_h \cdot \tilde{\nabla}_h + \dot{Z}\frac{\partial}{\partial Z}\right)\left[\frac{\partial \tilde{z}}{\partial Z}\right]\end{aligned}$$

Plugging this into the incompressible continuity equation (3.23) gives:

$$\tilde{\nabla}_h \cdot \tilde{\mathbf{u}}_h + \frac{\partial \dot{Z}}{\partial Z} + \frac{1}{\frac{\partial \tilde{z}}{\partial Z}}\left(\tilde{\mathbf{u}}_h \cdot \tilde{\nabla}_h + \dot{Z}\frac{\partial}{\partial Z}\right)\left[\frac{\partial \tilde{z}}{\partial Z}\right] = 0$$

Multiplying both sides with $\frac{\partial \tilde{z}}{\partial Z}$ and applying the product rule of differentiation rule gives a 'divergence'-free form equation:

$$\tilde{\nabla}_h \cdot \left(\frac{\partial \tilde{z}}{\partial Z}\tilde{\mathbf{u}}_h\right) + \frac{\partial}{\partial Z}\left(\frac{\partial \tilde{z}}{\partial Z}\dot{Z}\right) = 0 \tag{3.40}$$

However, it should be highlighted since the coordinates Z is not orthonormal to x and y, the expression is merely by coincidence similar to the divergence of a vector field in the Cartesian coordinates . Since $\frac{\partial Z}{\partial z}(x,y,z) = \frac{g_z(x,y,z)}{g_0}$, by the reciprocal rule,

$$\frac{\partial \tilde{z}}{\partial Z}(x,y,Z) = \frac{g_0}{\tilde{g_z}(x,y,Z)} \tag{3.41}$$

Attention should be paid on the scalar fields and their dependence on coordinates. In particular, the effective vertical gravity g_z has to be treated with care in both coordinates system because it is used to defined the coordinate transformation as well. In the above expression, the transformation

$$g_z(x,y,\tilde{z}(x,y,Z)) = \tilde{g_z}(x,y,Z) \tag{3.42}$$

has been applied. It should also be highlighted that a closed form representation of $\tilde{g_z}$ is often absent because the closed form representation of the inverse coordinate transformation $z = \tilde{z}(x,y,Z)$ in general does not exists.

Hence, in terms of the physical quantities, the adapted continuity equation in the transformed coordinates (x,y,Z,t) is given by

$$\tilde{\nabla}_h \cdot \left(\frac{g_0}{\tilde{g_z}}\tilde{\mathbf{u}}_h\right) + \frac{\partial}{\partial Z}\left(\frac{g_0}{\tilde{g_z}}\dot{Z}\right) = 0, \tag{3.43}$$

which is known as the *adapted incompressible continuity equation* in the transformed (x,y,Z,t) coordinates. This equation will be applied when derivation of the adapted shallow water equation is performed in later section.

3.6.2. A Zeroth-Order Approximation

While the 'divergence'-free form of equation (3.43) may suit analytical investigation, this form does not favour characteristic scale analysis. A zeroth-order approximation to the quantity $\tilde{g_z}$ based on the physical argument will be proposed to simplify the expression.

The approximation is based on the Taylor-expansion of $g_z(x,y,z)$ along the z-direction over a fixed (x,y). Expanding g_z at $z = z_0(x,y)$ gives

$$g_z(x,y,z) = \left[g_z\right]_{@z_0(x,y)} + \left[\frac{\partial g_z}{\partial z}\right]_{@z_0(x,y)}(z - z_0) + h.o.t., \tag{3.44}$$

where $h.o.t.$ refers to the higher order term. However, recall that the effective gravity $g_z = g_0 + g_z'$ consists of the sum of a constant reference gravity g_0 and the perturbing gravity g_z' components. Hence the quantity $\frac{\partial g_z}{\partial z}$ contains purely the perturbing component, that is,

$$\left[\frac{\partial g_z}{\partial z}\right]_{@z_0(x,y)} = \left[\frac{\partial g_z'}{\partial z}\right]_{@z_0(x,y)}. \tag{3.45}$$

However, the characteristic scale analysis, which will be presented in the next section, suggests that the magnitude of $\left\|\left[\frac{\partial g_z'}{\partial z}\right]_{@z_0(x,y)}(z - z_0)\right\|$ in the Ocean is much less than $\left[g_z\right]_{@z_0(x,y)}$, that is,

$$\left\|\left[\frac{\partial g_z'}{\partial z}\right]_{@z_0(x,y)}(z - z_0)\right\| \ll \left[g_z\right]_{@z_0(x,y)} \tag{3.46}$$

Hence a zeroth-order approximation is sufficiently made to g_z

$$g_z(x,y,z) \approx \left[g_z\right]_{@z_0(x,y)}, \tag{3.47}$$

which makes $g_z(x,y,z)$ independent of z. It follows that $\tilde{g_z}$ is independent of Z as well. In particular, since the mean-sea level $z = z_0(x,y)$ is mapped into $Z = 0$, equation (3.47) in terms of the transformed coordinates is given by

$$\tilde{g_z}(x,y,Z) \approx \tilde{g_z}(x,y,0). \tag{3.48}$$

However, now that both g_z and the transformed $\tilde{g_z}$ are no longer dependent on the vertical coordinates, hence it makes no difference between g_z and $\tilde{g_z}$. To simplify the notation, the tilde on $\tilde{g_z}$ will be omitted.

Therefore, equation (3.43) can be approximated by

$$\tilde{\nabla}_h \cdot \left(\frac{g_0}{g_z}\tilde{\mathbf{u}}_h\right) + \frac{g_0}{g_z}\frac{\partial \dot{Z}}{\partial Z} \approx 0. \tag{3.49}$$

The expression (3.49) can manipulated algebraically so that a more handy equation for analysis can be obtained. Expanding the horizontal gradient $\tilde{\nabla}_h \cdot \left(\frac{g_0}{\tilde{g_z}}\tilde{\mathbf{u}}_h\right)$ and multiplying every term with $\frac{\tilde{g_z}}{g_0}$ give

$$\frac{g_z}{g_0}\frac{g_0}{g_z}\tilde{\nabla}_h \cdot \tilde{\mathbf{u}}_h + \tilde{\mathbf{u}}_h \cdot \frac{g_z}{g_0}\tilde{\nabla}_h\left(\frac{g_0}{g_z}\right) + \frac{g_z}{g_0}\frac{g_0}{g_z}\frac{\partial \dot{Z}}{\partial Z} \approx 0$$

$$\tilde{\nabla}_h \cdot \tilde{\mathbf{u}}_h + \tilde{\mathbf{u}}_h \cdot \tilde{\nabla}_h\left(\ln\left(\frac{g_0}{g_z}\right)\right) + \frac{\partial \dot{Z}}{\partial Z} \approx 0$$

Hence an alternative form of (3.49) is given by

$$\tilde{\nabla}_h \cdot \tilde{\mathbf{u}}_h - \tilde{\mathbf{u}}_h \cdot \tilde{\nabla}_h\left(\ln\left(\frac{g_z}{g_0}\right)\right) + \frac{\partial \dot{Z}}{\partial Z} \approx 0 \tag{3.50}$$

In addition, to simplify the scale analysis, the term $\ln\left(\frac{\tilde{g_z}}{g_0}\right)$ can also be linearised and approximated. Recall the definition of $g_z = g_0 + g_z'$, hence it follows

$$\frac{g_z}{g_0} = 1 + \frac{g_z'}{g_0}$$

Therefore for $\|\frac{g_z'}{g_0}\| \ll 1$, linearisation of the logarithm function $\ln$ gives,

$$\ln\left(\frac{g_z}{g_0}\right) \approx \frac{g_z'}{g_0} \tag{3.51}$$

To sum up, if the following conditions are satisfied,

$$\left\|\left[\frac{\partial g_z'}{\partial z}\right]_{@z_0(x,y)}(z - z_0)\right\| \ll [g_z]_{@z_0(x,y)}, \tag{3.52a}$$

$$\|g_z'\| \ll g_0, \tag{3.52b}$$

the adapted incompressible continuity equation (3.43) can be approximated to zeroth-order by

$$\tilde{\nabla}_h \cdot \tilde{\mathbf{u}}_h + \frac{\partial \dot{Z}}{\partial Z} - \tilde{\mathbf{u}}_h \cdot \tilde{\nabla}_h\left(\frac{g_z'}{g_0}\right) \approx 0 \tag{3.53}$$

REMARK: In order to consider the first-order or even higher-order approximation, it suffices to consider higher-order terms in the Taylor expansion of g_z in equation (3.44), which is unnecessary in the case of ocean wave since the zeroth-order approximation is reasonably accurate already.

3.7. Adapted Horizontal Momentum Equation

3.7.1. Adapted Momentum Equation under the Hydrostatic Approximation

In this section, the hydrostatic approximation discussed in section 3.5.3 will be applied to simplify the adapted momentum equation after Z-transformation (3.25). Recall the decomposition of pressure $\tilde{p}$ into the hydrostatic $\tilde{p}_s$ and dynamic $\tilde{p}_d$ components:

$$\tilde{p}(x, y, Z, t) = \tilde{p}_s(x, y, Z) + \tilde{p}_d(x, y, Z, t)$$

The hydrostatic pressure $\tilde{p}_s$ is again given by equation (3.28), which suggests

$$\frac{\partial \tilde{p}_s}{\partial Z} = -\rho \frac{\partial \tilde{\Phi}}{\partial Z}$$

Rearranging equation (3.37) gives

$$\frac{\partial \tilde{p}}{\partial Z} + \rho \frac{\partial \tilde{\Phi}}{\partial Z} = \frac{\partial \tilde{p}_d}{\partial Z} \tag{3.54}$$

In addition, recall that the horizontal gradient of hydrostatic pressure $\tilde{\nabla}_h \tilde{p}_s$ vanishes according to equation (3.35):

$$\tilde{\nabla}_h \tilde{p}_s = \vec{0} \tag{3.55}$$

Therefore collecting the results of equations (3.37) and (3.55) in the momentum equation under Z-transformation (3.25), the adapted momentum equation is given by

$$\rho \left[\frac{D\tilde{\mathbf{u}}_h}{dt} \right] = -\tilde{\nabla}_h \tilde{p}_d + \frac{\partial \tilde{p}_d}{\partial Z} \frac{\partial Z}{\partial z} \tilde{\nabla}_h(\tilde{z}) \tag{3.56}$$

This equation is known as the *adapted horizontal momentum equation* in the Z-coordinates.

The last term $\tilde{\nabla}_h(\tilde{z})$ on the right-hand side of equation (3.56) is known as the Jacobian involved in the transformation of coordinates from the physical coordinates (x, y, z, t) to (x, y, Z, t). The mathematical properties and its physical implication will be presented in the following section.

3.7.2. Explicit Expression for the Jacobian term

Recall that the definition of $\tilde{\nabla}_h$ is given by

$$\tilde{\nabla}_h(\tilde{z}) = \left.\frac{\partial z}{\partial x}\right|_Z \hat{e_1} + \left.\frac{\partial z}{\partial y}\right|_Z \hat{e_2}$$

The vertical line with subscript Z refers to partial derivatives keeping Z unchanged.

It has been discussed in the section 3.2.3 that, given the definition of coordinate function $Z = Z(x, y, z)$ given by equation (3.10), the inverse coordinate function $z = z(x, y, Z)$ exists and is unique in the weakly non-uniform gravitation field. Although the explicit form of the function $z = z(x, y, Z)$ is absent, fortunately, it is still possible to compute $\left.\frac{\partial z}{\partial x}\right|_Z$ and $\left.\frac{\partial z}{\partial y}\right|_Z$ indirectly.

Consider the total differential of the coordinate functions $Z = Z(x, y, z)$ and $z = z(x, y, Z)$:

$$dZ = \frac{\partial Z}{\partial x} dx + \frac{\partial Z}{\partial y} dy + \frac{\partial Z}{\partial z} dz \tag{3.57}$$

$$dz = \left.\frac{\partial z}{\partial x}\right|_Z dx + \left.\frac{\partial z}{\partial y}\right|_Z dy + \frac{\partial \tilde{z}}{\partial Z} dZ \tag{3.58}$$

By setting $dy = 0$ and $dZ = 0$ in equation (3.58), the ratio dz/dx is given by $\left.\frac{\partial z}{\partial x}\right|_Z$:

$$dz = \left.\frac{\partial z}{\partial x}\right|_Z dx \tag{3.59}$$

Hence setting $dy = 0$ and $dZ = 0$ in equation (3.57) gives:

$$0 = \frac{\partial Z}{\partial x} dx + \frac{\partial Z}{\partial z} dz \iff dz = -\frac{\partial Z}{\partial x} \Big/ \frac{\partial Z}{\partial z} dx, \tag{3.60}$$

provided that $\frac{\partial Z}{\partial z} \neq 0$. Therefore by comparing equations (3.59) and (3.60), a closed form expression for $\left.\frac{\partial \tilde{z}}{\partial x}\right|_Z$ is obtained:

$$\left.\frac{\partial \tilde{z}}{\partial x}\right|_Z = -\frac{\partial Z}{\partial x} \Big/ \frac{\partial Z}{\partial z} \tag{3.61}$$

Similarly by setting $dx = 0$ and $dZ = 0$, an expression for $\left.\frac{\partial \tilde{z}}{\partial y}\right|_Z$ can be obtained:

$$\left.\frac{\partial \tilde{z}}{\partial y}\right|_Z = -\frac{\partial Z}{\partial y} \Big/ \frac{\partial Z}{\partial z} \tag{3.62}$$

REMARK: In tensor calculus, these are quantities are the vertical component in the covariant basis when transformation $Z = Z(x, y, z)$ is performed.

3.7.3. Explicit Computation for the Jacobian term

With an explicit expression for $\frac{\partial \tilde{z}}{\partial x}\big|_Z$ and $\frac{\partial \tilde{z}}{\partial y}\big|_Z$, given by equations (3.61) and (3.62), the Jacobian term $\tilde{\nabla}_h(\tilde{z})$ can be computed explicitly.

Recall the Z-transformation was given by equation (3.10):

$$Z = z + \frac{\Phi'(x, y, z)}{g_0} - Z_0(x, y) \tag{3.63}$$

where $Z_0(x,y) = z_0(x,y) + \frac{\Phi'_0(x,y)}{g_0}$. Recall $z = z_0(x, y)$ is the hydrostatic sea level at the horizontal physical coordinates (x, y) and $\Phi'_0(x, y) = \Phi'(x, y, z_0(x, y))$ is the perturbing geopotential at the mean sea level $(x, y, z_0(x, y))$.

Denote g'_x and g'_y to be

$$g'_x = -\frac{\partial \Phi'}{\partial x} \tag{3.64a}$$

$$g'_y = -\frac{\partial \Phi'}{\partial y} \tag{3.64b}$$

Then differentiating (3.63) gives

$$\frac{\partial Z}{\partial x} = \frac{1}{g_0}\frac{\partial \Phi'}{\partial x} - \frac{\partial Z_0}{\partial x} = -\frac{g'_x}{g_0} - \frac{\partial Z_0}{\partial x} \tag{3.65a}$$

$$\frac{\partial Z}{\partial y} = \frac{1}{g_0}\frac{\partial \Phi'}{\partial y} - \frac{\partial Z_0}{\partial y} = -\frac{g'_y}{g_0} - \frac{\partial Z_0}{\partial y} \tag{3.65b}$$

Now consider the derivative of function $Z_0 = z_0(x,y) + \frac{\Phi'(x,y,z_0(x,y))}{g_0}$. Note that the subscript $@z_0(x,y)$ means the quantities in the square brackets are evaluated at the mean-sea level $(x, y, z) = (x, y, z_0(x, y))$.

$$\begin{aligned}\frac{\partial Z_0}{\partial x} &= \frac{\partial z_0}{\partial x} + \frac{1}{g_0}\left[\frac{\partial \Phi'}{\partial x} + \frac{\partial \Phi'}{\partial z}\frac{\partial z_0}{\partial x}\right]_{@z_0(x,y)} \\ &= \frac{\partial z_0}{\partial x} + \left[-\frac{g'_x}{g_0}\right]_{@z_0(x,y)} + \left[\frac{g'_z}{g_0}\right]_{@z_0(x,y)}\frac{\partial z_0}{\partial x} \\ &= \left[1 + \frac{g'_z}{g_0}\right]_{@z_0(x,y)}\frac{\partial z_0}{\partial x} + \left[-\frac{g'_x}{g_0}\right]_{@z_0(x,y)}\end{aligned}$$

Note that in the above derivation, g_0 is a constant and $z_0(x, y)$ is independent of vertical coordinates z, hence at each z-coordinate they are identical. Similarly $\frac{\partial Z_0}{\partial x}$ can be computed. These give rise to

$$\frac{\partial Z_0}{\partial x} = \left[1 + \frac{g'_z}{g_0}\right]_{@z_0(x,y)}\frac{\partial z_0}{\partial x} - \frac{1}{g_0}\left[g'_x\right]_{@z_0(x,y)} \tag{3.66a}$$

$$\frac{\partial Z_0}{\partial y} = \left[1 + \frac{g'_z}{g_0}\right]_{@z_0(x,y)}\frac{\partial z_0}{\partial y} - \frac{1}{g_0}\left[g'_y\right]_{@z_0(x,y)} \tag{3.66b}$$

The physical meaning of these quantities will be discussed in the next section 3.7.4. Therefore $\frac{\partial Z}{\partial x}$ and $\frac{\partial Z}{\partial y}$ can be computed explicitly

$$\frac{\partial Z}{\partial x} = -\frac{g'_x - \left[g'_x\right]_{@z_0(x,y)}}{g_0} - \left[1 + \frac{g'_z}{g_0}\right]_{@z_0(x,y)}\frac{\partial z_0}{\partial x} \tag{3.67a}$$

$$\frac{\partial Z}{\partial y} = -\frac{g'_y - \left[g'_y\right]_{@z_0(x,y)}}{g_0} - \left[1 + \frac{g'_z}{g_0}\right]_{@z_0(x,y)}\frac{\partial z_0}{\partial y} \tag{3.67b}$$

Recall also that from equation (3.11),

$$\frac{\partial Z}{\partial z} = 1 + \frac{g'_z}{g_0}$$

Hence plugging this together with equations (3.67) into the closed form expressions (3.61) and (3.62) yields two lengthy formulas,

$$\left.\frac{\partial \tilde{z}}{\partial x}\right|_Z = \frac{\frac{g'_x - [g'_x]_{@z_0(x,y)}}{g_0} + \left[1 + \frac{g'_z}{g_0}\right]_{@z_0(x,y)} \frac{\partial z_0}{\partial x}}{1 + \frac{g'_z}{g_0}} \tag{3.68a}$$

$$\left.\frac{\partial \tilde{z}}{\partial y}\right|_Z = \frac{\frac{g'_y - [g'_y]_{@z_0(x,y)}}{g_0} + \left[1 + \frac{g'_z}{g_0}\right]_{@z_0(x,y)} \frac{\partial z_0}{\partial y}}{1 + \frac{g'_z}{g_0}}. \tag{3.68b}$$

After some algebraic manipulations, their physical meanings will become clear. This will be presented in the following section.

3.7.4. Physical Interpretation of the Jacobian term

Equation (3.68) reveals that several physical quantities come into effect to determine the Jacobian $\tilde{\nabla}_h(\tilde{z})$. It is noted that expression of equations (3.68a) and (3.68b) are identical except for the coordinates, it suffices to consider and discuss one of them for the physical interpretation. In particular, the equation (3.68a) in x direction will be focused on.

Multiplying the reference gravity g_0 to both the nominator and denominator of equation (3.68a) gives

$$\left.\frac{\partial z}{\partial x}\right|_Z = \frac{g'_x - [g'_x]_{@z_0(x,y)} + [g_0 + g'_z]_{@z_0(x,y)} \frac{\partial z_0}{\partial x}}{g_0 + g'_z} \tag{3.69}$$

However, recall that $g_z(x,y,z) = g_0 + g'_z(x,y,z)$ is the effective gravity in the vertically downwards direction at the point (x,y,z). Hence $[g_z]_{@z_0(x,y)} = g_0 + [g'_z]_{@z_0(x,y)}$ is the effective vertical gravity evaluated at the mean-sea level $(x,y,z_0(x,y))$.

Denote also $\Delta[g_x] = \Delta[g_x](x,y,z) = g'_x(x,y,z) - [g'_x]_{@z_0(x,y)}$ to be the difference between the x-component of effective gravity g_x at point (x,y,z) and the point at mean-sea level $(x,y,z_0(x,y))$. Hence $\left.\frac{\partial z}{\partial x}\right|_Z$ can be expressed as

$$\left.\frac{\partial z}{\partial x}\right|_Z = \frac{[g_z]_{@z_0(x,y)}}{g_z} \frac{\partial z_0}{\partial x} + \frac{\Delta[g_x]}{g_z} \tag{3.70}$$

Similarly $\left.\frac{\partial z}{\partial x}\right|_Z$ can be defined:

$$\left.\frac{\partial z}{\partial x}\right|_Z = \frac{[g_z]_{@z_0(x,y)}}{g_z} \frac{\partial z_0}{\partial y} + \frac{\Delta[g_y]}{g_z} \tag{3.71}$$

Since that $z_0 = z_0(x,y)$ is the hydrostatic mean-sea level at horizontal coordinates (x,y), the term $\frac{\partial z_0}{\partial x}$ in (3.70) and $\frac{\partial z_0}{\partial y}$ in (3.71) thus measures the slope of the mean-sea level. On the other hand, the dimensionless quantities $[g_z]_{@z_0(x,y)}/g_z$, $\Delta[g_x]/g_z$ and $\Delta[g_y]/g_z$ measure the ratio of the horizontal gravity, relative to mean-sea level, to the vertical gravity.

The scale analysis of all quantities involved will be presented in the next session.

3.8. Characteristic Scale Analysis of the Continuity Equation

3.8.1. Notation of the Characteristic Scales

Denote, with respect to Z coordinate, L_h and U_h to be the horizontal length and velocity scale, L_v and U_v to be their vertical counterparts. In other words, express

$$u, v = U_h u^* \tag{3.72a}$$

$$\dot{Z} = U_v \dot{Z}^* \tag{3.72b}$$

$$x, y = L_h x^* \tag{3.72c}$$

$$Z = L_v Z^* \tag{3.72d}$$

so that $u^*, \dot{Z}^*, x^*, Z^*$ are dimensionless and scales with order of magnitude $\mathcal{O}(1)$. Also, define σ_h to be the horizontal scale of the gradient of relative gravity perturbation $G = \frac{g_z'}{g_0}$, that is

$$\tilde{\nabla}_h G = \sigma_h G^* \tag{3.73}$$

where G^* is also dimensionless with order $\mathcal{O}(1)$.

3.8.2. Validity of Approximations

In the sections 3.6.2, two approximations have been made to derive the zeroth-order approximation of the continuity equation (3.53). The two approximation are valid only if (3.52a) and (3.52b) are satisfied. In this section, the validity of these conditions in the ocean will be illustrated.

Magnitude of g_z' in the Open Ocean

In the open ocean, the typical value of perturbing gravity g_z' is of order 0.01 ms^{-2}, while the reference gravity g_0 is of order 10 ms^{-2}. Therefore the order of size of $\frac{g_z'}{g_0}$ is given by

$$\frac{g_z'}{g_0} \sim \mathcal{O}(10^{-3}) \tag{3.74}$$

which is much less than 1. Hence the condition (3.52b) is satisfied, so that the linearisation of the logarithm function $\ln\left(1+\frac{g_z'}{g_0}\right) \approx \frac{g_z'}{g_0}$ is justified. Note that this approximation is only required to perform the characteristics scale analysis, but not the derivation of depth-integrated continuity equation which will be presented in the later sections.

Magnitude of $\frac{\partial g_z'}{\partial z}$ in the Open Ocean

In the open ocean, the typical variation of the perturbing gravity g_z' between the surface and the bottom of the ocean at most of order 100milliGal. Note that the quantity $z - z_0$, which measures vertical distance between a point and the mean-sea level, is at maximum when the bottom floor is considered $z = S_B$.

Therefore, denoting Δg_z to be scale of $\frac{\partial g_z'}{\partial z}(z - z_0)$, Δg_z is then given by

$$\Delta g_z \sim \mathcal{O}\left(100\text{milliGal}\right) = \mathcal{O}(10^{-3}\ \text{ms}^{-2}) \tag{3.75}$$

Note that Δg_z is much less than the reference gravity $g_0 \approx 10$ ms^{-2}. Hence the condition (3.52a) is also valid in the ocean.

To sum up, the empirical scales discussed in equation (3.74) and (3.75) indicate that the equation (3.53) is a reasonable approximation to the exact adapted incompressible continuity equation given by equation (3.43) in the setting of the open ocean.

3.8.3. Dimensionless Continuity Equation

Considering the characteristic scale of each of the terms in the continuity equation (3.53) yields:

$$\tilde{\nabla}_h \cdot \tilde{\mathbf{u}}_h = \frac{U_h}{L_h}\left(\tilde{\nabla}_h^* \cdot \tilde{\mathbf{u}}_h^*\right) \tag{3.76}$$

$$\frac{\partial \dot{Z}}{\partial Z} = \frac{U_v}{L_v}\left(\frac{\partial \dot{Z}^*}{\partial Z^*}\right) \tag{3.77}$$

$$\tilde{\mathbf{u}}_h \cdot \tilde{\nabla}_h\left(\frac{g_z'}{g_0}\right) = U_h \sigma_h \left(\tilde{\mathbf{u}}_h \cdot \tilde{\nabla}_h^* G^*\right) \tag{3.78}$$

Plugging these quantities into the continuity equation (3.53) gives:

$$\frac{U_h}{L_h}\left(\tilde{\nabla}_h^* \cdot \tilde{\mathbf{u}}_h^*\right) + \frac{U_v}{L_v}\left(\frac{\partial \dot{Z}^*}{\partial Z^*}\right) - \left[U_h \sigma_h \left(\tilde{\mathbf{u}}_h \cdot \tilde{\nabla}_h^* G^*\right)\right] = 0$$

Rearranging and grouping terms gives

$$\frac{U_h}{L_h}\left[\tilde{\nabla}_h^* \cdot \tilde{\mathbf{u}}_h^* - L_h \sigma_h \left(\tilde{\mathbf{u}}_h \cdot \tilde{\nabla}_h^* G^*\right)\right] + \frac{U_v}{L_v}\left(\frac{\partial \dot{Z}^*}{\partial Z^*}\right) = 0 \tag{3.79}$$

Horizontal Length Scales in the Ocean

By a similar consideration in the first square bracket in equation (3.79), the term $L_h \sigma_h \left(\tilde{\mathbf{u}}_h \cdot \tilde{\nabla}_h^* G\right)$ is comparable to $\tilde{\nabla}_h^* \cdot \tilde{\mathbf{u}}_h^*$ only if the dimensionless quantity α, given by the product of horizontal length scale of motion and horizontal gradient of relative gravity perturbation $\alpha = L_h \sigma_h$ is of order of magnitude equal than $\mathcal{O}(1)$, that is,

$$\alpha = L_h \sigma_h \sim \mathcal{O}(1) \tag{3.80}$$

Typical value of $\sigma_h = \mathcal{O}\left(\tilde{\nabla}_h G\right)$ ranges from $\mathcal{O}(10^{-11}\mathrm{m}^{-1})$ to $\mathcal{O}(10^{-7}\mathrm{m}^{-1})$ on the mean-sea level. Hence the length scale of the motion should be of at least order of magnitude $10^6\mathrm{m} = 10^3\mathrm{km}$, which is of the same scale with tidal motion.

Case 1, $\alpha \ll \mathcal{O}(1)$**:** When the condition (3.80) is not satisfied in the way that $\alpha \ll 1$, the term $L_h \sigma_h \left(\tilde{\mathbf{u}}_h \cdot \tilde{\nabla}_h^* G\right)$ in equation (3.79) can be neglected. Hence the continuity equation (3.53) in the transformed coordinates is further simplified and is given by:

$$\tilde{\nabla}_h \cdot \tilde{\mathbf{u}}_h + \frac{\partial \dot{Z}}{\partial Z} = 0, \tag{3.81}$$

whose form resembles the incompressible continuity equation in the physical coordinates system. However, it is reminded again that the coordinate Z is not orthogonal to (x, y), and thus this is not a divergence-free form.

Consider the balancing of the scales in equation (3.81) gives

$$\frac{U_h}{L_h} + \frac{U_v}{L_v} = 0$$
$$U_v \sim \mathcal{O}\left(\frac{L_v U_h}{L_h}\right)$$

Recall that $\delta = \frac{L_v}{L_h}$ is the aspect ratio of the motion, hence

$$U_v \sim \mathcal{O}(\delta U_h) \tag{3.82}$$

which suggests a constraint on the vertical velocity scale U_v, given certain aspect ration δ and horizontal velocities scale U_h. In the shallow water, i.e. $\delta \ll 1$, U_v is thus very small relative to U_h. Hence, the vertical momentum equation can be abandoned.

Case 2, $\alpha \sim \mathcal{O}(1)$**:** When the condition (3.80) is satisfied, the continuity equation (3.53) keeps its form

$$\tilde{\nabla}_h \cdot \tilde{\mathbf{u}}_h + \frac{\partial \dot{Z}}{\partial Z} - \left(\tilde{\mathbf{u}}_h \cdot \tilde{\nabla}_h\right)\left(\frac{g_z'}{g_0}\right) = 0$$

Since $\alpha \sim \mathcal{O}(1)$, both $\tilde{\nabla}_h \cdot \tilde{\mathbf{u}}_h$ and $\left(\tilde{\mathbf{u}}_h \cdot \tilde{\nabla}_h\right)\left(\frac{g_z'}{g_0}\right)$ scales with $\frac{U_h}{L_h}$. It follows that balancing the scale gives rise to the same result as equation (3.82)

$$U_v \sim \mathcal{O}(\delta U_h). \tag{3.83}$$

Case 3, $\alpha \gg \mathcal{O}(1)$**:** This corresponds to a strongly varying gravitational field on the Earth surface, which is not observed. In such case, the dominant balance in the continuity equation results in

$$\frac{\partial \dot{Z}}{\partial Z} - (\tilde{\mathbf{u}}_h \cdot \tilde{\nabla}_h)(\frac{g'_z}{g_0}) \approx 0, \tag{3.84}$$

which will not be studied in this project since it is physically absent on the Earth.

3.9. Characteristic Scale Analysis of the Momentum Equation

The characteristic scale analysis of the Momentum Equation presented in this section is not very standard. The common way to conduct the scale analysis is to derive the full momentum equation in all coordinates and consider the characteristic scales of each variable. However, since the momentum equation in the direction along the transformed vertical coordinate Z was not derived, this standard approach does not work.

However, a closer look of the horizontal momentum equation (3.22) suggests an alternative to derive information of the characteristic scales. Although this alternative is not entirely rigorous, it provides a handy and sensible argument to the characteristic scales of the terms in the momentum equation.

Recall that the horizontal momentum equation in the transformed coordinate Z is given by equation (3.56):

$$\rho\left[\frac{D\tilde{\mathbf{u}}_h}{dt}\right] = -\tilde{\nabla}_h \tilde{p}_d + \frac{\partial \tilde{p}_d}{\partial Z}\frac{\partial Z}{\partial z}\tilde{\nabla}_h(\tilde{z})$$

The main difference between the adapted horizontal momentum equation and the standard one is the extra term $\frac{\partial \tilde{p}_d}{\partial Z}\frac{\partial Z}{\partial z}\tilde{\nabla}_h(\tilde{z})$ on the right-hand side of the equation. Hence, it suffices to give an estimate of the order of magnitude of this term.

In this section the characteristic scales of variables are defined using also the notation in equation (3.72).

3.9.1. The scale of the term $\frac{D\tilde{\mathbf{u}}_h}{dt}$

It is reminded that Characteristic scales of variables in the transformed coordinates (x, y, Z, t) are defined in equation (3.72). It is reminded here about the notation

$$\frac{D\tilde{\mathbf{u}}_h}{dt} = \frac{\partial \tilde{\mathbf{u}}_h}{\partial t}\bigg|_Z + \tilde{u}\frac{\partial \tilde{\mathbf{u}}_h}{\partial x}\bigg|_Z + \tilde{v}\frac{\partial \tilde{\mathbf{u}}_h}{\partial y}\bigg|_Z + \dot{Z}\frac{\partial \tilde{\mathbf{u}}_h}{\partial Z}\bigg|_Z$$

have been used. Therefore denote, in addition, the time scale of the motion to be T,

$$\frac{D\tilde{\mathbf{u}}_h}{dt} \sim \mathcal{O}(\max(\frac{U_h}{T}, \frac{U_h^2}{L_h}, \frac{U_v U_h}{L_v}))$$

By equation (3.82) or (3.83), which is always valid on the Earth surface, the above scale simplifies into

$$\frac{D\tilde{\mathbf{u}}_h}{dt} \sim \mathcal{O}\big(\max(\frac{U_h}{T}, \frac{U_h^2}{L_h})\big). \tag{3.85}$$

3.9.2. The scale of the non-linear pressure gradient terms

It is noted that the pressure gradient involves an additional term $\frac{\partial \tilde{p}_d}{\partial Z}\frac{\partial Z}{\partial z}$ after the coordinate transformation.

Recall that the pressure $\tilde{p}(x, y, Z, t)$ has been decomposed into the hydrostatic $\tilde{p}_s$ and dynamic $\tilde{p}_d$ parts: $\tilde{p} = \tilde{p}_s + \tilde{p}_d$. Correspondingly the the pressure $p = p(x, y, z, t)$ in the physical coordinates has also been decomposed into $p = p_s + p_d$. It is reminded here about the notation of scalar field in different coordinates systems: $\tilde{p}_d(x, y, Z, t) = p_d(x, y, z(x, y, Z), t)$. The relation between $\frac{\partial p_d}{\partial z}$ and $\frac{\partial \tilde{p}_d}{\partial Z}$, by the chain rule, is given by

$$\frac{\partial \tilde{p}_d}{\partial Z} = \frac{\partial p_d}{\partial z}\frac{\partial \tilde{z}}{\partial Z} \tag{3.86}$$

Note that by the reciprocal rule $\frac{\partial \tilde{z}}{\partial Z}\frac{\partial Z}{\partial z} = 1$. Hence it yields:

$$\frac{\partial \tilde{p}_d}{\partial Z}\frac{\partial Z}{\partial z} = \frac{\partial p_d}{\partial z} \tag{3.87}$$

Therefore, it is sufficient to consider the characteristic scale of $\frac{\partial p_d}{\partial z}$. This can be done via the vertical momentum equation in standard Cartesian coordinates (x, y, z):

$$\frac{\partial w}{\partial t} + u\frac{\partial w}{\partial x} + v\frac{\partial w}{\partial y} + w\frac{\partial w}{\partial z} = \frac{-1}{\rho}\frac{\partial p}{\partial z} - (g_0 + g_z') \tag{3.88}$$

Considering the hydrostatic balance in the vertical momentum equation in the Cartesian coordinates gives

$$\frac{\partial p_s}{\partial z} = -\rho(g_0 + g_z') \tag{3.89}$$

Hence what remains in the momentum equation (3.88) is only the dynamic pressure p_d

$$\frac{Dw}{dt} = \frac{-1}{\rho}\frac{\partial p_d}{\partial z} \tag{3.90}$$

Note that the notation of material derivatives

$$\frac{Dw}{dt} = \frac{\partial w}{\partial t} + u\frac{\partial w}{\partial x} + v\frac{\partial w}{\partial y} + w\frac{\partial w}{\partial z}$$

have been used.

Notations of Characteristic Scales in the Physical Coordinates (x, y, z, t)

In order to perform the characteristic scale analysis for equation (3.90), it is necessary to define the characteristic scales again but in the original (x, y, z, t) coordinates.

Denote, with respect to the Cartesian coordinates (x, y, z, t), the characteristic length scale of the horizontal motion and its velocity u, v to be L_H and U_H respectively. Similarly for the vertical motion with velocity w, denote its length scale and velocity scale to be L_V and U_V. It is reminded again that Characteristic scales of variables in the transformed coordinates (x, y, Z, t) are defined in equation (3.72). To summarise, it follows

$$\begin{aligned} x, y &\sim \mathcal{O}(L_H) \\ u, v &\sim \mathcal{O}(U_H) \\ z &\sim \mathcal{O}(L_V) \\ w &\sim \mathcal{O}(U_V) \end{aligned}$$

Relations between Characteristic Scales in the Two Coordinates Systems

The relation between the characteristic scale in the two different coordinates should be examined and deal with care. Recall the transformation formulas for the horizontal velocities u and v in the two coordinates are given by

$$\begin{aligned} \tilde{u}(x, y, Z, t) &= u(x, y, z(x, y, Z), t) \\ \tilde{v}(x, y, Z, t) &= v(x, y, z(x, y, Z), t) \end{aligned}$$

which suggest u and v are essentially the same quantity with $\tilde{u}$ and $\tilde{v}$. It naturally follows that their scales are identical, that is $U_h = U_H$. Similar consideration gives also $L_h = L_H$.

For the vertical length scale, recall that the jacobian of the transformation is given by

$$\frac{\partial Z}{\partial z} = 1 + \frac{g_z'}{g_0}$$

Since it is assumed that $\frac{g_z'}{g_0} \ll 1$, hence it is expected that

$$\frac{\partial Z}{\partial z} \sim \mathcal{O}(1)$$

and thus the vertical length scale in both coordinates are of the same characteristic order, that is,

$$L_v \approx L_V$$

so that the aspect ratio of the motion $\delta = L_v/L_h \approx L_V/L_H$ remains approximately invariant in both coordinates.

To sum up, the relation between the characteristic scales are summarised as:

$$L_h = L_H \tag{3.91a}$$
$$U_h = U_H \tag{3.91b}$$
$$L_v \approx L_V \tag{3.91c}$$

Scale Analysis of Equation (3.90)

It has been shown in Pedlosky 1979 that

$$U_V \sim \mathcal{O}(\frac{L_V U_H}{L_H}), \tag{3.92}$$

However, using the relationship between the two characteristic scales (3.91), the scales in (3.92) can thus be expressed also by

$$U_V \sim \mathcal{O}(\delta U_h), \tag{3.93}$$

Denote $\max(a, b)$ to be the maximum of a and b. It follows from (3.93) that $\frac{Dw}{dt}$ scales with

$$\begin{aligned}\frac{Dw}{dt} &\sim \mathcal{O}(\max(\frac{U_V}{T}, \frac{U_h U_V}{L_h}, \frac{U_V^2}{L_v})) \\ &\sim \mathcal{O}(\max(\frac{\delta U_h}{T}, \frac{\delta U_h^2}{L_h}, \frac{\delta^2 U_h^2}{L_v})) \\ &\sim \mathcal{O}(\delta \cdot \max(\frac{U_h}{T}, \frac{U_h^2}{L_h})),\end{aligned}$$

Note that according to equation (3.85), $\max(\frac{U_h}{T}, \frac{U_h^2}{L_h})$ is the characteristic scale of $\frac{D\tilde{\mathbf{u}}_h}{dt}$. In order to emphasise that scale of the vertical momentum $\rho\frac{Dw}{dt}$ is dependent on the horizontal momentum $\rho\frac{D\tilde{\mathbf{u}}_h}{dt}$, denote

$$\rho\frac{Dw}{dt} \sim \mathcal{O}(\delta \cdot \rho\frac{D\tilde{\mathbf{u}}_h}{dt}) \tag{3.94}$$

By equation (3.90), an estimate to the scale of vertical gradient of dynamic pressure p_d is thus given by

$$\frac{\partial p_d}{\partial z} \sim \mathcal{O}(\delta \cdot \rho\frac{D\tilde{\mathbf{u}}_h}{dt}) \tag{3.95}$$

and therefore from equation (3.87):

$$\frac{\partial \tilde{p}_d}{\partial Z}\frac{\partial Z}{\partial z} \sim \mathcal{O}(\delta \cdot \rho\frac{D\tilde{\mathbf{u}}_h}{dt}) \tag{3.96}$$

3.9.3. The scale of the Jacobian term

It is noted that the term Jacobian term $\tilde{\nabla}_h(\tilde{z})$ is involved in the momentum equation after the coordinate transformation.

Recall that equation (3.70) and (3.71) provides two physically insightful formula for the Jacobian $\tilde{\nabla}_h(\tilde{z})$:

$$\left.\frac{\partial \tilde{z}}{\partial x}\right|_Z = \frac{[g_z]_{@z_0(x,y)}}{g_z}\frac{\partial z_0}{\partial x} + \frac{\Delta[g_x]}{g_z}$$
$$\left.\frac{\partial \tilde{z}}{\partial y}\right|_Z = \frac{[g_z]_{@z_0(x,y)}}{g_z}\frac{\partial z_0}{\partial y} + \frac{\Delta[g_y]}{g_z}$$

Denote the vertical and horizontal length scale of mean-sea level z_0 to be M_h and M_v respectively, that is,

$$\frac{\partial z_0}{\partial x}, \frac{\partial z_0}{\partial y} \sim \mathcal{O}(\frac{M_h}{M_v}) \tag{3.97}$$

Denote also the scale of vertical gravity g_z by G_v. Note that $[g_z]_{@z_0(x,y)}$ scales also with G_v, hence

$$\frac{[g_z]_{@z_0(x,y)}}{g_z} \approx 1 \tag{3.98}$$

In practice the order of $\Delta[g_x]$ and $\Delta[g_y]$ depends on location, denote the order of these quantity by

$$\frac{\Delta[g_x]}{g_z}, \frac{\Delta[g_y]}{g_z} \sim \mathcal{O}(\frac{\Delta G_h}{G_v}) \tag{3.99}$$

Therefore, the Jacobian $\tilde{\nabla}_h(\tilde{z})$ scales with

$$\left.\frac{\partial z}{\partial x}\right|_Z, \left.\frac{\partial z}{\partial y}\right|_Z \sim \mathcal{O}(\max(\frac{M_h}{M_v}, \frac{\Delta G_h}{G_v})) \tag{3.100}$$

Typical values of M_h and M_v are $\mathcal{O}(100\text{ km})$ and $\mathcal{O}(1\text{-}10\text{ m})$ respectively. The horizontal length scale of z_0 varies depending on location on the Earth.

$$\frac{M_h}{M_v} \sim \mathcal{O}(10^{-4} \text{ or } 10^{-5}) \tag{3.101}$$

In the ocean, the perturbing gravity is always weak, compared with the uniform reference gravity g_0. In terms of order of magnitudes,

$$g_0 \approx 10\text{ ms}^{-2} \tag{3.102}$$
$$g_z' \sim \mathcal{O}(10^{-4}\text{ ms}^{-2} \text{ to } 0.01\text{ ms}^{-2}) \tag{3.103}$$
$$g_x', g_y' \sim \mathcal{O}(10^{-4}\text{ ms}^{-2} \text{ to } 10^{-3}\text{ ms}^{-2}) \tag{3.104}$$

It is reminded that $g_z = g_0 + g_z'$, $g_x = g_x'$ and $g_y = g_y'$. Hence in equation (3.70) and (3.71), the quantities are of order

$$\frac{[g_z]_{@z_0(x,y)}}{g_z} = 1 + \mathcal{O}(10^{-3}) \tag{3.105}$$

which justifies equation (3.98). On the other hand,

$$\frac{\Delta G_h}{G_v} \leq \mathcal{O}(10^{-4}) \tag{3.106}$$

The $\leq$ sign is used to indicate the largest possible scale, because the differences of g_x and g_y between two locations are evaluated in $\Delta[g_x]$ and $\Delta[g_y]$. In particular, the closer a point is to the mean-sea level, the smaller this term is.

Therefore, in the open ocean, according to equation (3.100), the terms $\left.\frac{\partial z}{\partial x}\right|_Z$ and $\left.\frac{\partial z}{\partial y}\right|_Z$ are of order of magnitude:

$$\left.\frac{\partial z}{\partial x}\right|_Z, \left.\frac{\partial z}{\partial y}\right|_Z \leq \mathcal{O}(10^{-4}) \tag{3.107}$$

3.9.4. Short Conclusions

To sum up, in the general case of shallow water flow, the extra term in the adapted horizontal momentum equation $\frac{\partial \tilde{p}_d}{\partial Z}\frac{\partial Z}{\partial z}\tilde{\nabla}_h(\tilde{z})$ scales with:

$$\frac{\partial \tilde{p}_d}{\partial Z}\frac{\partial Z}{\partial z}\tilde{\nabla}_h(\tilde{z}) \sim \mathcal{O}(\delta \cdot \rho \frac{D\tilde{\mathbf{u}}_h}{dt} \cdot \max(\frac{M_h}{M_v}, \frac{\Delta G_h}{G_v})) \tag{3.108}$$

The shallowness assumption states that $\delta \ll 1$. Given the situation in the open ocean (3.107), the quantity $\delta \cdot \max(\frac{M_h}{M_v}, \frac{\Delta G_h}{G_v})$ is very small. Hence compared with $\rho\frac{D\tilde{\mathbf{u}}_h}{dt}$, the term $\frac{\partial \tilde{p}_d}{\partial Z}\frac{\partial Z}{\partial z}\tilde{\nabla}_h(\tilde{z})$ is negligible. Hence the adapted horizontal momentum is reduced into

$$\rho\frac{D\tilde{\mathbf{u}}_h}{dt} = -\tilde{\nabla}_h\tilde{p}_d, \tag{3.109}$$

which is called the *adapted horizontal momentum equation* in the shallow water.

It is expected in the deep water, where the configuration $\delta \ll 1$ is not valid, the term $\frac{\partial \tilde{p}_d}{\partial Z}\frac{\partial Z}{\partial z}\tilde{\nabla}_h(\tilde{z})$ is no longer negligible. However, an aspect ratio $\delta \approx 1$ will imply $L_h \approx L_v$. In order to satisfy the the condition (3.80) such that the gravity variation is 'felt' by the fluid motion, the vertical length scale L_v of the motion has to scale with $\frac{1}{\sigma_h}$, which is at least 10^7 m, which is much greater than the average depth of ocean ≈ 4000 m. Hence the deep water scenario will be unrealistic on the Earth and will not be studied in this project.

3.10. Derivation of Adapted Shallow Water Equations

In this section, the adapted shallow water model, which is capable of dealing with the weakly non-uniform gravity, will be derived.

3.10.1. Boundary Conditions

In the classical shallow water model, boundary conditions are needed to be imposed on both the surface of the fluid and the bottom floor over which the fluid flow. In this section, the boundary condition for the fluid in the transformed coordinates will be presented.

Surface: Kinematic Boundary Conditions

In the physical coordinates (x, y, z, t), typically the kinematic boundary condition on fluid surface $z = S(x, y, t)$ is imposed, which suggests a fluid element on the surface-interface always remains on the interface. Mathematically the kinematic boundary condition is given by:

$$\frac{D}{dt}(z - S) = 0, \text{ at } z = S(x, y, t)$$

or equivalently,

$$w = \frac{\partial S}{\partial t} + \mathbf{u}_h \cdot \nabla_h S \tag{3.110}$$

where u,v and w are the velocities in x, y and z direction.

A natural expectation of the analogy to equation (3.110) in the transformed coordinates (x, y, Z, t) is given by

$$\dot{Z} = \frac{\partial \tilde{S}}{\partial t} + \tilde{\mathbf{u}}_h \cdot \tilde{\nabla}_h \tilde{S} \tag{3.111}$$

However, equation (3.111) should be examined carefully because of the coordinate transformation. It turns out that, fortunately, equation (3.110) and (3.111) are equivalent and thus equation (3.111) correctly describe the kinematic boundary condition to the surface of the fluid in the transformed coordinates (x, y, Z, t) as well. The proof will be given in the next section. Readers who are not interested may skip it.

Equivalence between the expressions (3.110) and (3.111)

To show the equivalence between (3.110) and (3.111), it suffices to express the quantities given in equation (3.110) by the transformed coordinates (x, y, Z, t). The 'translation' from the physical coordinates (x, y, z, t) to the transformed coordinates (x, y, Z, t) of each term will be presented separately.

By equation (2.23), the vertical velocity w is translated into $\tilde{w}$ by

$$\tilde{w} = \frac{\partial \tilde{z}}{\partial t}\bigg|_Z + \tilde{\mathbf{u}}_h \cdot \tilde{\nabla}_h(\tilde{z}) + \dot{Z}\frac{\partial \tilde{z}}{\partial Z}$$

Since the inverse coordinate transformation $\tilde{z} = \tilde{z}(x, y, Z)$ is time-independent, $\frac{\partial \tilde{z}}{\partial t}\big|_Z = 0$. Thus the vertical velocity w on the left-hand sides of equation (3.110) is given by:

$$\tilde{w} = \tilde{\mathbf{u}}_h \cdot \tilde{\nabla}_h(\tilde{z}) + \dot{Z}\frac{\partial \tilde{z}}{\partial Z} \tag{3.112}$$

To translate the derivative of $S(x, y, t)$ into $\tilde{S}(x, y, t)$, it is necessary to consider the relation between S and $\tilde{S}$ first, which is already given by equation (3.16):

$$\tilde{S}(x, y, t) = S(x, y, t) + \frac{\Phi'(x, y, S(x, y, t))}{g_0} - Z_0(x, y)$$

Then consider the time-derivative of $\tilde{S}(x, y, t)$, by the chain rule:

$$\frac{\partial \tilde{S}}{\partial t} = \frac{\partial S}{\partial t} + \frac{1}{g_0}\left[\frac{\partial \Phi'}{\partial z}\right]_{@S(x,y,t)}\frac{\partial S}{\partial t}$$

Since $g'z = \frac{\partial \Phi'}{\partial z}$ and recall that $\frac{\partial Z}{\partial z} = 1 + \frac{g'_z}{g_0}$, $\tilde{S}(x, y, t)$ can be simply expressed by

$$\frac{\partial \tilde{S}}{\partial t} = \frac{\partial S}{\partial t}\left[\frac{\partial Z}{\partial z}\right]_{@S(x,y,t)}$$

The spatial-derivatives of $\tilde{S}(x, y, t)$ can be computed similarly and give

$$\begin{aligned}
\frac{\partial \tilde{S}}{\partial x} &= \frac{\partial S}{\partial x}\left[\frac{\partial Z}{\partial z}\right]_{@S(x,y,t)} - \frac{[g_x]_{@S(x,y,t)}}{g_0} - \frac{\partial Z_0}{\partial x} \\
\frac{\partial \tilde{S}}{\partial y} &= \frac{\partial S}{\partial y}\left[\frac{\partial Z}{\partial z}\right]_{@S(x,y,t)} - \frac{[g_y]_{@S(x,y,t)}}{g_0} - \frac{\partial Z_0}{\partial y},
\end{aligned}$$

where $g_x = -\frac{\partial \Phi'}{\partial x}$ and $g_y = -\frac{\partial \Phi'}{\partial x}$.

The above equations may seem complicated at first glance. However, recall that by equation (3.65),

$$\begin{aligned}
\left[\frac{\partial Z}{\partial x}\right]_{@S(x,y,t)} &= -\frac{[g_x]_{@S(x,y,t)}}{g_0} - \frac{\partial Z_0}{\partial x} \\
\left[\frac{\partial Z}{\partial y}\right]_{@S(x,y,t)} &= -\frac{[g_y]_{@S(x,y,t)}}{g_0} - \frac{\partial Z_0}{\partial y}.
\end{aligned}$$

In addition, by equation (3.61) and (3.62), $\frac{\partial Z}{\partial x}$ and $\frac{\partial Z}{\partial y}$ can be related to $\frac{\partial \tilde{z}}{\partial x}\big|_Z$ and $\frac{\partial \tilde{z}}{\partial y}\big|_Z$ respectively by

$$\begin{aligned}
\left[\frac{\partial \tilde{z}}{\partial x}\bigg|_Z\right]_{@\tilde{S}(x,y,t)} &= -\left[\frac{\partial Z}{\partial x}\right]_{@S(x,y,t)} \Big/ \left[\frac{\partial Z}{\partial z}\right]_{@S(x,y,t)} \\
\left[\frac{\partial \tilde{z}}{\partial y}\bigg|_Z\right]_{@\tilde{S}(x,y,t)} &= -\left[\frac{\partial Z}{\partial y}\right]_{@S(x,y,t)} \Big/ \left[\frac{\partial Z}{\partial z}\right]_{@S(x,y,t)}
\end{aligned}$$

Therefore the quantities $\frac{\partial S}{\partial t}$ and $\mathbf{u}_h \cdot \nabla_h S$ are 'translated' to be

$$\frac{\partial S}{\partial t} = \frac{\partial \tilde{S}}{\partial t}\left[\frac{\partial \tilde{z}}{\partial Z}\right]_{@S(x,y,t)} \tag{3.115a}$$

$$\mathbf{u}_h \cdot \nabla_h S = \tilde{\mathbf{u}}_h \cdot \left(\tilde{\nabla}_h \tilde{S} + \tilde{\nabla}_h(\tilde{z})\right)\left[\frac{\partial \tilde{z}}{\partial Z}\right]_{@S(x,y,t)} \tag{3.115b}$$

Note that in the above expressions, terms expressed in the physical coordinates (x, y, z, t) are placed on the left-hand sides, while the terms expressed in the transformed coordinates (x, y, Z, t) are placed on the right-hand sides.

Putting the translated w by (3.112) and translated $\frac{DS}{dt}$ by (3.115) into the kinematic boundary condition in the physical coordinates (3.110) gives

$$\begin{aligned}
\tilde{\mathbf{u}}_h \cdot \tilde{\nabla}_h(\tilde{z}) + \dot{Z}\frac{\partial \tilde{z}}{\partial Z} &= \frac{\partial \tilde{S}}{\partial t}\left[\frac{\partial \tilde{z}}{\partial Z}\right] + \tilde{\mathbf{u}}_h \cdot \left(\tilde{\nabla}_h \tilde{S}\right)\left[\frac{\partial \tilde{z}}{\partial Z}\right] + \tilde{\mathbf{u}}_h \cdot \left(\tilde{\nabla}_h(\tilde{z})\right) \\
\dot{Z}\frac{\partial \tilde{z}}{\partial Z} &= \frac{\partial \tilde{S}}{\partial t}\left[\frac{\partial \tilde{z}}{\partial Z}\right] + \tilde{\mathbf{u}}_h \cdot \left(\tilde{\nabla}_h \tilde{S}\right)\left[\frac{\partial \tilde{z}}{\partial Z}\right] \\
\dot{Z}\frac{\partial \tilde{z}}{\partial Z} &= \left[\frac{\partial \tilde{S}}{\partial t} + \tilde{\mathbf{u}}_h \cdot \left(\tilde{\nabla}_h \tilde{S}\right)\right]\left[\frac{\partial \tilde{z}}{\partial Z}\right]
\end{aligned}$$

Note that all quantities are evaluated at $Z = \tilde{S}(x, y, t)$ and thus the subscript $@\tilde{S}(x, y, t)$ notation has been dropped. Since the quantity $\frac{\partial \tilde{z}}{\partial Z}$ does not vanish, the boundary condition (3.110) in the physical coordinates is thus equivalent to the boundary condition (3.111)

$$w = \frac{\partial S}{\partial t} + \mathbf{u}_h \cdot \nabla_h S \iff \dot{Z} = \frac{\partial \tilde{S}}{\partial t} + \tilde{\mathbf{u}}_h \cdot \tilde{\nabla}_h \tilde{S}, \tag{3.116}$$

which completes the proof.

Bottom: Zero Normal Flow Boundary Conditions

In the physical coordinates (x, y, z, t), given the time-independent bottom topography $z = S_B(x, y)$, typically the boundary condition that the normal flow to the bottom vanishes is imposed. This suggests equivalently that a fluid element initially lying on the bottom will always remains on bottom. Mathematically the kinematic boundary condition is given by:

$$\frac{D}{dt}(z - S_B) = 0, \text{ at } z = S_B(x, y, t)$$

or equivalently,

$$w = \mathbf{u}_h \cdot \nabla_h S_B \tag{3.117}$$

where u,v and w are the velocities in x, y and z direction.

Repeating the argument discussed in the section for the surface boundary condition, and noting that $S_B(x, y)$ can be regarded as a special case of $S(x, y, t)$ where the time-dependence is absent, it can be shown that the equivalent boundary condition in the transformed coordinates (x, y, Z, t) is given by

$$\dot{Z} = \tilde{\mathbf{u}}_h \cdot \tilde{\nabla}_h \tilde{S}_B. \tag{3.118}$$

3.10.2. Adapted Depth-Averaged Continuity Equation

Additional Assumption: Gravity

Recall in equation (3.47), it has been **approximated** that the gravity variation g'_z is independent of the vertical coordinates, which is justified by the condition (3.52a),

$$g_z(x, y, z) \approx g_z(x, y, z_0(x, y)) \tag{3.119}$$

or equivalently in the transformed (x, y, Z) coordinates

$$\tilde{g_z}(x, y, Z) \approx \tilde{g_z}(x, y, 0), \tag{3.120}$$

since the mean-sea level $z = z_0(x, y)$ is mapped to $Z = 0$.

Another physical justification of this approximation is that in the standard shallow water model, the fluid is considered to be 'layerised'. By depth-averaging, the dependence on the vertical coordinates z of the horizontal velocities is removed. Hence the standard shallow water model is essentially a 'semi-3D' model.

Here in the adapted model the assumption of independence of vertical coordinates is extended also the the gravity g_z. Hence it is justifiable also to *a priori* take a depth-independent vertical gravity perturbation g_z', which gives the assumption (3.120).

Additional Assumption: Horizontal Velocities

Another assumption is that the horizontal velocity $\tilde{\mathbf{u}}_h$ is independent of Z, which is an exact analogy to the assumption that the horizontal velocities are vertically-independent in the standard shallow water model. Quantitatively this assumption is given by

$$\tilde{\mathbf{u}}_h = \tilde{\mathbf{u}}_h(x, y). \tag{3.121}$$

Depth-Integration

Rearranging the exact adapted incompressible continuity equation (3.43) gives

$$\frac{\partial}{\partial Z}\left(\frac{g_0}{\tilde{g}_z}\dot{Z}\right) = -\tilde{\nabla}_h \cdot \left(\frac{g_0}{\tilde{g}_z}\tilde{\mathbf{u}}_h\right), \tag{3.122}$$

Integrating the adapted continuity equation (3.122) over depth from $Z = \tilde{S}_B$ to arbitrary $Z = \tilde{S}$ gives

$$\int_{\tilde{S}_B}^{\tilde{S}} \frac{\partial}{\partial \check{Z}}\left(\frac{g_0}{\tilde{g}_z}\dot{Z}\right) d\check{Z} = -\int_{\tilde{S}_B}^{\tilde{S}} \tilde{\nabla}_h \cdot \left(\frac{g_0}{\tilde{g}_z}\tilde{\mathbf{u}}_h\right) d\check{Z}$$

Note that $\check{Z}$ is a dummy variable used in the integration. Since by equation (3.47) $\tilde{g}_z(x, y, Z)$ cab be approximated by $\tilde{g}_z(x, y, 0)$ to the zeroth-order, the integration is straight-forward and gives

$$\frac{g_0}{\tilde{g}_z}\left(\dot{Z}(x, y, \tilde{S}, t) - \dot{Z}(x, y, \tilde{S}_B, t)\right) \approx -(\tilde{S} - \tilde{S}_B)\left[\tilde{\nabla}_h \cdot \left(\frac{g_0}{\tilde{g}_z}\tilde{\mathbf{u}}_h\right)\right]$$

The boundary conditions for $\dot{Z}(x, y, \tilde{S}, t)$ and $\dot{Z}(x, y, \tilde{S}_B, t)$ are respectively given by (3.111) and (3.118). This gives rise to

$$\frac{g_0}{\tilde{g}_z}\left(\frac{\partial \tilde{S}}{\partial t} + \tilde{\mathbf{u}}_h \cdot \tilde{\nabla}_h(\tilde{S} - \tilde{S_B})\right) \approx -(\tilde{S} - \tilde{S}_B)\left[\tilde{\nabla}_h \cdot \left(\frac{g_0}{\tilde{g}_z}\tilde{\mathbf{u}}_h\right)\right]$$

Note the water depth $\tilde{D}$ in the transformed coordinates is given by $\tilde{D} = \tilde{S} - \tilde{S}_B$. Also note that $\tilde{S}_B$ is time-independent. Thus the depth-integrated continuty equation is given by

$$\frac{g_0}{\tilde{g}_z}\left(\frac{\partial \tilde{D}}{\partial t} + \tilde{\mathbf{u}}_h \cdot \tilde{\nabla}_h \tilde{D}\right) \approx -\tilde{D}\left[\tilde{\nabla}_h \cdot \left(\frac{g_0}{\tilde{g}_z}\tilde{\mathbf{u}}_h\right)\right]$$

By the product rule, the expression can be expressed in a concise way, which will be known as the *adapted depth-integrated continuity equation* in the shallow water:

$$\frac{\partial}{\partial t}\left(\frac{g_0}{\tilde{g}_z}\tilde{D}\right) + \tilde{\nabla}_h \cdot \left(\frac{g_0}{\tilde{g}_z}\tilde{D}\tilde{\mathbf{u}}_h\right) \approx 0 \tag{3.123}$$

Note that in the above expression, the quantity $\frac{g_0}{\tilde{g}_z}$ can also be given by $\frac{g_0}{\tilde{g}_z} = \frac{\partial \tilde{z}}{\partial Z}$. By equation (3.20), the adapted depth-integrated continuity equation (3.123) can thus be interpreted informally as

$$\frac{\partial D}{\partial t} + \tilde{\nabla}_h \cdot \left(D\tilde{\mathbf{u}}_h\right) \approx 0,$$

which looks like the the depth-integrated continuity in the classical case with uniform gravity. Note that this interpretation is informal since the horizontal divergence operator $\tilde{\nabla}_h$ is defined in the transformed coordinates (x, y, Z, t), while the physical water depth D is defined in the physical coordinates (x, y, z, t).

The depth-integrated continuity equation (3.123) can be expanded in an alternative form to favour the derivation of the adapted shallow water wave equation and numerical computations. Multiplying every term in equation (3.123) by $\frac{\tilde{g}_z}{g_0}$ and expanding the horizontal divergence term gives

$$\frac{\partial \tilde{D}}{\partial t} + \frac{\tilde{g}_z}{g_0}\tilde{D}\tilde{\mathbf{u}}_h \cdot \tilde{\nabla}_h\left(\frac{g_0}{\tilde{g}_z}\right) + \frac{\tilde{g}_z}{g_0}\frac{g_0}{\tilde{g}_z}\tilde{\nabla}_h \cdot \left(\tilde{D}\tilde{\mathbf{u}}_h\right) \approx 0$$

Note that the quantity $\frac{\tilde{g}_z}{g_0}\tilde{\nabla}_h\left(\frac{g_0}{\tilde{g}_z}\right)$ can be given by $-\tilde{\nabla}_h\left[\ln\left(\frac{\tilde{g}_z}{g_0}\right)\right]$. Hence an alternative and equivalent form to (3.123) is given by

$$\frac{\partial \tilde{D}}{\partial t} + \tilde{\nabla}_h \cdot \left(\tilde{D}\tilde{\mathbf{u}}_h\right) \approx \tilde{D}\tilde{\mathbf{u}}_h \cdot \tilde{\nabla}_h\left(\ln\left(\frac{\tilde{g}_z}{g_0}\right)\right) \tag{3.124}$$

3.10.3. Adapted Momentum Equation

In the remaining sections of this chapter, all variables, scalar fields and vector fields and their derivatives are expressed in the transformed coordinates (x, y, Z, t) unless otherwise specified. The notation tilde will thus be dropped to simplify the notation.

Recall that the simplified momentum equation (3.109) has the following form in the shallow water:

$$\rho\frac{D\mathbf{u}_h}{dt} = -\nabla_h p_d, \tag{3.125}$$

where ρ is the density of fluid, u_h is the horizontal velocities and p_d is the dynamic component of the pressure.

In order to obtained a closed system of equations with the adapted depth-averaged continuity equation, equation (3.39) is integrated over depth:

$$\int_{S_B}^{Z}\left(\frac{\partial p}{\partial \check{Z}}\right)d\check{Z} = -\rho\int_{h}^{Z}\left(\frac{\partial \Phi}{\partial \check{Z}}\right)d\check{Z}$$

Note that by equation (3.7), $\frac{\partial \Phi}{\partial Z} = g_0$, imposing the boundary condition of pressure on the free fluid surface: $p(x, y, S, t) = p_0$ leads to:

$$p(x, y, Z, t) - p_0 = -\rho g_0(Z - S)$$

Hence it follows that

$$\frac{\partial p}{\partial x} = \rho g_0\frac{\partial S}{\partial x} \tag{3.126a}$$

$$\frac{\partial p}{\partial y} = \rho g_0\frac{\partial S}{\partial y} \tag{3.126b}$$

Therefore using equation (3.35), (3.109) and (3.126), the *adapted horizontal momentum equation* in the shallow water is given by:

$$\frac{\partial u}{\partial t} + u\frac{\partial u}{\partial x} + v\frac{\partial u}{\partial y} = -g_0\frac{\partial S}{\partial x} \tag{3.127a}$$

$$\frac{\partial v}{\partial t} + u\frac{\partial v}{\partial x} + v\frac{\partial v}{\partial y} = -g_0\frac{\partial S}{\partial y} \tag{3.127b}$$

or equivalently

$$\frac{\partial \mathbf{u}_h}{\partial t} + \mathbf{u}_h \cdot \nabla\mathbf{u}_h = -g_0\nabla_h S \tag{3.128}$$

3.11. Derivation of Adapted Wave Equation in Shallow Water

Let the hydrostatic thickness of the fluid layer be $D_0(x,y)$. D_0 is therefore the difference in vertical coordinates Z between the mean-sea level and the ocean floor. Denote $\eta = \eta(x,y,t)$ to be the relative surface elevation of the fluid to the mean-sea level, that is,

$$\eta = D - D_0 \tag{3.129}$$

In this section it is assumed that $\eta \ll D_0$, which suggests only small-amplitude motions on the surface will be considered. These small amplitudes represent free oscillations or waves on a fluid surface.

In addition it is further assumed $\mathbf{u}_h$ is small enough, such that the advection term $\mathbf{u}_h \cdot \nabla_h \mathbf{u}_h$ can be neglected compared to $\frac{\partial \mathbf{u}_h}{\partial t}$ in equation (3.128). To sum up, it is assumed that

$$\eta \ll D_0$$
$$\mathbf{u}_h \cdot \nabla_h \mathbf{u}_h \ll \frac{\partial \mathbf{u}_h}{\partial t}$$

Consider a slight deviation from *quiescent* state of the fluid, which is given by

$$u = 0 + u'$$
$$v = 0 + v'$$
$$D = D_0 + \eta$$

and plug these into the adapted momentum equation (3.128) and the adapted depth-averaged continuity equation (3.124). By keeping only the first order perturbations it is obtained that:

$$\frac{\partial u'}{\partial t} = -g_0 \frac{\partial \eta}{\partial x} \tag{3.130a}$$
$$\frac{\partial v'}{\partial t} = -g_0 \frac{\partial \eta}{\partial y} \tag{3.130b}$$
$$\frac{\partial \eta}{\partial t} + \nabla_h \cdot (D_0 \mathbf{u}_h') = D_0 \mathbf{u}_h' \cdot \nabla_h \left(\ln\left(\frac{g_z}{g_0}\right) \right) \tag{3.130c}$$

Define the mass flux $\mathbf{U} = (u'D_0, v'D_0) = (U,V)$, it then follows

$$\frac{\partial U}{\partial t} = -g_0 D_0 \frac{\partial \eta}{\partial x} \tag{3.131a}$$
$$\frac{\partial V}{\partial t} = -g_0 D_0 \frac{\partial \eta}{\partial y} \tag{3.131b}$$
$$\frac{\partial \eta}{\partial t} + \nabla_h \cdot \mathbf{U} = \mathbf{U} \cdot \nabla_h \left(\ln\left(\frac{g_z}{g_0}\right) \right) \tag{3.131c}$$

The system of first-order partial differential equations (3.131) is known as the governing equation for the *adapted shallow water wave*. Numerical computation will be based on the system of equations (3.131).

It is noted that the depth-averaged continuity equation (3.131c) can be expressed equivalently by a 'conservative' form

$$\frac{\partial}{\partial t}\left(\frac{\eta}{g_z}\right) + \nabla_h \cdot \left(\frac{\mathbf{U}}{g_z}\right) = 0 \tag{3.132}$$

However, this form does not bring additional insight to the physics nor bring convenience to numerical computation. Hence the form in (3.131c) will be used and analysed.

3.11.1. The Second-Order Wave Equation

It is also possible to derive a second-order partial differential equations. Partially differentiate equation (3.131c) with respect to t gives:

$$\frac{\partial^2 \eta}{\partial t^2} + \nabla_h \cdot \left(\frac{\partial \mathbf{U}}{\partial t}\right) = \frac{\partial \mathbf{U}}{\partial t} \cdot \nabla_h \left(\ln\left(\frac{g_z}{g_0}\right) \right) \tag{3.133}$$

Noting that from equation (3.131a) and (3.131b), $\frac{\partial \mathbf{U}}{\partial t} = -g_0 D_0 \nabla_h \eta$. Substituting this into the equation (3.133), the *adapted shallow water wave equation* is finally obtained:

$$\frac{\partial^2 \eta}{\partial t^2} - \nabla_h \cdot \left(g_0 D_0 \nabla_h \eta\right) = -g_0 D_0 \nabla_h \left(\ln\left(\frac{g_z}{g_0}\right)\right) \cdot \nabla_h \eta \tag{3.134}$$

Note that when $g_z' = 0$ so that $g_z = g_0$, the right-hand side of equation (3.134) vanishes and equation (3.134) reduces to the classical shallow water gravity wave equation.

If the depth-averaged continuity equation (3.131c) of the form (3.132) is used, the above equation becomes

$$\frac{\partial^2 \eta}{\partial t^2} = g_z \nabla_h \cdot \left(\frac{g_0 D_0}{g_z} \nabla_h \eta\right) \tag{3.135}$$

which is an equivalent expression to (3.134).

3.11.2. The Mathematical Characteristics of the Adapted Shallow Water Wave

To end this chapter, the mathematical characteristics of (3.131) is highlighted. Since $g_0 \tilde{D}_0$ is strictly positive, denote:

$$c(x,y) = \sqrt{g_0 \tilde{D}_0}.$$

Readers are reminded that g_0 is the reference gravity and $\tilde{D}_0$ is the hydrostatic water depth in the transformed coordinates.

In equation (3.20) of section 3.3.2, it has been suggested that when the vertical component of the gravity field $g_z(x,y,z)$ is independent of the vertical z coordinates, the relation between the depth of fluid in the transformed coordinates $\tilde{D}$ and the physical coordinates D is given by

$$\tilde{D}(x,y,t) = D(x,y,t)\left[\frac{\partial Z}{\partial z}\right] = D(x,y,t)\left[1 + \frac{g_z'(x,y)}{g_0}\right]. \tag{3.136}$$

Applying the transformation rule to $\tilde{D}_0$ suggested in equation (3.136), in terms of the water depth D_0 in the physical coordinates, the wave speed $c(x)$ becomes

$$c(x) = \sqrt{g_0 D_0 \left[1 + \frac{g_z'(x)}{g_0}\right]} = \sqrt{g_z D_0}. \tag{3.137}$$

Readers are reminded that the effective gravity $g_z(x) = g_0 + g_z'(x)$ and time-averaged water depth $D_0(x)$ are both spatially dependent.

Equation (3.131) is then expressed in the form of:

$$\frac{\partial \eta}{\partial t} + \nabla_h \cdot \mathbf{U} = \mathbf{U} \cdot \nabla_h \left(\ln\left(\frac{g_z}{g_0}\right)\right) \tag{3.138a}$$

$$\frac{\partial U}{\partial t} + c^2 \frac{\partial \eta}{\partial x} = 0 \tag{3.138b}$$

$$\frac{\partial V}{\partial t} + c^2 \frac{\partial \eta}{\partial y} = 0 \tag{3.138c}$$

Defining $\underline{q} = (\eta, U, V)^T$, the system of equation (3.138) can thus be expressed in a system of linear hyperbolic equations

$$\frac{\partial \underline{q}}{\partial t} + A_x \frac{\partial \underline{q}}{\partial x} + A_y \frac{\partial \underline{q}}{\partial y} = \underline{R}(\underline{q}, g_z) \tag{3.139}$$

where

$$A_x = \begin{pmatrix} 0 & 1 & 0 \\ c^2 & 0 & 0 \\ 0 & 0 & 0 \end{pmatrix}$$

and

$$A_y = \begin{pmatrix} 0 & 0 & 1 \\ 0 & 0 & 0 \\ c^2 & 0 & 0 \end{pmatrix}$$

with the source term

$$\underline{R} = \begin{pmatrix} \mathbf{U} \cdot \nabla_h \left(\ln\left(\frac{g_z}{g_0}\right) \right) \\ 0 \\ 0 \end{pmatrix}$$

It is worthwhile to remind once more that the above equations are defined on the transformed coordinates (x, y, Z, t). The solution of equation (3.139) should be converted back to (x, y, z, t) in order to be comparable with the solutions from standard gravity wave equation as well as the actual observation and measurement data.

The next questions to ask are, naturally, how the extra source term $\underline{R}$ (in contrast to the standard wave equation) will affect η and how the effects look like after being translated back to physical coordinates (x, y, z, t). This will be discussed in the next chapter.

3.11.3. Conservation of Potential Vorticity

Define the vorticity of shallow fluid to be $\zeta = \frac{\partial v}{\partial x} - \frac{\partial u}{\partial y}$ and water depth to be $D = D(x, y, t)$. In the standard shallow water model with uniform gravity, the potential vorticity Π given by

$$\Pi = \frac{\zeta}{D}, \tag{3.140}$$

is a conserved quantity, namely, the material derivative of Π is zero:

$$\frac{D\Pi}{dt} = 0 \tag{3.141}$$

It will be demonstrated that the same quantity is no longer conserved in the adapted shallow water model.

Recall the depth-averaged momentum equation (3.128), which has the same form as the standard depth-averaged momentum equation:

$$\frac{\partial \mathbf{u}_h}{\partial t} + \mathbf{u}_h \cdot \nabla \mathbf{u}_h = -g_0 \nabla_h S$$

The vorticity equation can be obtained by cross-differentiating the two components of the horizontal velocity in the adapted momentum equation, which eventually gives

$$\frac{D\zeta}{dt} = -\zeta \nabla \cdot \mathbf{u}_h \tag{3.142}$$

The detailed derivation can be found in any introductory Geophysical Fluid Dynamics textbook.

Recall that the depth-averaged continuity equation (3.124) is given by

$$\frac{D}{dt}(\tilde{D}) + \tilde{D} \nabla_h \cdot \mathbf{u}_h = \tilde{D} \mathbf{u}_h \cdot \nabla_h \left(\ln\left(\frac{\tilde{g}_z}{g_0}\right) \right), \tag{3.143}$$

where $\tilde{D} = \tilde{D}(x, y, t)$ is the depth of the fluid layer in the transformed coordinates.

After some algebraic manipulations on (3.142) and (3.143), it can be shown that

$$\tilde{D} \frac{D\zeta}{dt} - \zeta \frac{D}{dt}(\tilde{D}) = -\tilde{D} \zeta \mathbf{u}_h \nabla \ln\left(\frac{\tilde{g}_z}{g_0}\right)$$

$$\Leftrightarrow \quad \frac{D}{dt}\left(\frac{\zeta}{\tilde{D}}\right) = -\frac{\zeta}{\tilde{D}} \mathbf{u}_h \nabla \ln\left(\frac{\tilde{g}_z}{g_0}\right)$$

In other words, the standard potential vorticity $\Pi = \frac{\zeta}{\tilde{D}}$ is no longer a conserved quantity in the adapted shallow water model. Readers are reminded here that $\tilde{D}$ refers to the water depth in the transformed coordinates.

However, by noting that the quantity $\frac{\tilde{g}_z}{g_0}$ is time-independent, the above expression can be rewritten as

$$\begin{aligned} & \frac{\partial}{\partial t}\left(\frac{\zeta}{\tilde{D}}\right) + \mathbf{u}_h \cdot \nabla\left(\frac{\zeta}{\tilde{D}}\right) = -\frac{\zeta}{\tilde{D}}\mathbf{u}_h \frac{g_0}{\tilde{g}_z}\nabla\left(\frac{\tilde{g}_z}{g_0}\right) \\ \Leftrightarrow \quad & \frac{\partial}{\partial t}\left(\frac{\tilde{g}_z}{g_0}\frac{\zeta}{\tilde{D}}\right) + \frac{\tilde{g}_z}{g_0}\mathbf{u}_h \cdot \nabla\left(\frac{\zeta}{D}\right) = -\frac{\zeta}{\tilde{D}}\mathbf{u}_h \nabla\left(\frac{\tilde{g}_z}{g_0}\right) \\ \Leftrightarrow \quad & \frac{\partial}{\partial t}\left(\frac{\tilde{g}_z}{g_0}\frac{\zeta}{\tilde{D}}\right) + \mathbf{u}_h \cdot \nabla\left(\frac{\tilde{g}_z}{g_0}\frac{\zeta}{\tilde{D}}\right) = 0 \end{aligned}$$

In other words, in the transformed coordinates an adapted potential velocity Π_a can be defined as

$$\Pi_a = \frac{\tilde{g}_z}{g_0}\frac{\zeta}{\tilde{D}} \tag{3.144}$$

such that the material derivative of Π_a vanishes, that is

$$\frac{D\Pi_a}{dt} = 0. \tag{3.145}$$

In other words, a conserved quantity in the adapted shallow water model is found to be the adapted potential vorticity.

4

One-Dimensional Adapted Wave Equation

In this chapter, the one-dimensional adapted wave equation will be discussed. The exact solution will be derived. Quantitative and qualitative behaviour of the solution will examined.

4.1. Diagnostic Formalism for the One-dimensional Adapted Wave Equation

Consider the one dimensional case of the adapted wave equation. For simplicity, it is also defined that $G(x) = \ln(\frac{g_z(x)}{g_0})$ and wave speed $c(x) = \sqrt{g_z D_0(x)}$. Equation (3.131) can thus be written as:

$$\frac{\partial \tilde{\eta}}{\partial t} + \frac{\partial \tilde{U}}{\partial x} = \tilde{U}\frac{\partial}{\partial x}(G) \tag{4.1a}$$

$$\frac{\partial \tilde{U}}{\partial t} + c^2\frac{\partial \tilde{\eta}}{\partial x} = 0 \tag{4.1b}$$

Note that variables marked with a tilde are defined in the transformed coordinates.

Consider an ansatz to the surface elevation $\tilde{\eta}$

$$\tilde{\eta}(x,t) = \tilde{\eta}_0(x)\exp(-i\omega t), \tag{4.2}$$

which is harmonic in time. Denote partial derivative by subscripts. Then (4.1) becomes:

$$-i\omega\tilde{\eta}_0 e^{-i\omega t} + \tilde{U}_x = \tilde{U}G_x$$
$$\tilde{U}_t + c^2(\tilde{\eta}_0)_x e^{-i\omega t} = 0$$

Rearranging gives:

$$\tilde{U}_x - G_x\tilde{U} = i\omega\tilde{\eta}_0 e^{-i\omega t}$$
$$\tilde{U}_t = -c^2(\tilde{\eta}_0)_x e^{-i\omega t}$$

Multiplying the integrating factor $e^{-G(x)}$ to both equations, the two equations can be written as

$$(\tilde{U}e^{-G})_x = e^{-i\omega t}\left[i\omega\tilde{\eta}_0 e^{-G}\right]$$
$$(\tilde{U}e^{-G})_t = e^{-i\omega t}\left[-c^2(\tilde{\eta}_0)_x e^{-G}\right]$$

Let $\tilde{u} = \tilde{U}e^{-G}$, consider the mixed second order derivative:

$$\tilde{u}_{xt} = +e^{-i\omega t}\left[\omega^2\tilde{\eta}_0\right]e^{-G}$$
$$\tilde{u}_{tx} = -e^{-i\omega t}\left[c^2(\tilde{\eta}_0)_{xx} - c^2G_x(\tilde{\eta}_0)_x + 2cc_x(\tilde{\eta}_0)_x\right]e^{-G}$$

Consider the case where both $\tilde{U}(x,t)$ and $G(x)$ are continuously differentiable, it follows that $\tilde{u}_{xt} = \tilde{u}_{tx}$, which leads to the equation:

$$-\omega^2\tilde{\eta}_0 = c^2(\tilde{\eta}_0)_{xx} - c^2G_x(\tilde{\eta}_0)_x + 2cc_x(\tilde{\eta}_0)_x$$

Rearranging gives:

$$(\tilde{\eta}_0)_{xx} + (2\frac{c_x}{c} - G_x)(\tilde{\eta}_0)_x + \frac{\omega^2}{c^2}(\tilde{\eta}_0) = 0, \tag{4.3}$$

which is a second order ordinary differential equation with variable coefficients. The equation can be transformed by taking $P(x) = \frac{2c_x}{c} - G_x$ and $Q(x) = \frac{\omega^2}{c^2}$, and defining a transform coordinate r implicitly by

$$\ln r = \ln(\tilde{\eta}_0) + \frac{1}{2}\int P(x)dx = \ln(\tilde{\eta}_0) + \ln c - \frac{1}{2}G. \tag{4.4}$$

Then equation (4.3) can be transformed into $r_{xx} + [Q(x) - \frac{1}{2}P_x - \frac{1}{4}P^2]r = 0$, or in our context:

$$r_{xx} + \left[\frac{\omega^2}{c^2} - \frac{1}{2}\left(2\frac{cc_{xx} - (c_x)^2}{c^2} - G_{xx}\right) - \frac{1}{4}\left(2\frac{c_x}{c} - G_x\right)^2\right]r = 0 \tag{4.5}$$

Now recall that $G(x)$ is given by $\ln\left(\frac{g_z}{g_0}\right)$. Hence G_x and G_{xx} are respectively given by

$$G_x(x) = \frac{1}{g_z}\frac{dg_z}{dx} \tag{4.6}$$

$$G_{xx}(x) = \frac{1}{g_z}\left[\frac{d^2g_z}{dx^2} - \frac{1}{g_z}\left(\frac{dg_z}{dx}\right)^2\right] \tag{4.7}$$

Define two dimensionless quantities

$$E = \frac{\omega^2}{c^2{k_0}^2}, \tag{4.8a}$$

$$V = \frac{1}{2{k_0}^2}\left[2\frac{c_{xx}}{c} - 2\frac{(c_x)^2}{c^2} - \frac{1}{g_z}\frac{\partial^2 g_z}{\partial x^2} + \frac{1}{g_z^2}\left(\frac{\partial g_z}{\partial x}\right)^2\right] + \frac{1}{4{k_0}^2}\left(2\frac{c_x}{c} - \frac{1}{g_z}\frac{\partial g_z}{\partial x}\right)^2, \tag{4.8b}$$

where k_0 is an arbitrarily chosen constant, which will be called reference wavenumber. For instance, k_0 can be chosen as the wavenumber of the incoming wave in a closed physical domain, or k_0 can be chosen as the characteristic wavenumber of waves in a physical domain.

The spatial derivatives of $c(x)$ using the definition of (3.137) are given by

$$\frac{\partial c}{\partial x} = \frac{1}{2c}\left[g_z\frac{\partial D_0}{\partial x} + \frac{\partial g_z}{\partial x}D_0\right] \tag{4.9}$$

$$\frac{\partial^2 c}{\partial x^2} = \frac{-1}{4c^3}\left[g_z\frac{\partial D_0}{\partial x} + \frac{\partial g_z}{\partial x}D_0\right]^2 + \frac{1}{2c}\left[g_z\frac{\partial^2 D_0}{\partial x^2} + 2\frac{\partial g_z}{\partial x}\frac{\partial D_0}{\partial x} + \frac{\partial^2 g_z}{\partial x^2}D_0\right] \tag{4.10}$$

Plugging these derivatives of $c(x)$ into the expression of the dimensionless quantity $V(x)$ given by equation (4.8), surprisingly, all terms involving g_z cancel out. $V(x)$ is greatly simplified into

$$V(x) = \frac{1}{4{k_0}^2{D_0}^2}\left[2D_0\frac{\partial^2 D_0}{\partial x^2} - \left(\frac{\partial D_0}{\partial x}\right)^2\right], \tag{4.11}$$

which suggests the quantity $V(x)$ is independent of effective gravity g_z itself.

On the other hand, the expression of E preserves the dependence on the effective gravity g_z, which is given by

$$E(x) = \frac{\omega^2}{g_z D_0 {k_0}^2}. \tag{4.12}$$

To sum up, in terms of the variables expressed in the physical coordinates, the dimensionless quantities E and V can be expressed as

$$E(x) = \frac{\omega^2}{g_z D_0 {k_0}^2}, \tag{4.13a}$$

$$V(x) = \frac{1}{4{k_0}^2 {D_0}^2}\left[2D_0\frac{\partial^2 D_0}{\partial x^2} - \left(\frac{\partial D_0}{\partial x}\right)^2\right], \tag{4.13b}$$

which are very handy expressions to be used for further analysis.

Equation (4.5) can be expressed simply by a simple second-order differential equation

$$r_{xx} + \left[(E(x) - V(x)){k_0}^2\right]r = 0, \tag{4.14}$$

whose form resembles the one-dimensional, time-independent Schrodinger equation in Quantum Mechanics.

While E is strictly positive, the dimensionless quantity V can be positive or negative, depending on the spatial configuration of wave speed $c(x)$ and the effective gravity $g_z(x)$. The types of solutions to the equation (4.14) are determined by the sign of $E - V$. This indicates that the dimensionless quantity $\kappa^*(x)$

$$\kappa^*(x) = \sqrt{E(x) - V(x)} \tag{4.15}$$

can serve as a *diagnostic* tool to a priori determine the type of wave dynamics. The two types of solutions will be discussed in the next section.

An ansatz to the 'Schrodinger equation' (4.14) will be applied

$$r(x) = A(x)\exp(iS(x)), \tag{4.16}$$

where $A(x)$ is the wave amplitude and $S(x)$ is the generalised phase function.

Depending on the sign of the diagnostic variable $\kappa^*(x) = \sqrt{E(x) - V(x)}$, two types of wave dynamics are possible.

4.1.1. Case 1: Oscillatory Mode $E > V$

The first type of wave dynamics corresponds to the case when κ^* is real, or equivalently $E > V$. In addition, if the wave amplitude $A(x)$ varies slowly relative to phase function $S(x)$, based on the JWKB-approximation (Jeffreys, 1924; Brillouin, 1926; Kramers, 1926; Wentzel, 1926), it can be shown that the solution to the Schrodinger equation (4.14), when $E \gg V$, is given by

$$A(x) = \frac{1}{(\sqrt{(E-V)}k_0)^{\frac{1}{2}}} \tag{4.17}$$

$$S(x) = \pm\int\sqrt{(E-V)}k_0 dx \tag{4.18}$$

so that r is

$$r \sim \frac{\exp(\pm i\int\sqrt{(E-V)}k_0 dx)}{(\sqrt{(E-V)}k_0)^{\frac{1}{2}}}$$

The symbol ' $\sim$' here refers to that r is a linear combination of the two possible fundamental solutions.

Transformation of r to $\tilde{\eta}_0$ via equation (4.4) gives

$$\tilde{\eta}_0 \sim \frac{\sqrt{g_z}}{\sqrt{g_0}c(\sqrt{(E-V)}k_0)^{\frac{1}{2}}}\exp(\pm i\int\sqrt{(E-V)}k_0 dx), \tag{4.19}$$

which is oscillatory in x with amplitudes scaled by a spatially-dependent function $\frac{\sqrt{g_z}}{\sqrt{g_0}c(\sqrt{(E-V)}k_0)^{\frac{1}{2}}}$. Waves which satisfy the condition $E > V$ will be called as waves in the *oscillatory mode*.

Note that the solution in (4.19) can be expressed equivalently by the diagnostic quantity $\kappa^*(x) = \sqrt{E(x) - V(x)}$

$$\tilde{\eta}_0 \sim \frac{\sqrt{g_z}}{\sqrt{g_0}c(\kappa^*(x)k_0)^{\frac{1}{2}}}\exp(\pm i\int\kappa^*(x)k_0 dx). \tag{4.20}$$

The significance of this alternative expression will be presented in the following sections.

4.1.2. Case 2: Growth/Decay mode $E < V$

On the other hand, when κ^* is imaginary, or equivalently $E < V$ in some region, and additionally the phase function $S(x)$ varies slowly relative to the amplitude $A(x)$, it can then be shown that the Schrodinger equation (4.14) has exponential solutions

$$A(x) = \frac{1}{(\sqrt{(V-E)}k_0)^{\frac{1}{2}}} \tag{4.21}$$

$$S(x) = \pm i \int \sqrt{(V-E)}k_0 dx \tag{4.22}$$

so that r is

$$r \sim \frac{\exp(\pm \int \sqrt{(V-E)}k_0 dx)}{(\sqrt{(V-E)}k_0)^{\frac{1}{2}}}$$

Transformation of r to $\tilde{\eta}_0$ via equation (4.4) gives

$$\tilde{\eta}_0 \sim \frac{\sqrt{g_z}}{\sqrt{g_0}c(\sqrt{(V-E)}k_0)^{\frac{1}{2}}} \exp(\pm \int \sqrt{(V-E)}k_0 dx), \tag{4.23}$$

which is no longer oscillatory in nature. In Quantum Mechanics, this correspond to the 'tunneling' effect. 'Waves' with this properties will be called as waves in the *growth/decay mode*.

The physical meaning and the significance of the two dimensionless quantities E and V, as well as the diagonstic quantity κ^* will be discussed in the next section.

4.1.3. The Physical Meanings of E and V

When the oscillatory mode is considered, firstly recall that a plane wave with wavenumber k and amplitude A is given by

$$\tilde{\eta}_0 = A \exp(\pm ikx). \tag{4.24}$$

Comparing it with the oscillatory mode solution, assuming $\kappa^* = \sqrt{E-V}$ is independent of x, given in equation (4.19) suggests that

$$k = \kappa^* k_0, \tag{4.25a}$$

$$A \sim \frac{\sqrt{g_z}}{\sqrt{g_0}c(\kappa^* k_0)^{\frac{1}{2}}} \tag{4.25b}$$

These indicate that the dimensionless quantity $\kappa^* = \sqrt{(E-V)}$ is a scaling factor for the reference wavenumber k_0 to become the actual wavenumber k. If $\kappa^* > 1$, then the observed wavenumber will be greater than the reference wave, or equivalently the observed wavelength is shorter than the reference wavelength. The other way round applies for $\kappa^* < 1$.

Since $\kappa* = \sqrt{E-V}$ is now a constant, it no longer controls the spatial variation of wave amplitude $A(x)$. Neglecting all the spatially constant terms in the wave amplitude $A(x)$, $A(x)$ is proportional to $\frac{1}{\sqrt{D_0}}$ only:

$$A \sim \frac{\sqrt{g_z}}{c} = \frac{1}{\sqrt{D_0}}. \tag{4.26}$$

The growth/decay mode is considerably more complicated. Recall that for exponential function, $\exp(\lambda x)$, λ is the growth factor ($\lambda > 0$) or the decay constant ($\lambda < 0$) which controls the rate of change of the exponential function. Comparing the growth/decay mode (4.23) with an exponential function

$$\tilde{\eta}_0 \sim A \exp(\pm \lambda x). \tag{4.27}$$

gives

$$\lambda = \sqrt{(V-E)}k_0,$$
$$A \sim \frac{\sqrt{g_z}}{\sqrt{g_0}c(\sqrt{(V-E)}k_0)^{\frac{1}{2}}} \sim \frac{\sqrt{g_z}}{c} = \frac{1}{\sqrt{D_0}}$$

This indicates that the quantity $\sqrt{(V-E)}k_0$, controls the attenuation of waves.

Together with a scaling factor A, which effectively scales with $\frac{1}{\sqrt{D_0}}$ only, the actual variation of $\tilde{\eta}_0$ may be faster or slower than $\exp(\pm\lambda x)$. Test cases will be studied in later sections.

4.1.4. Final Remarks on the Definitions of Diagnostic Variables E and V

It is noted that (4.14) differs from the one-dimensional Schrodinger equation by that the 'energy' E is no longer a constant but a function of spatial coordinates (x, y).

It is possible to get rid of the dependence of $E(x)$ on x by an additional step of horizontal coordinate transformation. The advantage of doing so is that only one diagnostic variable $V(x)$, derived from the topographic profile, is needed. The $V(x)$ can be interpreted as the 'potential' function for the wave energy E to ride on. This favours a direct analogy between the quantum mechanical system and surface gravity waves in terms of the analysis on scattering and transmission mechanisms. The details can be found in Maas(1996).

With the present definition of $E(x)$ and $V(x)$ in (4.14), the main advantage is that the information derived from the diagnostic variables directly tells the field of wavenumber $k(x)$ and surface elevation $\eta(x)$ in the physical coordinates without an inverse coordinate transformation. Mathematically the two approaches are identical despite the difference in the physical interpretation. For simplicity, the present definitions will be applied in the remaining text.

4.2. Methodology of Constructing Test Cases

In this section, the methodology to create test cases in order to study the one-dimensional adapted wave equation (4.1) will be presented.

There will be two types of test cases. The first type is purely hypothetical, with unrealistic values of the gravity g_z and water depth D_0. This type of test case is set up to verify the analytic results discussed in the previous sections. The values of parameters for the hypothetical configuration are given in Table 4.1.

The quantity Maximum Perturbing Gravity Δg_z and the Maximum Perturbing Mean-Sea Level ΔD_0 estimate the local maximum of the perturbing gravity field $g_z(x, y)$ and the local maximum of the mean-sea level $z_0(x, y)$. The quantity 'half-life' distance $r_{\frac{1}{2}}$ is a parameter that estimates the distance needed for both the perturbing gravity $g_z'(x, y)$ and the mean-sea level $z_0(x, y)$ to decrease to half of its local maximum. This parameter restricts the gradients of the perturbing gravity field $g_z'(x, y)$ and the mean-sea level $z_0(x, y)$.

Another type of test cases are created to mimic the actual physical setting in the ocean. In particular, two types of shallow water waves in the ocean - Tsunami waves and Tidal waves - will be considered as test case to study the adapted wave equation (4.1). The set of parameters which approximates the actual ocean is proposed in Table 4.2. The parameters in Table 4.2 represent the gravity perturbations g_z' that are solely due to local topographical features and exclude the effect of the Earth's rotation. There will be a separate test case which handles the gravity variation due to the Earth's rotation.

Global Maps of the perturbing gravity and relative mean-sea level are attached in Figure 4.1 and 4.2, from which the Maximum Perturbing Gravity Δg_z and Maximum Perturbing Mean-Sea Level ΔD_0 are estimated.

The value of 'half-life' distance $r_{\frac{1}{2}}$ is roughly estimated based on actual observation data, which suggests an order of magnitude with $\mathcal{O}(100\ \text{km})$. It should be highlighted that the parameters in Table 4.2 are very rough estimates and are expected to be accurate to the order of magnitude only.

As a final remark, a brief introduction to the figures in the same format as Figure 4.3 is given:

- All subplots share the same x-axis representing the relative spatial position, which is normalised to the reference wavelength.

Physical Parameters	Values
Reference Gravity, g_0	$10\ \text{ms}^{-2}$
Mean Depth of Fluid, $\bar{D}_0$	$10\ \text{m}$
Amplitude of incoming wave, η_0	$1\ \text{m}$
Period of incoming wave, T	12 seconds
Angular speed of incoming wave, ω	$\frac{2\pi}{T} = 0.5236\ \text{s}^{-1}$
Reference wavelength, λ_0	$T\sqrt{g_0 D_0} = 120\ \text{m}$
Reference wavenumber, k_0	$\frac{2\pi}{\lambda_0} = 0.05236\ \text{m}$
Maximum Perturbing Gravity, Δg_z	$\pm 2\ \text{ms}^{-2}$
Maximum Perturbing Mean-Sea Level, ΔD_0	$\pm 1\ \text{m}$
'Half-life' Distance, $r_{\frac{1}{2}}$	$\lambda_0 = 120\ \text{m}$
Numerical Parameters	**Values**
Spatial domain of computation	$x \in [0, 5\lambda_0]$ or $[-5\lambda_0, 5\lambda_0]$
Temporal domain of computation	$t \in [0, 12T]$
Number of grid cells	1200
Left Boundary condition	Incoming sinusoidal wave
Right Boundary condition	Outflow boundary

Table 4.1: Configuration for the hypothetical numerical simulations

- The first subplot in the figures show the surface elevation both when the gravity perturbation is present (purple line) and absent (green line). It is reminded that when the two lines almost overlap, only the green line is observable.
- The second subplot outline the difference in surface elevation between the test case and the reference case.
- The third subplot gives the spatial variation of the perturbation of gravity (blue line) and the perturbation of water depth (red line).
- The final subplot plots the spatial dependence of the two diagnostic variables $E(x)$ and $V(x)$ discussed in the previous sections.

4.3. Test Case 1: Uniform Water Depth

In this section, artificial scenarios where the water depth of the ocean is uniform is considered as a test case for the one-dimensional adapted wave equation (4.1).

4.3.1. Rationale and Configuration of Test Case 1

In this first test case, an artificial scenario where the ocean floor $z = S_B(x)$ is adjusted according to the mean-sea level $z = z_0(x)$, such that the time-averaged depth of the ocean $D_0(x) = z_0(x) - S_B(x) = \bar{D}$ is constant at all x.

Since the water depth $D_0(x)$ is no longer spatially dependent, its derivatives vanish. The expression $V(x)$ in (4.13) are thus zero everywhere. Define the reference wavelength k_0 by

$$k_0 = \frac{\omega}{\sqrt{g_0 \bar{D}}}, \tag{4.28}$$

which represents the expected wavelength of the wave when the water depth is constant and the gravity is uniform. The expression for the dimensionless variable E and V are thus given by

$$E(x) = \frac{\omega^2}{g_z \bar{D} {k_0}^2} = \frac{1}{1 + \frac{g_z'}{g_0}} = \frac{g_0}{g_z}, \tag{4.29a}$$

$$V(x) = 0. \tag{4.29b}$$

Physical Parameters	**Values**
Reference Gravity, g_0	9.806228 ms^{-2}
Mean Depth of Ocean, $\bar{D}$	4000 m
Maximum Perturbing Gravity, Δg_z	50 mGal = 0.0005 ms^{-2}
Maximum Perturbing Mean-Sea Level, ΔD_0	50 m
'Half-life' Distance, $r_{\frac{1}{2}}$	500 km
Period of Tsunami wave, T_{tsu}	45 minutes
Period of Tidal wave, T_{tidal}	12 hours
Amplitude of incoming wave, η_0	5 m
Numerical Parameters	**Values**
Spatial domain of computation	$x \in [0, \lambda_0]$ or $[-\lambda, \lambda_0]$
Temporal domain of computation	$t \in [0, 4T]$
Number of grid cells	1200
Left Boundary condition	Incoming sinusoidal wave
Right Boundary condition	Outflow boundary

Table 4.2: Parameters used to mimic the actual physical setting in the Ocean and its waves

Readers are reminded that the effective gravity g_z is given by $g_z = g_0 + g_z'$.

Since $V(x)$ is zero everywhere, the diagnostic variable $\kappa^* = \sqrt{E - V}$ is always real and waves in oscillatory mode solution proposed in (4.19) are always expected. Using the definition of wave speed $c(x)$ in (3.137), equation (4.19) indicates that the plane wave solution to the adapted wave equation is

$$\tilde{\eta}_0 \sim \frac{g_z^{\frac{1}{4}}}{\sqrt{g_0^{\frac{3}{2}} \bar{D} k_0}} \exp(\pm i \int \sqrt{\frac{g_0}{g_z}} k_0 dx). \tag{4.30}$$

Since the effective gravity $g_z(x)$ is decomposed into an uniform component g_0 and small perturbing component g_z' by $g_z(x) = g_0 + g_z'$ and $g_z' \ll g_0$, it justifies a first-order approximation of $\sqrt{\frac{g_0}{g_z}}$ by

$$\sqrt{\frac{g_0}{g_z}} = \left(1 + \frac{g_z'}{g_0}\right)^{-\frac{1}{2}} \approx 1 - \frac{g_z'}{2g_0} \tag{4.31}$$

Hence

$$\exp(\pm i \int \sqrt{\frac{g_0}{g_z}} k_0 dx) \approx \exp\big(\pm i(k_0 x - \frac{k_0}{2g_0} \int g_z' dx)\big), \tag{4.32}$$

If, furthermore, over a small region in which the perturbing gravity g_z' does not vary greatly in space such that the integral $\int g_z'(x) dx$ can be approximated by $g_z'(x)x$, solution (4.30) becomes

$$\tilde{\eta}_0 \sim g_z^{\frac{1}{4}} \exp\big(\pm i k_0 (1 - \frac{g_z'}{2g_0}) x\big). \tag{4.33}$$

Note that the terms g_0 and k_0 in the amplitude component of (4.30) are constants and thus do not contribute to the actual changes. Comparing the approximate solution (4.33) with the standard plane wave $\exp(\pm ikx)$ indicates that the perturbing gravity g_z' locally rescales the reference wavenumber k_0 into the actual wavenumber k over which the gravity perturbation g_z' is approximately constant by

$$k(x) = k_0 (1 - \frac{g_z'}{2g_0}). \tag{4.34}$$

Figure 4.1: Global gravity anomaly (Courtesy NASA)

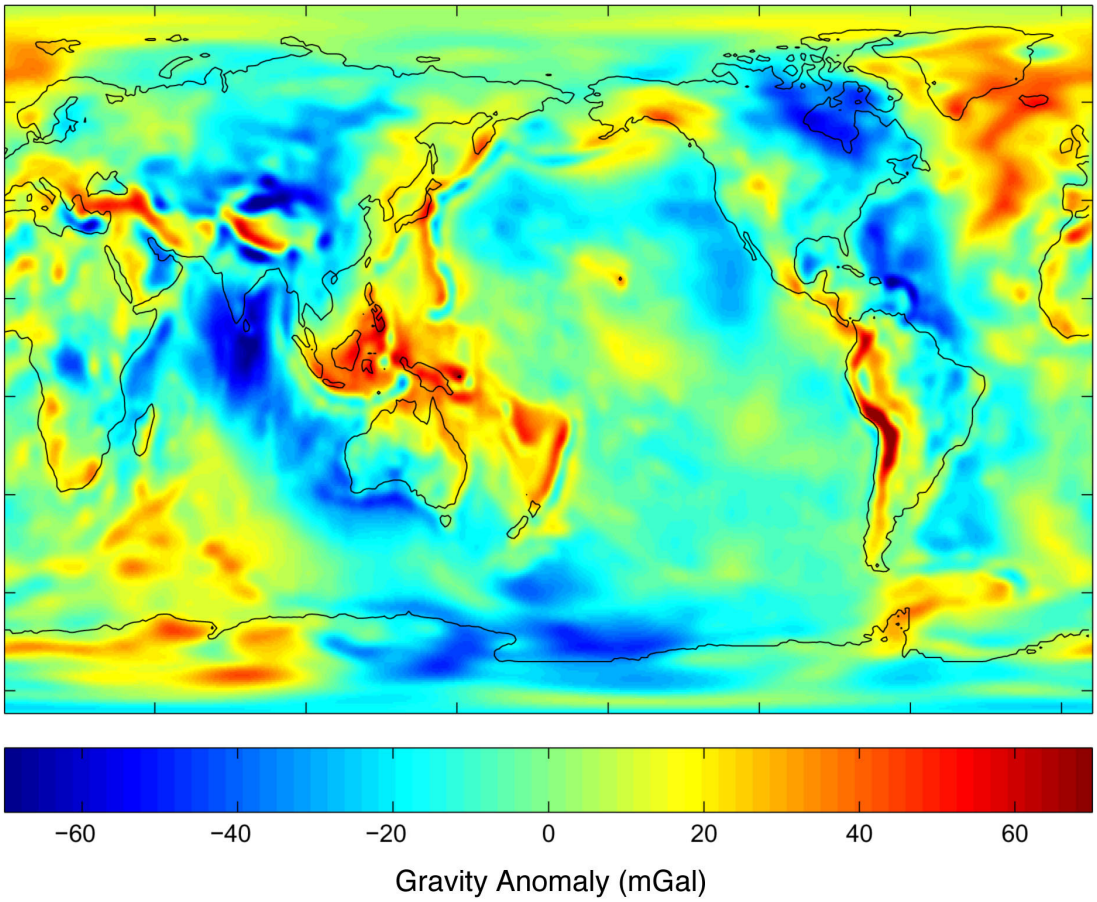

Hence it is expected that when waves propagates into a region with positive gravity variation g_z, the waves will appear to be elongated and vice versa.

Transforming $\tilde{\eta}_0$ back into the physical coordinates gives

$$\eta_0 = \frac{\tilde{\eta}_0}{\frac{\partial Z}{\partial z}} \sim g_z^{-\frac{3}{4}} \exp(\pm i \int \sqrt{\frac{g_0}{g_z}} k_0 dx). \tag{4.35}$$

This suggests that, if the water depth $D_0(x) = \bar{D}$ is constant over space x in the physical space, the surface wave amplitude scales spatially with $\left[g_z(x)\right]^{-\frac{3}{4}}$.

The solution provided in (4.35) can be equivalently expressed in terms of $\kappa^*(x)$ by noting that

$$\kappa^*(x) = \sqrt{\frac{g_0}{g_z(x)}}, \tag{4.36}$$

which, by (4.35), leads to

$$\eta_0 \sim (\kappa^*)^{\frac{3}{2}} \exp\left(\pm i \int \kappa^* k_0 dx\right). \tag{4.37}$$

This can also be derived directly from the general equation (4.20). It can be seen that the diagnostic variable κ^* controls entirely the qualitative behaviour of the solution.

Figure 4.2: Relative elevation of global mean-sea level (Courtesy European Space Agency)

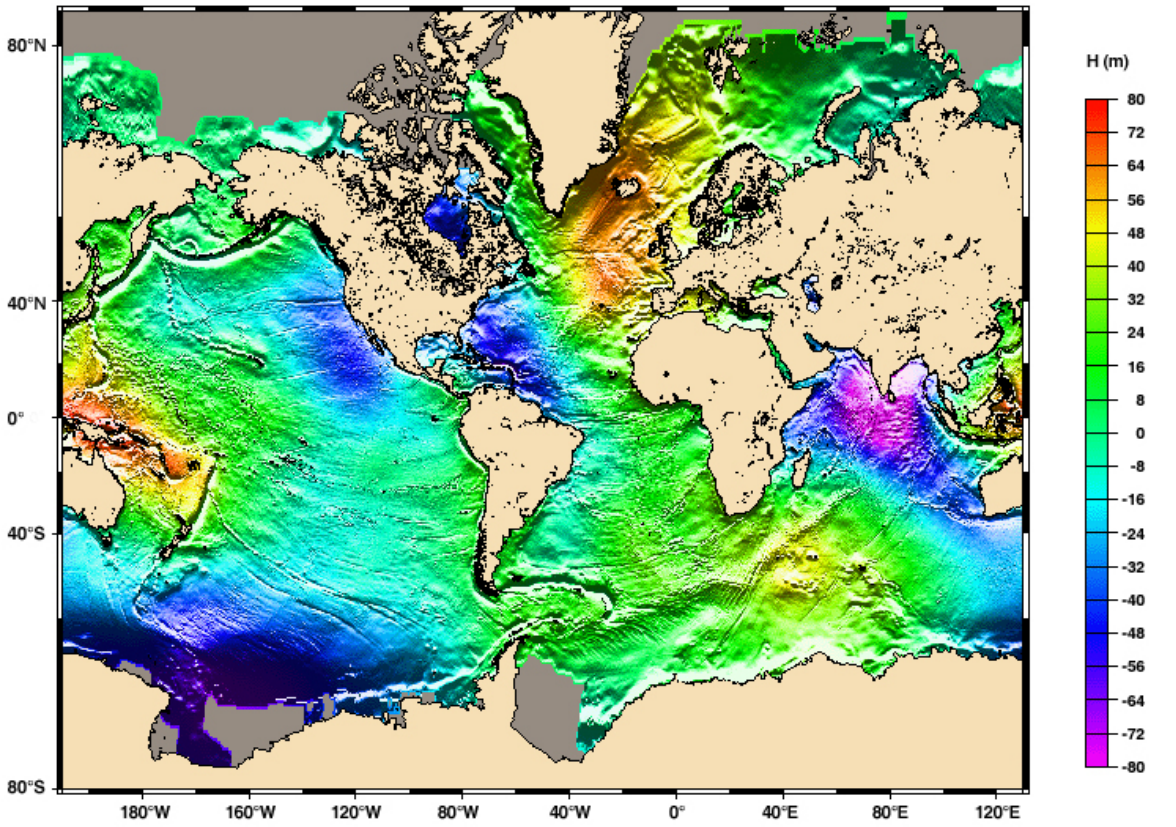

4.3.2. Test Case 1a: Uniform Water Depth + Exponential Gravity Perturbation

Consider an artificial scenario where the magnitude of perturbing gravity $g'_z(x)$ decreases exponentially from $x = 0$ in the positive x-direction, and λ is the positive decay constant. That is,

$$D_0(x) = \bar{D} \tag{4.38}$$
$$g'_z(x) = \Delta g_z \exp(-\lambda x) \tag{4.39}$$

such that the effective gravity g_z is given by

$$g_z(x) = g_0 + g'_z(x) = g_0 + \Delta g_z \exp(-\lambda x) \tag{4.40}$$

Note that only the domain $x \geq 0$ is considered and Δg_z can be positive or negative. Thus Δg_z represents the gravity perturbation at point $x = 0$, which is also the maximum magnitude of gravity perturbation in the interested domain.

It follows from the definition of the reference wavelength k_0 in (4.28) and the simplified definition of E and V in (4.29) that

$$E = \frac{g_0}{g_0 + \Delta g_z \exp(-\lambda x)},$$
$$V = 0.$$

Equation (4.35) indicates that the solution to the adapted wave equation in the physical space, is

$$\eta_0 \sim \left[g_0 + \Delta g_z e^{-\lambda x}\right]^{-\frac{3}{4}} \exp\left(\pm i \frac{2}{\lambda} \arctan\left(\sqrt{\frac{g_0 + \Delta g_z e^{-\lambda x}}{g_0}} \right) \right). \tag{4.41}$$

If Δg_z is positive such that the effective gravity $g_z(x)$ decreases over positive x-direction, the amplitude of the surface wave will grow over space x while the observed wavelength of the surface waves will contract at decreasing rates.

1a.i: Hypothetical Scenario Numerical simulations have been conducted to verify the claims based on the hypothetical scenarios with parameters given in Table 4.1. Figure 4.3 and 4.4 give two examples of the instantaneous solution of the adapted wave equation with positive and negative gravity perturbation respectively. The actual parameters are given in the titles of the figures.

Readers are reminded that the blue dotted lines in the first plot of the figures are the reference solution which corresponds to the scenario with no gravity nor water depth variation. The wavenumber of the reference solution is the reference wavenumber k_0 used to define the dimensionless quantities E and V.

It can be noted that the theoretical bounds (black dots) plotted using the theoretical wave amplitude, which scales with $g_z^{-\frac{3}{4}}$ is derived in equation (4.35), fits very well with the amplitudes of numerical solution (red lines). The observed wavelength of the numerical solution is also consistent with the theoretical prediction in (4.35), which scales reciprocally with κ^* relative to the reference wavelength in the reference solution (blue dotted lines). In particular, when $\kappa^* > 1$, the observed wavelength to contracted with a factor $\frac{1}{\kappa^*}$ relative to the reference wavelength λ_0 and vice verse.

1a.ii: Physical Scenario To mimic the actual gravity field on the Earth, the decay constant λ needs to be determined. However, in reality the gravity perturbation g_z' never decays exponentially. To give a realistic estimation of the decay constant, recall that the 'half-life' distance $r_{\frac{1}{2}}$ for exponential functions is given by

$$r_{\frac{1}{2}} = \frac{\ln(2)}{\lambda}, \tag{4.42}$$

over which the gravity perturbation g_z' decreases by a half. Hence λ is approximated using the value of 'half-life' distance $r_{\frac{1}{2}}$ listed in Table 4.3

Parameters	Values
Decay constant, λ	$\frac{\ln(2)}{500\text{ km}} = 1.3862 \times 10^{-6}\text{ m}^{-1}$

Table 4.3: Parameters used to mimic the actual gravity perturbation by exponential function

Based on the parameters in Table 4.2 and 4.3, numerical solutions have been found for the adapted wave equations (4.1). Figure 4.5 and 4.6 show the simulation results for positive and negative gravity perturbations. It can be noted from both Figure 4.5 and 4.6 that the solutions of test cases nearly coincide with the reference case solution.

The difference between the surface elevation of the test case and the reference case are given in the second subplot of the figures. It can be noted that the difference is maximally of order $\mathcal{O}(10^{-4}\text{ m})$. Given that the actual amplitude of ocean surface wave is of order $\mathcal{O}(1\text{ m})$, the relative difference of surface elevation induced by the gravity is of order $\mathcal{O}(\frac{10^{-4}\text{ m}}{1\text{ m}}) = \mathcal{O}(10^{-4})$, which indicates that the variation of surface elevation due to the gravity perturbation can be neglected in practice.

Nonetheless, comparing the solutions in Figure 4.5 and 4.6 also reveals another interesting feature. In Figure 4.5 where the gravity perturbation is positive, there are periodically small wiggles in the solution. The small wiggles cannot be observed in Figure 4.6 with negative gravity perturbation. The reasons of the presence of these wiggles are unclear. A possible reason could be numerical errors involved in defining flux at some particular grid cells. Another reason could be there exists some natural 'resonant' frequencies of oscillation associated to the positive gravity perturbation. This may be rationalised by the wave trapping mechanism seen in both surface waves and quantum mechanics, in which the wave amplitude field is exponential when energy E is smaller than V locally. Further investigation is needed to confirm the claim. In any case, since the magnitude of the wiggles are minimal, they are neglected for the purpose of this project.

4.3.3. Test Case 1b: Uniform Water Depth + Gaussian Gravity Perturbation

Consider the case again that the Bathymetry is uniform so that $D_0(x) = \bar{D}_0$. The gravity perturbation g_z' is, however, taken by the Gaussian function

$$g_z'(x) = \Delta g_z \exp\left(\frac{-x^2}{2\sigma^2}\right), \tag{4.43}$$

where Δg_z is a real constant and $\sigma > 0$ is the dispersion parameter, a parameter that controls the spread of the perturbation. The domain of interest is the entire x-axis.

It follows from the definition of the reference wavelength k_0 in (4.28) and the simplified definition of E and V in (4.29) that

$$E = \frac{g_0}{g_0 + \Delta g_z \exp\left(\frac{-x^2}{2\sigma^2}\right)},$$
$$V = 0.$$

A gravity perturbation g_z' modelled by the Gaussian function mimics an excess or deficit of mass in the ocean floor near $x = 0$. The case $\Delta g_z > 0$ represents there is excess mass beneath the ocean floor and thus induces extra gravity. An important parameter that measures the spread of the Gaussian function is the **Full width at half maximum (FWHM)**, which is given by

$$FWHM = \sqrt{2\ln(2)}\sigma. \tag{4.44}$$

From the expression (4.43), when $x = \sqrt{2\ln(2)}\sigma$, the value of the gravity perturbation is half of its peak located at $x = 0$.

1b.i: Hypothetical Scenario Numerical simulations have been conducted based on the hypothetical scenarios with parameters given in Table 4.1. Figure 4.7 and 4.8 give two examples of the instantaneous solution of the adapted wave equation with positive and negative gravity perturbation respectively. The actual parameters are given in the titles of the figures.

It can be noted again that the theoretical bounds fit well with the amplitudes of waves in the numerical solution. Also, while the waves propagate through the region with gravity perturbation, they experience a phase change, as predicted from solution (4.35).

If the dispersion parameter σ is lowered by one order of magnitude to 'localise' the gravity perturbation, it can be noted from Figure (4.9) and (4.10) that the difference between the test case waves and reference waves (second subplot) are qualitatively different from that of the non-localised versions in Figure 4.7 and 4.8, namely, there are periodic differences between the test case waves and reference waves in the 'incoming' section of the wave (domain of $x < 0$) where the 'waves' should have not experienced any variation in gravity.

To investigate the reason behind the periodic difference, the test case waves are examined at an earlier instant when the wave signals have not arrived the region with gravity perturbation. Figure 4.11 and 4.12 give two examples.

It can be observed that the difference between the test case waves and reference waves before the test case waves hit the region with gravity variation is minimal. These imply that the period difference seen in Figure 4.7 and 4.8 are very likely to be caused by reflection of waves at the region with localised gravity variation. This motivates the studies of the reflection-transmission mechanisms due to gravity perturbation, will be discussed in the next test case.

1b.ii: Physical Scenario To mimic the actual gravity variation, the parameter σ is chosen such that the *FWHM*= 500 km as in Table 4.4 .

Parameters	Values
Dispersion parameter, σ	$\frac{500\text{ km}}{\sqrt{2\ln(2)}} = 4.2466 \times 10^5$ m

Table 4.4: Parameters used to mimic the actual gravity perturbation by gaussian function

Numerical simulations have also been conducted to study the effect of the Gaussian gravity perturbation in a more realistic setting, based on the hypothetical scenarios with parameters given in Table 4.2 and 4.4.

The first group of studies are based on Tsunami waves with wave period T taken as $T = 45$ minutes. Figure 4.13 and 4.14 show two examples of the solutions at some time.

The second group of studies are based on the tidal waves which has period $T = 12$ hours. Figure 4.15 and 4.16 give a numerical solution at certain time to the adapted wave equation with incoming tidal waves, based on parameters given in Table 4.2 and 4.4.

It can be seen in both the cases of tidal and tsunami waves that the instantaneous difference between the test case waves and reference waves are maximally of order $\mathcal{O}(10^{-3}\ \mathrm{m})$, which indicates that in practice the effects of gravity on the amplitude of ocean surface wave can hardly be measured.

Comparing the difference between test case and reference waves (second subplots) in the tsunami waves from Figure 4.13 or 4.14 with that in the tidal waves in Figure 4.15 or 4.16, it can be noted that similar patterns respectively with the hypothetical cases in Figure 4.7 or 4.8 with Figure 4.9 or 4.10 have occured. These highlight the importance of the 'locality' of the gravity perturbation, which is measured relative to the wavelength of the waves. This provides another direction to study the reflection-transmission mechanisms of waves in the next test case.

Short Conclusions from Test Case 1

- When the depth is uniform, the amplitude A of surface waves scales with the magnitude of gravity by $A \sim g_z^{-\frac{3}{4}}$.
- It appears to be possible to reflect ocean surface wave by gravity variation. The 'locality' of the gravity perturbation, measured relative to the wavelength of surface waves, seems to be a factor also in controlling the amplitude of reflected waves.
- The gravity perturbation in the ocean is relatively more 'localised' to tidal waves than tsunami waves. Reflection of tidal waves due to gravity perturbation is more likely than tsunami waves.
- Depsite the theoretical implications, the gravity variation in the actual ocean is too small to affect any tsunami waves or tidal wave practically.

4.4. Test case 2: Reflection and Scattering of Surface Waves by Varying Gravity

4.4.1. Rationale and Configuration of Test Case 2

In test case 1, it has been noted that the gravity variation seems to play a role in reflecting ocean surface waves. In this section, the surface waves under several artificial configurations of gravity fields will be studied analytically. The goal of this chapter is to understand the reflection of surface waves by gravity.

4.4.2. Test case 2a: Gravity Step

The first case to study is the simple configuration with piecewise constant gravity field g_z:

$$g_z(x) = \begin{cases} g_l, & x \le 0 \\ g_r, & x > 0 \end{cases} \tag{4.45}$$

where g_1 and g_2 are constants. The water depth $D_0(x)$ is constant everywhere.

Based on the general solution (4.37), the spatial structure of the surface surface wave $\eta(x)$ should be

$$\eta(x) \sim \begin{cases} \exp\left(\pm i\kappa_l^* k_0 x\right), & x \le 0 \\ \exp\left(\pm i\kappa_r^* k_0 x\right), & x > 0 \end{cases} \tag{4.46}$$

where $k_0 = \frac{\omega}{\sqrt{g_0 \bar{D}}}$, $\kappa_l^* = \sqrt{\frac{g_0}{g_l}}$ and $\kappa_r^* = \sqrt{\frac{g_0}{g_r}}$ are constants.

Consider a sinusoidal incoming surface wave from the $x = -\infty$, with incoming amplitude A and wavenumber $\kappa_1^* k_0$. Suppose the incoming wave partially reflects at $x = 0$, thus it is expected that the spatial solution of the wave is

$$\eta(x) = \begin{cases} A\exp(i\kappa_l^* k_0 x) + B\exp(-i\kappa_l^* k_0 x), & x \le 0 \\ F\exp(i\kappa_r^* k_0 x), & x > 0 \end{cases} \tag{4.47}$$

In addition, it is assumed that

1. The surface elevation $\eta(x)$ is continuous everywhere. (4.48a)
2. Its first derivative $\frac{d\eta}{dx}$ is also continuous everywhere. (4.48b)

It can then be shown that after algebraic manipulation

$$\frac{B}{A} = \frac{\kappa_l^* - \kappa_r^*}{\kappa_l^* + \kappa_r^*} \tag{4.49}$$

$$\frac{F}{A} = \frac{2\kappa_l^*}{\kappa_l^* + \kappa_r^*} \tag{4.50}$$

Expressing $\frac{B}{A}$ and $\frac{F}{A}$ in terms of the gravity gives the reflection and transmission coefficients in uniform water depth:

$$\frac{B}{A} = \frac{\sqrt{g_r} - \sqrt{g_l}}{\sqrt{g_l} + \sqrt{g_r}} \tag{4.51}$$

$$\frac{F}{A} = \frac{2\sqrt{g_r}}{\sqrt{g_l} + \sqrt{g_r}} \tag{4.52}$$

These indicate the greater the ratio $\frac{g_l}{g_r}$ is, the greater reflection of surface waves is. Also, if the gravity g_r in the region of $x > 0$ is smaller than that of g_l in $x < 0$, a π-phase shift is expected in the reflected wave.

The reflection coefficient $R = \frac{|B|^2}{|A|^2}$ and transmission coefficient $T = \frac{|F|^2}{|A|^2}$ are thus given by

$$R = \frac{(\kappa_l^* - \kappa_r^*)^2}{(\kappa_l^* + \kappa_r^*)^2} = \frac{(\sqrt{g_r} - \sqrt{g_l})^2}{(\sqrt{g_l} + \sqrt{g_r})^2} \tag{4.53}$$

$$T = \frac{4{\kappa_l^*}^2}{(\kappa_l^* + \kappa_r^*)^2} = \frac{4g_r}{(\sqrt{g_l} + \sqrt{g_r})^2}. \tag{4.54}$$

Note that $R + T = 1$.

4.4.3. Test case 2b: Gravity Well

The next configuration is a three-section piecewise constant gravity field g_z:

$$g_z(x) = \begin{cases} g_a, & \text{Region a}^-\text{: } x \le -L \\ g_b, & \text{Region b: } -L < x \le L \\ g_a, & \text{Region a}^+\text{: } x > L \end{cases} \tag{4.55}$$

with an expected solution

$$\eta(x) = \begin{cases} A\exp(i\kappa_a^* k_0 x) + B\exp(-i\kappa_a^* k_0 x), & \text{Region a}^-\text{: } x \le -L \\ C\exp(i\kappa_b^* k_0 x) + D\exp(-i\kappa_b^* k_0 x), & \text{Region b: } -L < x \le L \\ F\exp(i\kappa_a^* k_0 x), & \text{Region a}^+\text{: } x > L \end{cases} \tag{4.56}$$

where $k_0 = \frac{\omega}{\sqrt{g_0 D}}$, $\kappa_a^* = \sqrt{\frac{g_0}{g_a}}$ and $\kappa_b^* = \sqrt{\frac{g_0}{g_b}}$ are real constants.

This configuration can be interpreted as an infinite domain with gravity g_a, together with a gravity perturbation of magnitude $g_b - g_a$ in region b: $(-L, L)$. The water depth $D_0(x) = \bar{D}$ is constant for all x. Imposing the same conditions (4.48), it can be shown that

$$R_{ab} \equiv \frac{|B|^2}{|A|^2} = \frac{4(\kappa_a^{*2} - \kappa_b^{*2})^2 \sin^2(2\kappa_b^* k_0 L)}{16\kappa_a^{*2}\kappa_b^{*2} + 4(\kappa_a^{*2} - \kappa_b^{*2})^2 \sin^2(2\kappa_b^* k_0 L)} \tag{4.57}$$

$$T_{ab} \equiv \frac{|C|^2}{|A|^2} = \frac{4\kappa_a^{*2}(\kappa_a^* + \kappa_b^*)^2}{16\kappa_a^{*2}\kappa_b^{*2} + 4(\kappa_a^{*2} - \kappa_b^{*2})^2 \sin^2(2\kappa_b^* k_0 L)} \tag{4.58}$$

$$R_{bc} \equiv \frac{|D|^2}{|A|^2} = \frac{4\kappa_a^{*2}(\kappa_a^* - \kappa_b^*)^2}{16\kappa_a^{*2}\kappa_b^{*2} + 4(\kappa_a^{*2} - \kappa_b^{*2})^2 \sin^2(2\kappa_b^* k_0 L)} \tag{4.59}$$

$$T_{bc} \equiv \frac{|F|^2}{|A|^2} = \frac{16\kappa_a^{*2}\kappa_b^{*2}}{16\kappa_a^{*2}\kappa_b^{*2} + 4(\kappa_a^{*2} - \kappa_b^{*2})^2 \sin^2(2\kappa_b^* k_0 L)}, \tag{4.60}$$

where R_{ab} and T_{ab} are the reflection and transmission coefficients at the interface of Region a$^-$ and b relative to the incoming waves. Analogously the same definition applies for R_{cd} and T_{cd} at the interface of Region b and a$^+$. In terms of the values of gravity, these coefficients are given by

$$R_{ab} \equiv \frac{|B|^2}{|A|^2} = \frac{4(g_b - g_a)^2 \sin^2(2\kappa_b^* k_0 L)}{16 g_a g_b + 4(g_b - g_a)^2 \sin^2(2\kappa_b^* k_0 L)} \tag{4.61}$$

$$T_{ab} \equiv \frac{|C|^2}{|A|^2} = \frac{4g_b(\sqrt{g_a} + \sqrt{g_b})^2}{16 g_a g_b + 4(g_a - g_b)^2 \sin^2(2\kappa_b^* k_0 L)} \tag{4.62}$$

$$R_{bc} \equiv \frac{|D|^2}{|A|^2} = \frac{4g_b(\sqrt{g_b} - \sqrt{g_a})^2}{16 g_a g_b + 4(g_a - g_b)^2 \sin^2(2\kappa_b^* k_0 L)} \tag{4.63}$$

$$T_{bc} \equiv \frac{|F|^2}{|A|^2} = \frac{16 g_a g_b}{16 g_a g_b + 4(g_b - g_a)^2 \sin^2(2\kappa_b^* k_0 L)}, \tag{4.64}$$

Note that also $R_{ab}^2 + T_{bc}^2 = 1$.

The reflection coefficient R_{ab} indicates that the amplitude of the reflected waves do not only depend on the perturbing gravity $g_b - g_a$, but also the length of region $b = 2L$ where the perturbation gravity is added, and the wavenumber of waves in region b, given by $k_b = \kappa_b^* k_0$.

Given the values of gravity g_a and g_b and a positive integer n, it is noted that when $k_b = \frac{n\pi}{2L}$, the reflection coefficient $R_{ab} = 0$; when $k_b = \frac{(2n+1)\pi}{2(2L)}$, the reflection coefficient attends its maximum with $\frac{4(g_b - g_a)^2}{16 g_a g_b + 4(g_b - g_a)^2}$. In the particular case when the perturbation in gravity is highly 'localised' relative to the wavelength of the waves such that $2Lk_b \to 0$, it is expected that the reflection of waves is not very likely.

Based on this preliminary study, it should be expected that, since the wavelengths of tidal waves are much larger than the length scales of the region with gravity perturbation, tidal waves are anyway not very likely to be reflected by the gravity variation.

For the tsunami waves whose wavelengths are comparable to the characteristic lengths of area with gravity perturbation, in theory, whether the reflection take places depends on the actual wavelengths and size of region with gravity perturbation.

However, a closer look of the reflection coefficient R_{ab} reveals that since the gravity perturbation $g_b - g_a$ in practice is maximally with order of magnitude $\mathcal{O}(10^{-2}\ \text{ms}^2)$, while the gravity g_a or g_b both are roughly 10ms^2 in practice, the reflection coefficient R_{ab} is maximally with order of magnitude $\mathcal{O}(10^{-6})$. Hence in practice, with the current measurement facilities, it is not expected that the reflected tidal or tsunami wave induced purely by the gravity variation will be measurable.

4.4.4. Short Conclusions from Test case 2

- Reflection and Transmission of surface waves by gravity variation is possible
- Despite the theoretical possibility, the actual variation of gravity field seems to be insufficient in reflection any ocean surface wave in an observable manner

In the next test case, another effect of the gravity anomaly will be focused, namely, its induced variation on the mean-sea level $z_0(x,y)$, or the sea-surface topography.

4.5. Test Case 3: Non-Flat Sea-Surface Topography

4.5.1. Rationale and Configuration of Test Case 3

The term sea-surface topography refers to the spatial variation of mean-sea level z_0 due to non-uniform distribution of gravity. Typically variation ΔD_0 can amount up to ± 80m, which gives a relative variation to the water depth D_0 in the ocean by $\frac{\Delta D_0}{\bar{D}_0} \sim \mathcal{O}(\frac{80\text{m}}{4000\text{m}}) = \mathcal{O}(10^{-2})$, which is much larger than the relative variation of gravity $= \frac{g_z'}{g_0} \sim \mathcal{O}(10^{-5})$.

In Test case 3, the ocean floor $z = S_B(x)$ is assumed to be flat, that is, $S_B(x)$ is a constant. However, due to the presence of spatially dependent gravity perturbation g_z', the mean-sea level z_0 varies in space. Hence the water depth $D_0(x) = z_0(x) - S_B$ becomes also spatially dependent and its variation are predominantly given by the mean-sea level.

For simplicity, it is assumed in this section that the water depth $D_0(x)$ can be decomposed into a uniform component $\bar{D}$ and spatially dependent perturbing component $D_0'(x)$. Furthermore, it is assumed that the perturbing gravity $g_z'(x)$ and the perturbing component of the water depth $D_0(x)$ are linearly related. In other words, it is assumed that

$$g_z(x) = g_0 + g_z'(x) \tag{4.65}$$

$$D_0(x) = \bar{D} + D_0'(x) \tag{4.66}$$

with

$$D_0'(x) \propto g_z'(x). \tag{4.67}$$

Readers are reminded that, however, while the sea-surface topography mimics the spatial variation perturbing gravity field, there is no definite correlation between the magnitude of the gravity field g_z' and the mean-sea level z_0.

Recall the definition of the diagnostic variables E and V, given by equation (4.8),

$$E(x) = \frac{\omega^2}{g_z D_0 {k_0}^2},$$

$$V(x) = \frac{1}{4{k_0}^2 {D_0}^2}\left[2D_0\frac{\partial^2 D_0}{\partial x^2} - \left(\frac{\partial D_0}{\partial x}\right)^2\right],$$

By choosing the reference wavenumber k_0 to be

$$k_0 = \frac{\omega}{\sqrt{g_0 \bar{D}}}, \tag{4.69}$$

The expression for E and V becomes

$$E(x) = \frac{1}{\left[1+\frac{g_z'}{g_0}\right]\left[1+\frac{D_0'}{\bar{D}}\right]}, \tag{4.70a}$$

$$V(x) = \frac{g_0\bar{D}}{\omega^2}\left[\frac{(D_0')_{xx}}{2D_0} - \frac{[(D_0')_x]^2}{4(D_0)^2}\right]. \tag{4.70b}$$

Note that for small perturbations of gravity $g_z' \ll g_0$ and water depth $D_0' \ll \bar{D}$, the quantity E is approximately equal to 1.

If the the variation of the water depth is too 'small', in the sense that both $\frac{g_0\bar{D}}{\omega^2}\frac{(D_0')_{xx}}{D_0}$ and $\frac{g_0\bar{D}}{\omega^2}\frac{[(D_0')_x]^2}{(D_0)^2}$ in $V(x)$ do not scale with order of magnitude of at least $\mathcal{O}(10^{-1})$, the diagnostic quantity $\kappa^*(x) = E(x) - V(x)$ can be approximated by dropping the contribution from $V(x)$

$$\kappa^*(x) \approx E(x) = \frac{1}{\left[1+\frac{g_z'}{g_0}\right]\left[1+\frac{D_0'}{\bar{D}}\right]} > 0. \tag{4.71}$$

The oscillatory solution (4.20) can thus be applied and the solution in the transformed coordinates is given by

$$\tilde{\eta}_0 \sim (\frac{g_z}{D_0})^{\frac{1}{4}} \exp(\pm i \int \frac{k_0}{\sqrt{[1+\frac{g_z'}{g_0}][1+\frac{D_0'}{\bar{D}}]}} dx). \tag{4.72}$$

Transforming $\tilde{\eta}_0$ back to η_0 defined in physical coordinates gives

$$\eta_0 \sim (\frac{1}{g_z^{\frac{3}{4}} D_0^{\frac{1}{4}}}) \exp(\pm i \int \frac{k_0}{\sqrt{[1+\frac{g_z'}{g_0}][1+\frac{D_0'}{\bar{D}}]}} dx), \tag{4.73}$$

which suggests the wave amplitude $A(x)$ scales spatially with $g_z^{-\frac{3}{4}} D_0^{-\frac{1}{4}}$.

Recall that when the gravity is uniform, the wave amplitude scales spatially with $D_0^{-\frac{1}{4}}$. Now with the spatial variation in gravity, there is an extra scaling factor $g_z^{-\frac{3}{4}}$ for the wave amplitude.

4.5.2. Test case 3a: Exponential Water Depth + Exponential Gravity Perturbation

In this test case, the ocean floor $S_B(x)$ is flat but the mean-sea level z_0 contains a perturbing component which decays exponentially. Therefore, the perturbing water depth $D_0'(x)$ and the perturbing gravity $g_z'(x)$ are given by

$$D_0'(x) = \Delta D_0 \exp(-\lambda x) \tag{4.74a}$$
$$g_z(x) = \Delta g_z \exp(-\lambda x), \tag{4.74b}$$

where ΔD_0 and Δg_z are constants which represents the maximum values of perturbation in water depth D_0 and gravity g_z. λ is a constant which measures the rate of decay of the perturbation. Note that only the domain of positive x is considered. The expression of E and V given by equation (4.70) thus becomes

$$E(x) = \frac{1}{[1+\frac{\Delta g_z}{g_0}\exp(-\lambda x)][1+\frac{\Delta D_0}{\bar{D}_0}\exp(-\lambda x)]} \tag{4.75a}$$
$$V(x) = \left(\frac{g_0 \bar{D}_0}{\omega^2}\right)\left(\frac{\lambda^2}{4}\right)\left[\frac{\Delta D_0 e^{-\lambda x} + 2\bar{D}_0}{(\bar{D}_0 + \Delta D_0 e^{-\lambda x})^2}(\Delta D_0 e^{-\lambda x})\right]. \tag{4.75b}$$

It can be shown that $V(x)$ attains its maximum on the domain $x \geq 0$ at $x = 0$. Note that $V(0)$ is given by

$$V(0) = \left(\frac{g_0 \bar{D}_0}{\omega^2}\right)\left(\frac{\lambda^2}{4}\right)\left[\frac{\Delta D_0 + 2\bar{D}_0}{(\bar{D}_0 + \Delta D_0)^2}(\Delta D_0)\right] \tag{4.76}$$

Using the parameters listed in Table 4.2 and 4.3, for tsunami waves the dimensionless quantity $V(0)$ is of the order of magnitude $\mathcal{O}(10^{-7})$ and for tidal waves the quantity$V(0)$ is of the order of magnitude $\mathcal{O}(10^{-6})$. Meanwhile the order of magnitude of E is $\mathcal{O}(1)$. These justify the approximation $\kappa^* = E - V \approx E$ in the approximation (4.71) and offer validity to the solution (4.73).

3a.i: Hypothetical Scenario Based on the parameters and configuration listed in Table 4.1, numerical solutions to the one-dimensional adapted wave equation (4.1) have been found. Figure 4.17 gives an example of the numerical solution when the gravity perturbation is positive. It is noted that $V(x) << E(x)$ and thus the approximation (4.71) is valid.

It can also be noted from Figure 4.17 that the amplitude of waves fits well with the theoretical prediction given in the general solution (4.73). Comparing Figure 4.17 with Figure 4.3 reveals that the phase difference between the test case wave and reference wave is enlarged when the perturbation of sea-surface elevation is considered. This is not unexpected since $\kappa^*(x)$ is scaled with a extra factor $\frac{1}{1+\frac{D_0'}{\bar{D}}}$ in (4.71) compared with (4.29) when the variation of water depth D_0 is excluded.

3a.ii: Physical Scenario Numerical solutions based on the parameters associated with tsunami and tidal waves listed in Table 4.2 and 4.3 are obtained. Figure 4.18, 4.19, 4.20 and 4.21 give some examples of the numerical solutions.

Figure 4.20 and 4.21 show that the instantaneous difference between the test case wave and reference has an order of magnitude $\mathcal{O}(0.01\text{ m})$, which is much greater than the $\mathcal{O}(10^{-4}\text{ m})$ in Figure 4.5 and 4.6 without the perturbation in water depth. This indicates that the perturbation of the mean-sea level is much more likely to affect the wave dynamics than the gravity perturbation itself, despite the fact that the difference is still unlikely to be measured by any observational tools.

Similarly to the case without mean-sea level perturbation, it is noted from the instantaneous difference between the test case wave and reference wave in Figure 4.20 that there are small-amplitude periodic wiggles. The detailed mechanism of the emergence of these wiggles will be analysed.

4.5.3. Test case 3b: Gaussian Water Depth + Gaussian Gravity Perturbation

In this test case, the ocean floor $S_B(x)$ is again flat. The gravity and mean-sea level $z_0(x)$ are perturbed with a Gaussian function. In other words,

$$D_0'(x) = \Delta D_0 \exp\left(\frac{-x^2}{2\sigma^2}\right), \tag{4.77a}$$

$$g_z(x) = \Delta g_z \exp\left(\frac{-x^2}{2\sigma^2}\right), \tag{4.77b}$$

with σ being the dispersion parameter which measures the spread of the peak of the Gaussian function.

It follows from equation (4.70) that the expression of E and V becomes

$$E(x) = \frac{1}{\left[1 + \frac{\Delta g_z}{g_0} e^{\frac{-x^2}{2\sigma^2}}\right]\left[1 + \frac{\Delta D_0}{\bar{D}_0} e^{\frac{-x^2}{2\sigma^2}}\right]}, \tag{4.78a}$$

$$V(x) = \left(\frac{g_0 \bar{D}_0}{\omega^2}\right)\left(\frac{-1}{4\sigma^4}\right)\left[\frac{(2\sigma^2 - x^2)\Delta D_0 e^{\frac{-x^2}{2\sigma^2}} + 2(\sigma^2 - x^2)\bar{D}_0}{(\bar{D}_0 + \Delta D_0 e^{\frac{-x^2}{2\sigma^2}})^2}\right](\Delta D_0 e^{\frac{-x^2}{2\sigma^2}}) \tag{4.78b}$$

Since the numerical solutions of the hypothetical scenario based on the parameters given in Table 4.1 do not provide much additional insight, they are omitted in this report.

3b: Physical Scenario Numerical solution for incoming tsunami and tidal waves are transmitted to a region with Gaussian gravity and mean-sea level perturbation are obtained. The parameters for the computation are listed in Table 4.2 and 4.3. Figure 4.22, 4.23, 4.24 and 4.25 give some examples of the numerical solutions.

These figures are very similar to Figure 4.13, 4.14, 4.15 and 4.16 except that the instantaneous difference between the test case wave and reference wave is much larger when the perturbation of the mean-sea level is taken into account. This is not unexpected given the general solution given in (4.73).

4.5.4. Short Conclusions from Test case 3

- When the water depth is perturbed together with the gravity, the amplitude A of surface waves scales with the magnitude of gravity by $A \sim g_z^{-\frac{3}{4}} D_0^{-\frac{1}{4}}$.
- It is more likely to reflect ocean surface wave by the variation of gravity-induced mean-sea level than the gravity itself.
- Despite the theoretical implications, the gravity-induced mean-sea level variation in the actual ocean is still too small to induce any observable changes on tsunami wave or tidal wave in practice.

4.6. Test Case 4: Global Variation of Gravity

4.6.1. Rationale and Configuration of Test Case 4

Due to the presence of centrifugal force, the effective gravity g_z near the equator on the Earth is significantly lower than that in near the pole. An empirically-based formula know as the **International Gravity Formula**, is often used to evaluate the theoretical gravity g_r at different latitude ϕ. The formula is cited here

$$g_r(\phi) = g_e(1 + A\sin^2(\phi) - B\sin^2(2\phi)^2), \tag{4.79}$$

where $g_e = 9.780327$ m/s^2 is the gravity at equator, $A = 0.0053024$ and $B = 0.0000058$ are empircally determined constants.

The plot of g_r over latitude is given in Figure 4.26. It can be noted that the gravity is weakest in the equator at roughly 9.78 ms^{-2} and strongest near the pole with approximately 9.83 ms^{-2}.

4.6.2. Test Case 4a: Surface Waves on an Arc

To simplify the analysis, the waves motion along an arc on Earth's surface is considered. This is achieved by projecting the latitude ϕ on single spatial coordinates x, which is given by

$$x = R_E\phi, \tag{4.80}$$

where $R_E = 6371$ km is an estimated radius of Earth.

With the projection, the effective gravity g_z can be thus expressed in the form of

$$g_z(x) = g_0 + g_z'(x) \tag{4.81}$$

by choosing the reference gravity g_0 and perturbing gravity $g_z'(x)$ as

$$g_0 = g_e \tag{4.82}$$

$$g_z'(x) = g_e(A\sin^2(\frac{x}{R_E}) - B\sin^2(\frac{2x}{R_E})) \tag{4.83}$$

Furthermore, consider the case where the water depth D_0 is uniformly equal to 4000m everywhere along the arc. This makes the diagnostic variable $V(x)$ given in (4.13) becomes strictly zero.

It has been demonstrated in test case 1, that when the water depth is uniform, the surface elevation η_0 in the physical coordinates is given by equation (4.35)

$$\eta_0 \sim g_z^{-\frac{3}{4}}\exp(\pm i\int\sqrt{\frac{g_0}{g_z}}k_0 dx),$$

where $k_0 = \frac{\omega}{\sqrt{g_0 D_0}}$ is a reference wavelength.

This suggests when given surface waves with wavenumber k_0 and amplitude η_0 at the equator propagate towards the pole with stronger gravity, the wavenumber will appear to decrease to $k_1 = \sqrt{\frac{g_0}{g_z}}k_0 \approx \sqrt{\frac{9.78}{9.83}}k_0 \approx 0.9984k_0$ and the wave amplitude will appear to increase to $\eta_1 = \left(\frac{g_z}{g_0}\right)^{-\frac{3}{4}}\eta_0 \approx 1.0023\eta_0$. In other words, a maximally 0.3% percentage change of wavelength and amplitude would be experienced by the ocean surface waves due to the meridional gravity gradient on the Earth.

With the present measurement facilities, it will be extremely challenging, if not impossible, to isolate the minimal effects of gravity variation on surface waves from other factors such as the non-uniform bathymetry, tidal forcing and wind-forcing. This makes empirical analysis of global scale ocean surface waves impractical.

4.6.3. Short Conclusions from Test case 4

- In test case 4 the meridional gravity variation due to rotation of Earth is reviewed.
- In an idealistic scenario where one-dimensional surface waves are considered in a uniformly-deep ocean, it has been shown with the aid of test case 1 that the meridional gravity gradient is not strong enough to induce any observable changes on surface waves in practice.

4.7. Conclusions from One-Dimensional Adapted Shallow Water Waves

In this chapter, analytical solutions to the adapted shallow water waves derived in Chapter 3 in one-dimensional space were studied. The analytical solutions were also verified numerically in both hypothetical and geophysical scenarios.

Surface waves in fluid with uniform depth are studied in test case 1. The analytical solutions are verified by numerical solution. Reflection and transmission of surface waves due to gravity perturbation were examined both numerically and analytically in test case 2.

In test case 3, the effects of non-flat sea-surface topography on the adapted shallow water waves are studied both analytically and numerically. It has been shown that the surface waves in practice are more sensitive to the induced sea-surface topography than the gravity variation itself.

In test case 4, the gravity variation due to Earth's rotation, which are much stronger than that originated from topographical features, are studied. However, it is demonstrated that the gravity perturbation is still insufficient in making any observable effects in the actual ocean.

To sum up, the one-dimensional studies reveals it is highly unlikely for surface waves in the ocean to be altered in an observable manner due to the gravity variation. This justifies the traditional assumption that the gravity is taken to be a constant uniformly in space in the studies of surface waves.

Figure 4.3: Numerical Simulations with Positive Exponential Gravity Perturbation; Hypothetical Scenario

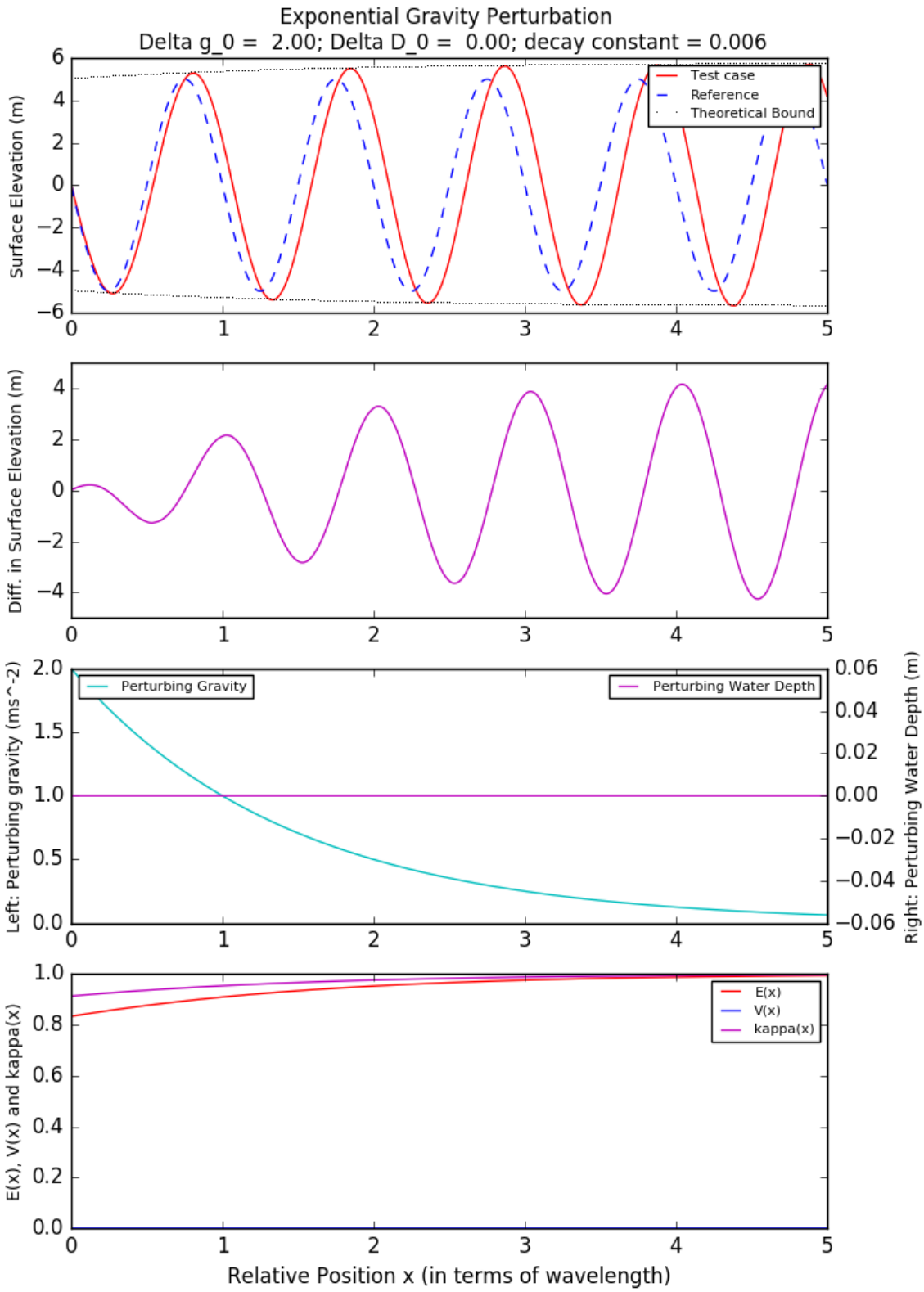

Figure 4.4: Numerical Simulations with Negative Exponential Gravity Perturbation; Hypothetical Scenario

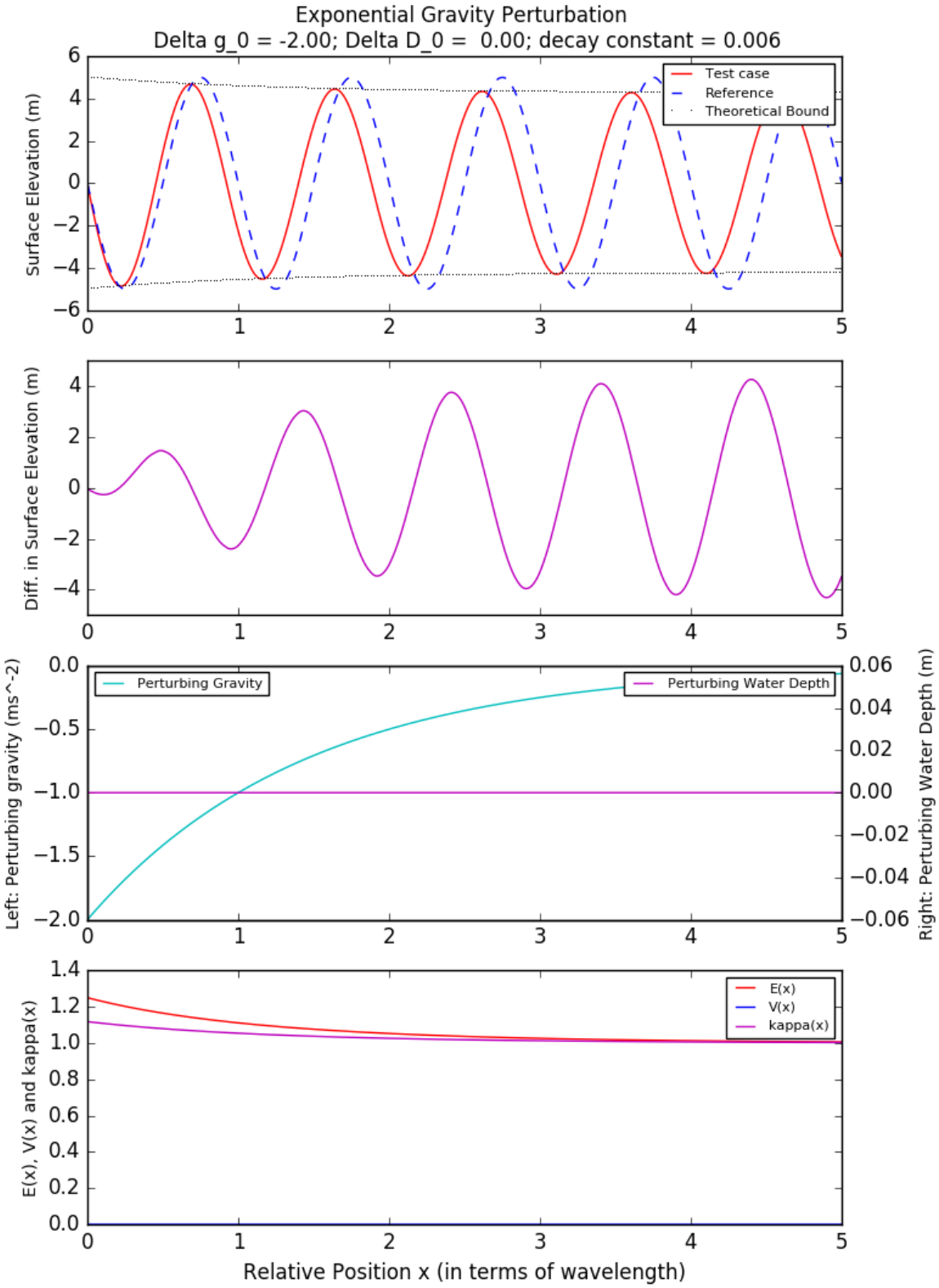

Figure 4.5: Numerical Simulations with Positive Exponential Gravity Perturbation; Physical Scenario - Incoming tidal wave

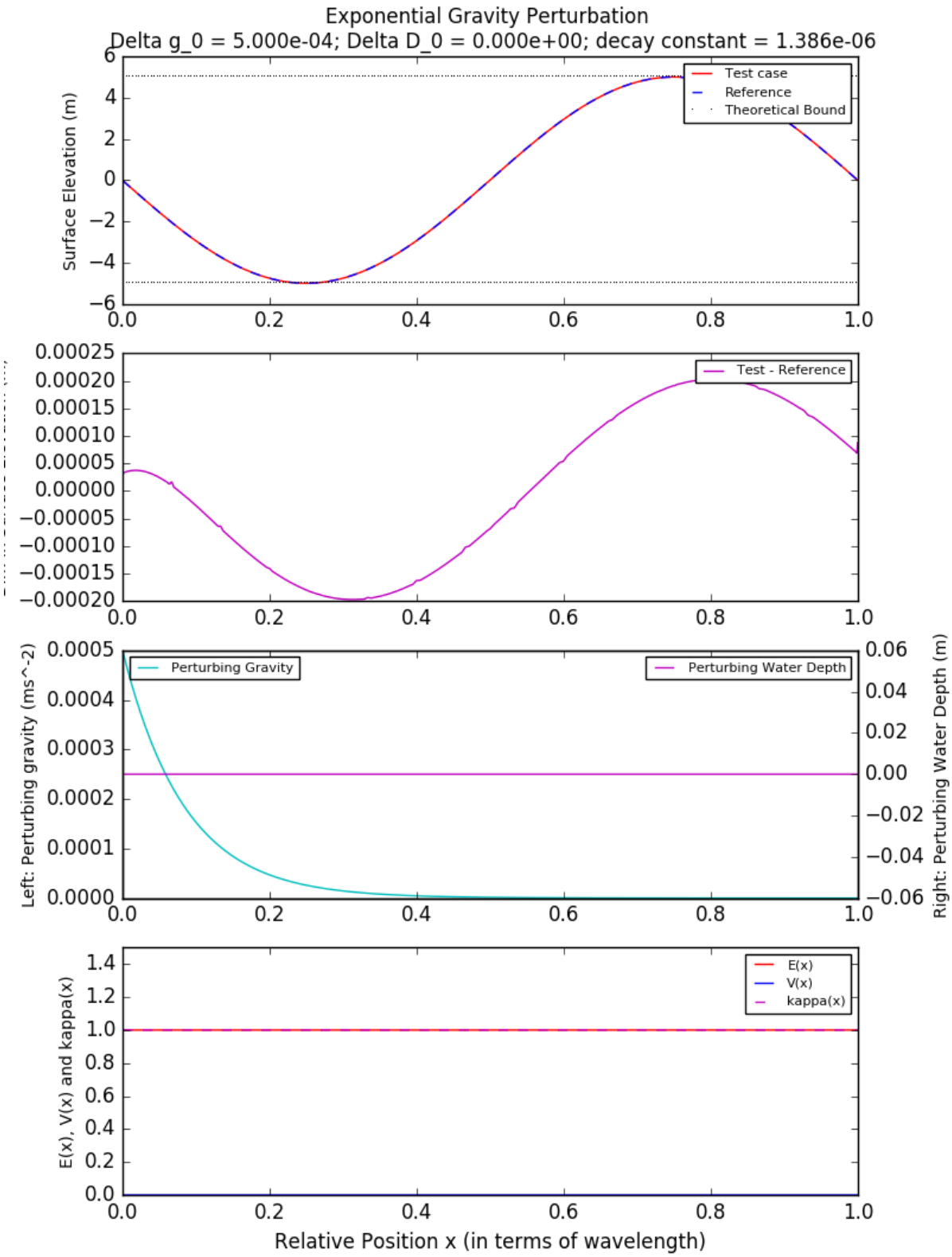

Figure 4.6: Numerical Simulations with Negative Exponential Gravity Perturbation; Physical Scenario - Incoming tidal wave

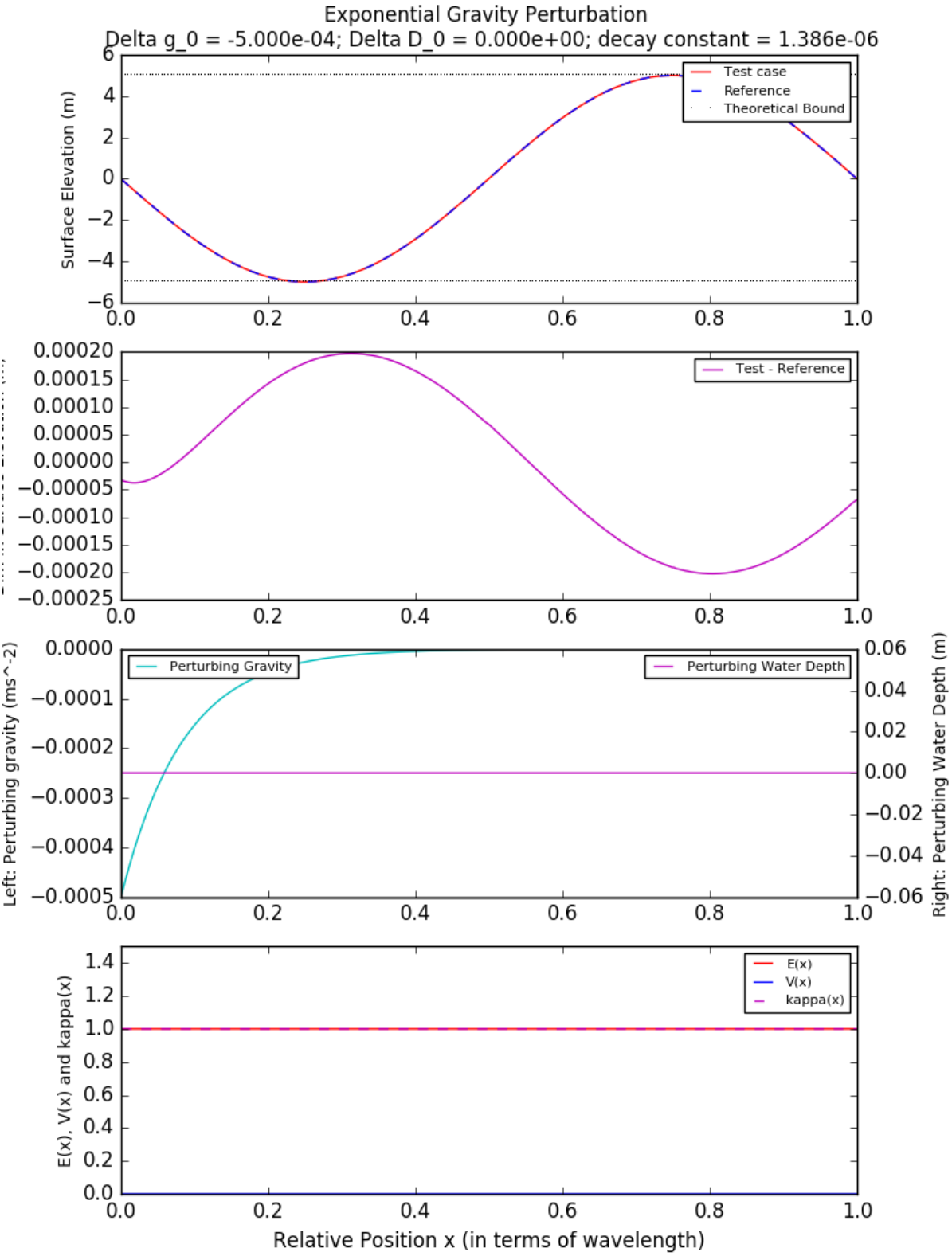

Figure 4.7: Numerical Simulations with Positive Gaussian Gravity Perturbation; Hypothetical Scenario

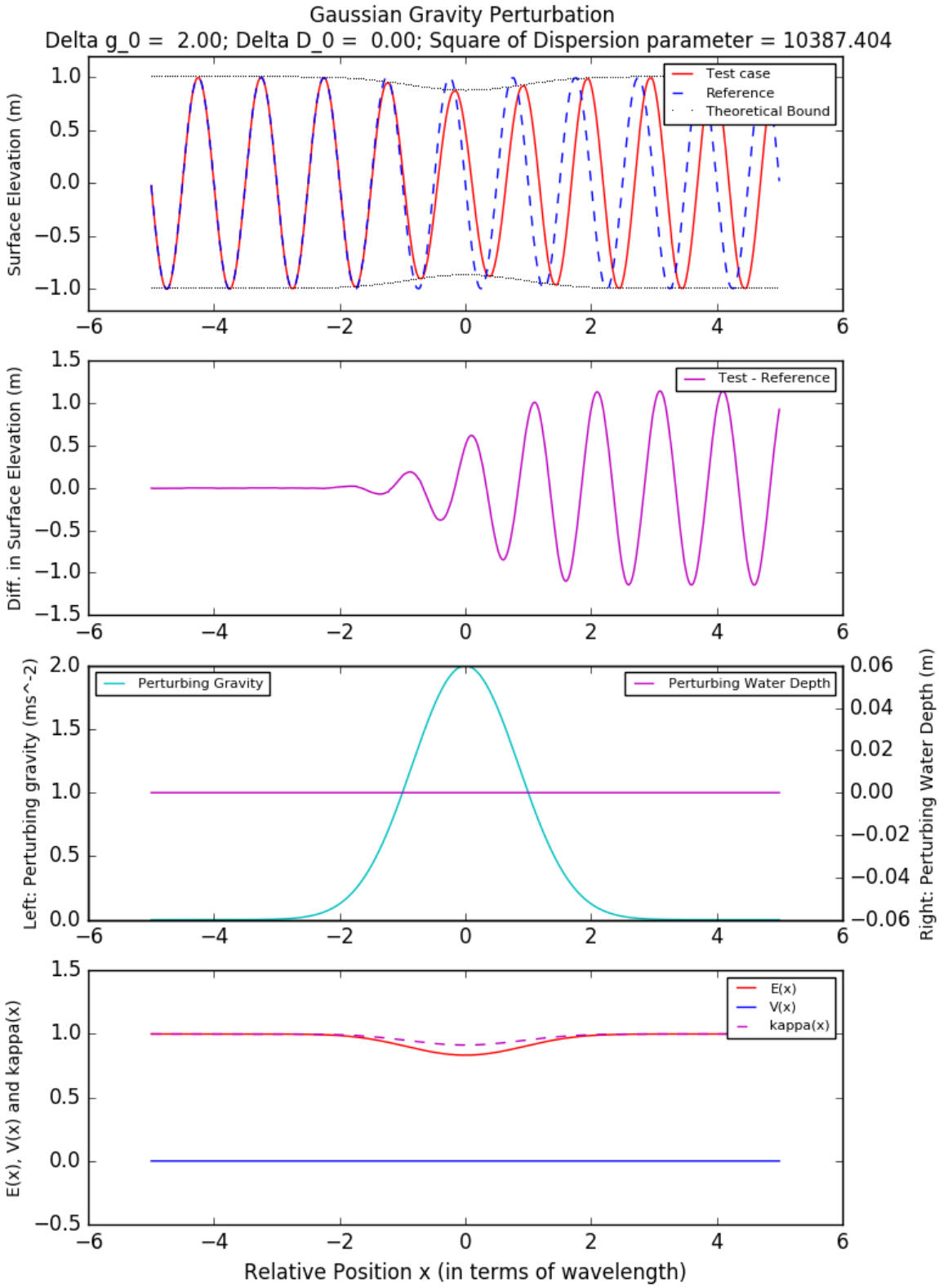

Figure 4.8: Numerical Simulations with Negative Gaussian Gravity Perturbation; Hypothetical Scenario

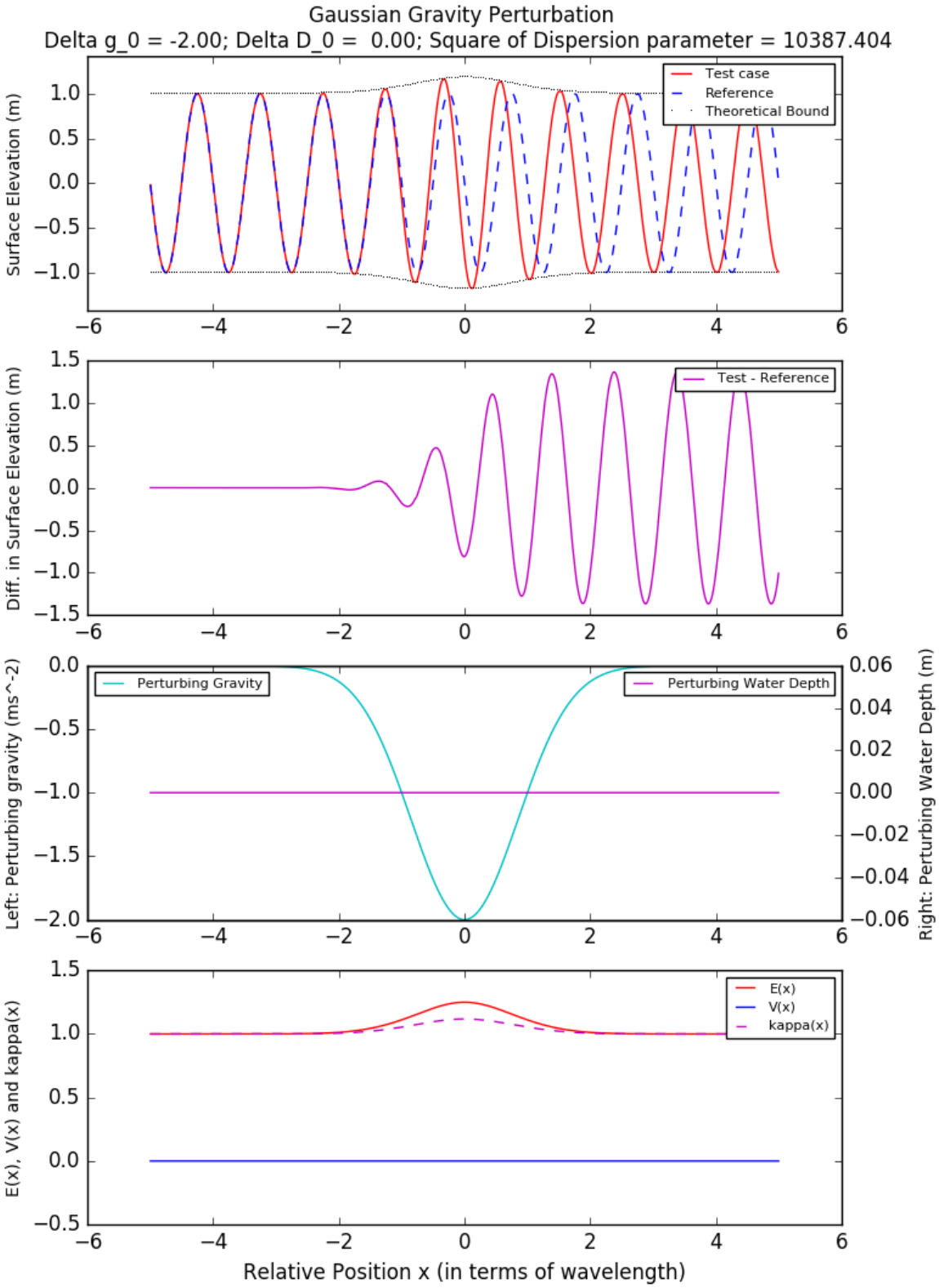

Figure 4.9: Numerical Simulations with Positive Gaussian Gravity Perturbation; Hypothetical Scenario; Localised Gravity Perturbation

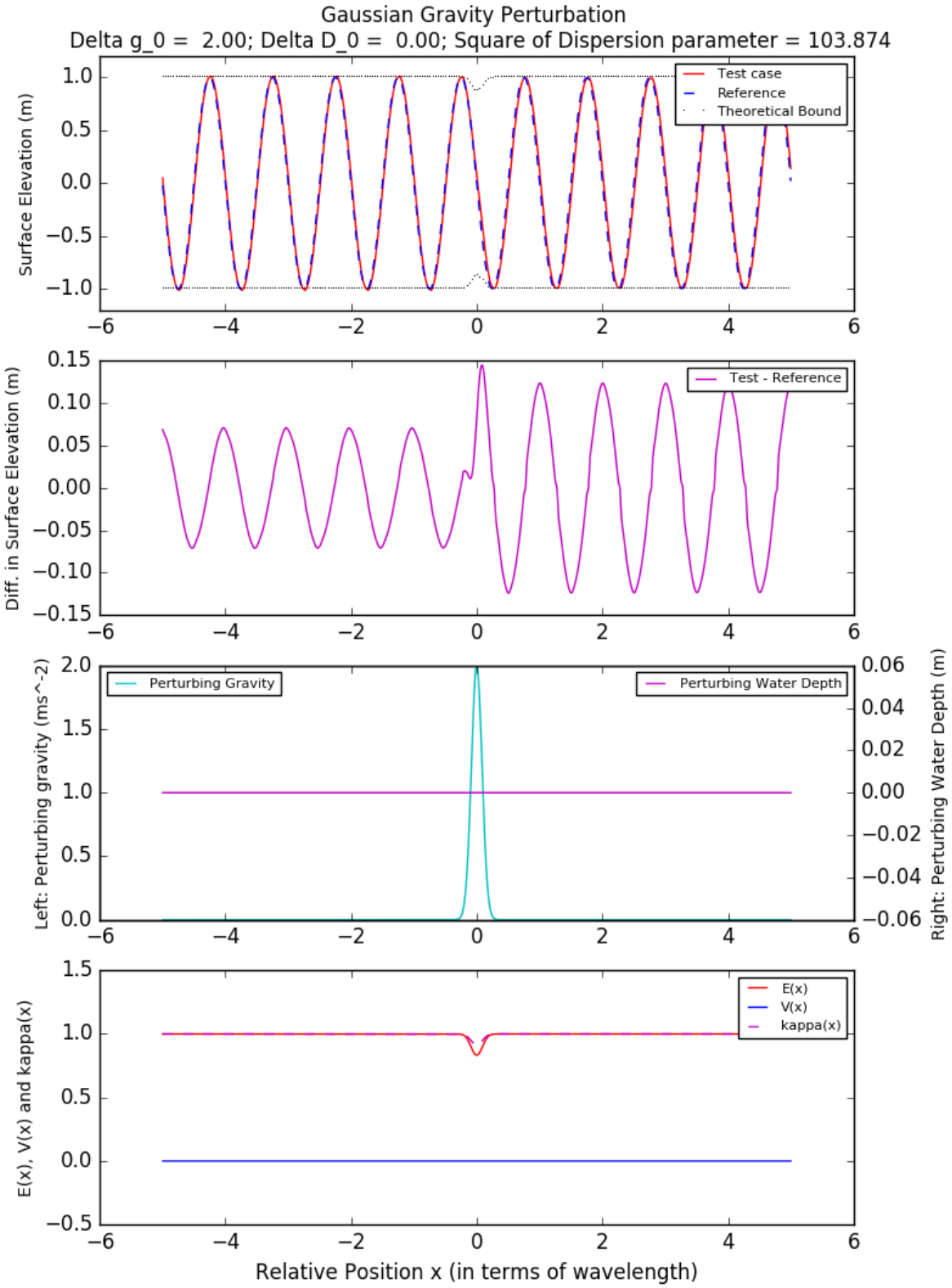

Figure 4.10: Numerical Simulations with Negative Gaussian Gravity Perturbation; Hypothetical Scenario; Localised Gravity Perturbation

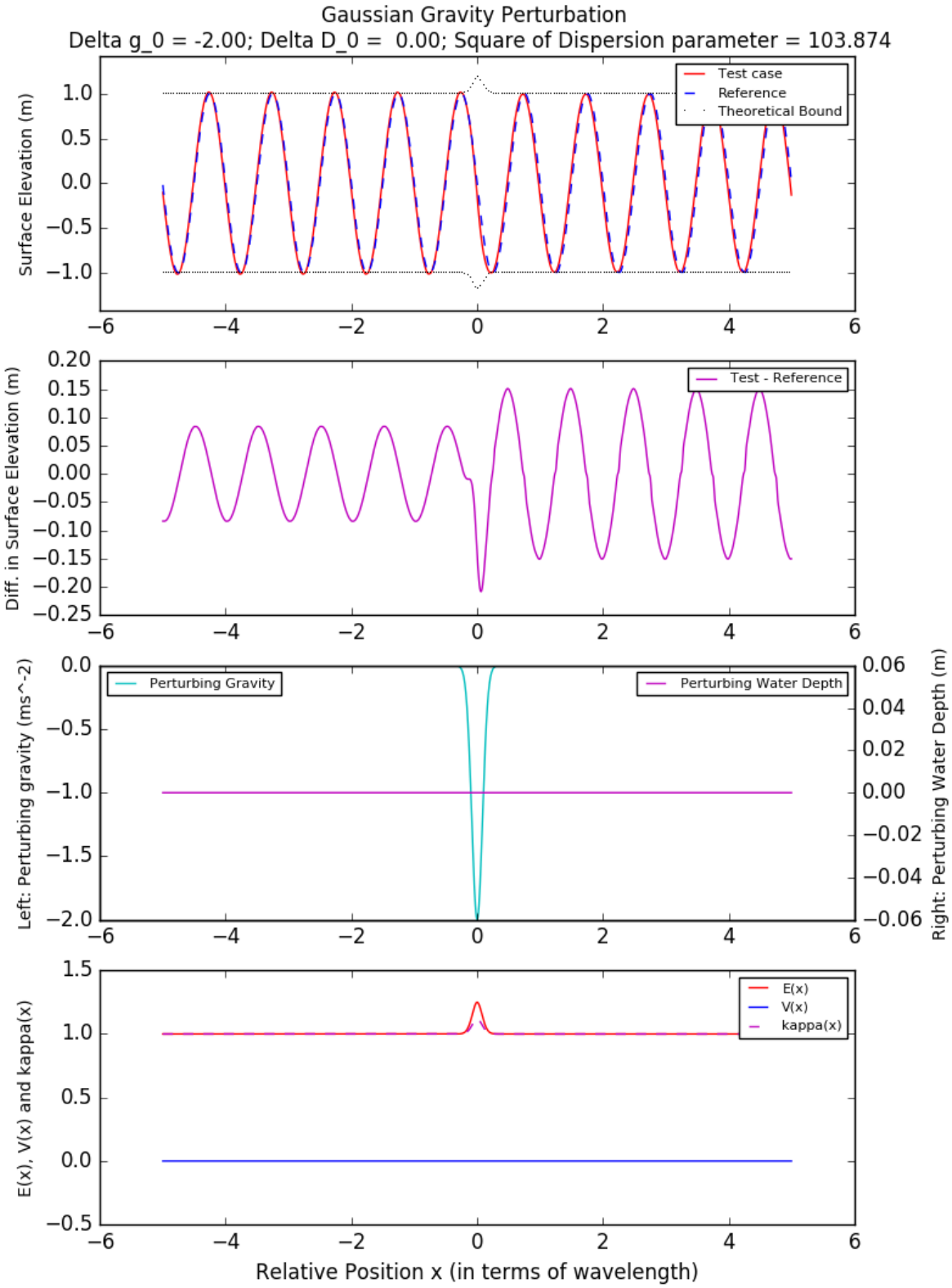

Figure 4.11: Numerical Simulations with Positive Gaussian Gravity Perturbation; Hypothetical Scenario

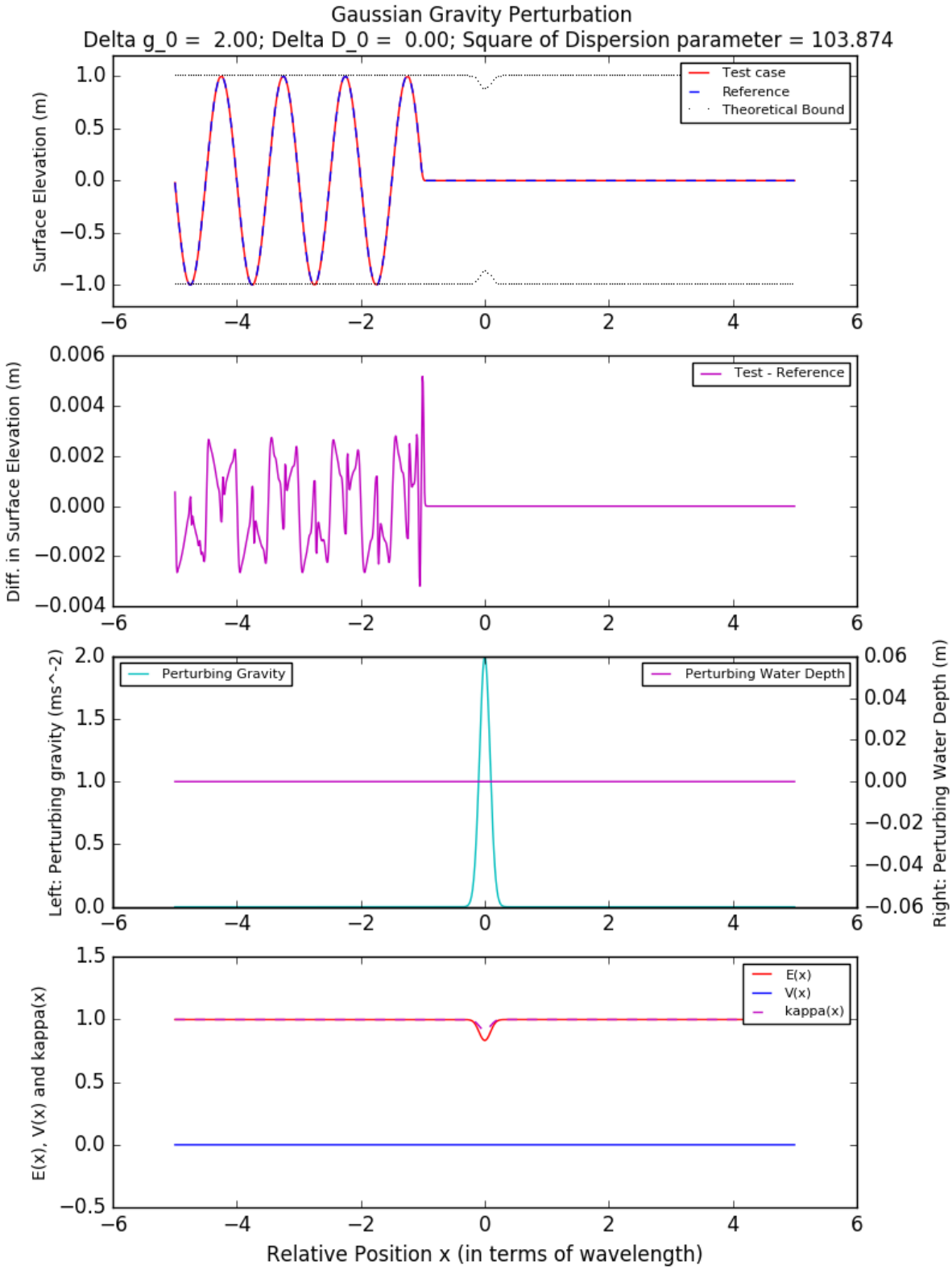

Figure 4.12: Numerical Simulations with Negative Gaussian Gravity Perturbation; Hypothetical Scenario

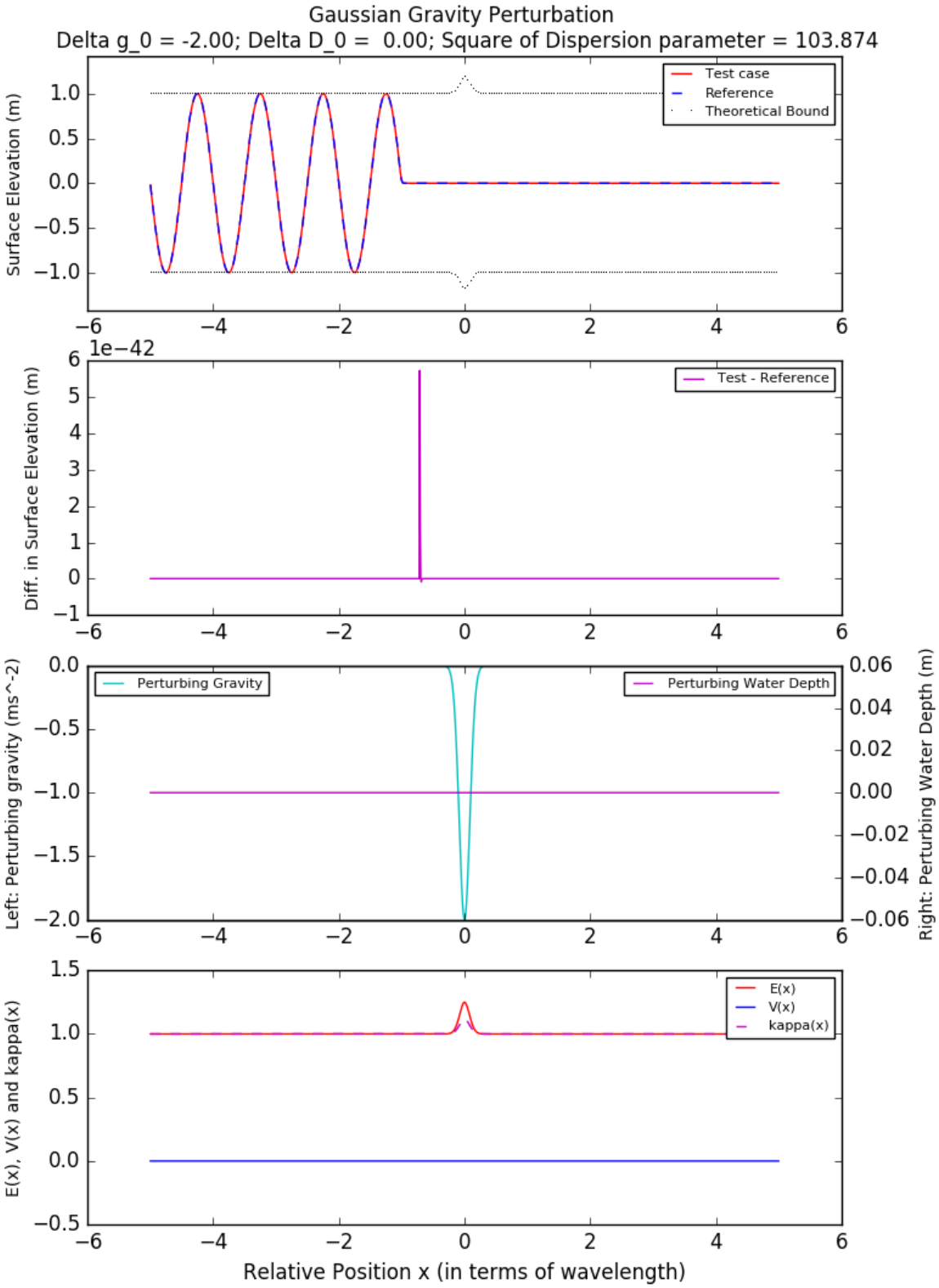

Figure 4.13: Numerical Simulations with Positive Gaussian Gravity Perturbation; Physical Scenario - Incoming Tsunami Waves

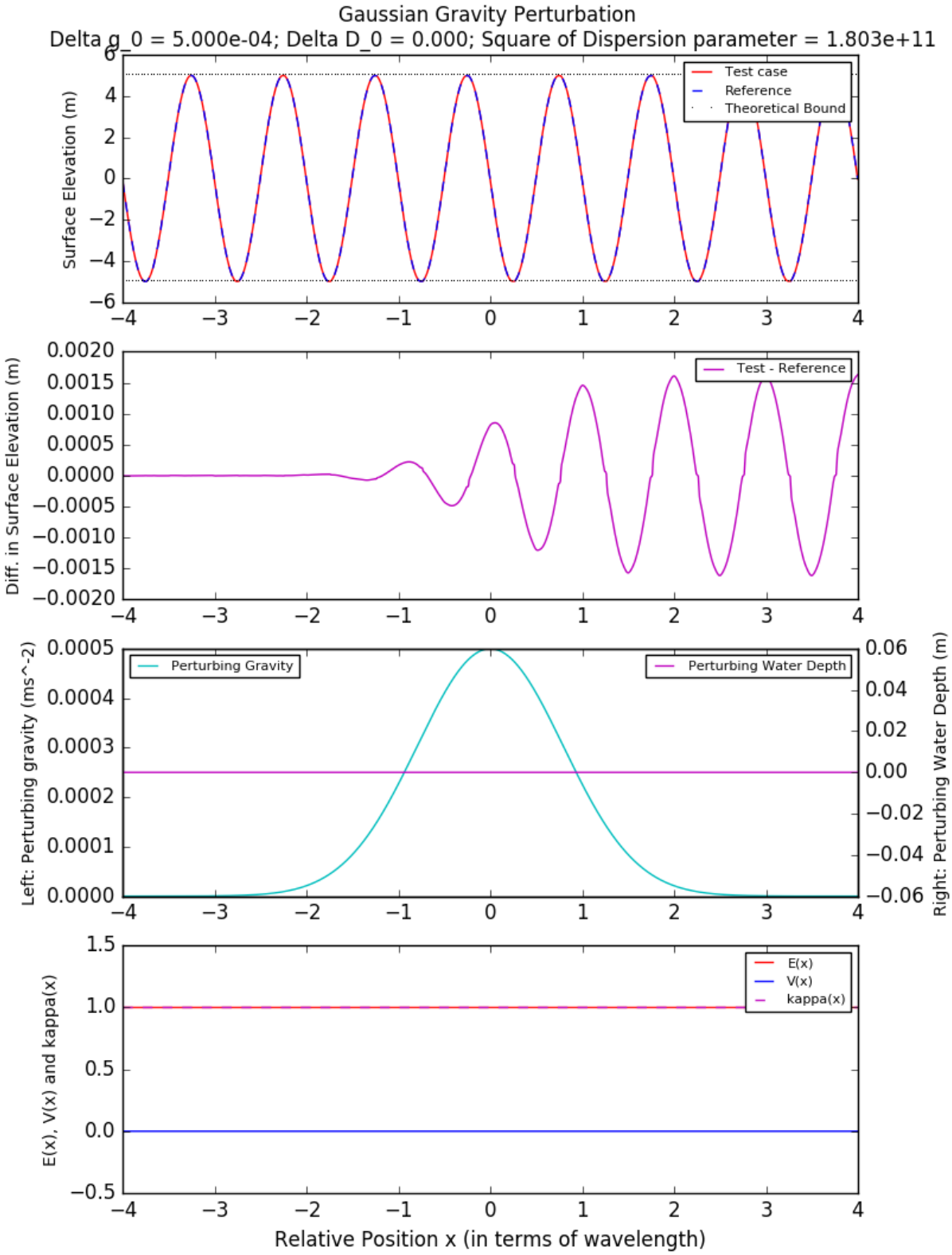

Figure 4.14: Numerical Simulations with Negative Gaussian Gravity Perturbation; Physical Scenario - Incoming Tsunami Waves

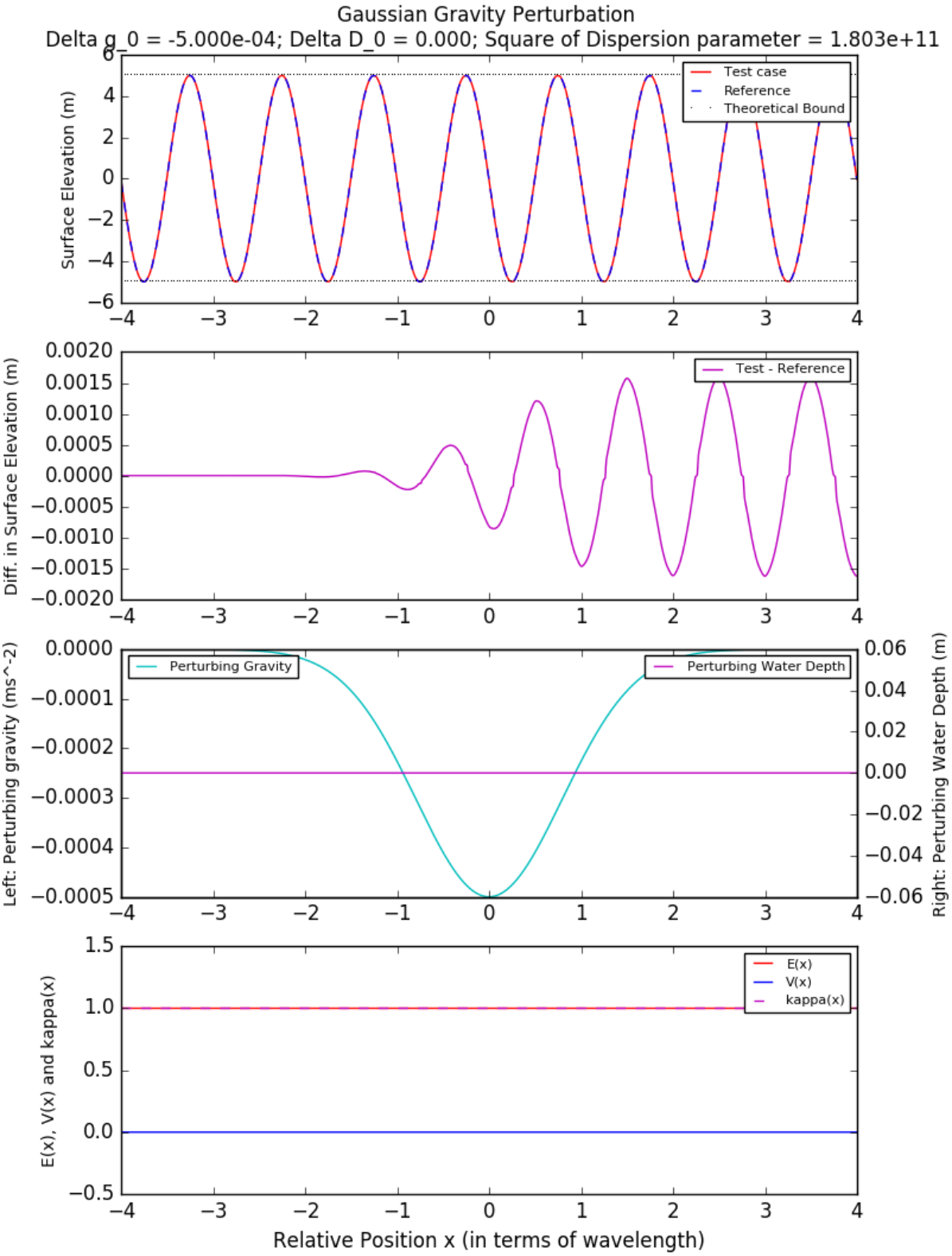

Figure 4.15: Numerical Simulations with Positive Gaussian Gravity Perturbation; Physical Scenario - Incoming Tidal waves

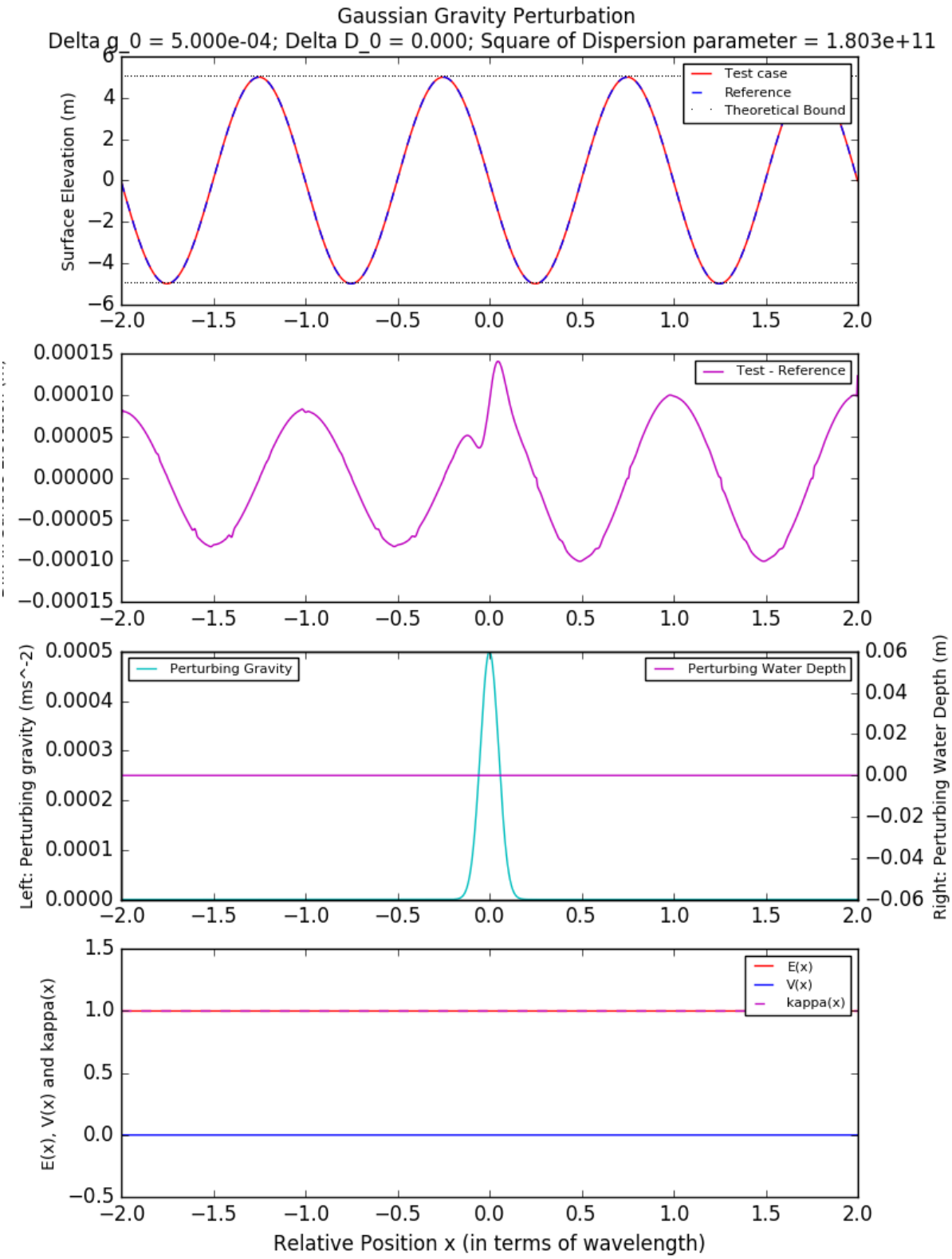

Figure 4.16: Numerical Simulations with Negative Gaussian Gravity Perturbation; Physical Scenario - Incoming Tidal waves

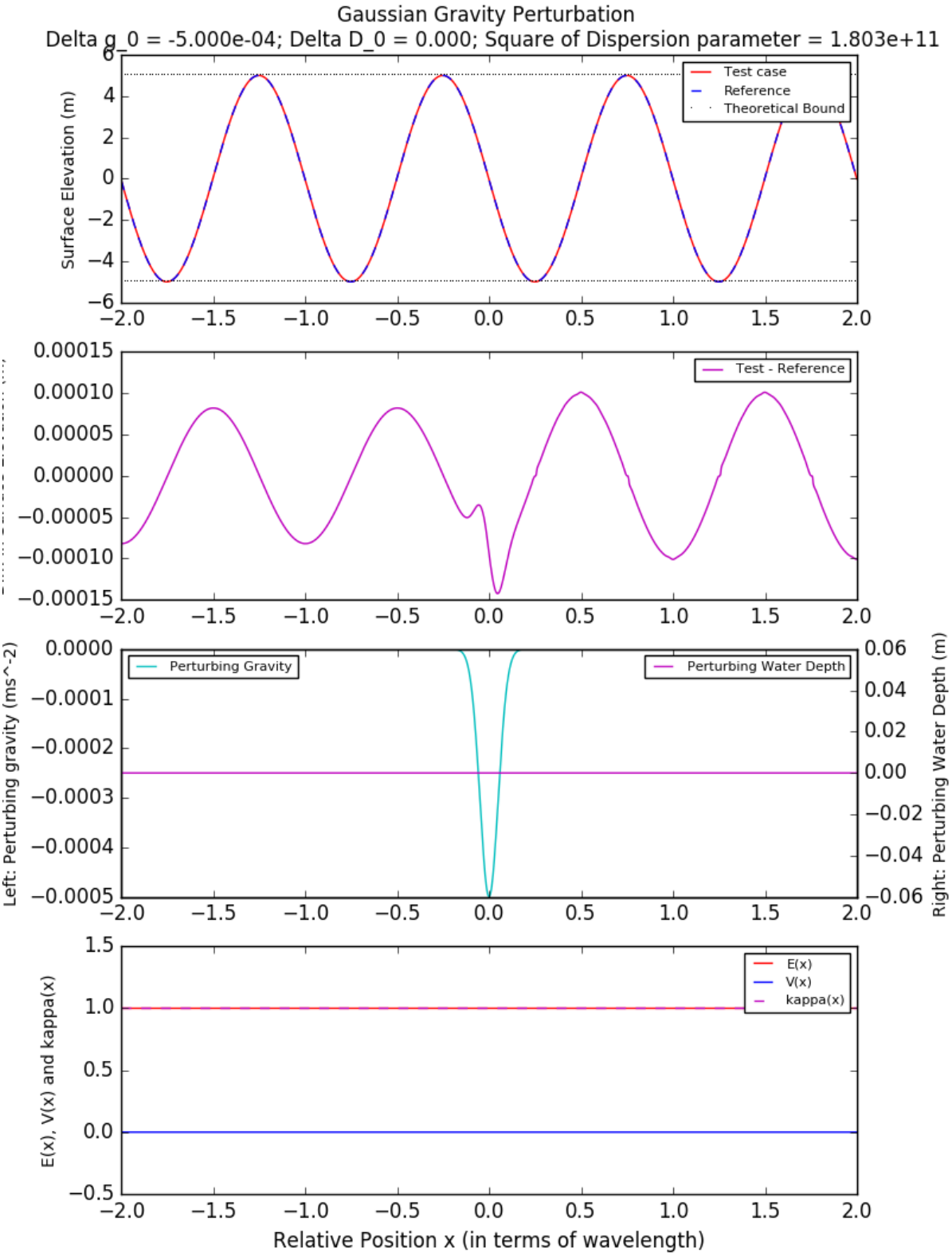

Figure 4.17: Numerical Simulations with Positive Exponential Gravity and Mean Sea-Level Perturbation; Hypothetical Scenario

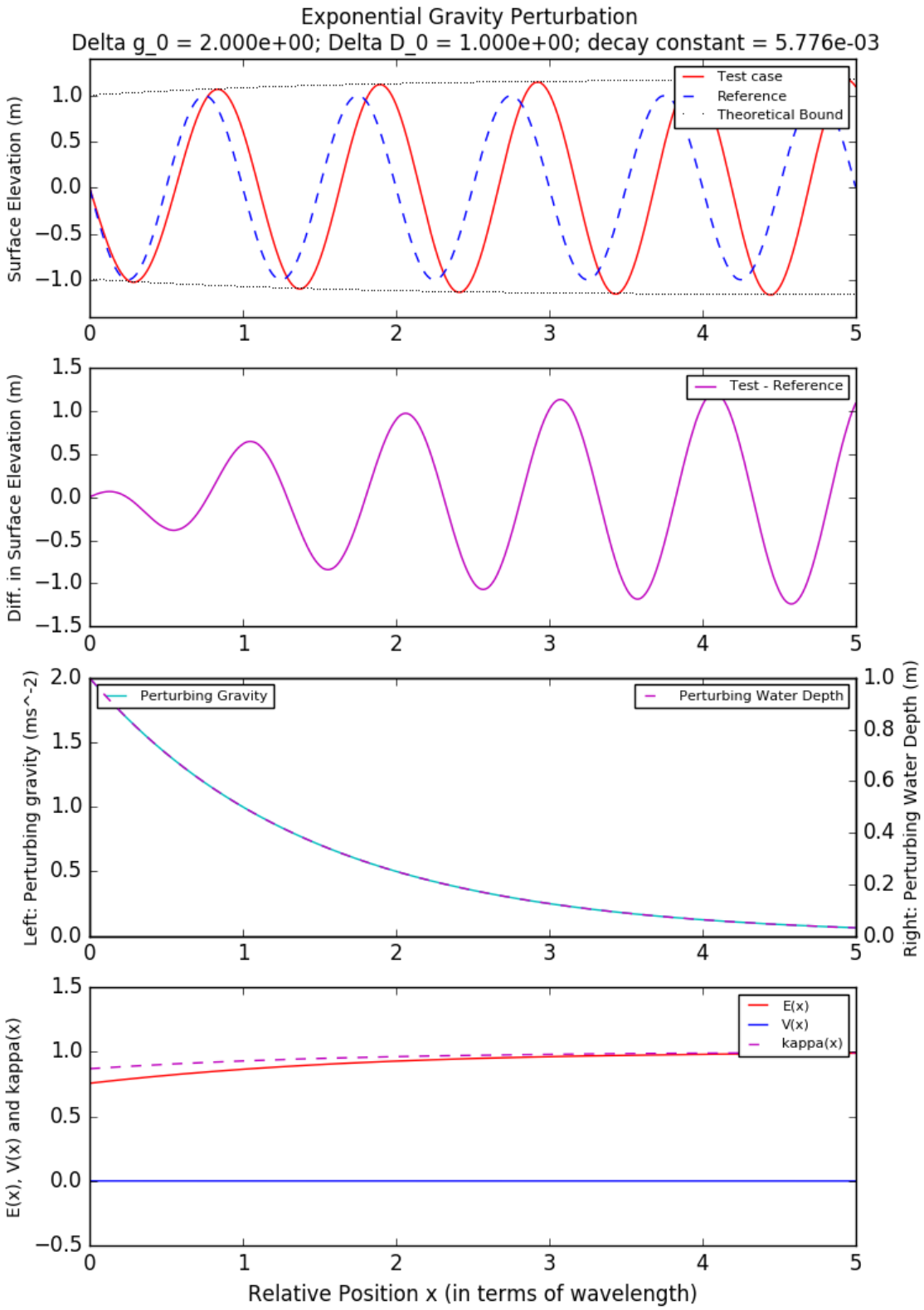

Figure 4.18: Numerical Simulations with Positive Exponential Gravity and Mean Sea-Level Perturbation; Physical Scenario - Incoming Tsunami Waves

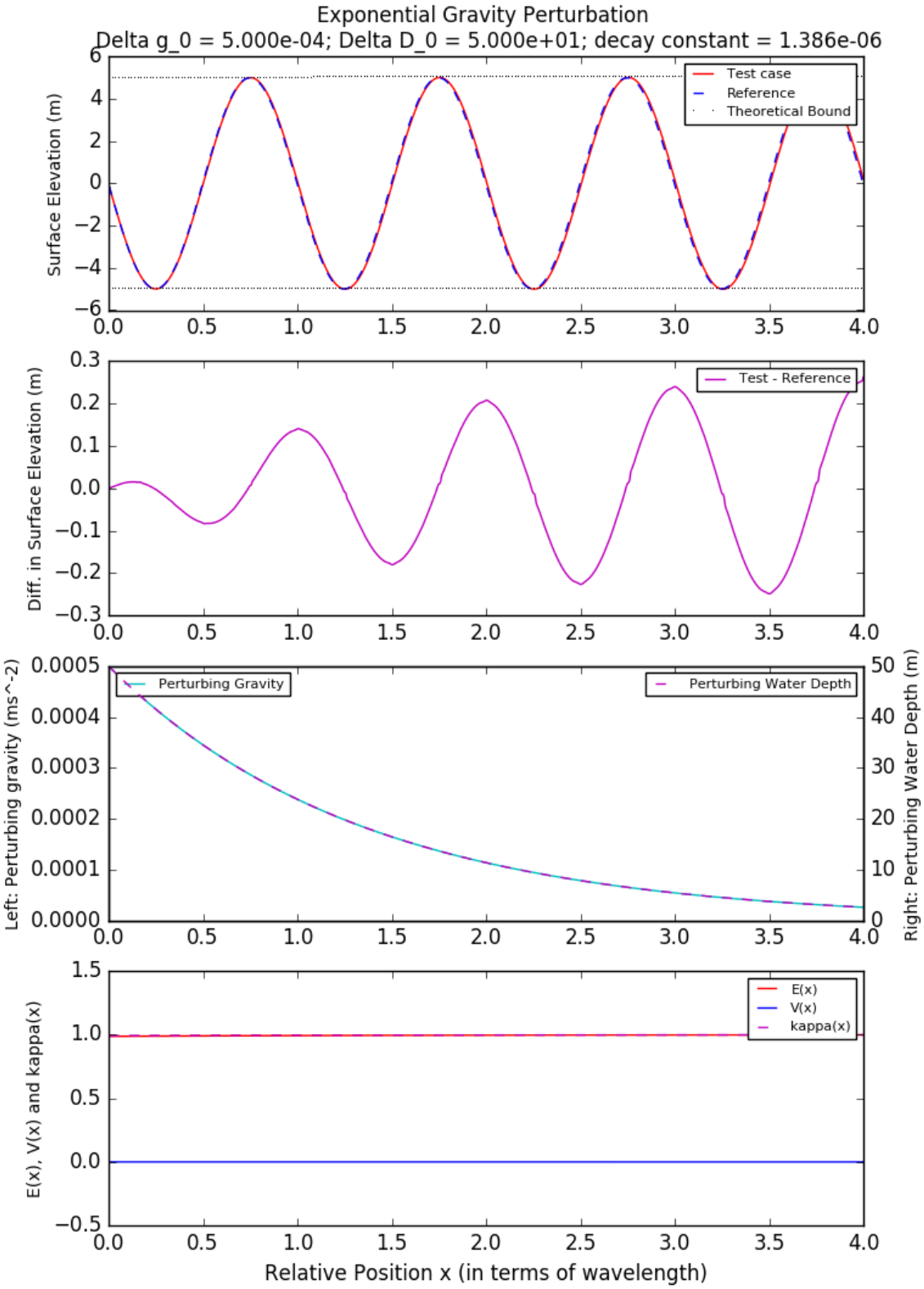

Figure 4.19: Numerical Simulations with Negative Exponential Gravity and Mean Sea-Level Perturbation; Physical Scenario - Incoming Tsunami Waves

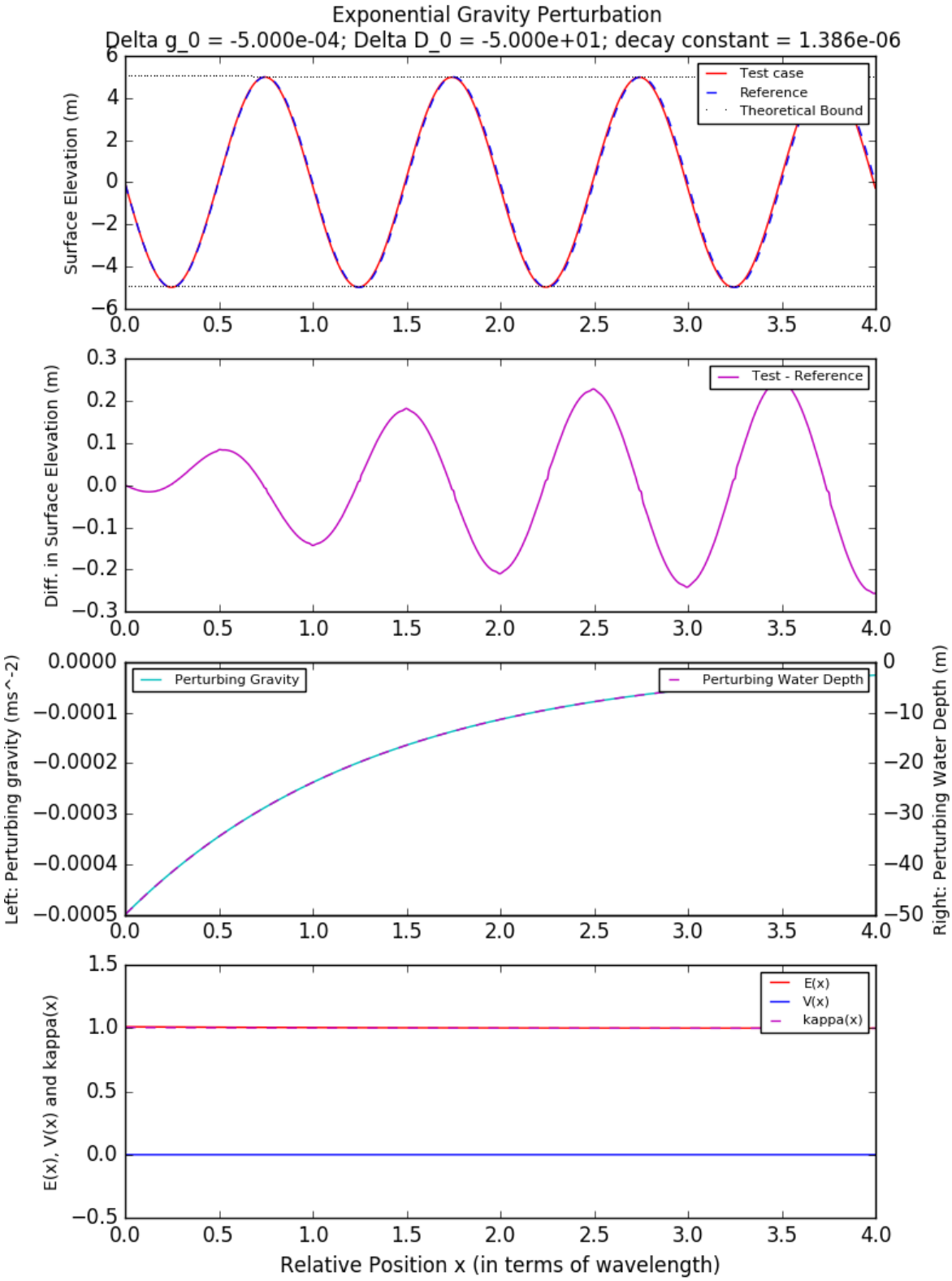

Figure 4.20: Numerical Simulations with Positive Exponential Gravity and Mean Sea-Level Perturbation; Physical Scenario - Incoming Tidal Waves

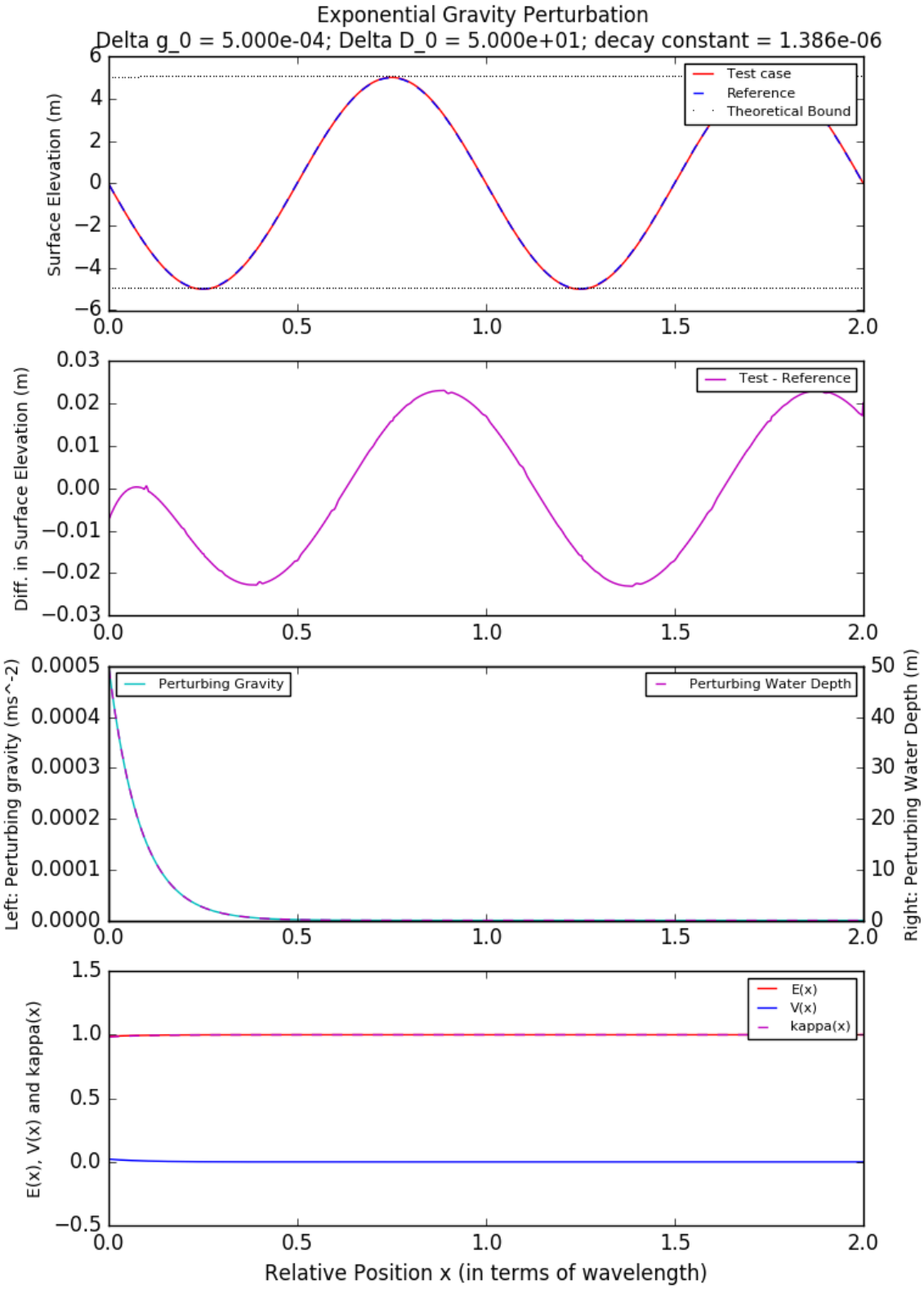

Figure 4.21: Numerical Simulations with Negative Exponential Gravity and Mean Sea-Level Perturbation; Physical Scenario - Incoming Tidal Waves

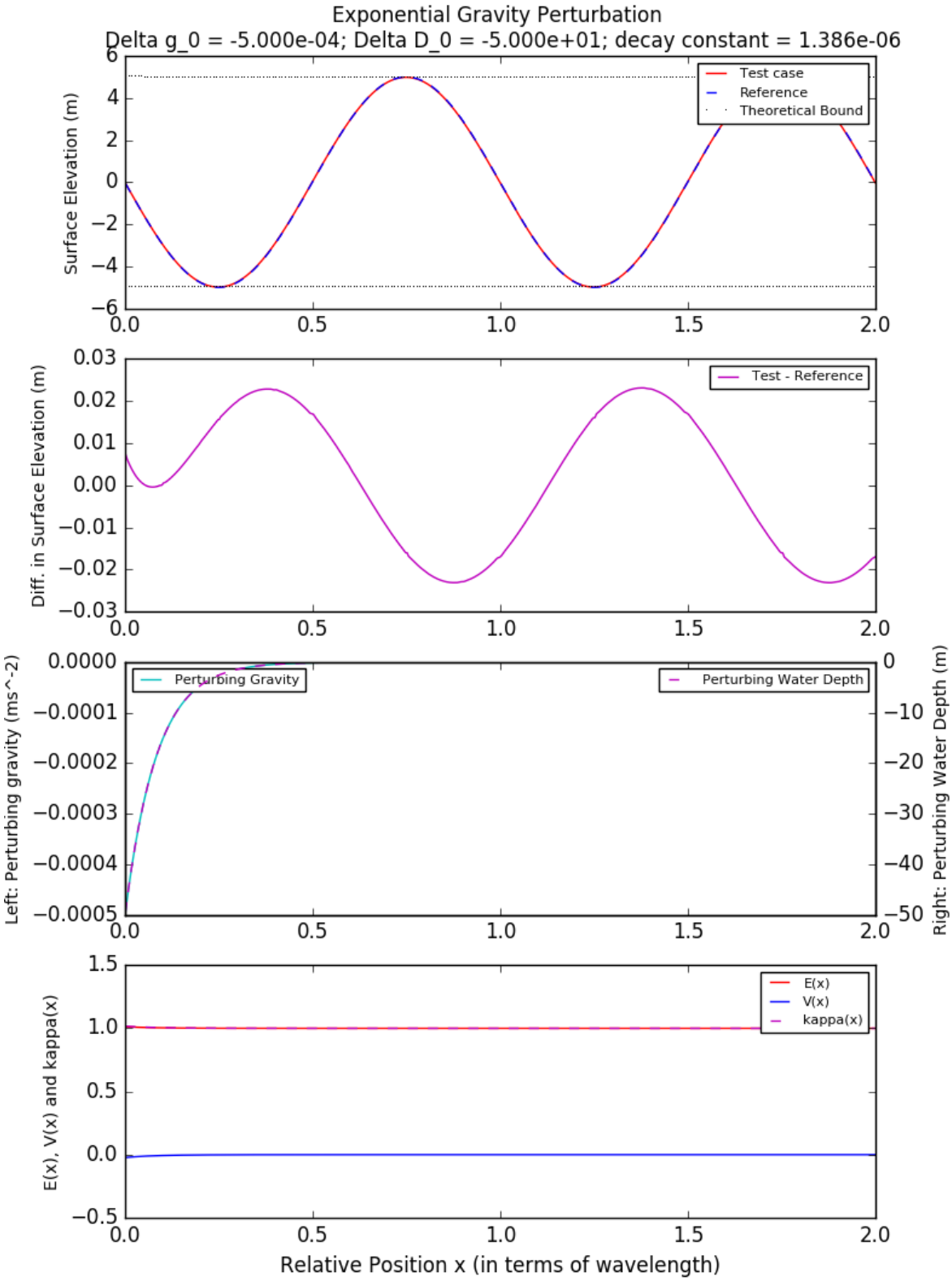

Figure 4.22: Numerical Simulations with Positive Gaussian Gravity and Mean-Sea Level Perturbation; Physical Scenario - Incoming Tsunami Waves

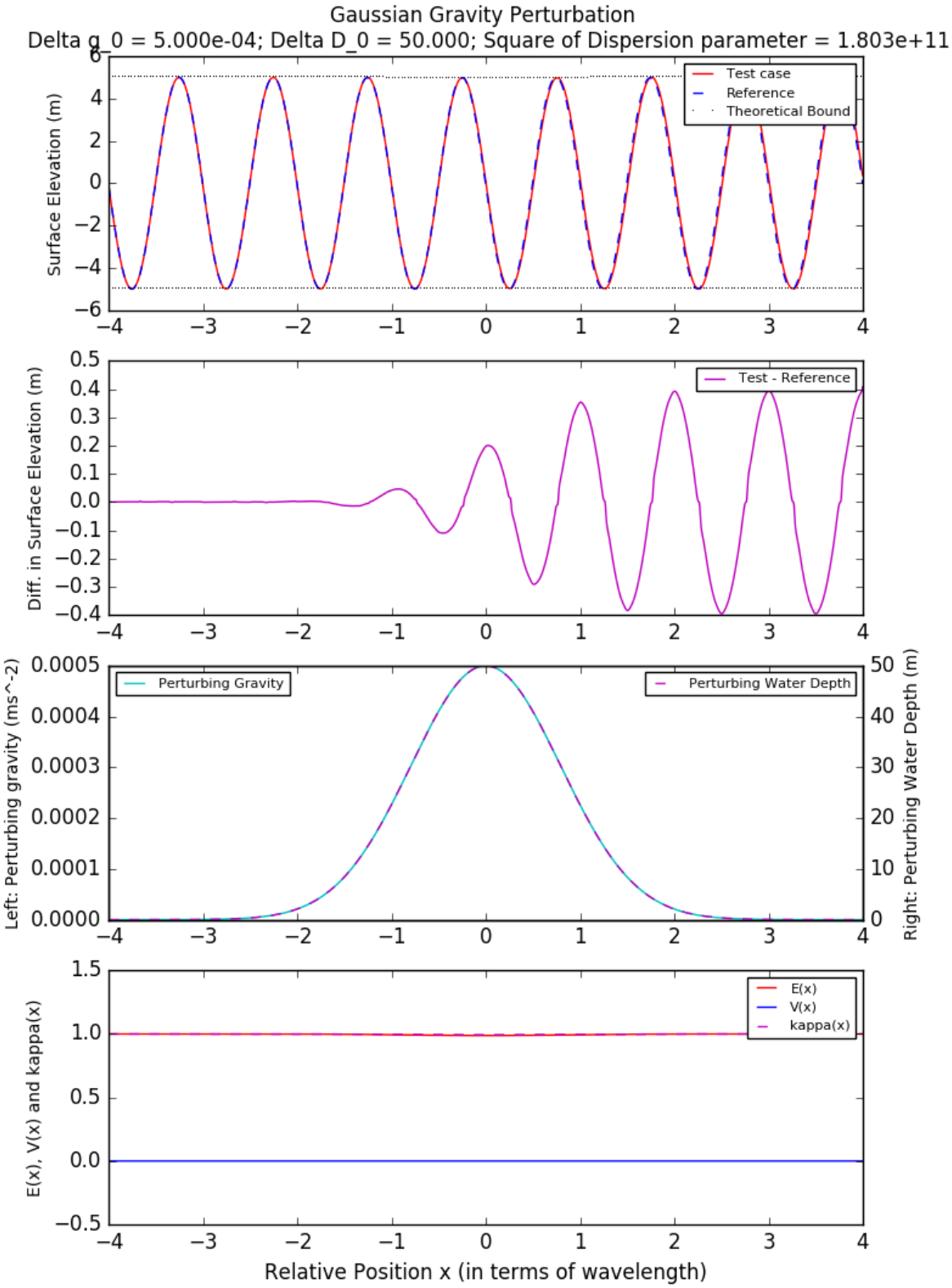

Figure 4.23: Numerical Simulations with Negative Gaussian Gravity and Mean-Sea Level Perturbation; Physical Scenario - Incoming Tsunami Waves

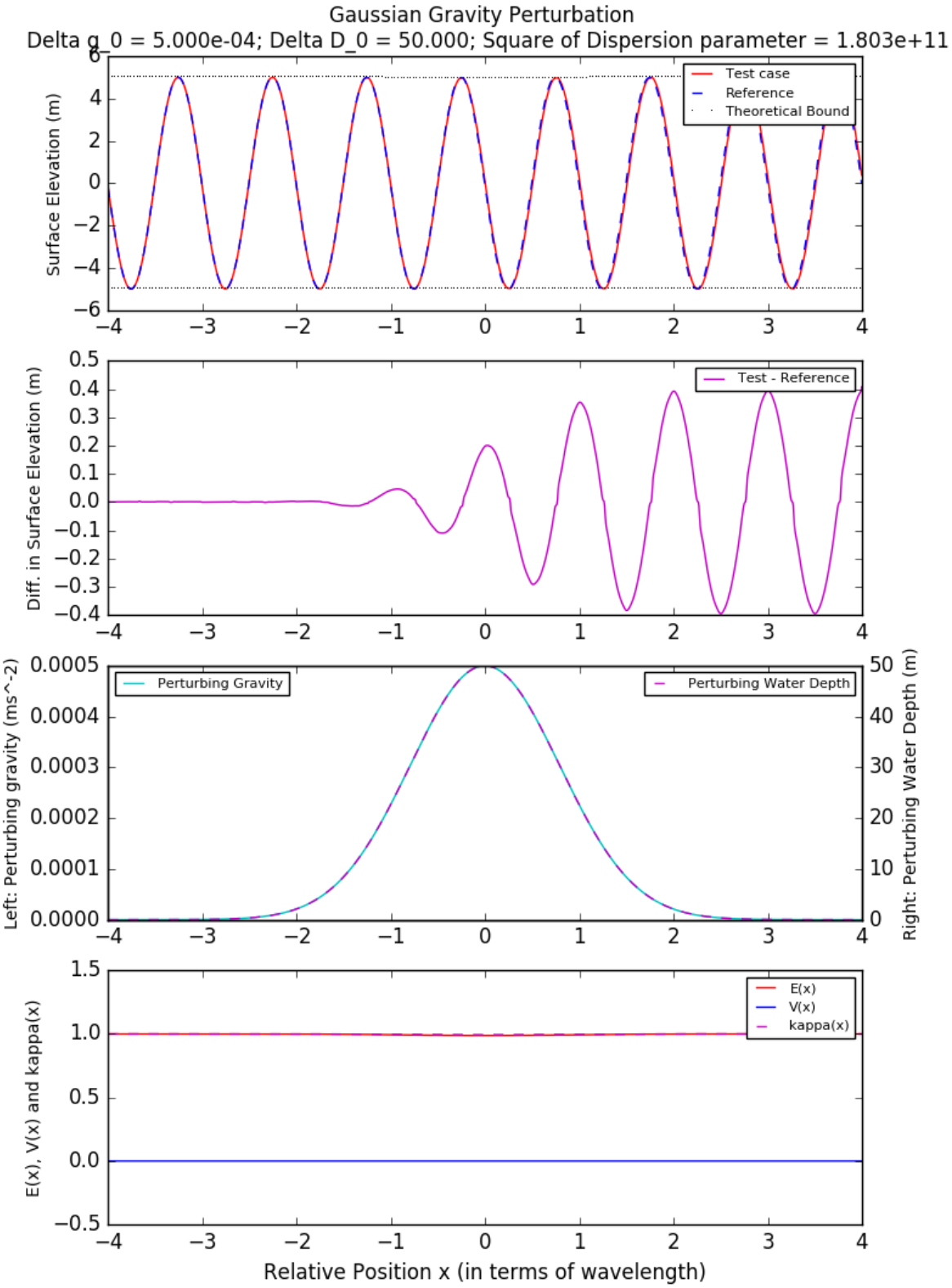

Figure 4.24: Numerical Simulations with Positive Gaussian Gravity and Mean-Sea Level Perturbation; Physical Scenario - Incoming Tidal waves

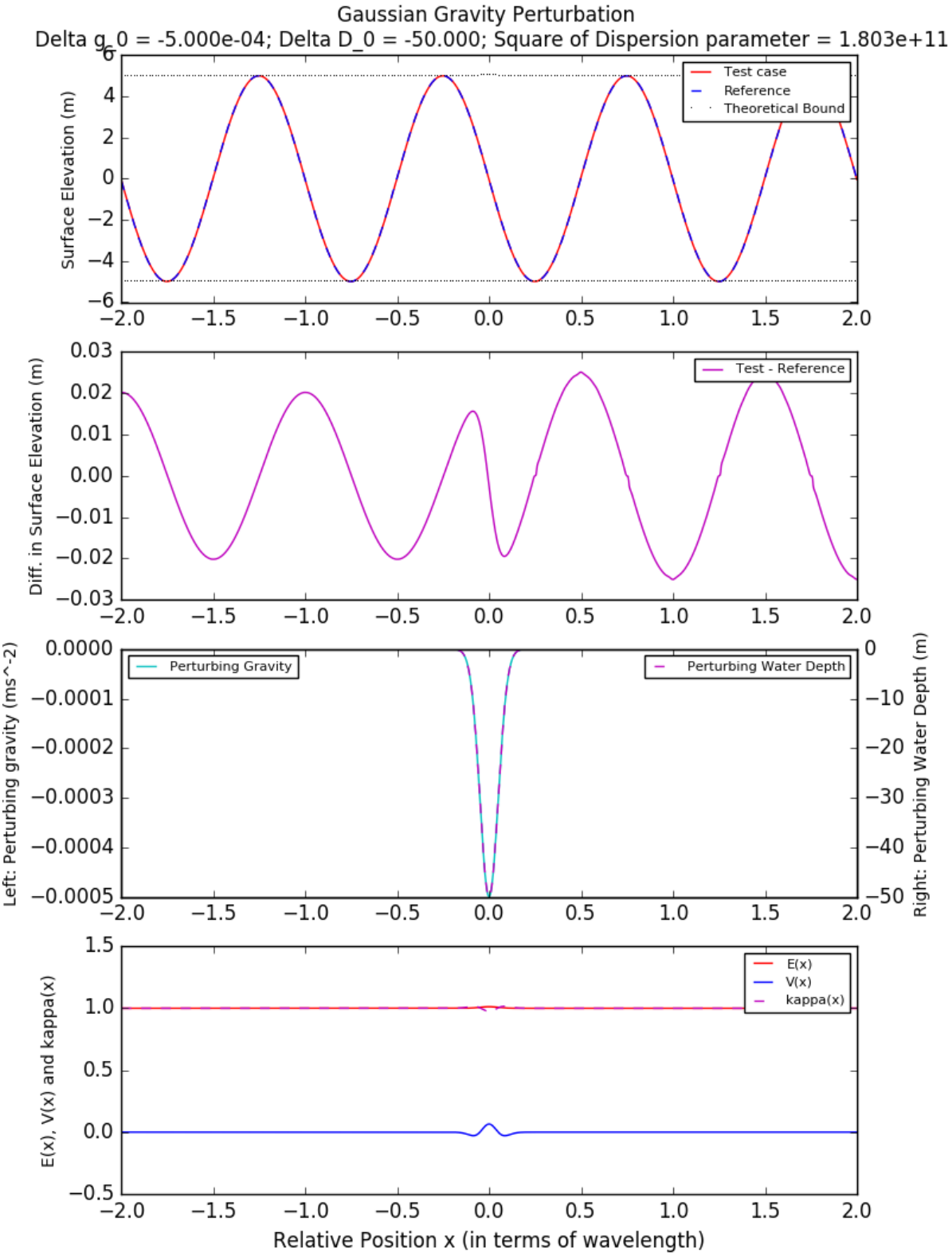

Figure 4.25: Numerical Simulations with Negative Gaussian Gravity and Mean-Sea Level Perturbation; Physical Scenario - Incoming Tidal waves

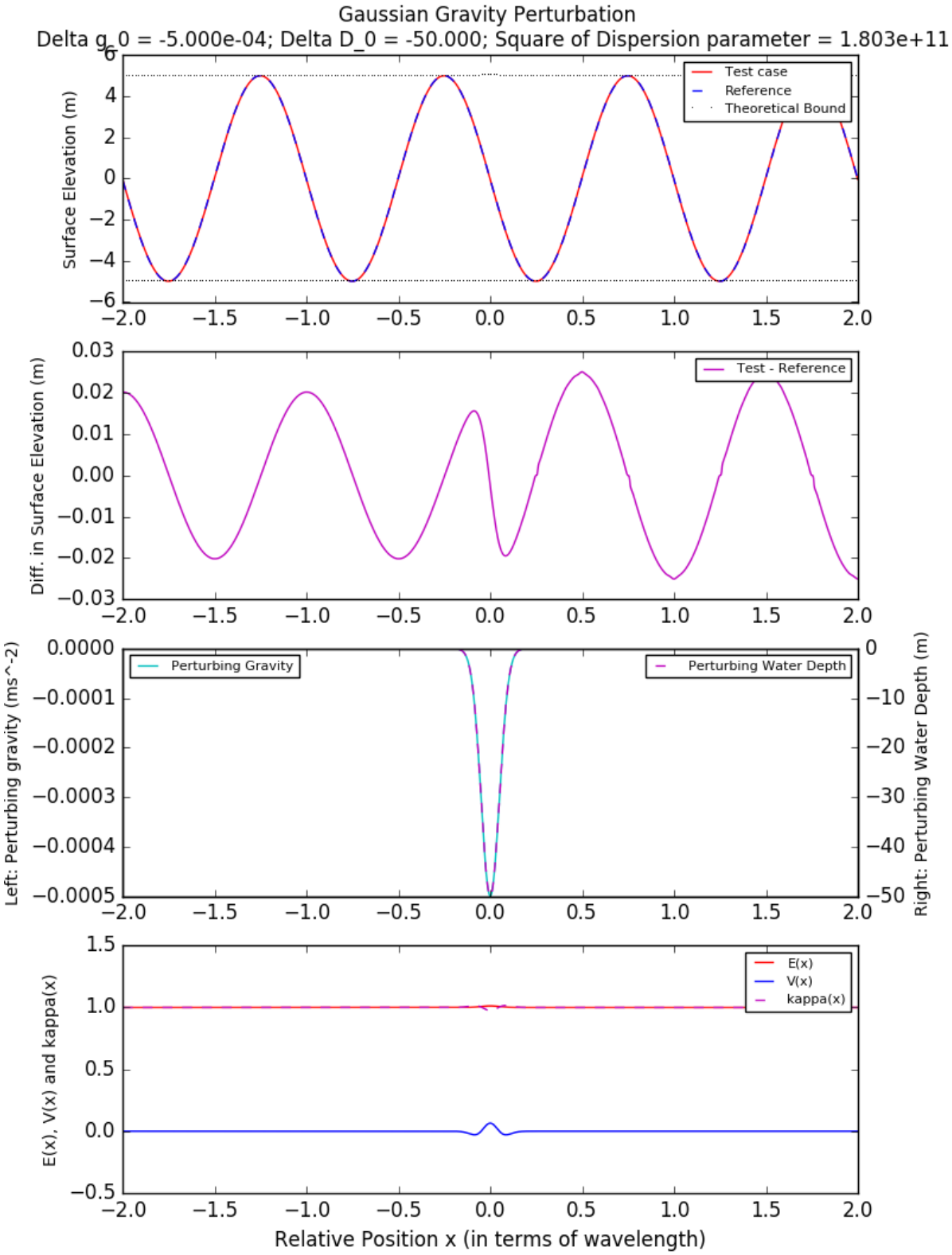

Figure 4.26: Global Variation of Gravity

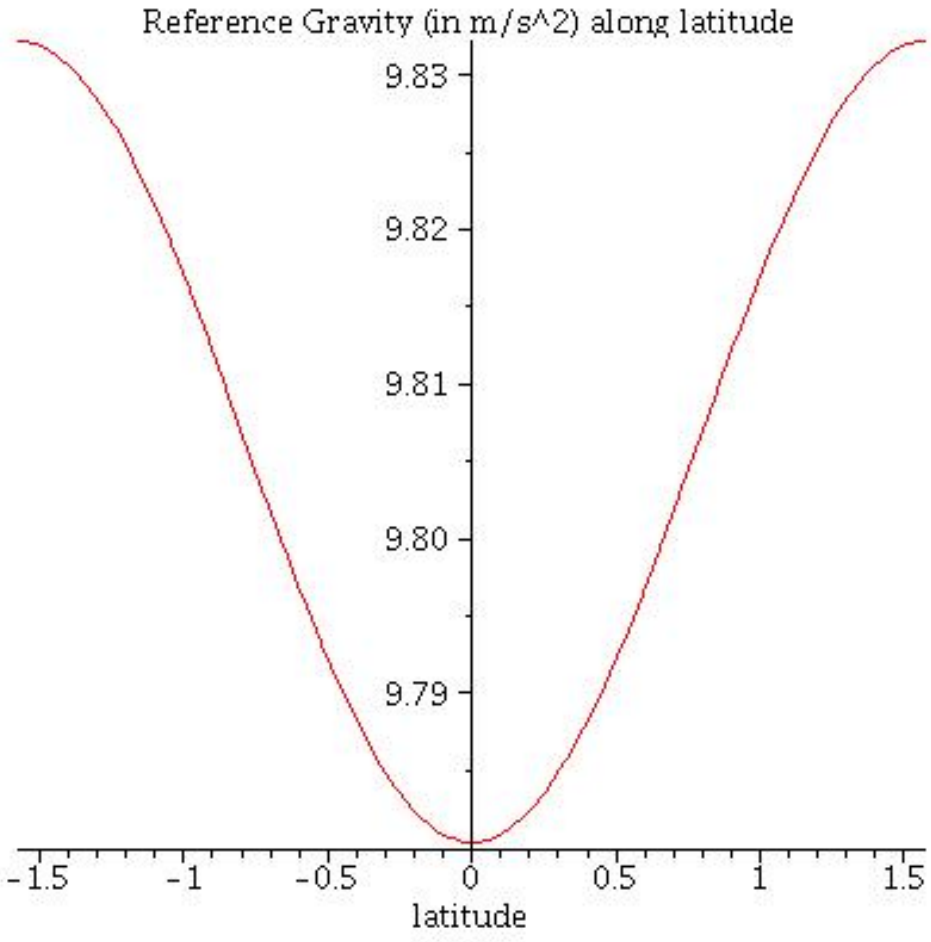

5

Two-Dimensional Adapted Wave Equation

In this chapter, the two-dimensional adapted wave equation will be discussed. Numerical solutions will be investigated. Quantitative and qualitative behaviour of the solutions will be examined.

5.1. Diagnostic Formalism: Limitations

Recall that the set of equations (3.138) given by,

$$\begin{aligned}
&\frac{\partial \eta}{\partial t} + \nabla_h \cdot \mathbf{U} = \mathbf{U} \cdot \nabla_h \left(\ln\left(\frac{g_z}{g_0}\right) \right), \\
&\frac{\partial U}{\partial t} + c^2 \frac{\partial \eta}{\partial x} = 0, \\
&\frac{\partial V}{\partial t} + c^2 \frac{\partial \eta}{\partial y} = 0,
\end{aligned}$$

governs the small-amplitude surface waves in a spatially varying gravity field on a two-dimensional plane.

Motivated by the treatment in one-dimensional space, a time-harmonic ansatz to the surface elevation $\eta(x,y,t) = \eta_0(x,y)e^{-i\omega t}$ is chosen to solve (3.138). This eventually gives rises to the second-order partial differential equation:

$$\nabla^2 \eta_0 + \nabla \ln\left(\frac{c^2}{g_z}\right) \cdot \nabla \eta_0 + \frac{\omega^2}{c^2}\eta_0 = 0, \tag{5.1}$$

which is the two-dimensional generalisation of (4.3).

Motivated by the one-dimensional case as in equation 4.4, applying a coordinate transformation given by

$$\ln r = \ln \eta_0 + \frac{1}{2}\ln\left(\frac{c^2}{g_z}\right), \tag{5.2}$$

equation (5.1) becomes into

$$\nabla^2 r + \left[\frac{\omega^2}{c^2} - \left(\frac{1}{c}\nabla^2 c + \frac{3}{4{g_z}^2}\|\nabla g_z\|^2 - \frac{1}{2g_z}\nabla^2 g_z - \frac{1}{cg_z}\nabla c \cdot \nabla g_z\right)\right] r = 0 \tag{5.3}$$

Using the definition of $c(x,y) = \sqrt{g_z D}$ given by (3.137), the above transformed differential equation can be simplified into

$$\nabla^2 r + \left[E(x,y) - V(x,y)\right]{K_0}^2 r = 0 \tag{5.4}$$

where $E(x,y)$ and $V(x,y)$ are given by

$$E(x,y) = \frac{\omega^2}{g_z D {K_0}^2} \tag{5.5a}$$

$$V(x,y) = \frac{1}{4{K_0}^2}\left(\frac{2}{D}\nabla^2 D - \frac{1}{D^2}\|\nabla D\|^2\right) \tag{5.5b}$$

and $K_0 = \sqrt{{k_0}^2 + {l_0}^2}$ is the magnitude of a reference plane-wave wavevector $\vec{K}_0 = (k_0, l_0)$, which is a constant. It is noted that (5.4) is similar to the two-dimensional time-independent Schrodinger equation, except that the 'energy' E is a function of spatial coordinates (x,y) instead of a constant. This is the two-dimensional generalisation to (4.14).

In spite of the similarity, the two-dimensional time-independent 'Schrodinger' equation (5.4) is not as useful as the one-dimensional one (4.14) discussed in the previous chapter. This is because, given the magnitude of wavevector K_0, there are infinitely many possible wavevector $\vec{K}_0$ that give rises to the same K_0. Such degeneracy complicates the analysis to the equation (5.4). Therefore the diagnostic formalism will not be further developed in this thesis.

5.2. Test Cases and Numerical Simulations

5.2.1. Rationale and Limitations

Rather than the analytical solutions, in this chapter only the numerical solutions to the two-dimensional adapted shallow water wave equations (3.138) will be considered. This is because in the one-dimensional studies, it has been shown that the gravity variation on the Earth surface is only able to create very minimal changes for surface waves. The outcome of this chapter is to show that the effects caused by the spatially-varying gravity field on ocean surface waves is also minimal in the three-dimensional space as well.

5.2.2. Methodology and Configurations of Test Cases

Numerical Configurations

The parameters used for constructing test cases are given in Tables 5.1 and 5.2. The parameters are obtained in the same manner as in the one-dimensional configurations in Table 4.1 and 4.2. The detailed meanings of each quantity have been discussed in section 4.2.

Similar to the one-dimensional studies, the hypothetical setting given by Table 5.1 targets at showing the qualitative features while the physical setting given by 5.2 aims at providing insight about the surface waves in the actual ocean.

The numerical simulations are carried out using CLAWPACK, an open-source software package to solve systems of hyperbolic equations numerically.

Explanation of Figures

Each of the figures shown in the following sections include four subplots. Each subplot represents a scalar field at a certain instant. All subplots share identical x-axis and y-axis, which mark the normalised x and y-coordinates. The normalisation is relative to the wavelength of the prescribed incoming waves. The colour in the subplots represents the instantaneous value of the scalar field, with a colourbar below the subplots. The ticks in the colour bar represents the maximum and minimum value of the instantaneous scalar field.

From left to right, the first subplot gives the surface elevation of reference waves. This serves as a yardstick for comparison with the second subplot, which gives the surface elevation of the test waves. The test waves usually differ from the reference waves by the presence of gravity perturbation, water depth perturbation or both. Details will be specified in the caption of the figures.

The third subplot shows the perturbation field of either the gravity or water depth. The final subplot gives the instantaneous difference between the test waves and reference waves. This provides a handy tool to preliminarily investigate the effects of the gravity or depth perturbation on the waves. Readers are reminded that the instantaneous difference in surface elevation is not a very rigorous tool to study the transmission-reflection mechanism of surface waves scattered by topography. A more sophisticated tool should consider the time-independent surface elevation field by time-averaging. Yet for the purpose of this chapter, such analysis is omitted.

Physical Parameters	**Values**
Reference Gravity, g_0	10 ms^{-2}
Mean Depth of Fluid, D_0	10 m
Amplitude of incoming wave, η_0	1 m
Period of incoming wave, T	6 seconds or 120 seconds
Reference wavelength, λ_0	$T\sqrt{g_0 D_0} = 60$ m or 1200 m
Maximum Perturbing Gravity, Δg_z	± 2 ms^{-2}
Maximum Perturbing Mean-Sea Level, ΔD_0	± 2 m
'Half-life' Distance, $r_{\frac{1}{2}}$	$\lambda_0 = 120$ m
Numerical Parameters	**Values**
Spatial domain of computation	$x \in [-5\lambda_0, -5\lambda_0]$ or $[-2.5\lambda_0, 2.5\lambda_0]$ $y \in [-2.5\lambda_0, 2.5\lambda_0]$
Temporal domain of computation	$t \in [0, 12T]$
Number of grid cells	250×250
Left Boundary condition	Incoming sinusoidal waves
Right Boundary condition	Outflow boundary
Bottom Boundary condition	Outflow boundary
Top Boundary condition	Outflow boundary

Table 5.1: Configuration for the hypothetical numerical simulations

5.3. Test case 1: Hypothetical Surface Waves

In this test case, the surface waves based on parameters given in Table 5.1 will be studied.

5.3.1. Test case 1a: Depth Perturbation vs Uniform Gravity and Depth

To begin with, the classical case of uniform water depth perturbed with a two-dimensional Gaussian function is reviewed. The gravity is uniform as in the classical theory. Figure 5.1 to 5.4 give the simulation results. The fourth subplot, which measures the instantaneous difference between the surface elevations of test and reference waves, serves as a preliminary indicator of the scattered wave due to the topographical feature.

Figure 5.1: Hypothetical Waves with Gaussian Depth Perturbation. FWHM=120 m, $\Delta D = 2$ m, wavelength=60 m. Reference: $\Delta D = 0$, $\Delta g = 0$.

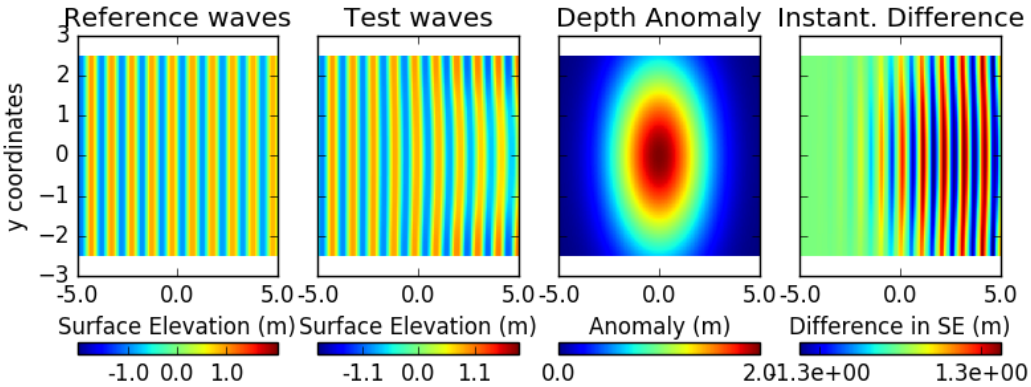

It can be noted by comparing 5.1 and 5.3 that the dispersion of perturbation significantly affects the spatial structure of scattered waves. For a highly-localised (relative to the wavelengths) perturbed depth, such as in Figure 5.3 or 5.4, the depth perturbation acts like a point-source for near-circular scattered waves. It is also noted that when the depth perturbation is positive, representing a bottom

Physical Parameters	**Values**
Reference Gravity, g_0	9.806228 ms^{-2}
Mean Depth of Ocean, $\bar{D}$	4000 m
Maximum Perturbing Gravity, Δg_z	50 mGal = 0.0005 ms^{-2}
Maximum Perturbing Mean-Sea Level, ΔD_0	50 m
'Half-life' Distance, $r_{\frac{1}{2}}$	500 km
Period of Tsunami wave, T_{tsu}	45 minutes
Period of Tidal wave, T_{tidal}	12 hours
Reference Tsunami wavelength, λ_{tsu}	540 km
Reference Tidal wavelength, λ_{tidal}	8640 km
Amplitude of incoming wave, η_0	5 m
Numerical Parameters	**Values**
Spatial domain of computation (tsunami)	$x \in [-5\lambda, -5\lambda]$ $y \in [-2.5\lambda, 2.5\lambda]$
Spatial domain of computation (tidal)	$x \in [-2.5\lambda, -2.5\lambda]$ $y \in [-2.5\lambda, 2.5\lambda]$
Temporal domain of computation	$t \in [0, 12T]$
Number of grid cells	250×250
Left Boundary condition	Incoming sinusoidal wave
Right Boundary condition	Outflow boundary
Bottom Boundary condition	Outflow boundary
Top Boundary condition	Outflow boundary

Table 5.2: Parameters used to mimic the actual physical setting in the Ocean and its waves

pit, in addition to the near-circular scattered waves, other small-amplitude waves are also excited.

On the other hand, for a dispersive perturbation as in Figure 5.1 or 5.2 such that the perturbed area is comparable to the wavelength, the depth perturbation refracts and scatters plane waves. In particular, when the plane waves propagate over a circular bottom pit, the plane waves are refracted away and diverged from the pit. On the other hand, when the planes waves propagate over a subsurface mountain, the waves converge towards the centre of mountain.

5.3.2. Test case 1b: Gravity Perturbation vs Uniform Gravity and Depth

In the next step, the case in which a uniform gravity field is perturbed Gaussianly will be studied. Figure 5.5 to 5.8 outline the numerical simulations where Gaussian gravity perturbations are added to homogeneous gravity and water depth medium.

It can be noted that the figures are very similar to those in Test case 1a, which deals with waves in perturbed water depth. This motivates the comparison between the perturbation in gravity and depth, which will be presented in the next section.

5.3.3. Test case 1c: Gravity Perturbation vs Depth Perturbation

Recall in Table 5.1 that the both the uniform and perturbed components of gravity and water depth are chosen to be equal in magnitude. This enables fair comparisons in this section.

In this test case, the test waves experience Gaussian gravity perturbation and the reference ones experience Gaussian water depth perturbation. Figure 5.9 to 5.12 give the simulation results.

It can be immediately noticed from the subplots of instantaneous differences that the waves scattered respectively by the gravity and depth perturbation are nearly identical. This is not unexpected since the scattering property is controlled by the wave speed field $c(x, y)$, given by

$$c(x, y) = \sqrt{g_z D_0},$$

with g_z and D_0 being the effective gravity and time-average water depth. In this test case the perturbation added respectively to g_z and D_0 are identical in both spatial distribution and magnitude, resulting

Figure 5.2: Hypothetical Waves with Gaussian Depth Perturbation. FWHM=120 m, $\Delta D = -2$ m, wavelength=60 m. Reference: $\Delta D = 0$, $\Delta g = 0$.

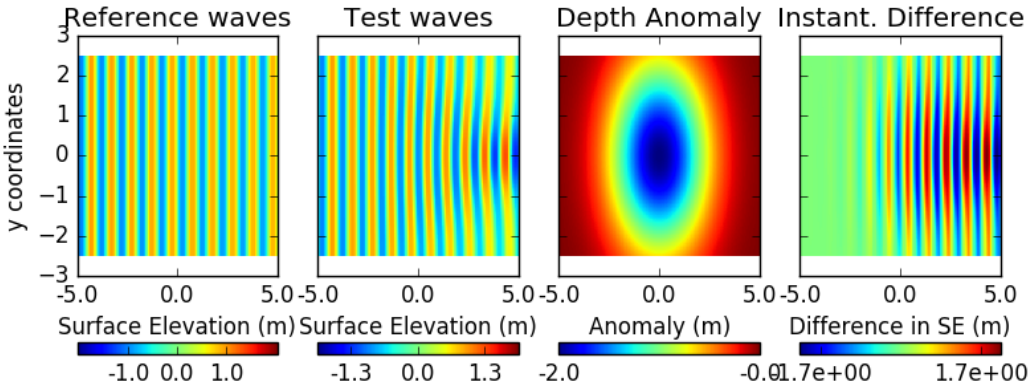

Figure 5.3: Hypothetical Waves with Gaussian Depth Perturbation. FWHM=120 m, $\Delta D = 2$ m, wavelength=1200 m. Reference: $\Delta D = 0$, $\Delta g = 0$.

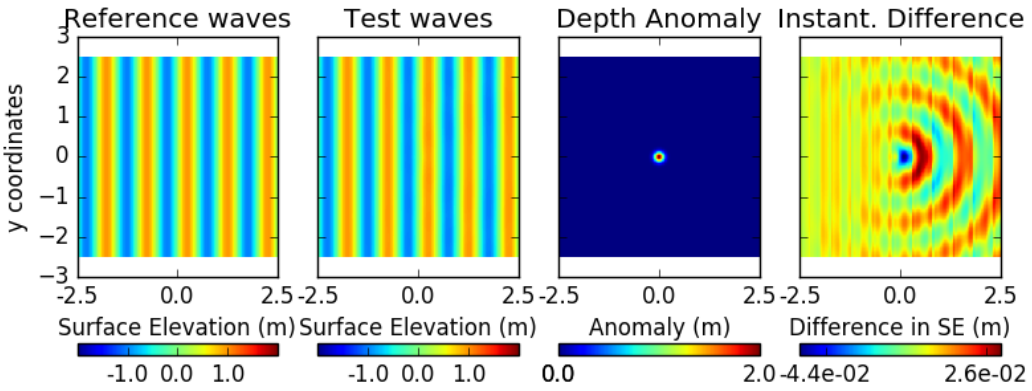

identical fields of wave speed $c(x, y)$ for both the test waves and reference waves. Hence the scattered waves are expected to be in phase.

Meanwhile, the instantaneous difference of surface elevation also reveals another feature in the adapted shallow water waves. Readers are reminded that the governing equations for the adapted shallow water waves (3.138) differ from the standard ones only by an additional term $\mathbf{U} \cdot \nabla \ln(\frac{g_z}{g_0})$ in the right-hand side of depth-averaged continuity equation. In the one-dimensional analytic studies given in Chapter 4 it has been shown that this additional term results in both changes of amplitude and wavenumber of waves. Reader may refer to the derivation of equation (4.73) for the details.

By comparing the subplots of the gravity perturbation field and the instantaneous differences in Figure 5.9 to 5.12, it is clear that the spatially varying gravity field in the two-dimensional space does a very similar job.

However, as discussed in Section 5.1, a handy diagnostic tool for wave dynamics in two-dimension is hard to obtain. A closed form expression as given in (4.73) may thus be difficult to obtain analytically. To overcome this limitation, the numerical solutions can be analysed to obtain the time-independent wave amplitude field. After removing the effects of scattered waves, the maximum amplitude over time at each numerical cell can be recorded to determine the spatial structure of the amplitude field. The results can thus be compared with the gravity field. For the purpose of this project, which focuses on ocean waves on the Earth surface, it will be demonstrated in the next test case that such analysis is unnecessary. Due to the time constraint, this analysis will be omitted in this project.

Figure 5.4: Hypothetical Waves with Gaussian Depth Perturbation. FWHM=120 m, $\Delta D = -2$ m, wavelength=1200 m. Reference: $\Delta D = 0$, $\Delta g = 0$.

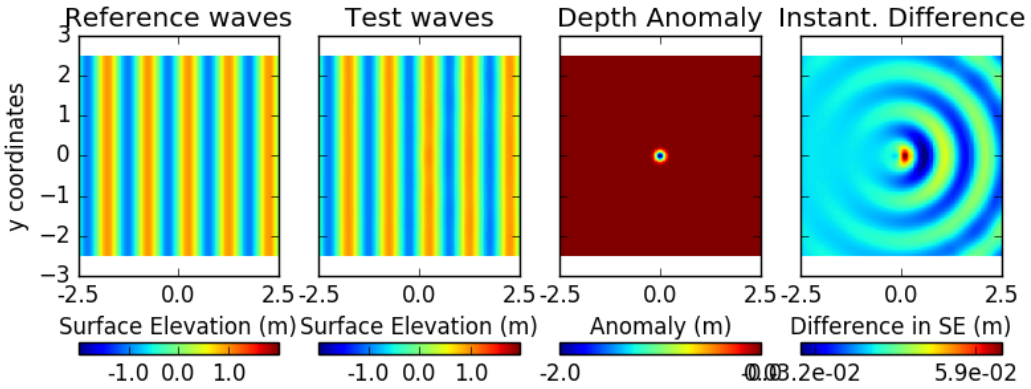

Figure 5.5: Hypothetical Waves with Gaussian Gravity Perturbation. FWHM=120 m, $\Delta g = 2$ ms^{-2}, wavelength=60 m. Reference: $\Delta D = 0$, $\Delta g = 0$.

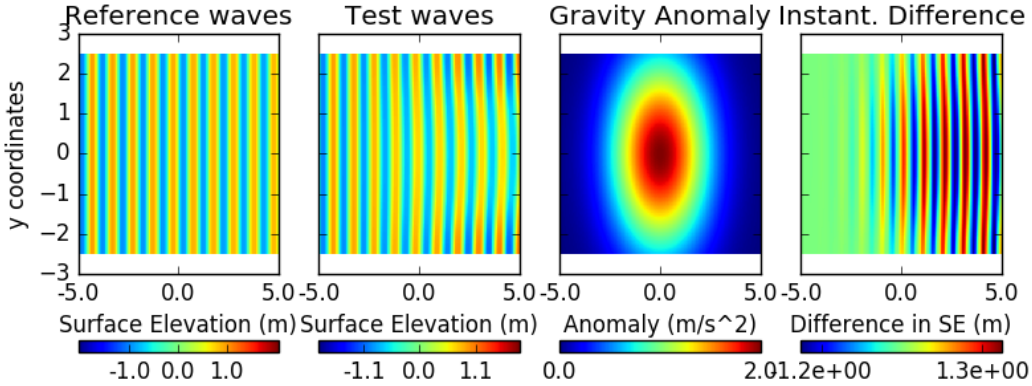

5.4. Test case 2: Physical Surface Waves

In this test case, the surface waves based on parameters given in Table 5.2 will be studied. Both idealistic tsunami and tidal waves will be reviewed.

5.4.1. Test case 2a: Gravity Perturbation vs Uniform Gravity and Depth

Based on the configuration given in Table 5.2, a Gaussian gravity perturbation with peak 50 mGal is added the uniform gravity field 9.80622 ms^{-2} in constant water depth 4 km in this test case. The surface waves are compared with the reference waves in which no perturbation is experienced.

Figure 5.13 and 5.14 give an account for the effects of the gravity perturbations on the tsunami waves in the actual ocean. Figure 5.15 and 5.16 on the other hand suggest the possible consequences when tidal waves propagate over a spatially-varying gravity field in the ocean.

It can be noted that since the wavelengths of tsunami waves are comparable to the length scale of the gravity perturbation area, the resulted scattered field is highly similar to the hypothetical test waves in Figure 5.5 and 5.5. On the other hand, the tidal waves are very similar to the hypothetical waves in 5.5 and 5.5 thanks to the similarity in relative length scales between wavelengths and gravity perturbation field.

It can be noted in all four figures from 5.13 and 5.16 that while the spatial structures of the scattered waves are very similar to the hypothetical scattered waves, the magnitudes of the scattered waves are maximally of order $\mathcal{O}(10^{-3}\text{m})$, which is much smaller than that in the hypothetical waves. This is not surprising since the relative size of the gravity perturbation is much smaller in the physical setting than that in the hypothetical cases.

Figure 5.6: Hypothetical Waves with Gaussian Gravity Perturbation. FWHM=120 m, $\Delta g = -2$ ms^{-2}, wavelength=60 m. Reference: $\Delta D = 0$, $\Delta g = 0$.

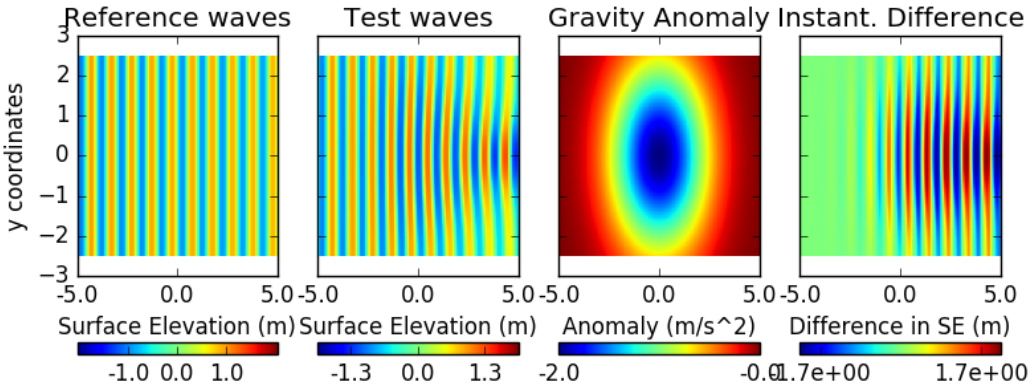

Figure 5.7: Hypothetical Waves with Gaussian Gravity Perturbation. FWHM=120 m, $\Delta g = 2$ ms^{-2}, wavelength=1200 m. Reference: $\Delta D = 0$, $\Delta g = 0$.

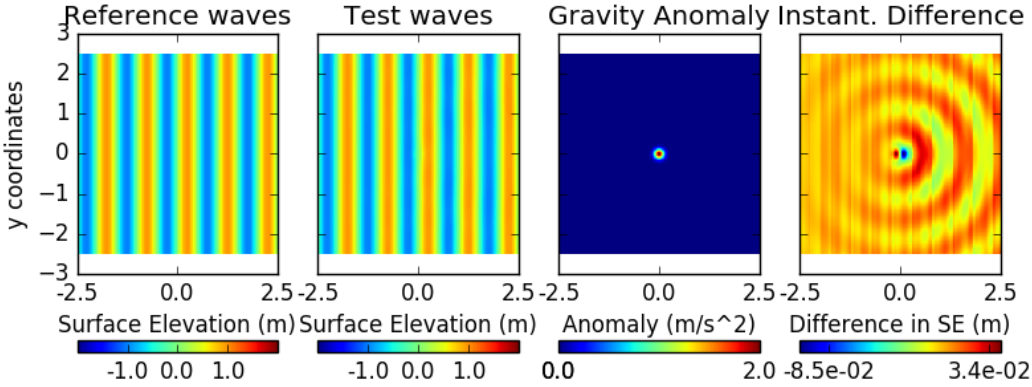

From the four figures from 5.13 and 5.16, it can be concluded that the spatially-varying gravity field alone on Earth surface only lead to minimal changes to the ocean surface waves.

5.4.2. Test case 2b: Gravity and Depth Perturbation vs Uniform Gravity and Depth

In this test case, the changes in surface elevation due to water depth perturbation is also taken into account. Same as the one-dimensional test cases given in the previous chapter, the changes in surface elevation are assumed to be linearly related to the gravity perturbation.

Figure 5.17 to 5.20 give the behaviour of tsunami and tidal waves in several physically representative scenarios. The configurations for each figure are specified in the captions.

The qualitative features in Figure 5.17 to 5.20 are very similar to Figure 5.13 and 5.14 respectively. The differences lie in the quantitative measures: when the depth perturbation is included, the scattered waves are at least $\mathcal{O}(10^{-2}m)$ larger in amplitude, which makes it possibly observable in the nature. In order to identify the cause for the increase in wave amplitude, the next test case is introduced.

5.4.3. Test case 2c: Gravity and Depth Perturbation vs Uniform Gravity and Depth Perturbation

In the final test case, the ocean surface waves which experienced both gravity and depth perturbation (test waves) are compared against the waves which only encountered depth perturbation (reference waves). Figure 5.21 to 5.24 give the corresponding scenarios. The purpose of the comparison is to 'filter out' the effects of depth perturbation from the combined perturbations. Hence the subplots of

Figure 5.8: Hypothetical Waves with Gaussian Gravity Perturbation. FWHM=120 m, $\Delta g = -2$ ms^{-2}, wavelength=1200 m. Reference: $\Delta D = 0$, $\Delta g = 0$.

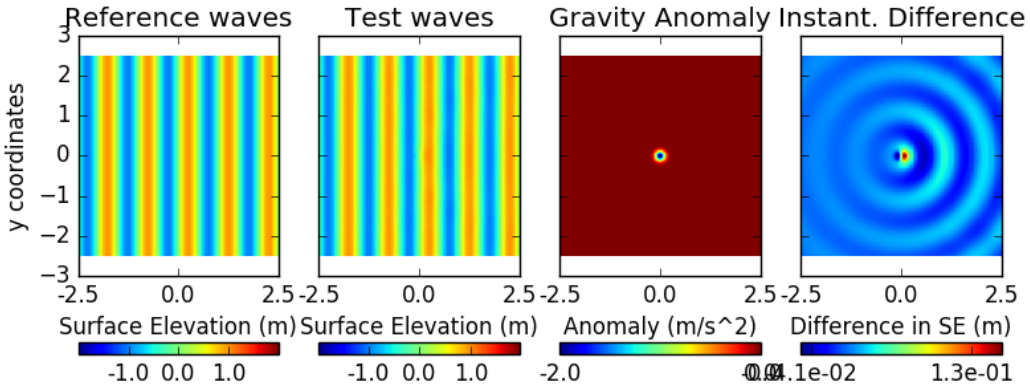

Figure 5.9: Hypothetical Waves with Gaussian Gravity Perturbation. FWHM=120 m, $\Delta g = 2$ ms^{-2}, wavelength=60 m. Reference: $\Delta D = 2$, $\Delta g = 0$.

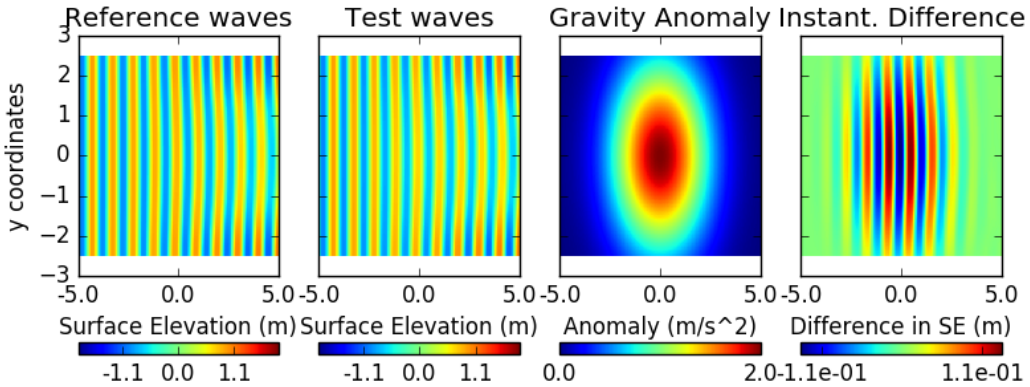

instantaneous difference between test and reference waves represents only the waves scattered by the gravity perturbation. It is highlighted that the 'filtering' is not rigorous since the scattered waves are not necessarily linear. However for the sake of an overview, the result is sufficient.

It can be directly observed from the plots of instantaneous difference that the order of magnitudes of wave amplitudes are similar to that in Figure 5.13 to 5.16. This implies that the gravity-induced depth perturbation is dominant in the combined effects.

The quantitative justification can also be noted from that fact that the gravity perturbation maximally corresponds to $\mathcal{O}(10^{-3}\%)$ change to the gravity, while the depth perturbation is capable of making up to $\mathcal{O}(1\%)$ change in the actual geophysical setting.

5.5. Conclusions from Test Cases

In the hypothetical test cases, it has been shown that the gravity perturbation scatters surface waves as what the depth does in the adapted shallow water model. It has also been noted that the field of wave amplitude is also associated with the gravity field, similar to the one-dimensional test cases studied in the previous chapter.

In the physical test cases, it becomes clear that while in practice the surface waves can be altered by the gravity perturbation, the effects are mainly attributed to the induced-changes of water depth. Based on the adapted shallow water model, the variations of gravity in itself are too weak to make up a huge difference for the ocean surface waves. In other words, the studies also justify the assumption of uniform gravity for surface waves in the geophysical setting on Earth surface.

Figure 5.10: Hypothetical Waves with Gaussian Gravity Perturbation. FWHM=120 m, $\Delta g = -2$ ms^{-2}, wavelength=60 m. Reference: $\Delta D = -2$, $\Delta g = 0$.

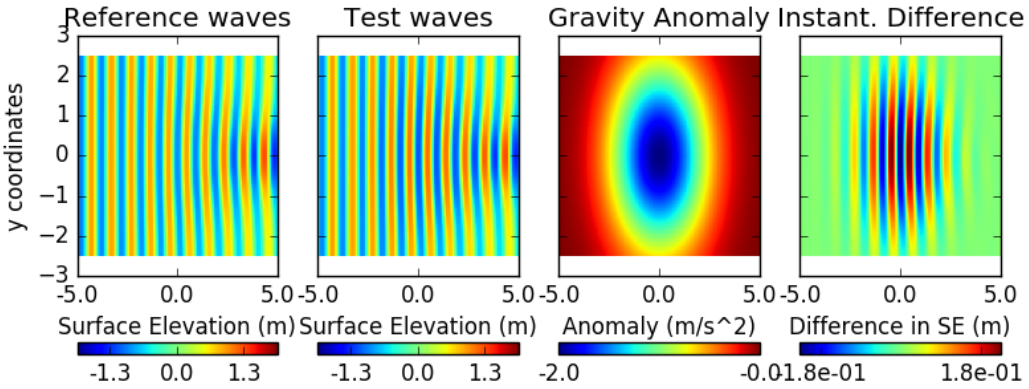

Figure 5.11: Hypothetical Waves with Gaussian Gravity Perturbation. FWHM=120 m, $\Delta g = 2$ ms^{-2}, wavelength=1200 m. Reference: $\Delta D = 2$, $\Delta g = 0$.

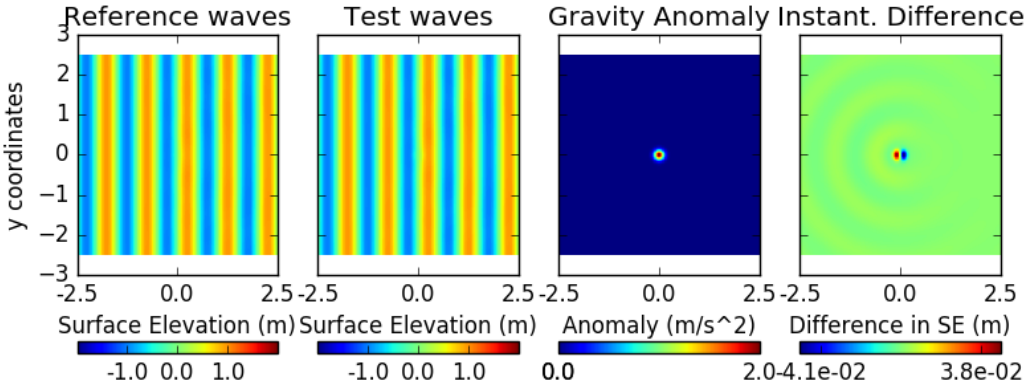

5.6. Final Remarks on Surface Waves on a Two-Dimension Plane

Typically on the two-dimension plane, the surface water waves are analysed by the ray theory, which assumes a slowly-varying medium for the wave propagation. It appears to be possible that the adapted shallow water waves equations (3.138) can be studied by the ray theory after certain adaptations. However, as seen in the test cases, the gravity variation on Earth is not strong enough to induce any observable difference. Hence the detailed analysis is not performed for the purpose of this project.

Interested readers may refer to any introductory text on wave dynamics in fluid, for instance, Pedlosky(2003), LeBlond and Mysak(1981) or Lighthill (1978), for the details of ray theory.

Readers are also reminded that the Coriolis force induced by the Earth's rotation are neglected in the test cases. In a more realistic modelling of large-scale ocean surface waves, the Coriolis force certainly plays a very important role and should never be omitted. Pedlosky(2003) provides a comprehensive introduction to the ocean surface waves in a rotating frame for interested readers.

Figure 5.12: Hypothetical Waves with Gaussian Gravity Perturbation. FWHM=120 m, $\Delta g = -2$ ms^{-2}, wavelength=1200 m. Reference: $\Delta D = -2$, $\Delta g = 0$.

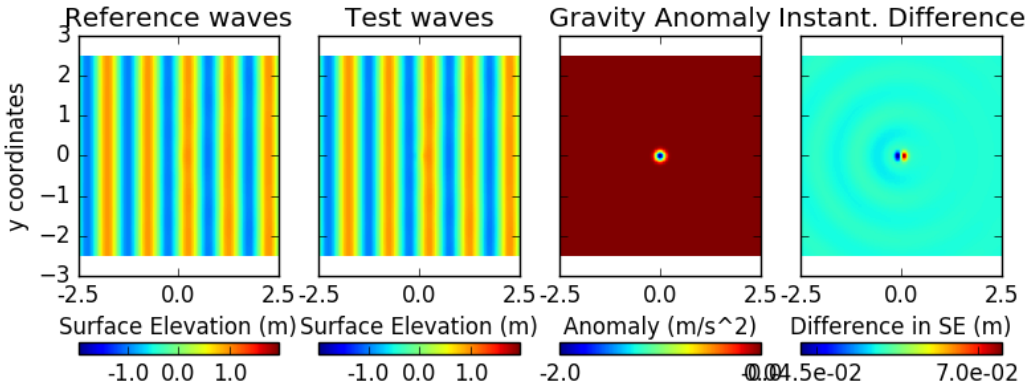

Figure 5.13: Physical Tsunami Waves with Gaussian Gravity Perturbation. FWHM=500 km, $\Delta g = 50$ mGal, wavelength=540 km. Reference: $\Delta D = 0$, $\Delta g = 0$.

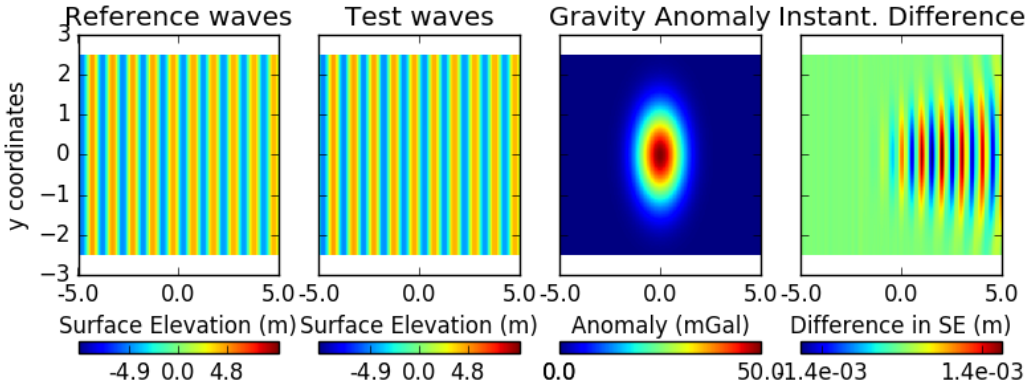

Figure 5.14: Physical Tsunami Waves with Gaussian Gravity Perturbation. FWHM=500 km, $\Delta g = -50$ mGal, wavelength=540 km. Reference: $\Delta D = 0$, $\Delta g = 0$.

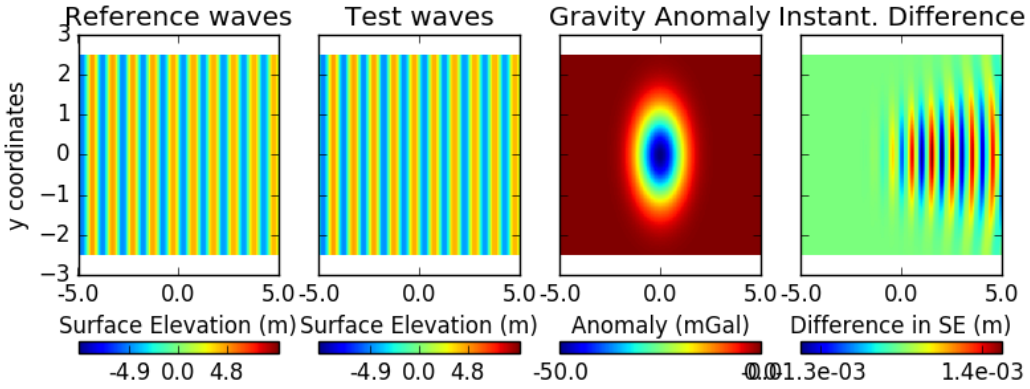

Figure 5.15: Physical Tidal Waves with Gaussian Gravity Perturbation. FWHM=500 km, $\Delta g = 50$ mGal, wavelength=8640 m. Reference: $\Delta D = 0$, $\Delta g = 0$.

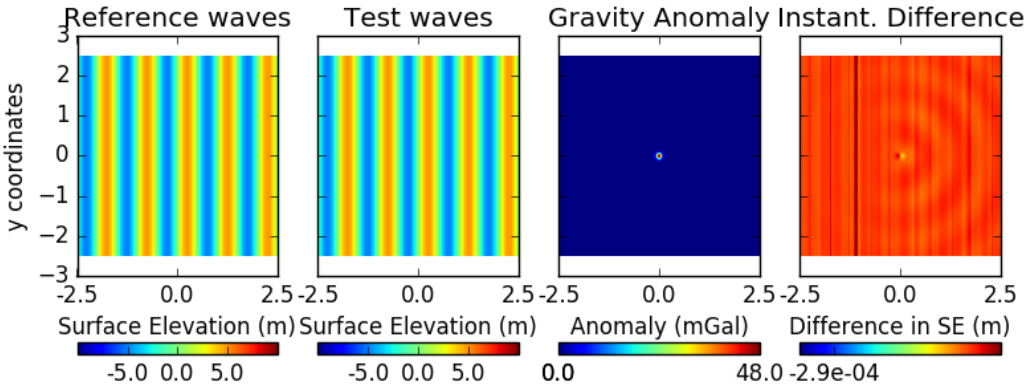

Figure 5.16: Physical Tidal Waves with Gaussian Gravity Perturbation. FWHM=500 km, $\Delta g = -50$ mGal, wavelength=8640 m. Reference: $\Delta D = 0$, $\Delta g = 0$.

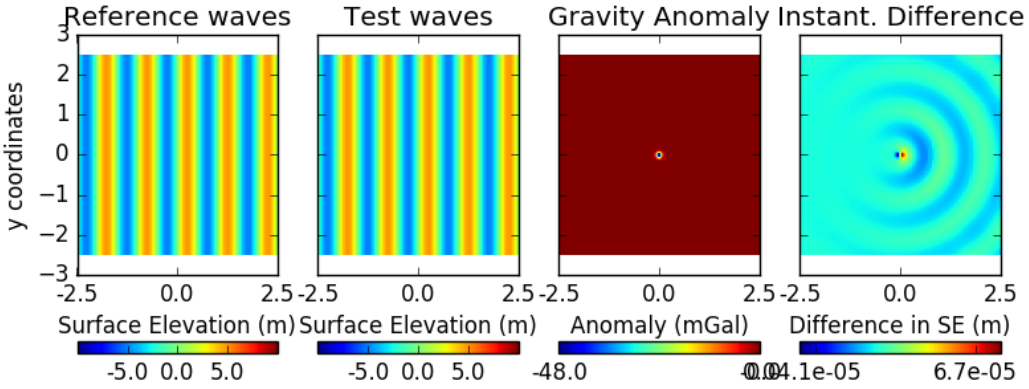

Figure 5.17: Physical Tsunami Waves with Gaussian Gravity Perturbation. FWHM=500 km, $\Delta g = 50$ mGal, $\Delta D = 50$ m, wavelength=540 km. Reference: $\Delta D = 0$, $\Delta g = 0$.

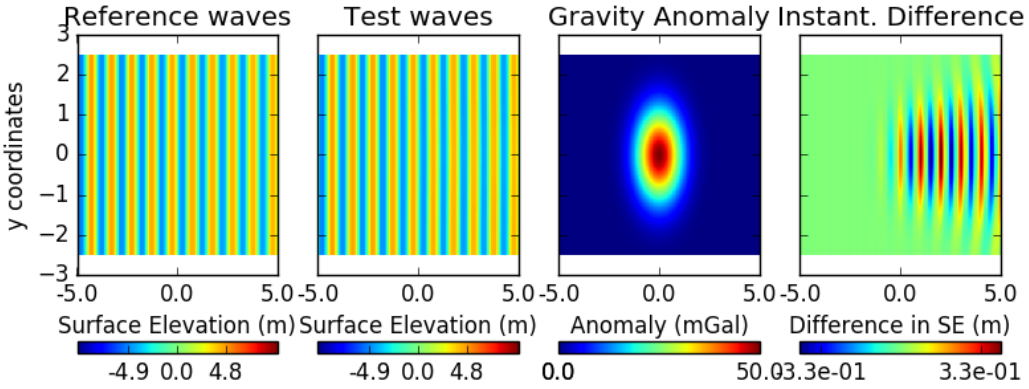

Figure 5.18: Physical Tsunami Waves with Gaussian Gravity Perturbation. FWHM=500 km, $\Delta g = -50$ mGal, $\Delta D = -50$ m, wavelength=540 km. Reference: $\Delta D = 0$, $\Delta g = 0$.

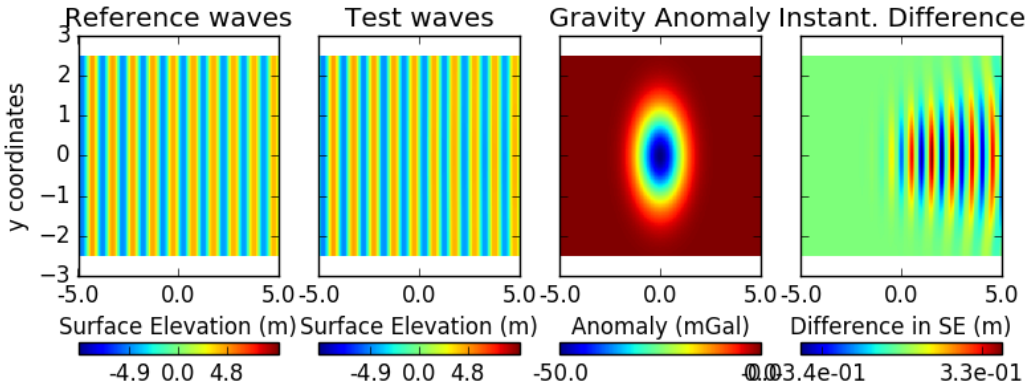

Figure 5.19: Physical Tidal Waves with Gaussian Gravity Perturbation. FWHM=500 km, $\Delta g = 50$ mGal, $\Delta D = 50$ m, wavelength=8640 m. Reference: $\Delta D = 0$, $\Delta g = 0$.

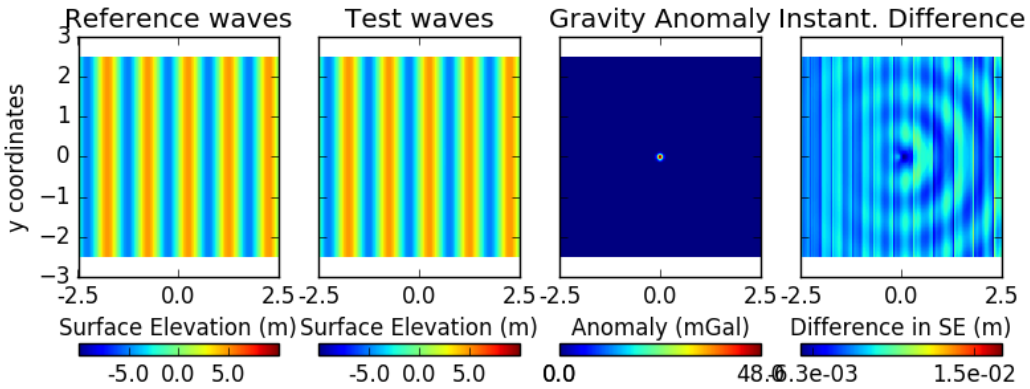

Figure 5.20: Physical Tidal Waves with Gaussian Gravity Perturbation. FWHM=500 km, $\Delta g = -50$ mGal, $\Delta D = -50$ m, wavelength=8640 m. Reference: $\Delta D = 0$, $\Delta g = 0$.

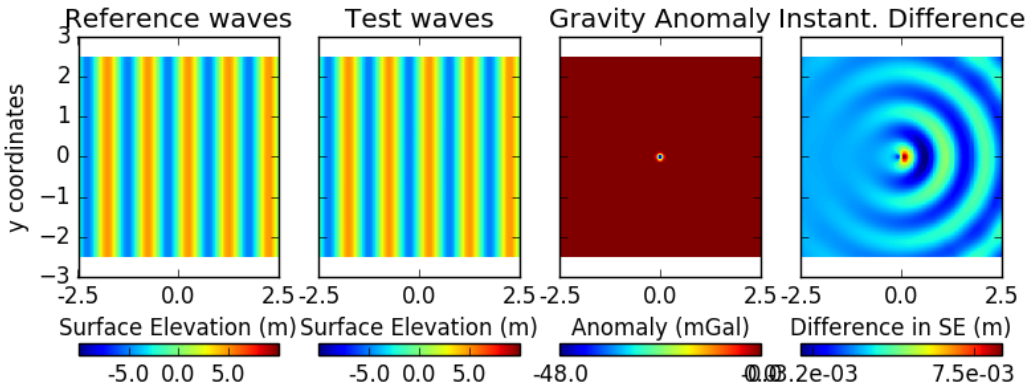

Figure 5.21: Physical Tsunami Waves with Gaussian Gravity Perturbation. FWHM=500 km, $\Delta g = 50$ mGal, $\Delta D = 50$ m, wavelength=540 km. Reference: $\Delta g = 0$, $\Delta D = 50$ m.

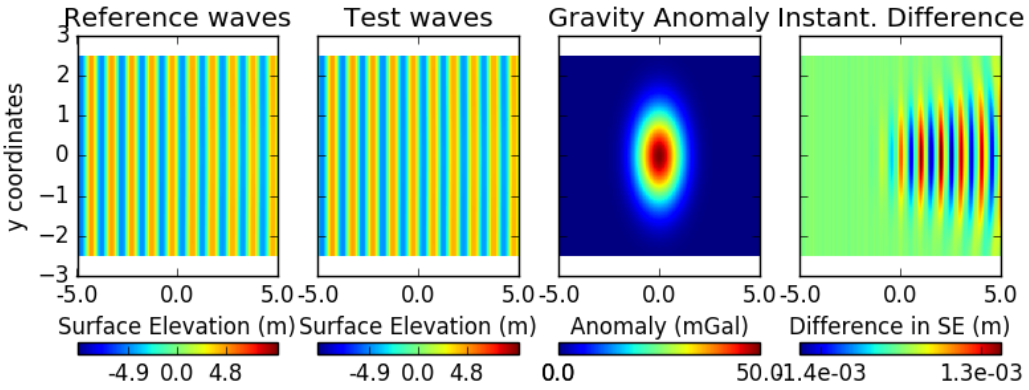

Figure 5.22: Physical Tsunami Waves with Gaussian Gravity Perturbation. FWHM=500 km, $\Delta g = -50$ mGal, $\Delta D = -50$ m, wavelength=540 km. Reference: $\Delta g = 0$, $\Delta D = -50$ m.

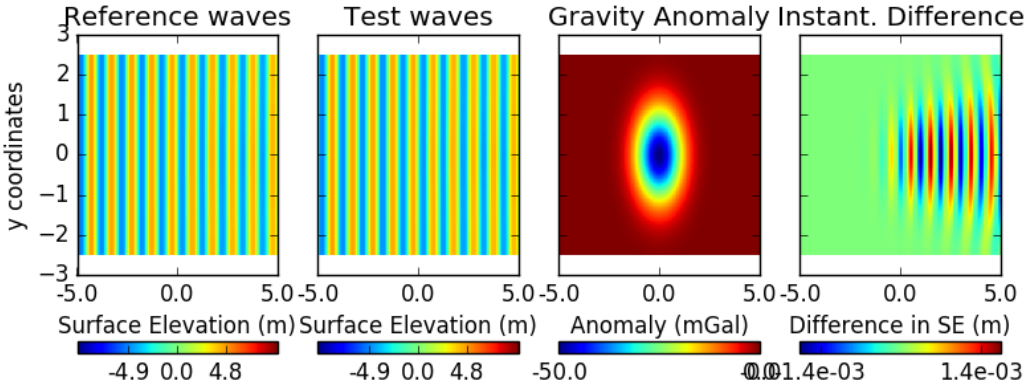

Figure 5.23: Physical Tidal Waves with Gaussian Gravity Perturbation. FWHM=500 km, $\Delta g = 50$ mGal, $\Delta D = 50$ m, wavelength=8640 m. Reference: $\Delta g = 0$, $\Delta D = 50$ m.

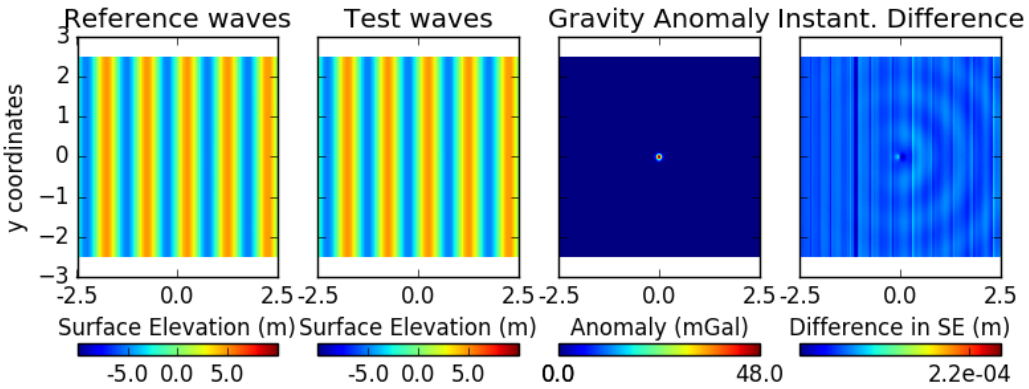

Figure 5.24: Physical Tidal Waves with Gaussian Gravity Perturbation. FWHM=500 km, $\Delta g = -50$ mGal, $\Delta D = -50$ m, wavelength=8640 m. Reference: $\Delta g = 0$, $\Delta D = -50$ m.

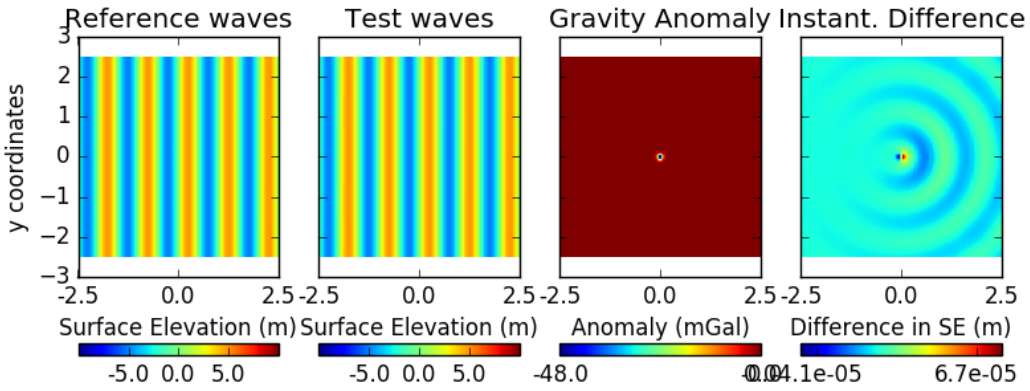

6

Generalised Airy's Linear Wave Theory

In this chapter, Airy's linear wave theory will be generalised for a general conservative gravitational field. The chapter begins with a variational formalism for surface gravity waves. The linear waves will then be studied in two-dimensional and three-dimensional space.

6.1. Derivation: Variational Formalism of Surface Gravity Waves

In this chapter, the variational formalism will be presented to derive a set of equations governing the surface gravity waves in a fluid.

Luke (1967) considered the free surface gravity waves in incompressible, irrotational and inviscid fluids, which allows the expression of velocity field $\mathbf{v}$ by a velocity potential ϕ such that $\mathbf{v} = \nabla\phi$. He proposed a Lagrangian variational scheme to derive both linear and non-linear waves. For a conservative gravity field $\mathbf{g} = -\nabla\Psi$ with geopotential Ψ and fluid of density ρ, the Lagrangian $\mathcal{L}$, also known as Luke's Lagrangian, is given by

$$\mathcal{L} = -\int_{t_0}^{t_1} \rho \left[\int_{V(t)} \left(\frac{\partial \phi}{\partial t} + \frac{1}{2}\|\nabla\phi\|^2 + \Psi \right) dV \right] dt, \tag{6.1}$$

where $V(t)$ is the control volume of fluid.

In Luke's paper only the special case where the gravity is uniform was discussed. That is, the special case of $\Psi = g_0 z$ where g_0 is a constant and z is the vertical coordinate in the Cartesian coordinates. In the following discussion a general Ψ and standard Cartesian coordinates (x, y, z) will be considered.

Similar to Luke's approach, a layer of horizontally unbounded fluid with surface elevation $z = \eta(x, y, t)$ and bottom-bed $z = -h(x, y)$ is considered. This leads to the Luke's Lagrangian:

$$\mathcal{L}(\phi, \eta) = -\int_{t_0}^{t_1} \rho \left[\int_{\mathcal{R}^2} \left(\int_{-h(x,y)}^{\eta(x,y,t)} \frac{\partial \phi}{\partial t} + \frac{1}{2}\|\nabla\phi\|^2 + \Psi dz \right) dA \right] dt, \tag{6.2}$$

where $\mathcal{R}^2$ refers to the whole horizontal plane.

The next steps follows directly from the standard procedure of calculus of variation. Based on the variation on velocity potential, the resulting equation is independent of the geopotential Ψ and gives:

$$\nabla^2\phi(x, y, z, t) = \frac{\partial^2 \phi}{\partial x^2} + \frac{\partial^2 \phi}{\partial y^2} + \frac{\partial^2 \phi}{\partial z^2} = 0, \tag{6.3}$$

subject to the boundary condition

$$\text{at } z = -h(x, y): \quad \frac{\partial \phi}{\partial x}\frac{\partial h}{\partial x} + \frac{\partial \phi}{\partial y}\frac{\partial h}{\partial y} = \frac{\partial \phi}{\partial z}, \tag{6.4a}$$

$$\text{at } z = \eta(x, y, t): \quad \frac{\partial \eta}{\partial t} + \frac{\partial \phi}{\partial x}\frac{\partial \eta}{\partial x} + \frac{\partial \phi}{\partial y}\frac{\partial \eta}{\partial y} = \frac{\partial \phi}{\partial z}. \tag{6.4b}$$

Meanwhile applying the variation of surface elevation gives rise to the equation containing Ψ

$$\text{at } z = \eta(x,y,t)\text{: } \frac{\partial \phi}{\partial t} + \frac{1}{2}\|\nabla\phi\|^2 + \Psi = P_a, \tag{6.5}$$

where P_a is the reduced atmospheric pressure, which can be taken as 0 without loss of generality. The detailed derivation of equations (6.3) and (6.4) can be found in Luke (1967) or Whitham's textbook "Linear and Nonlinear Waves" (1974). The detailed derivation of (6.5) shares the same procedure as the standard case where $\Psi = g_0 z$, which can be found also in Whitham's text.

The set of partial differential equations (6.3), (6.4) and (6.5) governs the surface gravity waves. It provides a framework to model non-linear surface gravity waves, which will not be studied in this thesis.

The Laplace equation (6.3) is an equivalent expression for the continuity equation of irrotational fluid. The equation (6.5) is Bernoulli's principle applied at the surface of the fluid, which stems from the momentum equation of fluid. It is noted from the governing equations that the gravity field plays a role only in (6.5), which is related to the momentum equation only.

6.2. One-Dimensional Surface Gravity Waves

6.2.1. Governing Equations for Linear Waves

The governing equations for surface waves (6.3) to (6.5) do not in general have closed-form solutions. To obtain analytic solution, the one-dimensional linear surface gravity waves in a general conservative gravity field will be studied first.

The one-dimensional waves are obtained by removing the y-coordinates in (6.3), (6.4) and (6.5), which gives

$$\frac{\partial^2 \phi}{\partial x^2} + \frac{\partial^2 \phi}{\partial z^2} = 0, \tag{6.6}$$

subject to the boundary condition

$$\text{at } z = -h(x)\text{: } \frac{\partial \phi}{\partial x}\frac{\partial h}{\partial x} = \frac{\partial \phi}{\partial z}, \tag{6.7a}$$

$$\text{at } z = \eta(x,t)\text{: } \frac{\partial \eta}{\partial t} + \frac{\partial \phi}{\partial x}\frac{\partial \eta}{\partial x} = \frac{\partial \phi}{\partial z}, \tag{6.7b}$$

and

$$\text{at } z = \eta(x,t)\text{: } \frac{\partial \phi}{\partial t} + \frac{1}{2}\left[\left(\frac{\partial \phi}{\partial x}\right)^2 + \left(\frac{\partial \phi}{\partial z}\right)^2\right] + \Psi = 0. \tag{6.8}$$

Define $z = \delta m(x)$ to be the mean-sea level, such that $\Psi(x, \delta m(x)) = \Psi_0$ for some known constant Ψ_0. For small amplitude motion $|\eta(x,t) - \delta m(x)| \ll h(x)$, following the procedure given by Airy (1841), the governing equations for linear surface wave is given by

$$\frac{\partial^2 \phi}{\partial x^2} + \frac{\partial^2 \phi}{\partial z^2} = 0, \tag{6.9}$$

subject to the linearised boundary conditions

$$\text{at } z = -h(x)\text{: } \frac{\partial \phi}{\partial z} + \frac{\partial \phi}{\partial x}\frac{\partial h}{\partial x} = 0, \tag{6.10a}$$

$$\text{at } z = \delta m(x)\text{: } \frac{\partial \eta}{\partial t} = \frac{\partial \phi}{\partial z}, \tag{6.10b}$$

$$\text{at } z = \delta m(x)\text{: } \frac{\partial \phi}{\partial t} - \Psi(x,\eta) = 0, \tag{6.10c}$$

The set of equation (6.9) and (6.10) is the governing equations for the linear surface gravity wave in fluid. It is also a generalisation of the Airy's linear wave theory for general conservative gravitational field.

Unlike the standard case where the the geopotential $\Psi(x,\eta)$ is simply given by $\Psi(x,\eta) = g_0\eta$, the geopotential Ψ is now a general function in spatial-coordinates (x,z). This brings difficulty in the pursuit of ansatz. In order to address this issue, a coordinate transformation scheme is proposed in the next section.

6.2.2. Motivation for the Coordinate Transformation

Recall that the geopotential $\Psi(x,z)$ satisfies the two-dimensional Laplace equation in free-space, that is,

$$\nabla^2\Psi = 0, \tag{6.11}$$

subject to suitable boundary conditions.

A classical result from complex analysis reveals that, if function $q_1(x,z)$ is a solution to the Laplace equation, there exists a harmonic conjugate $q_2(x,z)$ that also satisfies the Laplace equation. The function $q_2(x,z)$ satisfies the Cauchy-Riemann condition, namely,

$$\frac{\partial q_1}{\partial x} = \frac{\partial q_2}{\partial z}, \tag{6.12a}$$

$$\frac{\partial q_2}{\partial x} = -\frac{\partial q_1}{\partial z}. \tag{6.12b}$$

Note that $q_2(x,z)$ is unique up to a constant.

Define a time-independent orthogonal coordinate transformation $(x,y) \to (q_1,q_2)$, using the transformation rule:

$$q_2(x,z) = \frac{\Psi(x,z) - \Psi_0}{g_0}, \tag{6.13a}$$

$$q_1(x,z) = \text{harmonic conjugate of } q_2(x,z), \text{ subject to } q_1(0,\delta m(0)) = 0, \tag{6.13b}$$

where $\Psi_0 = \Psi(x,\delta m(x))$ is the mean-sea level potential and g_0 is a constant which takes the value of reference gravity.

Physically $q_2(x,y)$ measures the scaled potential difference at point (x,y) with the mean-sea level, which reduces into the Cartesian vertical coordinates z in the case of uniform gravity. Meanwhile, in the case of uniform gravity, q_1 is reduced into the Cartesian horizontal coordinates x. Both q_1 and q_2 are uniquely determined thanks to the condition in defining q_1.

6.2.3. Properties of the Conformal Coordinate Transformation

The very first property of the coordinate transformation is that u and v are orthogonal to each others.

Consider the contrapositive basis

$$\mathbf{a}^{(1)} = \nabla q_1 \tag{6.14a}$$

$$\mathbf{a}^{(2)} = \nabla q_2 \tag{6.14b}$$

Since the Cauchy-Riemann condition is satisfied, $\nabla q_1 \cdot \nabla q_2 = 0$, which implies the orthogonality between q_1 and q_2.

In addition, the Euclidean norm of ∇q_1 and ∇q_2 are equal due to the Cauchy-Riemann condition:

$$\|\nabla q_1\|^2 = \left(\frac{\partial q_1}{\partial x}\right)^2 + \left(\frac{\partial q_1}{\partial z}\right)^2 = \left(\frac{\partial q_2}{\partial z}\right)^2 + \left(-\frac{\partial q_2}{\partial x}\right)^2 = \|\nabla q_2\|^2, \tag{6.15}$$

which implies the contrapositive basis $\mathbf{a}^{(1)}$ and $\mathbf{a}^{(2)}$ are equal in norm.

It can then been shown that the covariant basis are therefore given by

$$\mathbf{a}_{(1)} = \frac{1}{\|\nabla q_2\|^2}\left[\frac{\partial q_2}{\partial z}, -\frac{\partial q_2}{\partial x}\right] = \frac{1}{\|\nabla q_1\|^2}\left[\frac{\partial q_1}{\partial x}, \frac{\partial q_1}{\partial z}\right] \tag{6.16}$$

$$\mathbf{a}_{(2)} = \frac{1}{\|\nabla q_1\|^2}\left[-\frac{\partial q_1}{\partial z}, \frac{\partial q_1}{\partial x}\right] = \frac{1}{\|\nabla q_2\|^2}\left[\frac{\partial q_2}{\partial x}, \frac{\partial q_2}{\partial z}\right] \tag{6.17}$$

With the explicit formulas for both the contrapositive and covariant basis, the metric tensors g^{ij} and g_{ij} are computed by $g^{ij} = \mathbf{a}^{(i)} \cdot \mathbf{a}^{(j)}$ and $g_{ij} = \mathbf{a}_{(i)} \cdot \mathbf{a}_{(j)}$:

$$g^{11} = g^{22} = \|\nabla q_1\|^2 = \|\nabla q_2\|^2 \tag{6.18}$$

$$g_{11} = g_{22} = \frac{1}{\|\nabla q_1\|^2} = \frac{1}{\|\nabla q_2\|^2} \tag{6.19}$$

$$g^{12} = g^{21} = g_{12} = g_{21} = 0 \tag{6.20}$$

The quantity $\sqrt{g} = \sqrt{g_{11}g_{22} - g_{12}g_{21}}$ is thus given by:

$$\sqrt{g} = \frac{1}{\|\nabla q_1\|^2} = \frac{1}{\|\nabla q_2\|^2} \tag{6.21}$$

Hence the differential operators in the transformed coordinates are well-defined.

6.2.4. Transformed Laplacian Operators and Laplace Equation

Applying the metric tensor, the Laplacian operator in the transformed coordinates is thus given by

$$\begin{aligned}\nabla^2\phi &= \frac{1}{\sqrt{g}}\frac{\partial}{\partial q_1}\left(\sqrt{g}g^{11}\frac{\partial\phi}{\partial q_1} + \sqrt{g}g^{12}\frac{\partial\phi}{\partial q_2}\right) + \frac{1}{\sqrt{g}}\frac{\partial}{\partial q_2}\left(\sqrt{g}g^{21}\frac{\partial\phi}{\partial q_1} + \sqrt{g}g^{22}\frac{\partial\phi}{\partial q_2}\right)\\ &= \|\nabla q_1\|^2\frac{\partial}{\partial q_1}\left(1\cdot\frac{\partial\phi}{\partial q_1}\right) + \|\nabla q_2\|^2\frac{\partial}{\partial q_2}\left(1\cdot\frac{\partial\phi}{\partial q_2}\right)\end{aligned}$$

But since $\|\nabla q_2\|^2 = \|\nabla q_1\|^2$, the Laplace equation is simply given by

$$\|\nabla q_2\|^2\left[\frac{\partial}{\partial q_1}\left(\frac{\partial\phi}{\partial q_1}\right) + \frac{\partial}{\partial q_2}\left(\frac{\partial\phi}{\partial q_2}\right)\right] = 0$$

or equivalently, when $\|\nabla q_2\| \neq 0$,

$$\frac{\partial^2\phi}{\partial {q_1}^2} + \frac{\partial^2\phi}{\partial {q_2}^2} = 0 \tag{6.22}$$

which preserves the structure of the Laplace equation in Cartesian coordinates.

6.2.5. Transformed Boundary condition

In the Cartesian coordinates, the geometry of bottom boundary $z = -h(x)$ and surface elevation $z = \eta(x,t)$ can be interpreted as given by two level-set $S_B(x,z)$ and $S(x,z,t)$ being equal to zero:

$$S_B(x,z) = z + h(x) = 0 \tag{6.23}$$

$$S(x,z,t) = z - \eta(x,t) = 0 \tag{6.24}$$

While the explicit expression for the inverse coordinate transformation from (x,y) to (q_1,q_2) is in general absent, its existence and uniqueness is guaranteed by the implicit function theorem. Hence, by denoting the inverse transformation by $(u,v) \to (x(q_1,q_2), z(q_1,q_2))$, it is equivalent to express the level-sets by

$$\tilde{S}_B(q_1,q_2) = S_B(x(q_1,q_2), z(q_1,q_2)) = z(q_1,q_2) + h(x(q_1,q_2)) = 0 \tag{6.25}$$

$$\tilde{S}(q_1,q_2,t) = S(x(q_1,q_2), z(q_1,q_2), t) = z(q_1,q_2) - \eta(x(q_1,q_2),t) = 0 \tag{6.26}$$

As long as the conditions of the implicit function theorem are satisfied, the level-sets $\tilde{S}_B(q_1,q_2) = 0$ and $\tilde{S}(q_1,q_2) = 0$ can be expressed by using q_2 as an independent coordinate, in other words, there exists well-defined function $\tilde{h}(q_1)$ and $\tilde{\eta}(q_1,t)$ such that the level-sets $\tilde{S}_B(q_1,q_2)$ and $\tilde{S}(q_1,q_2)$ are given by

$$\tilde{S}_B(q_1,q_2) = v + \tilde{h}(q_1) = 0 \tag{6.27}$$

$$\tilde{S}(q_1,q_2,t) = v - \tilde{\eta}(q_1,t) = 0 \tag{6.28}$$

By considering the total time-derivative of $\tilde{S}_B(q_1,q_2)$ and $\tilde{S}(q_1,q_2)$, the boundary condition in the transformed coordinates are thus given by

$$\text{at } q_2 = -\tilde{h}(q_1)\text{:}\quad \frac{\partial\phi}{\partial q_1}\frac{\partial h}{\partial q_1} = -\frac{\partial\phi}{\partial q_2}, \tag{6.29}$$

$$\text{at } q_2 = \tilde{\eta}(q_1,t)\text{:}\quad \frac{\partial\eta}{\partial t} + \frac{\partial\phi}{\partial q_1}\frac{\partial\eta}{\partial q_1} = \frac{\partial\phi}{\partial q_2}, \tag{6.30}$$

$$\text{at } q_2 = \tilde{\eta}(q_1,t)\text{:}\quad \frac{\partial\phi}{\partial t} + \frac{1}{2}|\nabla\phi|^2 - (g_0 q_2 - \Psi_0) = P_a \tag{6.31}$$

The arbitrary reduced pressure P_a can thus now be chosen as Ψ_0. Considering small-amplitude motion, the linearised boundary condition are thus given by

$$\text{at } q_2 = -\tilde{h}(q_1): \quad \frac{\partial \phi}{\partial q_1}\frac{\partial h}{\partial q_1} = -\frac{\partial \phi}{\partial q_2}, \tag{6.32a}$$

$$\text{at } q_2 = 0: \quad \frac{\partial \tilde{\eta}}{\partial t} = \frac{\partial \phi}{\partial q_2}, \tag{6.32b}$$

$$\text{at } q_2 = 0: \quad \frac{\partial \phi}{\partial t} - g_0\tilde{\eta} = 0 \tag{6.32c}$$

Readers are reminded that the mean-sea level $y = \delta m(x)$ is mapped into $v = 0$ under the coordinate transformation.

6.2.6. Short Summary

Together with the Laplace equation in the transformed coordinates (6.22), the boundary conditions (6.32) indicate that in the transformed orthogonal coordinates (q_1, q_2), surface waves are governed by exactly the same set of equations as in Cartesian coordinates with uniform gravity. Hence all results obtained from the standard Cartesian coordinates can be mapped one-to-one to the scenario with a spatially varying yet conservative gravity field, after the coordinate transformation suggested in (6.13).

The slight difference is, however, the interpretation of the physics. In the standard Cartesian coordinates with uniform gravity, the quantity water depth, which is the physical vertical length between the surface elevation and bottom boundary, is identified as a parameter to control the wave dynamics. In the transformed coordinates, however, it is clear that the true quantity which plays the role is the gravitation potential difference between the surface and bottom along the line of gravity. Figure 6.1 exemplifies a possible coordinates configuration. The coordinate systems for the adapted shallow water model is also exemplified in Figure 6.2 for reference.

Figure 6.1: Example: Conformal Coordinate System

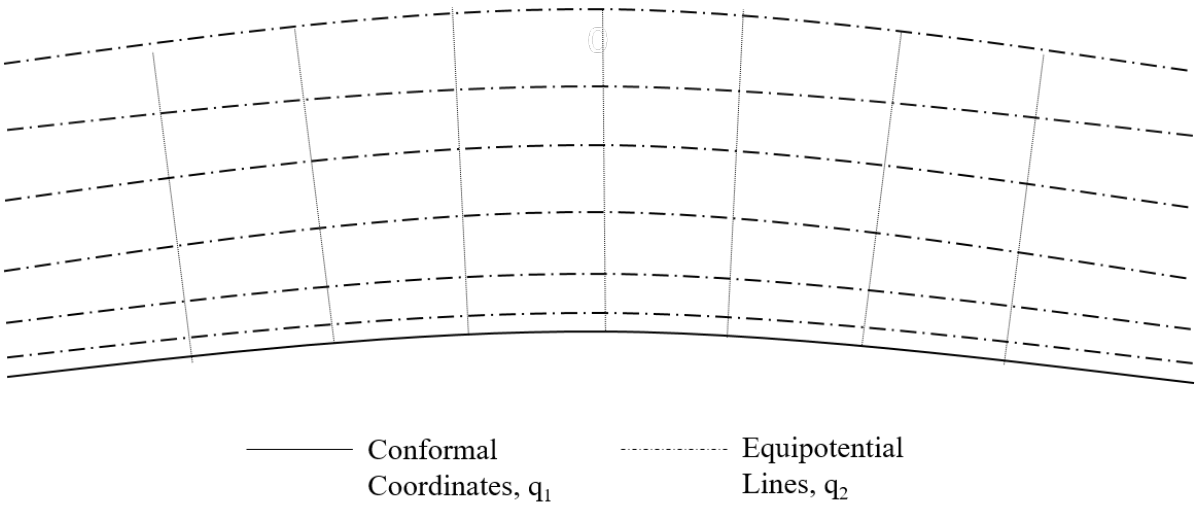

The difference, as seen in Figure 6.1 and 6.2, lies in the orthogonality of the coordinates.

However, readers are reminded that the conformal coordinate transformation only works in two-dimensional settings, thus enabling the studies of one-dimensional surface waves.

6.3. Test Cases for One-Dimensional Linear Waves

In this section, several test cases will be proposed to visualise the linear wave on a general conservative gravitational field.

Figure 6.2: Example: Coordinates for Adapted Shallow Water Model

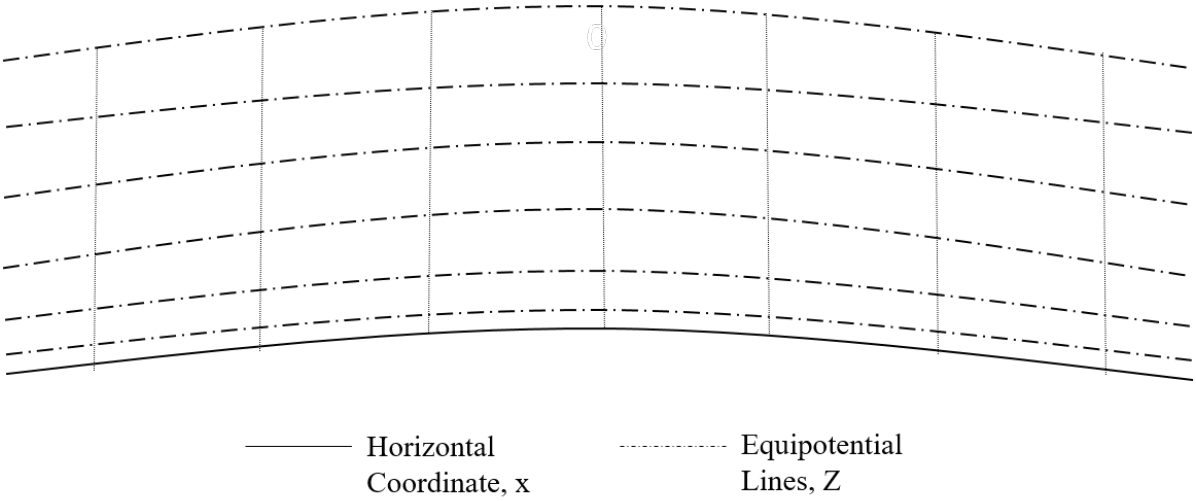

6.3.1. Example 1: Gravity with Inverse-law in 2D

Consider a solid circle of radius R_c with centre lying at the origin of the 2-dimensional plane, as in Figure 6.3. Solving the Poisson equation for the gravitational potential gives rise to a geopotential

$$\Psi(x,z) = g_0 \ln(\sqrt{x^2+z^2}),$$

in the domain $\{(x,y) : x^2+z^2 \geq {R_c}^2\}$, where g_0 is a positive constant.

This also gives rises to a central-forced gravitational field $\mathbf{F}(x,z) = -\nabla\Psi$:

$$\mathbf{F}(x,z) = -g_0\left(\frac{x}{x^2+z^2}\hat{x} + \frac{z}{x^2+z^2}\hat{z}\right), \tag{6.33}$$

whose direction is always pointing towards the origin and magnitude $\|\mathbf{F}(x,z)\| = \frac{g_0}{\sqrt{x^2+z^2}}$ is decaying inversely with the distance $r = \sqrt{x^2+z^2}$. Note that $\hat{x}$ and $\hat{z}$ are the unit vectors in the x and z-direction in the Cartesian plane.

Consider a fixed volume of fluid attached to the surface of the circle. The hydrostatic balance will keep the fluid in the domain $R_c \leq \sqrt{x^2+z^2} \leq R_s$, for some positive constant R_s

The coordinate transformation proposed in (6.13) are then given by

$$q_1(x,z) = \tan^{-1}(\frac{x}{z}) \tag{6.34a}$$

$$q_2(x,z) = \ln(\frac{\sqrt{x^2+z^2}}{R_s}) \tag{6.34b}$$

An explicit expression for the inverse coordinate transformation can be obtained. Manipulating the expression gives

$$\frac{x}{z} = \tan(q_1) \tag{6.35}$$

$$x^2+z^2 = \left[R_s e^{q_2}\right]^2, \tag{6.36}$$

which suggests the inverse transformation by

$$x(q_1,q_2) = R_s e^{q_2}\sin(q_1) \tag{6.37a}$$

$$z(q_1,q_2) = R_s e^{q_2}\cos(q_1) \tag{6.37b}$$

Figure 6.3: Schematic Sketch for Example 1 - a 2D Earth

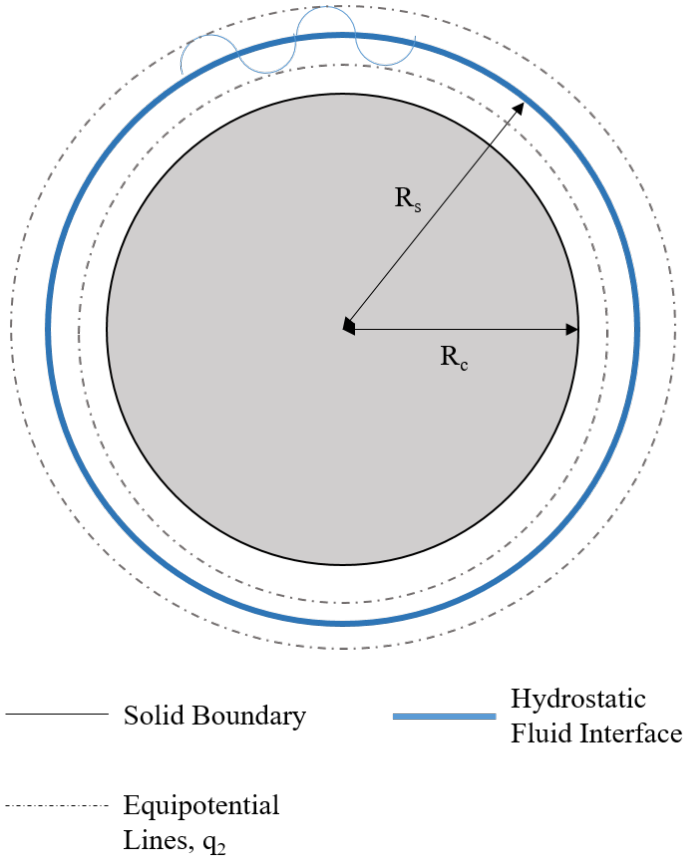

Using the forward and inverse coordinate transformation given in equation (6.34) and (6.37), the physical domain

$$\{(x,z) : \sqrt{x^2+z^2} \geq R_c\}$$

can be mapped into the domain

$$\{(q_1,q_2) : -\pi < q_1 \leq \pi, q_2 \geq -\tilde{h}_0\},$$

where $\tilde{h}_0 = \ln(\frac{R_s}{R_c})$ is denoted to simplify the notation.

It is noted that q_1 is chosen to be bounded to ensure the one-to-one correspondence between the physical coordinates and transformed coordinates. This additionally imposes the periodic boundary condition on the solution of Laplace equation (6.22), which requires that both the surface elevation $\eta(q_1,t)$ and velocity potential $\phi(q_1,q_2,t)$ in the transformed coordinates satisfy

$$\eta(-\pi,t) = \eta(\pi,t) \tag{6.38}$$
$$\phi(-\pi,q_2,t) = \phi(\pi,q_2,t), \tag{6.39}$$

in additional to the boundary conditions given in (6.32):

$$\text{at } q_2 = -: \ \frac{\partial \phi}{\partial q_2} = 0, \tag{6.40a}$$
$$\text{at } q_2 = 0: \ \frac{\partial \eta}{\partial t} = \frac{\partial \phi}{\partial q_2}, \tag{6.40b}$$
$$\text{at } q_2 = 0: \ \frac{\partial \phi}{\partial t} - g_0 \eta = 0. \tag{6.40c}$$

These altogether suggest the monochromatic surface waves with amplitude a, angular frequency ω and wave number k in the transformed coordinates (q_1, q_2), whose surface elevation $q_2 = \eta(q_1, t)$ and velocity potential $\phi(q_1, q_2, t)$ read

$$\eta(q_1, t) = a\cos(kq_1 - \omega t) \tag{6.41a}$$

$$\phi(q_1, q_2, t) = \left(\frac{\omega}{k}a\right)\frac{\cosh(k(q_2 + \tilde{h}_0))}{\sinh(k\tilde{h}_0)}\sin(kq_1 - \omega t) \tag{6.41b}$$

subject to the dispersion relation

$$\omega^2 = g_0 k \tanh(k\tilde{h}_0) \tag{6.42}$$

and the boundary condition

$$\begin{aligned}\cos(k\pi - \omega t) = \cos(-k\pi - \omega t), \forall t &\iff 0 = 2\sin(2k\pi)\sin(\omega t), \forall t \\ &\iff 2k\pi = n\pi \\ &\iff k = \frac{n}{2},\end{aligned}$$

with n being an integer. This indicates that the wave number k is quantised, limiting the modes of wave available, which is not surprising since the fluid remains attached on a circular domain. One can thus also denote the wave number by $k_n = \frac{n}{2}$ to emphasise its quantised nature.

Translating from the transformed coordinates (q_1, q_2) to the physical coordinates (x, y) via equation (6.37) reveals that the surface elevation $q_2 = \eta(q_1, t)$ is described by

$$\ln\left(\frac{\sqrt{x^2 + y^2}}{R_s}\right) = a\cos\left(k_n \tan^{-1}\left(\frac{x}{y}\right) - \omega t\right) \tag{6.43}$$

To make the expression more readable, the standard polar coordinates is now introduced

$$r^2 = x^2 + y^2 \tag{6.44}$$

$$\tan\theta = \frac{y}{x} \tag{6.45}$$

By noting the identity $\tan^{-1}(x) + \tan^{-1}(\frac{1}{x}) = sgn(x)\frac{\pi}{2}$, where $sgn(x)$ is the sign function, the expression for surface elevation (6.41a) becomes

$$r = \eta_r(\theta, t) = R_s \exp\left[a\cos\left(\omega t + k_n\theta - k_n sgn(\theta)\frac{\pi}{2}\right)\right]. \tag{6.46}$$

Note that the constant quantity $-k_n sgn(\theta)\frac{\pi}{2}$ corresponds to the phase shift which can be cancelled by shifting the time variable t. Hence the surface elevation is described by

$$r = \eta_r(\theta, t) = R_s \exp\left[a\cos(\omega t + k_n\theta)\right]. \tag{6.47}$$

Note that by fixing θ, the quantity $\exp\left[a\cos(\omega t + k_n\theta)\right]$ oscillates around 1 from $\exp(-a)$ and $\exp(a)$ in time. This indicates that the periodic variation of surface elevation takes place around of $r = R_s$, albeit not in a linear sinusoidal manner.

One can also reinterpret the equation (6.47) in the framework of harmonic waves. For the wave amplitude a in the transformed coordinates to be sufficiently small, the quantity $\exp\left[a\cos(\omega t + k_n\theta)\right]$ can be expanded as

$$\exp\left[a\cos(\omega t + k_n\theta)\right] = 1 + \sum_{i=1}^{\infty}\frac{a^i}{i!}\cos^i(\omega t + k_n\theta) \tag{6.48}$$

such that the surface elevation is given by

$$r = \eta_r(\theta, t) = R_s\left[1 + \sum_{i=1}^{\infty} \frac{a^i}{i!} \cos^i(\omega t + k_n\theta)\right]. \tag{6.49}$$

This indicates the presence of higher-order harmonics in the oscillation, when the waves are viewed in the physical coordinates.

Note that the coefficients of the i-th order harmonics $\cos^i(\omega t + k_n\theta), i \geq 2$, given by $\frac{a^i}{i!}$, decrease with the order i. Hence to first-order one can approximate the surface elevation also by

$$r = \eta_r(\theta, t) \approx R_s\left[1 + a\cos(\omega t + k_n\theta)\right] \tag{6.50}$$

or equivalently

$$r - R_s \approx A\cos(\omega t + k_n\theta), \tag{6.51}$$

where $A = R_s a$ can be considered as the wave amplitude of the linear wave.

6.3.2. Example 2a: Vertical Downwards Gravity with Perturbation

Figure 6.4: Schematic Sketch for Example 2

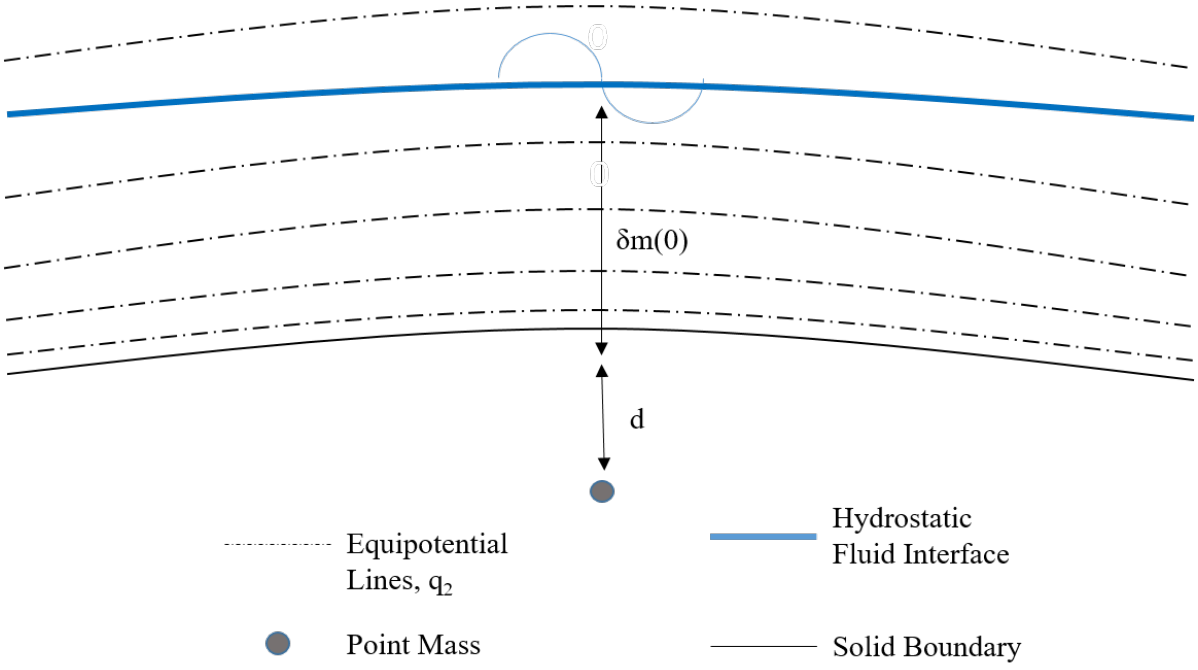

Consider a horizontal layer of fluid over a bottom boundary given by $z = -h(x)$. The uniform gravity field due to the Earth can be regarded as $\mathbf{g}_u = -g_0\hat{z}$, which points vertically downwards in the z-direction.

Suppose, in addition, there is an excess point mass located at $(x, z) = (0, -d)$ under the bottom boundary, that is, $d > h(0)$. This leads to an additional perturbing gravity field $\square\mathbf{g}$ given by

$$\square\mathbf{g}(x, z) = -\frac{(\delta m(0) + d)^2}{\delta m(0)} G_\epsilon\left(\frac{x}{x^2 + (z+d)^2}\hat{x} + \frac{z}{x^2 + (z+d)^2}\hat{z}\right), \tag{6.52}$$

such that also at the mean-sea level at $x = 0$, the perturbing gravity is simply given by $-G_\epsilon\hat{z}$. The magnitude of the perturbing gravity $\|\square\mathbf{g}\|$ is assumed to be much smaller than g_0. For simplicity denote $g_\epsilon = \frac{(\delta m(0)+d)^2}{\delta m(0)} G_\epsilon$. Figure 6.4 gives a schematic sketch for the configuration.

The total gravity field $\mathbf{g}(x,z)$ is given by the sum of the uniform component $\mathbf{g}_u$ and the perturbing component $\square\mathbf{g}$:

$$\mathbf{g}(x,z) = -\frac{g_\epsilon x}{x^2+(z+d)^2}\hat{x} - \left(g_0 + \frac{g_\epsilon z}{x^2+(z+d)^2}\right)\hat{z}, \tag{6.53}$$

which suggests the geopotential $\Psi(x,z)$ is given by

$$\Psi(x,z) = g_0 z + \frac{g_\epsilon}{2}\ln(x^2+(z+d)^2) + C, \tag{6.54}$$

where C is arbitrary constant.

The constant C is chosen by demanding $\Psi_0 = \Psi(x,\delta m(x)) = 0$, where $z = \delta m(x)$ is the mean-sea level. The transformation rules in equation (6.13) suggest the new set of coordinates (q_1,q_2) by

$$q_1(x,z) = x + \frac{g_\epsilon}{g_0}\tan^{-1}\left(\frac{x}{z+d}\right) \tag{6.55}$$

$$q_2(x,z) = z + \frac{g_\epsilon}{2g_0}\ln(x^2+(z+d)^2) \tag{6.56}$$

Suppose, in addition, the bottom solid boundary of the fluid $z=-h(x)$ is chosen such that the geopotential $\Psi(x,-h(x))$ also remains constant on the boundary. In other words, $z=-h(x)$ coincides with an equipotential line of the geopotential, such that the line $z=-h(x)$ can be mapped into $q_2=-h_0$ with h_0 being a constant.

Hence the boundary conditions suggested in (6.40) is also applicable in this example. This gives rises to the same monochromatic wave solution as in (6.41a) and (6.41b):

$$\eta(q_1,t) = a\cos(kq_1-\omega t) \tag{6.57}$$

$$\phi(q_1,q_2,t) = \left(\frac{\omega}{k}a\right)\frac{\cosh(k(q_2+\tilde{h}_0))}{\sinh(k\tilde{h}_0)}\sin(kq_1-\omega t) \tag{6.58}$$

subject to the dispersion relation

$$\omega^2 = g_0 k\tanh(k\tilde{h}_0). \tag{6.59}$$

Unfortunately an explicit inverse coordinate transformation from (q_1,q_2) to physical coordinates (x,z) is absent, which makes the analysis complicated.

Furthermore, both coordinate functions $q_1(x,z)$ and $q_2(x,z)$ do not converge as $r=\sqrt{x^2+y^2}\to\infty$, which makes the two limiting cases $r\to 0$ and $r\to\infty$ impotent in distinguishing different types of wave behaviour.

This motivates the studies of next example, which is based on a non-physical scenario.

6.3.3. Example 2b: Vertical Downwards Gravity with Perturbation

Consider the same physical setting in Example 2a except for the perturbing geopotential $\delta\Psi(x,z)$ that satisfies the Laplace equation, which is given by

$$\delta\Psi(x,z) = \frac{-G_\epsilon x}{x^2+(z+d)^2}. \tag{6.60}$$

This physically corresponds to a dipole of mass and negative-mass centred at $(x,z)=(0,-d)$. However, negative-mass is unlikely to be relevant to gravitational field on Earth.

Despite the physical irrelevance, the perturbing gravity field $\square\mathbf{g}$ is still considered:

$$\square\mathbf{g}(x,z) = -G_\epsilon\left(\frac{x^2-(z+d)^2}{[x^2+(z+d)^2]^2}\hat{x} + \frac{2x(z+d)}{[x^2+(z+d)^2]^2}\hat{z}\right), \tag{6.61}$$

where G_ϵ is a positive constant. This suggests for $|x|>|z+d|$, both the horizontal and vertical component of the perturbation gravity is always negative. This motivates a domain of interest given

by $\{(x,z) : x \geq z + d > 0\}$, where it appears as if there is a certain attractive mass on the left side of the domain of interest.

The magnitude of the perturbing gravity $\|\square\mathbf{g}\|$ given by

$$\|\square\mathbf{g}\| = \frac{G_\epsilon}{x^2 + (z+d)^2} \tag{6.62}$$

is assumed to be much smaller than g_0.

Hence the total gravity field $\mathbf{g}(x,z)$ is given by the sum of the uniform component $\mathbf{g}_u$ and $\square\mathbf{g}$:

$$\mathbf{g}(x,z) = -\frac{G_\epsilon(x^2 - (z+d)^2)}{[x^2 + (z+d)^2]^2}\hat{x} - \left(g_0 + \frac{2G_\epsilon x(z+d)}{[x^2 + (z+d)^2]^2}\right)\hat{z}, \tag{6.63}$$

which suggests the geopotential $\Psi(x,z)$:

$$\Psi(x,z) = g_0 z - \frac{G_\epsilon x}{x^2 + (z+d)^2} + C, \tag{6.64}$$

where C is an arbitrary constant.

The constant C in the geopotential is chosen by demanding $\Psi_0 = \Psi(x, \delta m(x)) = 0$, where $z = \delta m(x)$ is the mean-sea level. Hence $C = -g_0 \delta m(0)$. The transformation rules in equation (6.13) result in the new set of coordinates (q_1, q_2):

$$q_1(x,z) = x - \frac{G_\epsilon}{g_0}\frac{z+d}{x^2 + (z+d)^2} + \frac{G_\epsilon}{g_0(\delta m(0) + d)} \tag{6.65a}$$

$$q_2(x,z) = z - \frac{G_\epsilon}{g_0}\frac{x}{x^2 + (z+d)^2} - \delta m(0) \tag{6.65b}$$

Closed-form expressions for the inverse $x = x(q_1, q_2)$ and $z = z(q_1, q_2)$ actually exists and can be obtained by symbolic calculation using Maple or Mathematica. Yet the expression is lengthy and will not be presented here.

Consider again the case that the bottom solid boundary of the fluid $z = -h(x)$ coincides with an equipotential line of the geopotential, such that the line $z = -h(x)$ can be mapped into $q_2 = -h_0$ with h_0 being a constant. Note that d is assumed to be $d < h(x)$ such that the excess mass is embedded beneath the fluid.

The boundary conditions suggested in (6.40) becomes applicable. This gives rise to the monochromatic wave in (6.41a) and (6.41b):

$$\eta(q_1, t) = a\cos(kq_1 - \omega t) \tag{6.66}$$

$$\phi(q_1, q_2, t) = \left(\frac{\omega}{k}a\right)\frac{\cosh(k(q_2 + \tilde{h}_0))}{\sinh(k\tilde{h}_0)}\sin(kq_1 - \omega t) \tag{6.67}$$

subject to the dispersion relation

$$\omega^2 = g_0 k \tanh(k\tilde{h}_0) \tag{6.68}$$

Rewriting the equation for the surface elevation $q_2 = \eta(q_1, t) = a\cos(kq_1 - \omega t)$ by the physical coordinates (x,z) gives

$$z - \frac{G_\epsilon}{g_0}\frac{x}{x^2 + (z+d)^2} - \delta m(0) = a\cos\left[k(x - \frac{G_\epsilon}{g_0}\frac{z+d}{x^2 + (z+d)^2}) - \omega t + \theta_k\right], \tag{6.69}$$

where $\theta_k = k\frac{G_\epsilon}{g_0(\delta m(0)+d)}$ is a constant phase which can be eliminated by shifting the time t.

It is noted from the coordinate functions (6.65) that, in the far-field $|x| \gg (z+d)$ where the very weak perturbing gravity field points towards the negative x-direction, q_1 and q_2 can be approximated by

$$q_1(x,z) \approx x + \frac{G_\epsilon}{g_0(\delta m(0) + d)} \tag{6.70}$$

$$q_2(x,z) \approx z + \frac{G_\epsilon}{g_0 x} - \frac{\delta m(0)}{g_0} \tag{6.71}$$

Hence it is expected that in the far-field the surface elevation in (6.69) can be described approximately by

$$z \approx a\cos\left[kx - \omega t + \theta_k\right] - \frac{G_\epsilon}{g_0 x} + \frac{\delta m(0)}{g_0} \tag{6.72}$$

For sufficiently large $|x| \gg \frac{g_\epsilon}{g_0 a}$, the term $\frac{g_\epsilon}{g_0 x}$ becomes negligible to $a\cos(\cdot)$, then the wave number k and wave amplitude a the transformed coordinates (q_1, q_2), can be interpreted as also the wave number and amplitude of surface waves in the physical coordinates (x, z) in the far-field.

6.3.4. Example 2b: Numerical Visualisation and Comparison with Adapted Shallow Water Model

In order to examine the actual surface elevation in the physical coordinates, the level-set (x, z) described by (6.69) and the mean-sea level $q_2(x, z) = 0$ is visualised numerically using several configurations.

Figure 6.5: Surface Wave on fluid, spatially varying gravity field. Wavelength 50 m.

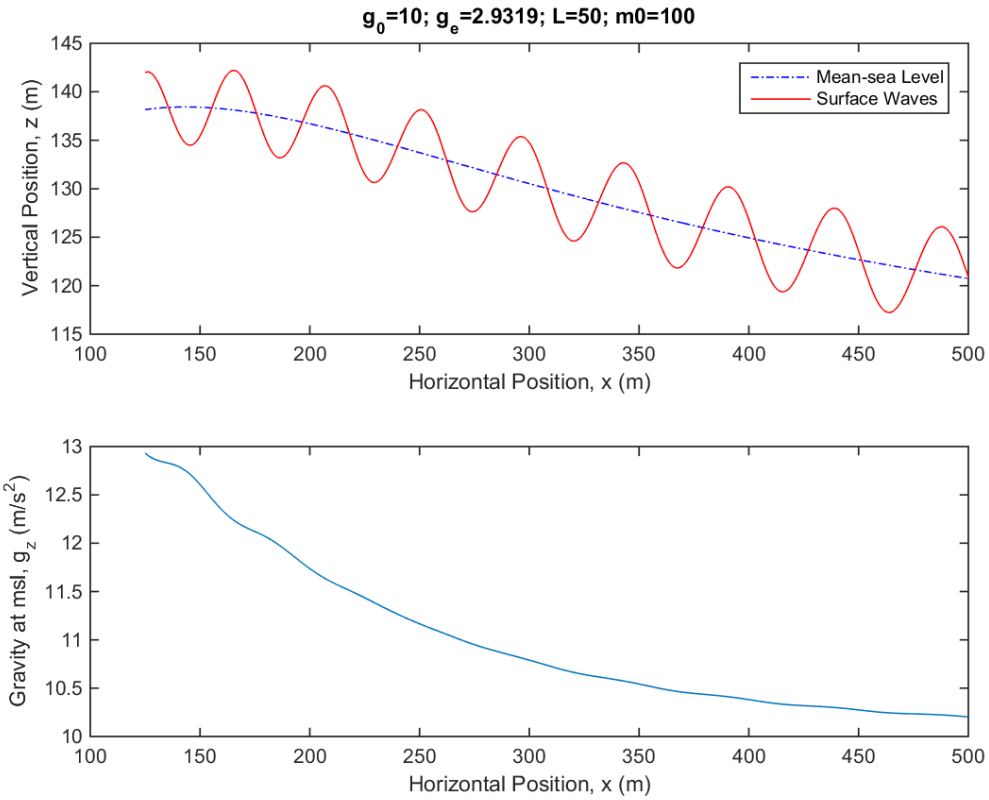

Figure 6.5 to 6.8 gave the instantaneous surface elevation and mean-sea level in some hypothetical scenarios at different wavelengths L. The second subplots in the figures plots the spatially varying gravity at the mean-sea level. The depth of the fluid layer is 100 m in the far-field when gravity perturbation is absent. The difference among the figure are only the wavelength (and thus period) of the waves, which are described in the caption of each figure.

It can be concluded from all the figures, in regions with stronger gravity and thus higher and steeper mean-sea level, an observer on a floating ship who aligns his local orthogonal coordinates along the mean-sea level would observe a longer wavelength yet smaller wave amplitude than the counterpart in the far-field. This is consistent with the results derived from the shallow water model.

In order to provide a more quantitative justification, the wave amplitude is compared with the theoretical wave amplitude given by the shallow water model.

Figure 6.6: Surface Wave on fluid, spatially varying gravity field. Wavelength 200 m.

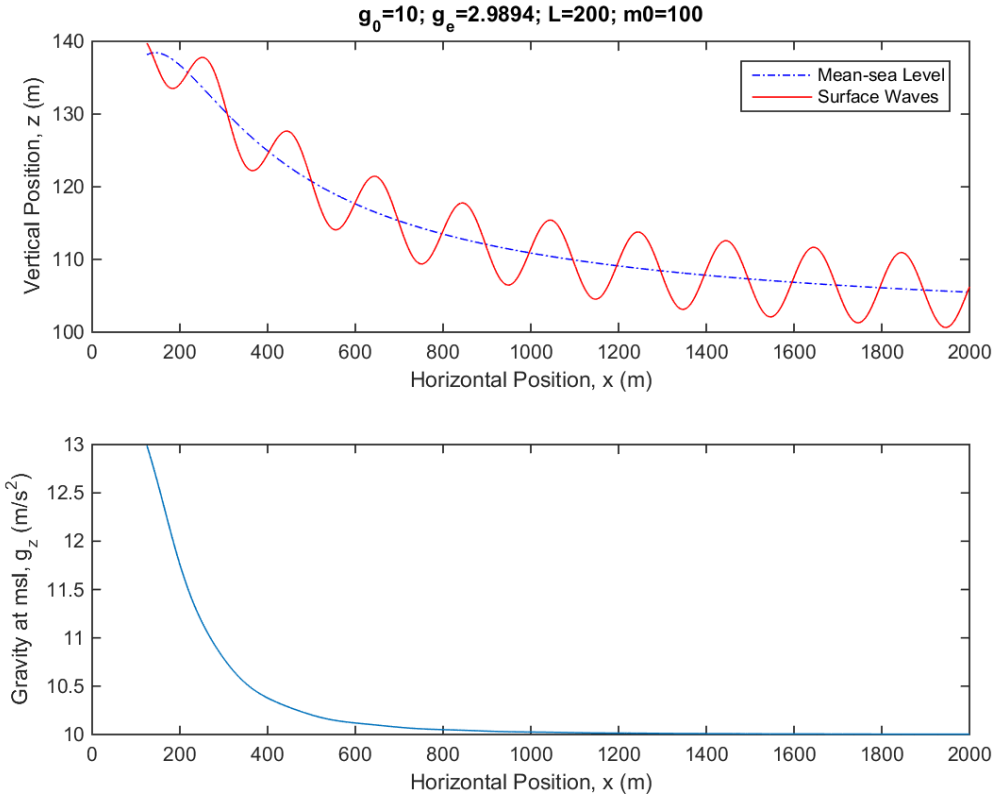

It has been shown in (4.35) that the wave amplitude in shallow water scales with $g_z^{-\frac{3}{4}}$, where $g_z(x)$ is the effective gravity at position x, on the surface of fluid with uniform water depth. It is recalled that in the shallow water model the horizontal coordinates are not transformed. The wave amplitude $a(x)$ at location x has been defined by

$$a(x) = \max\{|\eta(x,t) - \delta m(x)|, \forall t\} \tag{6.73}$$

where $z = \eta(x,t)$ is the surface elevation.

In order to make a fair comparison, the same definition of wave amplitude is applied to the surface elevation described by (6.69) in the generalised Airy's linear wave theory. The wave amplitudes are compared with the theoretical prediction by the shallow water models at different wavelengths and are given in Figure 6.9 to 6.12. It can be noted from the figures when the wavelengths of surface waves increases, such that the fluid is getting more 'shallow', the adapted shallow water model gains consistency with the generalised Airy's theory.

Readers are reminded that no unphysical approximation is made in the generalised Airy's linear wave theory. Thus this model is believed to be a more accurate model to describe surface waves in a general conservative gravity field. The consistency thus indirectly justifies the various approximations used in the derivation of the adapted shallow water model.

REMARK: Strictly speaking, the wavenumber k derived the should also be compared with the wavenumber field $k = k(x)$ from the adapted shallow water model. However a straightforward comparison is difficult since the surface waves derived by the generalised Airy's theory are described implicitly by the coordinates (x,z). It becomes unclear on how to define the wavenumber field $k = k(x)$ in the framework of generalised Airy's linear theory. Due to the time constraints, such analysis is omitted in this project. Further research is invited to explore this areas.

Figure 6.7: Surface Wave on fluid, spatially varying gravity field. Wavelength 1000 m.

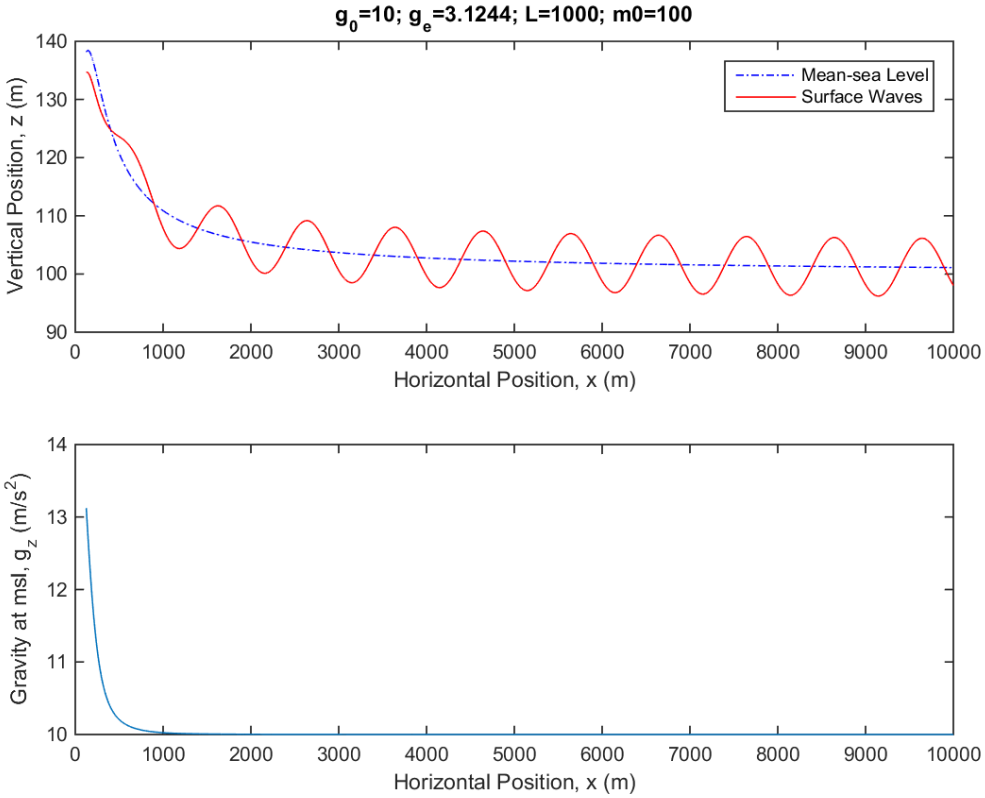

6.3.5. Conclusions from the One-Dimensional Waves

In the test cases, the surface waves in quiescent fluid with uniform 'generalised' water depth were studied. The effects of water depth on the surface waves are thus eliminated from the analysis.

In example 1, the scenario in which the gravity varies only in the transverse direction of waves is studied. It can be noted that the linear wave in the transformed coordinates can mapped non-linearly to derive the actual waves in the physical coordinates.

In example 2, a weak and spatially varying gravity perturbation is added to the uniform gravity field. Example 2a reveals the limitation of the choice of perturbing gravity field in the two-dimensional space. Example 2b shows the possibility of deriving insights from unphysical gravity field by confining a suitable domain of interest.

The result from example 2b shows qualitative consistency with the adapted shallow water model, which suggested the surface waves to be damped but elongated in region with stronger gravity in the physical space. Quantitative justification for the consistency in the wave amplitudes has also be provided.

6.3.6. Remarks on the General Variable Bathymetric Profiles

In the test cases only the uniform bathmetric profiles, namely, water depth $h(x) = h_0$ being constant after the coordinate transformation, is considered.

In the general case of a variable water depth $h(x)$, after applying once the coordinate transformation via (6.13) to reduce the spatially-varying gravity field into an uniform one, an additional step of conformal terrain-following coordinate transformation can be applied to derive the ansatz for the surface waves. Ruban(2004, 2005) discussed the detailed mathematical formalism of the more general time-dependent coordinate transformation via spectral methods. Viott(2013) outlined the numerical methods to solve the resulting system of equations based on non-linear iterative solver.

In this thesis since the gravity field is concerned, the details of variable bottom profiles will be omitted. Interested readers may refer to the literature suggested above.

Figure 6.8: Surface Wave on fluid, spatially varying gravity field. Wavelength 2000 m.

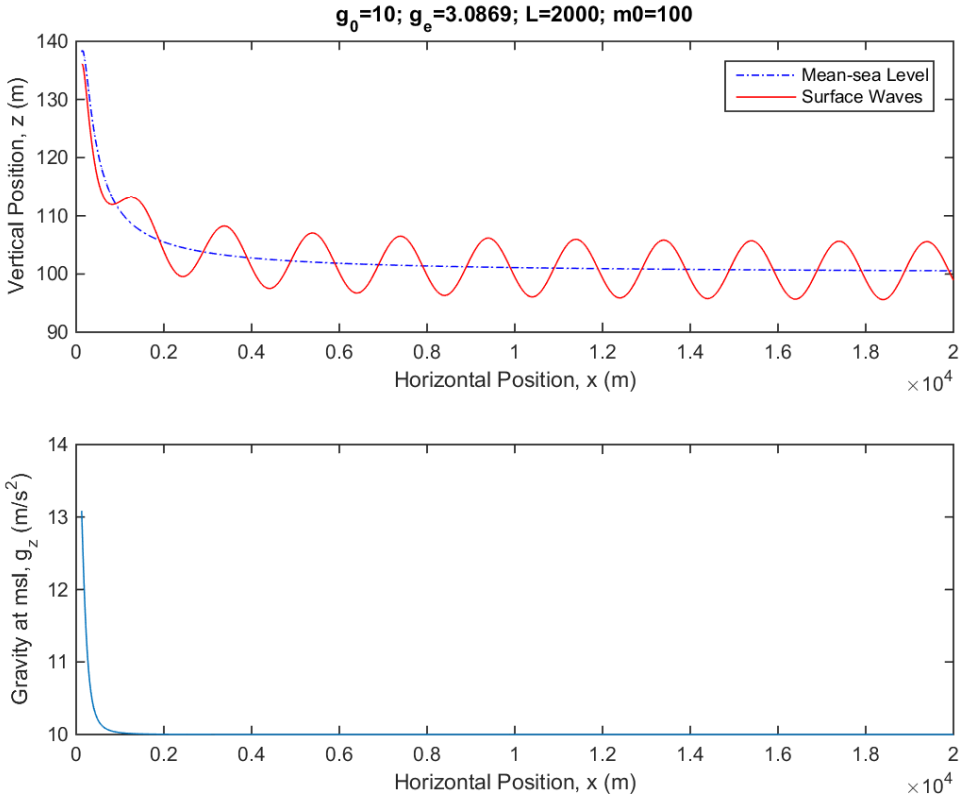

6.4. Discussion on the Three-Dimensional Potential

It is natural to seek a three-dimensional generalisation to the coordinate transformation schemes discussed to analyse the surface waves. It will be shown in an example that, while an analogous method to perform orthogonal coordinate transformation exists, the invariance property of the Laplacian operator cannot be preserved in general. The framework on which the coordinate transformation takes place will be presented in the next section before proceeding to an illustrating example.

6.4.1. coordinate transformation in Three-Dimensional Space

Analogous to the two-dimensional problem discussed in previous section, given a geopotential $\Psi(x,y,z)$ which satisfies the Laplace equation $\nabla^2\Psi = 0$, it is attempted to seek a coordinate transformation $(x,y,z) \to (q_1,q_2,q_3)$ such that the following three properties hold:

1. The transformation $(x,y,z) \to (q_1,q_2,q_3)$ is uniquely defined and the inverse uniquely exists in the interested domain.
2. The coordinates are orthogonal, that is $\nabla q_i \cdot \nabla q_j = \delta_{ij}$, where δ_{ij} is the Kronecker delta
3. The scalar function $q_3(x,y,z) = \frac{1}{g_0}(\Psi(x,y,z) - \Psi_0)$, such that $q_3(x,y,z)$ physically measures the scaled potential difference from the mean-sea level Ψ_0

The Property 3 directly gives the explicit formula of q_3. Hence it suffices to determine q_1 and q_2.

6.4.2. Trial 1: Clebsch Potential

For any divergence-free vector field $\mathbf{u}$ in $\mathcal{R}^3$ with

$$\nabla \cdot \mathbf{u} = 0,$$

Figure 6.9: Comparison of adapted shallow water model and generalised Airy's wave theory. Wavelength 50 m.

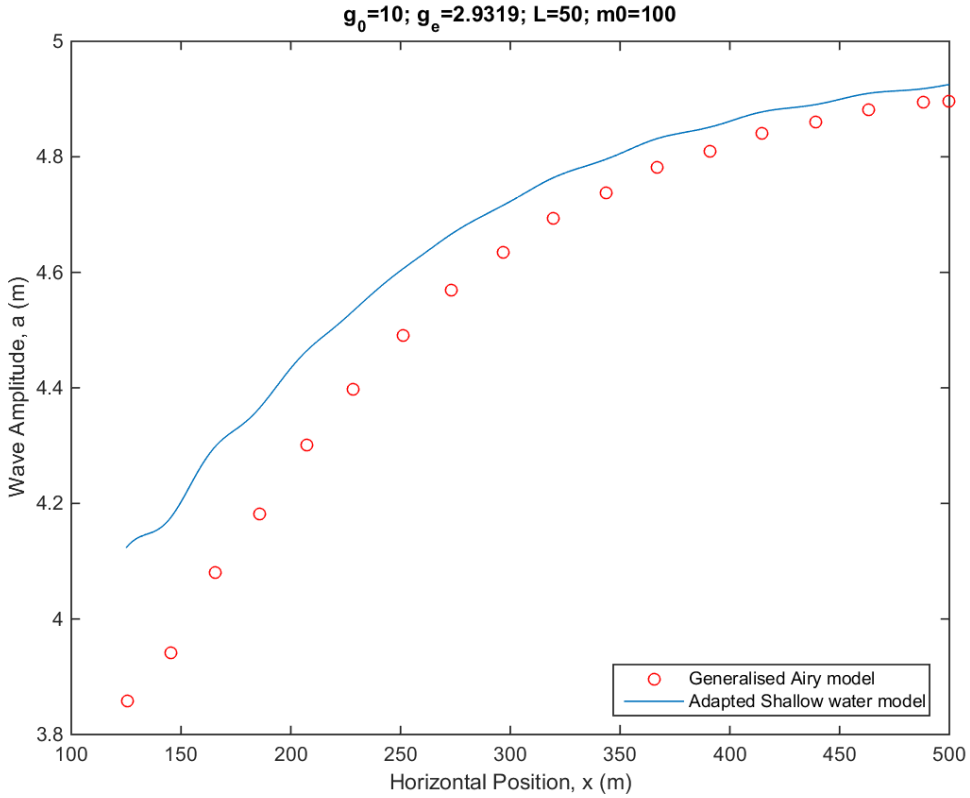

it can be proved via techniques from algebraic topology that there exists a vector potential $\mathbf{A}$ such that

$$\nabla \times \mathbf{A} = \mathbf{u}.$$

The detailed proof can be obtained from intermediate-level Analysis texts.

It is reminded that the vector potential $\mathbf{A}$ is not unique. For any scalar function f, the vector field $\mathbf{A}' = \mathbf{A} + \nabla f$ is also a vector potential for $\mathbf{u}$. This property is known as 'Gauge invariance'.

Clebsch (1857) showed that locally the vector potential $\mathbf{A}$ can be decomposed into

$$\mathbf{A} = \eta \nabla \xi,$$

where $\eta(x, y, z)$ and $\xi(x, y, z)$ are two scalar functions. It follows that

$$\mathbf{u} = \nabla \eta \times \nabla \xi,$$

which shows the the vector $\mathbf{u}$ is locally parallel to the intersection line of the surfaces η = constant and ξ = constant.

Based on the definition given in the previous section, since $q_3(x, y, z)$ satisfies the Laplace equation, the gradient of q_3, ∇q_3, is a divergence-free vector field. For the field $\mathbf{A}$ to be the vector potential of ∇q_3 such that $\nabla \times \mathbf{A} = \nabla q_3$, it then follows the coordinates function $q_1(x, y, z)$ and $q_2(x, y, z)$ can be chosen by

$$\mathbf{A} = q_1 \nabla q_2 \tag{6.74}$$

which leads to

$$\nabla q_3 = \nabla q_1 \times \nabla q_2, \tag{6.75}$$

If, in addition, ∇q_1 and ∇q_2 are orthogonal, (6.75) implies that ∇q_1, ∇q_2 and ∇q_3 are mutually orthogonal. Furthermore, considering the norm of vectors in (6.75), it can be noted that $\|\nabla q_3\| =$

Figure 6.10: Surface Wave on fluid, spatially varying gravity field. Wavelength 200 m.

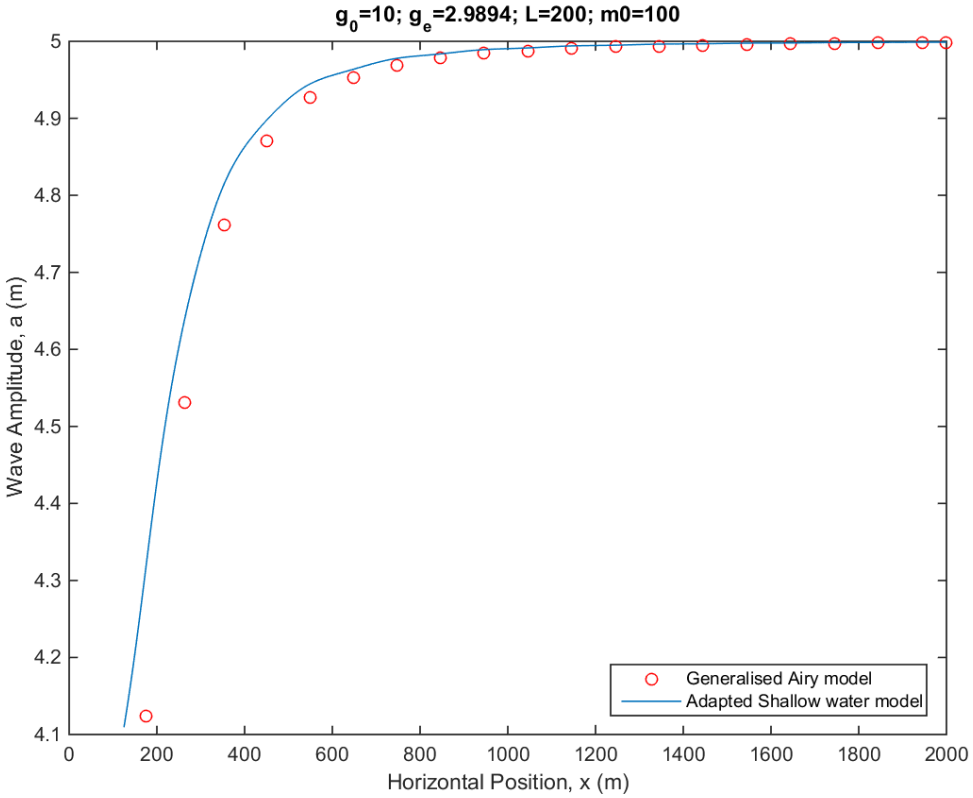

$\|\nabla q_1\|\|\nabla q_2\|$. In other words, unless all three vectors ∇q_i are unit vector, the coordinates will not be equal in norm.

It is noted that the two-dimensional conformal coordinates discussed in (6.13) is a special case under Clebsch's theory. If q_1 can be chosen such that $q_1(x,y)$ is independent of the vertical Cartesian coordinates z, by choosing $q_2(x,y,z) = z$, it follows that the coordinates $q_3(x,y)$ is also independent of z. The coordinates q_1 and q_3 satisfy the Cauchy-Riemann condition (6.12) automatically by the choice of q_2.

6.4.3. Example: Point-mass in three-dimensional space

Consider the gravitational potential induced by a sphere of radius R_c centred at the origin. To simplify the notation, standard spherical coordinates (r,θ,ϕ) with unit vectors $\hat{r},\hat{\theta},\hat{\phi}$ will be used. By proper rescaling the physical length r, the geopotential function $\Psi(r)$ is simply given by

$$\Psi(r) = -\frac{g_0}{r} \tag{6.76}$$

outside the sphere $r > R_c$, where g_0 is some positive constant. Suppose $r = R_s$ is the mean-sea level. It follows that the coordinate function $q_3(r,\theta,\phi)$ is simply given by

$$q_3(r,\theta,\phi) = -\frac{1}{r} + \frac{1}{R_s} \tag{6.77}$$

The contrapositive basis $\mathbf{a}^{(3)} = \nabla q_3$ is thus given by

$$\mathbf{a}^{(3)} = \nabla q_3 = \frac{1}{r^2}\hat{r} \tag{6.78}$$

Figure 6.11: Surface Wave on fluid, spatially varying gravity field. Wavelength 1000 m.

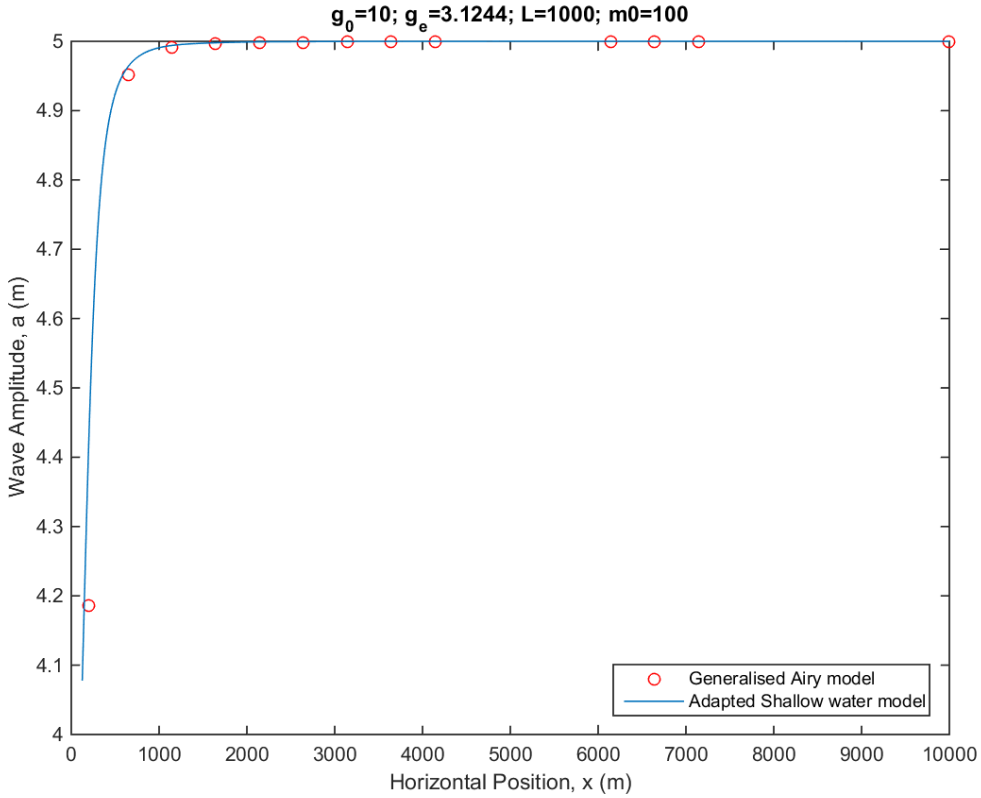

It can be shown that a possible vector potential $\mathbf{A}(r,\theta,\phi)$ to ∇q_3 such that $\nabla q_3 = \nabla \times \mathbf{A}$ is given by

$$\mathbf{A}(r,\theta,\phi) = \frac{1-\cos(\theta)}{r\sin(\theta)}\hat{\phi}, \text{ with } \sin(\theta) \neq 0 \tag{6.79}$$

To decompose $\mathbf{A}$ into the form $q_1 \nabla q_2$, a natural choice is done by

$$q_1 = 1-\cos(\theta) = 2\sin^2(\frac{\theta}{2}) \tag{6.80a}$$

$$q_2 = \phi. \tag{6.80b}$$

It then also follows that the corresponding contrapositive basis $\mathbf{a}^{(i)}$ are given by

$$\mathbf{a}^{(1)} = \nabla q_1 = \frac{\sin(\theta)}{r}\hat{\theta} \tag{6.81}$$

$$\mathbf{a}^{(2)} = \nabla q_2 = \frac{1}{r\sin(\theta)}\hat{\phi}. \tag{6.82}$$

It is noted that with this choice of q_i, the contrapositive basis $\mathbf{a}^{(i)}$ are all mutually orthogonal.

It then follows also that the covariant basis $\mathbf{a}_{(i)}$ are given by

$$\mathbf{a}_{(1)} = \frac{r}{\sin(\theta)}\hat{\theta} \tag{6.83}$$

$$\mathbf{a}_{(2)} = r\sin(\theta)\hat{\phi} \tag{6.84}$$

$$\mathbf{a}_{(3)} = r^2\hat{r}. \tag{6.85}$$

Figure 6.12: Surface Wave on fluid, spatially varying gravity field. Wavelength 2000 m.

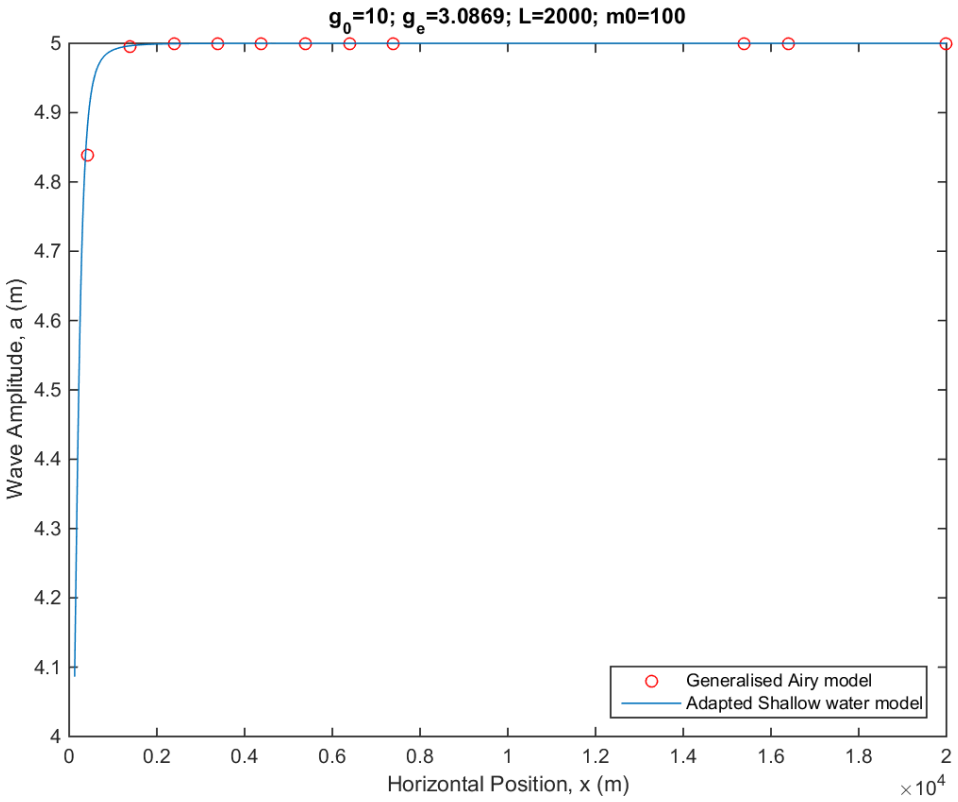

The metric tensor $g^{ij} = \mathbf{a}^{(i)} \cdot \mathbf{a}^{(j)}$ and $g_{ij} = \mathbf{a}_{(i)} \cdot \mathbf{a}_{(j)}$ are therefore given by

$$g^{11} = \frac{\sin^2(\theta)}{r^2},\ g^{22} = \frac{1}{r^2 \sin^2(\theta)},\ g^{33} = \frac{1}{r^4} \tag{6.86}$$

$$g_{11} = \frac{r^2}{\sin^2(\theta)},\ g_{22} = r^2 \sin^2(\theta),\ g_{33} = r^4 \tag{6.87}$$

and the quantity $\sqrt{g}$ is given by

$$\sqrt{g} = \sqrt{g_{11} g_{22} g_{33}} = r^4 \tag{6.88}$$

The Laplacian operator in the (q_1, q_2, q_3) are thus given by

$$\begin{aligned}
\nabla^2 f &= \frac{1}{\sqrt{g}} \frac{\partial}{\partial q_1}\left(\sqrt{g} g^{11} \frac{\partial f}{\partial q_1}\right) + \frac{1}{\sqrt{g}} \frac{\partial}{\partial q_2}\left(\sqrt{g} g^{22} \frac{\partial f}{\partial q_2}\right) + \frac{1}{\sqrt{g}} \frac{\partial}{\partial q_3}\left(\sqrt{g} g^{33} \frac{\partial f}{\partial q_3}\right) \\
&= \frac{1}{r^4} \frac{\partial}{\partial q_1}\left(r^4 \frac{\sin^2(\theta)}{r^2} \frac{\partial f}{\partial q_1}\right) + \frac{1}{r^4} \frac{\partial}{\partial q_2}\left(r^4 \frac{1}{r^2 \sin^2(\theta)} \frac{\partial f}{\partial q_2}\right) + \frac{1}{r^4} \frac{\partial}{\partial q_3}\left(r^4 \frac{1}{r^4} \frac{\partial f}{\partial q_3}\right) \\
&= \frac{1}{r^4} \frac{\partial}{\partial q_1}\left(r^2 \sin^2(\theta) \frac{\partial f}{\partial q_1}\right) + \frac{1}{r^4} \frac{\partial}{\partial q_2}\left(\frac{r^2}{\sin^2(\theta)} \frac{\partial f}{\partial q_2}\right) + \frac{1}{r^4} \frac{\partial^2 f}{\partial {q_3}^2}
\end{aligned}$$

To simplify the notation, considering the coordinate transformation q_3 in (6.77), it is also possible to recast

$$q_3' = q_3 - \frac{1}{R_s} \tag{6.89}$$

such that r and $\frac{\partial}{\partial q_3}$ can be expressed in terms of

$$r = \frac{-1}{q_3'} \tag{6.90}$$

$$\frac{\partial}{\partial q_3} = \frac{\partial}{\partial q_3'} \tag{6.91}$$

To recast $\sin^2(\theta)$ in terms of (q_1, q_2, q_3), applying trigonometric identities and using (6.80) give

$$\sin^2(\theta) = 4\cos^2(\frac{\theta}{2})\sin^2(\frac{\theta}{2}) = 4(1-\frac{q_1}{2})\frac{q_1}{2} = (2-q_1)q_1 \tag{6.92}$$

Therefore the Laplacian operator $\nabla^2 f$ in the (q_1, q_2, q_3) coordinates are given by

$$\nabla^2 f = {q_3'}^2 \frac{\partial}{\partial q_1}\left((2-q_1)q_1\frac{\partial f}{\partial q_1}\right) + \frac{{q_3'}^2}{(2-q_1)q_1}\frac{\partial^2 f}{\partial {q_2}^2} + {q_3'}^4\frac{\partial^2 f}{\partial {q_3'}^2}$$

Hence the Laplace equation (6.3) for the velocity potential ϕ is rewritten as

$$\nabla^2\phi = \frac{\partial}{\partial q_1}\left((2-q_1)q_1\frac{\partial f}{\partial q_1}\right) + \frac{1}{(2-q_1)q_1}\frac{\partial^2 f}{\partial {q_2}^2} + {q_3'}^2\frac{\partial^2 f}{\partial {q_3'}^2} = 0 \tag{6.93}$$

subject to the linearised boundary conditions

$$\text{at } q_3 = -\tilde{h}_0\text{: } \frac{\partial\phi}{\partial q_3'} = 0, \tag{6.94a}$$

$$\text{at } q_3 = 0\text{: } \frac{\partial\phi}{\partial q_3'} = \frac{\partial\eta}{\partial t}. \tag{6.94b}$$

together with an addition equation for surface elevation $q_3 = \eta(q_1, q_2, t)$:

$$\text{at } q_3 = 0\text{: } \frac{\partial\phi}{\partial t} + g_0\eta = 0, \tag{6.95}$$

Readers are reminded that q_3 and q_3' are different merely by a shift proposed in (6.89).

Equation (6.93) reveals that the Laplacian operator does not preserve the structure as that in the Cartesian coordinates.

As a first trial, consider a time-independent separable solution f to equation (6.93), that is, take $f(q_1, q_2, q_3') = Q_1(q_1)Q_2(q_2)Q_3(q_3')$, this gives rises to the partial differential equation:

$$\frac{(2-q_1)q_1}{Q_1(q_1)}\frac{d}{dq_1}\left((2-q_1)q_1\frac{dQ_1}{dq_1}\right) + \frac{1}{Q_2(q_2)}\frac{d^2Q_2}{d{q_2}^2} + \frac{(2-q_1)q_1{q_3'}^2}{Q_3(q_3')}\frac{d^2Q_3}{d{q_3'}^2} = 0 \tag{6.96}$$

For constant m, consider $\frac{d^2Q_2}{d{q_2}^2} = -m^2Q_2(q_2)$ such that $Q_2(q_2)$ is sinusoidal, the Laplace equation can then be separated into three ordinary differential equations:

$$\frac{d}{dq_1}\left((2-q_1)q_1\frac{dQ_1}{dq_1}\right) = [-l(l+1) + \frac{m^2}{(2-q_1)q_1}]Q_1(q_1), \tag{6.97a}$$

$$\frac{d^2Q_2}{d{q_2}^2} = -m^2Q_2(q_2), \tag{6.97b}$$

$$\frac{d^2Q_3}{d{q_3'}^2} = \frac{l(l+1)}{{q_3'}^2}Q_3(q_3'), \tag{6.97c}$$

where l is a constant.

After some attempts of solving, it turns out that the solution of (6.97) is equivalent to the separable solution of Laplace equation in the standard spherical coordinates by recasting (q_1, q_2, q_3) into (r, θ, ϕ), which reads

$$f(r,\theta,\phi) = \sum_{l=0}^{\infty}\sum_{m=0}^{l}(A_l r^l + B_l r^{(-l-1)})P_l^m(\cos(\theta))[S_m \sin(m\phi) + C_m \cos(m\phi)] \tag{6.98}$$

where P_l^m are the associated Legendre polynomials and A_l, B_l, S_m, C_m are some constants. This ansatz is known as spherical harmonics, which are discussed together with its applications extensively in many texts, such as Lebedev(1965).

In the particular case when $m = 0$, which suggests azimuthal symmetry in the ansatz, it appears that the order of the Legendre function l plays the role of wavenumber k for sinusoidal-types of waves. For integer k, the term $\cos(k\theta)$ can always be expressed uniquely by linear combination $P_l^0(\cos(\theta)), l \leq k$ with the aid of Chebyshev polynomial. The details can be found in texts on special functions, for example Lebedev(1965).

Conceptually, if the surface elevation $q_3 = \eta(q_1, q_2, t)$ is known everywhere at a given t, a boundary-value problem to the Laplace equation (6.93) with pure Neumann boundary conditions (6.94) is formed. It then follows the constants A_l, B_l, S_m, C_m and thus the instantaneous velocity potential can be determined. Meanwhile the additional equation (6.95) can fix the uniqueness issue of the solution resulted from the ill-posed pure Neumann boundary condition.

Unfortunately this approach by separation of variables does not appear to possess the capability in deriving a wave-like and inseparable ansatz for the surface elevation $\eta = \eta(k_1 q_1 + k_2 q_2 - \omega t)$ with arbitrary constants k_1 and k_2.

Further research shall be devoted to confirm the existence of such solutions and, if exists, an algorithm to obtain the solutions. The following sections outline alternative directions to obtain another set of coordinates, which may bring insights in constructing the wave-like ansatz.

6.4.4. Clebsch Potential: the Gauge Invariance

Readers are reminded again that vector potential $\mathbf{A}$ is unique only up to the Gauge transformation. It may be possible to choose a scalar function h such that the coordinates function q_1 and q_2, given by

$$\mathbf{A} + \nabla h = q_1 \nabla q_2, \tag{6.99}$$

fulfill the additional conditions

$$\|\nabla q_1\| = \|\nabla q_2\| = g^{11} = g^{22} = G. \tag{6.100}$$

In that case, the Laplacian operator becomes

$$\nabla^2 f = \frac{1}{\sqrt{g}}\frac{\partial}{\partial q_1}\left(\sqrt{g}G\frac{\partial f}{\partial q_1}\right) + \frac{1}{\sqrt{g}}\frac{\partial}{\partial q_2}\left(\sqrt{g}G\frac{\partial f}{\partial q_2}\right) + \frac{1}{\sqrt{g}}\frac{\partial}{\partial q_3}\left(\sqrt{g}g^{33}\frac{\partial f}{\partial q_3}\right) \tag{6.101}$$

which separates the transverse direction (q_1, q_2) of surface waves from the longitudinal direction q_3.

If, in additional, both

$$\sqrt{g}G = \sqrt{g}G(q_3) \tag{6.102}$$

$$\sqrt{g}g^{33} = \sqrt{g}G(q_3) \tag{6.103}$$

are only functions of q_3, then there exists symmetry in q_1 and q_2, namely q_1 and q_2 are interchangeable while preserving the Laplacian operator. The symmetry seems to provide a gateway to guarantee the existence of an arbitrarily-oriented wavevector $\vec{k} = (k_1, k_2)$ on the q_1-q_2 plane, which is a condition of the hyperbolicity of systems of partial differential equations.

However, the existence of h is not guaranteed and there is a lack of general procedure to obtain h. It is also uncertain whether it is possible to choose a coordinate such that q_1 and q_2 possess the symmetry properties described in the previous paragraph. Further research shall be conducted to rigorously understand the properties and explore this area.

6.4.5. Trial 2: Geometric Inspection

In this section another trial to choose proper coordinates is presented. Although it appears to be also a failing attempt, it does provide insight for the right direction to move forward.

Readers are reminded that for a given coordinate q_3, the goal has always been to seek two additional mutually-orthogonal coordinates q_1, q_2 which avoid cross-terms in the transformed Laplace equation. While the approach via Clebsch potential effectively generates the orthogonal coordinates, it does not seem to be effective in representing the physics in a mathematically concise manner.

For the particular example of point-mass geopotential, an alternative approach to propose the coordinate transformation is given by a direct inspection of the algebraic and geometry properties of the transformation. The inspection will be presented in this section.

Recall the coordinates function q_3 is given by (6.77)

$$q_3(r,\theta,\phi) = -\frac{1}{r} + \frac{1}{R_s},$$

which gives a contrapositive basis $\mathbf{a}^{(3)}$:

$$\mathbf{a}^{(3)} = \nabla q_3 = \frac{1}{r^2}\hat{r}$$

It can be noted that $\mathbf{a}^{(3)}$ is parallel to the unit vector $\hat{r}$. It is known that the unit vector $\hat{r}$ is orthonormal to $\hat{\theta}$ and $\hat{\phi}$. This suggests that, by choosing

$$q_1 = q_1(\theta) = \int \frac{d\theta}{\sin(\theta)} = \frac{1}{2}\ln\left(\frac{1-\cos(\theta)}{1+\cos(\theta)}\right) \tag{6.104}$$

$$q_2 = q_2(\phi) = \phi \tag{6.105}$$

which makes

$$\mathbf{a}^{(1)} = \nabla q_1 = \frac{1}{r\sin(\theta)}\hat{\theta} \tag{6.106}$$

$$\mathbf{a}^{(2)} = \nabla q_2 = \frac{1}{r\sin(\theta)}\hat{\phi}, \tag{6.107}$$

the contrapositive basis are mutually orthogonal. An additional property that $\mathbf{a}^{(1)}$ and $\mathbf{a}^{(2)}$ are equal in norm is also guaranteed. The covariant basis are then given by

$$\mathbf{a}_{(1)} = r\sin(\theta)\hat{\theta} \tag{6.108}$$

$$\mathbf{a}_{(2)} = r\sin(\theta)\hat{\phi} \tag{6.109}$$

$$\mathbf{a}_{(3)} = r^2\hat{r} \tag{6.110}$$

The metric tensor are computed and given by

$$g^{11} = g^{22} = \frac{1}{r^2\sin^2(\theta)};\ g^{33} = \frac{1}{r^4} \tag{6.111}$$

$$g_{11} = g_{22} = r^2\sin^2(\theta);\ g^{33} = r^4 \tag{6.112}$$

with the quantity $\sqrt{g} = \sqrt{g_{11}g_{22}g_{33}} = r^4\sin^2(\theta)$.

By recasting q_3 into q_3' in the same manner in (6.89), the inverse transformation from (q_1, q_2, q_3') are given by

$$\tanh(q_1) = -\cos(\theta) \tag{6.113}$$

$$q_2 = \phi \tag{6.114}$$

$$q_3' = \frac{-1}{r} \tag{6.115}$$

after some algebraic manipulation. It follows also that $\sin^2(\theta) = 1-\cos^2(\theta) = 1-\tanh^2(q_1) = \frac{1}{\cosh^2(q_1)}$.

Hence the Laplacian operator is given by

$$\nabla^2 f = \frac{1}{r^4 \sin^2(\theta)}\left[\frac{\partial}{\partial q_1}\left(r^2 \frac{\partial f}{\partial q_1}\right) + \frac{\partial}{\partial q_2}\left(r^2 \frac{\partial f}{\partial q_2}\right) + \frac{\partial}{\partial q_3}\left(\sin^2(\theta)\frac{\partial f}{\partial q_3}\right)\right] \tag{6.116}$$

$$= {q_3'}^4 \cosh^2(q_1)\left[\frac{1}{{q_3'}^2}\frac{\partial^2 f}{\partial q_1^2} + \frac{1}{{q_3'}^2}\frac{\partial^2 f}{\partial q_2^2} + \frac{1}{\cosh^2(q_1)}\frac{\partial^2 f}{\partial {q_3'}^2}\right] \tag{6.117}$$

The Laplacian equation on function $f(q_1, q_2, q_3)$ can thus be expressed by

$$\frac{\partial^2 f}{\partial q_1^2} + \frac{\partial^2 f}{\partial q_2^2} + \frac{{q_3'}^2}{\cosh^2(q_1)}\frac{\partial^2 f}{\partial {q_3'}^2} = 0. \tag{6.118}$$

Considering again the the separable solution $f(q_1, q_2, q_3) = Q_1(q_1)Q_2(q_2)Q_3(q_3')$ results in three ordinary differential equations

$$\frac{d^2 Q_1}{d{q_1}^2} = \left[\frac{-l(l+1)}{\cosh^2(q_1)} + m^2\right]Q_1(q_1), \tag{6.119a}$$

$$\frac{d^2 Q_2}{d{q_2}^2} = -m^2 Q_2(q_2), \tag{6.119b}$$

$$\frac{d^2 Q_3}{d{q_3'}^2} = \frac{l(l+1)}{{q_3'}^2}Q_3(q_3'), \tag{6.119c}$$

which turns out to give an equivalent ansatz as (6.97) after recasting the coordinates into the standard spherical coordinates (r, θ, ϕ). In other words, with this seemingly 'better' set of coordinates $(q_1(\theta), q_2(\phi), q_3(r))$, the ansatz to the Laplace equation one can seek is no different from the ansatz by choosing the standard coordinates (r, θ, ϕ).

This failing example highlights again the choice of coordinates actually implicitly restricts the ansatz one can obtain. With simple adaptation of the spherical coordinates, for example by $(q_1(\theta), q_2(\phi), q_3(r))$, it is very unlikely to generate an insightful ansatz. This again motivates the further studies outlined in section 6.4.4 for a general coordinate transformation given by $(q_1(r, \theta, \phi), q_2(r, \theta, \phi), q_3(r))$ satisfying the additional conditions (6.100) and (6.102).

6.5. Short Conclusions

In this chapter Airy's linear wave theory is generalised to deal with spatially non-uniform conservative gravitational field in two and three-dimensional space.

In the two dimensional space, an explicit scheme of coordinate transformation has been proposed to map the non-uniform conservative gravitational field into a uniform one, enabling the use of classical results to analyse surface gravity waves in fluid. It has also been demonstrated in test cases that the generalised linear wave theory is consistent with the adapted shallow water discussed in Chapter 3 in the long-wave limit.

In the three dimensional space, however, the magic does not work in a straightforward manner. It remains questionable whether a three-dimensional spatially-varying conservative field can be mapped into a uniform field. Several attempts have been made to create the coordinate transformation scheme in a special case but unfortunately unsuccessful. The reason of the failure has been analysed and new directions have been proposed for further research.

7

Conclusions and Further Research Directions

In this thesis, the effects of non-uniformity of gravity field on the fluid surface waves are studied analytically and numerically.

In chapter 3 to 5 the shallow water long waves are studied. With the aid of both analytical and numerical studies, it has been demonstrated that the actual variation of gravity field on Earth solely is not critical to surface waves in the ocean, despite all the possible changes in wave amplitude, wavenumber and wave scattering features induced by the gravity.

Despite this, it has been also illustrated that the sea-surface topography induced by the non-uniform gravity can possibly affect the wave dynamics, especially in waves scattering, via the changes in the time-averaged water depth. This implies that while it remains justifiable to assume constant gravity remains, the spatial variation of time-averaged surface elevation due to gravity on the ocean shall not be neglected. Hence the classical shallow water models remains applicable after properly taking account of the water depths. This also reveals the equivalence between a surface mountain in a non-uniform gravitatonal field and a seabed pit at the bottom in a uniform gravitational field, when it comes to surface waves dynamics.

In chapter 6 the generalised Airy's linear wave theory provided a qualitative justification to the seemingly unrealistic approximations and assumptions used in the derivation of adapted shallow water model. Unfortunately, the generalisation which builds upon conformal mapping is by-far only limited to the two-dimensional space. Further research is needed for the three-dimensional generalisation, in areas including the existence, uniqueness and algorithmic procedures for the three-dimensional orthogonal mapping.

Another unanswered question includes the analytic aspects of two-dimensional waves scattering in the adapted shallow water model, which appears to be possibly analysed by the standard techniques for waves scattering in general heterogeneous medium.

While it appears to be clear that the gravity force on the ocean is too weak to alter the surface waves, the theory developed in this thesis is not confined to surface waves on the ocean. In principle, it applies to fluid surface waves in any conservative and weakly non-linear force fields. It is therefore expected that analogous examples could be sought for in other physical scenarios, for instance, on planets with stronger variation of gravity pull, in charged fluid in conservative electromagnetic fields and so on.

A setback of this project is that the theories developed lack experimental or empirical verification. While the gravity variation on Earth is too weak to result in any observable changes in practice, the variation of restoring force to fluid surface waves can possibly be blown up in laboratory environments. This may be achieved by using electromagnetic forces for charged fluid. Another possible direction to conduct the experiment is by Direct Navier-Stokes simulation computationally. The validation of the theories propose a new topic for further research.

Bibliography

[1] A. Adcroft, J. Marshall and K. Emanuel. *Lecture Notes on Atmospheric and Oceanic Modeling*. Freely retrieve from http:www-paoc.mit.edu12.950_modelingnotesindex.htm. MIT.

[2] G.B. Airy. *Tides and waves*. Encyclopaedia Metropolitana. Mixed Sciences. 3:396, 1841.

[3] F. Barthelmes. *Definition of functionals of the geopotential and their calculation from spherical harmonic models*. Tech. rep., Helmholtz Centre Potsdam, GFZ, 2009.

[4] L.Brillouin. *La mecanique ondulatoire de Schroedinger: une methode generale de resolution par approximations successives*. Comptes Rendus de l'Academie des Sciences, 1926.

[5] A. Clebsch. *Uber eine allgemeine Transformation der hydrodynamischen Gleichungen*. J Reine Angew Math 54:293-313, 1857.

[6] S.S. Hough. *On the Application of Harmonic Analysis to the Dynamical Theory of the Tides. Part I. On Laplace's 'Oscillations of the First Species,' and on the Dynamics of Ocean Currents*. Philos. Trans. R. Soc, A. 189:201-257, 1897.

[7] H. Jeffrey. *On certain approximate solutions of linear differential equations of the second order*. Proceedings of the London Mathematical Society. 23: 428-436, 1924.

[8] H.A. Kramers. *Wellenmechanik und halbzaehlige Quantisierung*. Zeitschrift fuer Physik. 39 (10-11): 828-840, 1926.

[9] P.H. LeBlond, L.A. Mysak. *Waves in the Ocean*. Elsevier, 1981.

[10] N.N. Lebedev. *Special Functions and Their Applications*. Prentice-Hall. Englewood Cliffs, N.J:308pp, 1965.

[11] R.J. LeVeque. *Finite Volume Methods for Hyperbolic Problems*. Cambridge University Press, 2002.

[12] J.C. Luke. *A Variational Principle for a Fluid with a Free Surface*. Journal of Fluid Mechanics. 27 (2): 395-397, 1967.

[13] L.R. Maas. *Topographic filtering and reflectionless transmission of long waves*. J. Phys. Ocean., 27: 195-202, 1996.

[14] J. Marshall and R.A. Plume. *Atmosphere, Ocean and Climate Dynamics: An Introductory Text*. Academic Press, 2007.

[15] J. Pedlosky. *Geophysical Fluid Dynamics*. Springer-Verlag New York, 1979.

[16] J. Pedlosky. *Waves in the Ocean and Atmosphere: Introduction to Wave Dynamics*. Springer Science & Business Media, 2003.

[17] V.P. Ruban. *Water waves over a strongly undulanting bottom.*. Phys. Rev. E, 70:066302, 2004.

[18] V.P. Ruban. *Water waves over a time-dependent bottom: Exact description for 2D potential flows*. Physics Letter A. 340:194-200, 2005.

[19] D.L. Turcotte, G. Schubert. *Geodynamics*. Cambridge University Press, 2002.

[20] C. Viotti. D. Dutykh. F. Dias. *The Conformal-mapping Method for Surface Gravity Waves in the Presence of Variable Bathymetry and Mean Current*. Procedia IUTAM: VOL11. IUTAM Symposium on Nonlinear Interfacial Wave Phenomena from the Micro- to the Macro-Scale, 2013.

[21] G. Wentzel. *Eine Verallgemeinerung der Quantenbedingungen für die Zwecke der Wellenmechanik*. Proceedings of the London Mathematical Society. 23: 428-436.

[22] P. Wesseling. *Principles of Computational Fluid Dynamics*. Springer Science & Business Media, 2001